BEHAVIOUR OF REINFORCED CONCRETE SQUAT SHEAR WALLS WITH AND WITHOUT OPENINGS

A THESIS

Submitted by

SIVAGURU V

for the award of the degree

of

DOCTOR OF PHILOSOPHY

DEPARTMENT OF CIVIL ENGINEERING
INDIAN INSTITUTE OF TECHNOLOGY MADRAS
CHENNAI-600036

OCTOBER 2020

Dedicated to
My Father and
My Friend Magesh

THESIS CERTIFICATE

This is to certify that the thesis entitled **"BEHAVIOUR OF REINFORCED CONCRETE SQUAT SHEAR WALLS WITH AND WITHOUT OPENINGS"** submitted by **SIVAGURU V** to the Indian Institute of Technology, Madras for the award of the degree of **Doctor of Philosophy** is a bona fide record of research work carried out by him under my supervision. The contents of this thesis, in full or in parts, have not been submitted to any other Institute or University for the award of any degree or diploma.

Dr. G. Appa Rao
Professor & Research Guide
Department of Civil Engineering
Indian Institute of Technology Madras
Chennai – 600 036, India.

Place: Chennai

Date: November 2020

ACKNOWLEDGEMENT

I have great pleasure in recording deep sense of gratitude to my research guide, Prof. G. Appa Rao, Structural Engineering Division, Civil Engineering Department, IIT Madras, for his constant support, encouragement and guidance throughout my research stay. I express my heartfelt thanks to him for kindling a deep interest in the present study and the valuable time spent. I would like to thank him for providing facilities required for my research study and valuable suggestions and for constructive discussions and meticulously correction of thesis. Words are inadequate to acknowledge his affection and support.

I am thankful to Prof. Manusanthanam, Head, Department of Civil Engineering, and Prof. Ramamurthy, former Head of the Department of Civil Engineering, IIT Madras, for their valuable support during my research stay. I am very much thankful to my doctoral committee members, Prof. Amlan Kumar Sengupta, Prof. Benny Raphael, and Prof. C. Sujatha, for their valuable suggestions and encouragement during my research work.

I am grateful to Professors A Meher Prasad, Devdas Menon, C V R Murthy, R Satish Kumar, P Alugusundaramoorthy, B Nageshwara Rao, S T G Raghukanth, Arul Jayachandran, U Saravanan, Rupen Goswami, Arun Menon, Laxmi Priya, Alagappan and P Pradeep for their valuable suggestions. I wish to express my acknowledgement to Mr. T. Rajkumar, Mr. Balamurugan, Mr. Sathish, Mr. S. Padmanabhan, Mr. B. Krishnan, Mr. Vincent George, R. Murali, Mr. Ashok and all supporting and technical staff of the Structural Engineering Laboratory for their kind co-operation during experimental work. I am very much thankful to MHRD for providing a stipend for my financial support during Ph. D. under Regular Program.

I express my deep sense of gratitude to all my teachers and Prof. Daniel Thangaraj, Dr. K. R. Leelavathi and Mr. Nageshwaran from UCE Tindivanam. It would have been a daunting task to finish my research successfully, without the affection and moral support provided by my Parents Mr. K. Viswanathan and Mrs. V. TamilSelvi, Sisters Mrs.V. Kavitha, Mrs. V. Sridevi and Mrs. V. Radha, and their families. I thank my friends Kanaka Durga, Leon Raj, Poluraju, Nagesh, Kondal Raj, Amarvel, Yajurved Reddy, Abhinaya, Abishek Peri, Sagadevan, Kaviyarasan, Adsam Gideon, Vijaykumar, Omkar powar Sukumar, Vishwajit anand, Ratna Sai, Anjali Dhabu, Prathusha, Sevugan, Avinash, Chitra, Manikandan, Dinesh, Dhandapani, Gokul, Najeeb Sherif, and Jikhil Joseph for their support. I express my deep gratitude to the IIT Madras, for giving me great opportunity to be within it.

SIVAGURU V

ABSTRACT

KEYWORDS: *Reinforced concrete, shear wall, shear strength prediction, boundary element, utility opening, fibre reinforced concrete (FRC), Nonlinear Finite Element Analysis.*

Reinforced concrete shear walls are often found in high-rise buildings as lateral load resisting members produced by effects of earthquake and wind loads. Shear walls efficiently control performance and damage in buildings. Codes of practice and many researchers proposed empirical and semi-equations for predicting the shear strength of RC walls. Sixteen such predictive equations for finding shear strength have been collected; *IS 456-2000, ACI 318-14, ACI 318-19, ASCE/SEI 43-05, MCBC-04, EC 08-04, AIJ-99, AS 3600-09, NZ 3101.1-06, Barda et al. (1977), Wood (1990), Hernandez et al. (1980), Sánchez et al. (2010), Gulec et al. (2009), Kaseem et al. (2010), Luna et al. (2019).* Accuracy of such predictions is a great concern for designers and are highly deviating. Such deviation in prediction needs to be addressed. These predictions have been assessed through statistically based 333 selective experimental data points. A detailed statistical assessment has been performed. Statistical parameters such as mean, median, coefficient of variation, coefficient of determination, predictor error, scatter plot, frequency distribution and whisker plot has been evaluated for the sixteen equations and the best has been found. Deviation of predicted shear strength of RC walls as per existing equations has been inferred. Shear strength predictions by ACI 318-19 and Sánchez et al. (2010) are closely agreeable with experimental results. Though several factors influence shear strength of RC walls, role vertical and horizontal reinforcement, axial load, and boundary elements is still debatable. Main factors influencing shear strength of RC walls have been emphasised. Best predictions have been validated with accepted experimental results.

Performance of shear walls seems to be significantly influenced by shape of opening, its dimensions and location in walls. Even several national codes do not include provisions for detailing of reinforcement in shear walls with openings, but few national codes recommend additional corner reinforcement around openings. Further, strengthening of shear wall with openings also needs to be addressed. An attempt has been made to study behaviour of RC squat shear walls with utility opening by experimental analysis. Experimental programme

includes selection and processing of materials, dimensions and preparation of specimens, reinforcement detailing, test set-up, loading protocol and testing to understand horizontal strength and behaviour of RC shear walls with and without openings. Test series includes five one-third scaled reinforced concrete squat shear wall with and without opening. It is presumed that cantilever wall subjected to constant vertical load and static cyclic lateral load exhibits similar behaviour of shear wall under earthquake loading. Five shear walls that are designed for experimental study consist of without opening (SW-1.0), with concentric window opening (SW-1.0-CW), FRC with concentric window opening (SW-1.0-CW-FRC), with concentric door opening (SW-1.0-CD) and FRC with concentric door opening (SW-1.0-CD-FRC). Shear strength, shear strength degradation, lateral stiffness, ductility factor and energy dissipation capacity of shear walls have been found to be significantly affected due to openings. Reduction of shear strength, stiffness and energy dissipation of RC wall with opening is rapid during subsequent consecutive cycles after cycle in which maximum peak load occurs. Integrity, cracking resistance, shear strength, stiffness, ductility and energy dissipation capacity of the squat walls have been improved significantly by fibres randomly distributed in concrete with additional reinforcement detailing in corner regions of openings. Though shear strength predicted by ACI 318 equations in shear walls with openings is closely agreeable with test results, it does not state any shape of the opening. Further, as suggested by ACI 318 that weak plane coincides with a horizontal plane in opening, but it does not seem to be observed from experimental investigations.

Nonlinear finite element analysis (NFEA) has been performed for studying behaviour of squat RC shear walls under axial and lateral loads with utility openings. NFE package ANSYS 15.0 was used to model RC shear walls. Reinforced concrete has been modelled using discrete modelling technique and fibres are smeared in it. It has been observed that, presence of openings significantly affected shear strength and behaviour of shear walls. Fibres in concrete provided additional cracking resistance, which seems to be an alternate strengthening scheme for RC shear wall with functional openings.

TABLE OF CONTENTS

LIST OF FIGURES

LIST OF TABLES

NOTATIONS

A_{BE}	Gross area of the boundary element ($l_c \times b_c$)
A_{cv}	Total area of the defined section minus the area of the utility opening in that section
A_g	Gross area of concrete section in the direction of shear force
A_v	Area of horizontal reinforcement
A_{vf}	Area of total reinforcement crossing the shear plane
A_w	Area of the wall bounded by web thickness and web length
b_c	Breadth of boundary element
d	Distance from extreme compression fibre to centroid of longitudinal reinforcement
f_{ck}	Characteristic cube compressive strength of concrete
f_c'	Characteristic cylinder compressive strength of concrete
F_{vbe}	Shear force developed by vertical boundary element reinforcement
F_{vw}	Shear force developed by vertical web reinforcement
f_y	Yield strength of reinforcement
h_w	Height of shear wall
l_c	Length of boundary element
l_w	Length of shear wall
M_u	Moment about base of the wall
N_u	Axial load on shear wall
P	Axial load on Boundary Element
s	Spacing of horizontal reinforcement
t_w	Thickness of the wall
V_{BE}	Peak shear strength of shear wall with boundary elements
V_c	Shear strength contributed by concrete to the shear strength of shear wall
V_n	Peak shear strength of RC shear wall

V_s Shear strength contributed by steel to the shear strength of shear wall

λ Modification Factor to reflect the reduced mechanical properties of lightweight concrete relative to normal weight concrete of same weight concrete

ρ Reinforcement ratio of boundary element

ρ_h Horizontal web reinforcement ratio

ρ_{se} Combined horizontal and vertical reinforcement ratio per ASCE/SEI 43-05

ρ_v Vertical web reinforcement ratio

ρ_w Web Reinforcement

σ Axial stress on the shear wall

CHAPTER 1

INTRODUCTION

1.1 GENERAL

Earthquake is the shaking of the earth's surface, resulting in sudden release of energy in the Earth's lithosphere. This develops seismic waves on the surface of the earth. The earthquake can range in size from weak, which cannot be felt to those violent enough to propel objects and people into the air and can lead to severe destruction across the entire cities. There are several ways to measure the magnitude of an earthquake. The widely-used method is the Richter scale, developed by Charles F. Richter in 1934. The buildings resting on the ground experience motion at their bases due to shaking of the ground. Even though the base of the building moves with the ground, the roof tends to stay at its original position. This tendency to continue to remain in the original position is known as the inertia. Since the walls and columns are built in it, they drag the roof along with them. Due to the inertia of structural mass, seismic forces get induced in buildings. These forces generate lateral forces on buildings in response to the displacements induced at the ground level. Intensity of seismic forces induces based on not only on the intensity of earthquake but also on the mass and stiffness of the structure.

In the past, flexible structures were thought to perform better under these seismic induced forces as they attract less seismic forces due to their flexibility. During destructive earthquakes, failure induces due to excessive displacements and storey drift, which leads to severe damage of non-structural and structural members also.

Many philosophies for earthquake resistance design have been studied and recommended by many researchers. Three basic design philosophies are aimed at achieving the following.

- Adequate stiffness of elements so that during low-intensity earthquakes, elastic response can ensure utmost protection against damage of non-structural members.
- Adequate strength since moderate earthquakes do not result in structural damage.
- Adequate ductility and capability to dissipate energy so that building can be protected to a certain extent during severe earthquakes.

Apart from seismic forces, other forces also add to the lateral loads to buildings such as wind loads, blast or explosive loads and so on. Reinforced concrete walls in buildings are the best choices to fulfil these requirements. These walls reduce storey drift and consequently reduce non-structural damage. They are very strong in in-plane stiffness and shear strength. The brittle nature of reinforced concrete walls is the main challenge. To ensure safety, many codes of practice increase the base shear coefficient. Many techniques such as base isolation emerged to overcome such effects. These reinforced concrete shear walls are effective in resisting and transferring lateral loads. They are also efficient both in construction cost and suitable in minimizing earthquake damage of structural system. Considerable development in the design of RC walls for construction of buildings in the past few decades has been observed. Figure 1.1 shows a typical shear wall with boundary element.

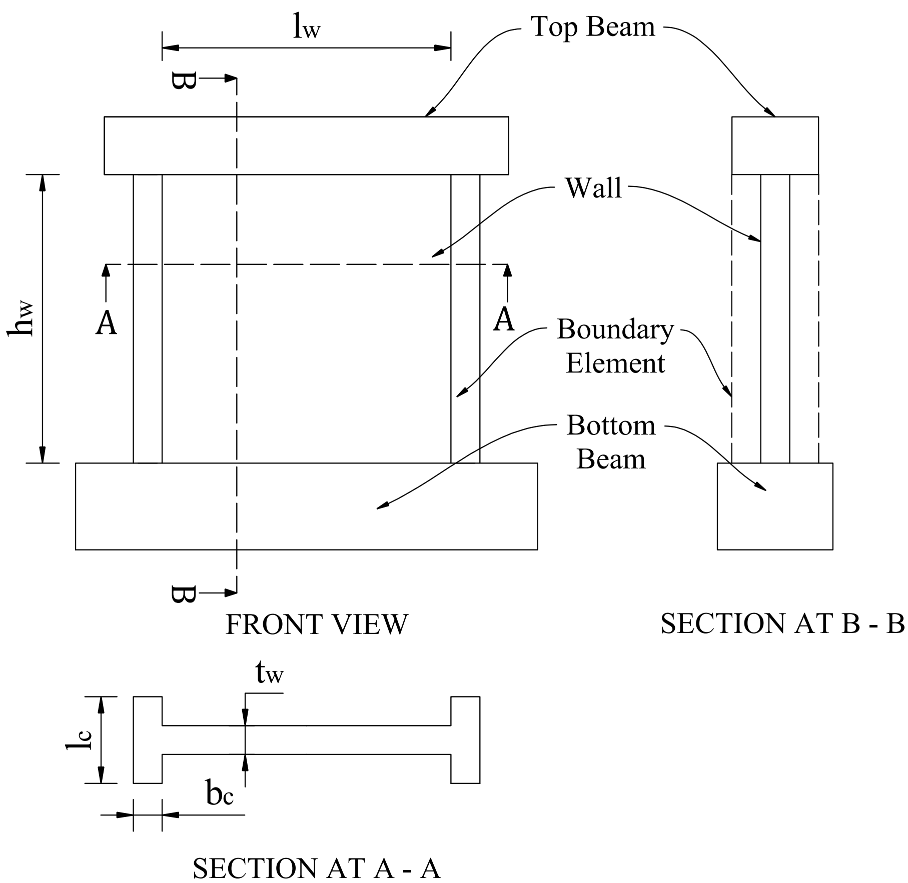

Fig. 1.1 Typical Shear wall

Behaviour of shear walls is primarily influenced by the ratio of applied moment-to-applied shear force, also called the aspect ratio (AR), ratio of height-to-length of the wall. Shear walls can resist lateral loads either by cantilever action as in slender walls or high-rise walls and by truss action in squat walls or low-rise walls. The slender walls predominantly fail in flexure, while the squat walls fail in shear.

Local buckling of web of walls can be minimized by providing minimum web thickness as recommended by researchers and codes of practices. Proper detailing and confinement can avoid in-plane splitting failure of walls. The studies show that the aspect ratio, wall thickness, reinforcement ratios, yield strength of steel and compressive of concrete, boundary elements and applied axial stress significantly influence the shear strength of shear walls. Importantly, the above parameters affect the behaviour of RC shear walls in terms of parameters such as ductility, stiffness degradation, energy dissipation, crack patterns and modes of failure. Using various software, many researchers carried out numerical investigations on reinforced concrete walls through various modelling approaches including finite element analysis, fibre analysis, lumped plasticity, multi-axial spring models etc.

Practically, openings such as doors, windows and other functional openings in shear walls are commonly accommodated. These walls with discontinuities need investigation for assessment of structural strength. Seismic response is significantly affected by size of openings and their location in the walls. Hence, research on the behaviour and strengthening of shear walls with openings is an important issue. The information on this aspect is still volatile, which needs more experimental and numerical studies. Also, very few studies have been carried out on strengthening of walls with openings.

1.2 DEVELOPMENT OF STRUCTURAL SEISMIC SYSTEM (FEMA 454)

Design of any building should ensure safety against earthquake forces. During the past 100 years, seismic design philosophy and details progressed from simply considering earthquakes to be similar to wind loads to a sophisticated understanding of the phenomenon of earth-shaking that induces in a building. On 18th April 1906, an earthquake struck along the coast of Northern California with an estimated moment magnitude of 7.8 and maximum Mercalli intensity of XI (*Extreme*). This earthquake is popularly known as the 1906 San Francisco Earthquake. After the San Francisco earthquake, concepts of building dynamic response gained interest. Hence, structural seismic system development can be divided into Pre 1906 San Francisco Earthquake, Early (1906–1945), Middle (1945–1960), Mature (1960–1985) and Creative (1985–Present) stages.

a. Pre 1906 San Francisco Earthquake

Before 1906, all residential buildings of low storey were constructed with light-frame wood with brick masonry bearing walls or wood-framed floors and roofs. In 1906, severe shaking lasted for 45 seconds in San Francisco which is also called the 1906 San Francisco Earthquake. Figure 1.2 shows the damage caused in San Francisco due to earthquake followed by fire accident. As a result, the earthquake damage tends to be more severe in the areas of soft ground. It is very clear after the 1906 San Francisco earthquake that the building damage is in relation to the ground conditions.

Fig. 1.2 San Francisco Earthquake damage, 1906

(Courtesy: Encyclopædia Britannica, Photo: Arnold Genthe)

In the aftermath of the San Francisco earthquake, awareness on seismic risk increased among engineers resulting in voluntary efforts on seismic-resistant design. The tall buildings which utilized steel-frame to support gravity loads performed well during the earthquake. General conclusion after the 1906 earthquake was that steel-framed building designed to support gravity loads and surrounded with well-proportioned anchored brick walls resist earthquake forces as the best structural system.

b. The Early Stage (1906 – 1940)

After the 1906 earthquake, a variety of new structural concepts have emerged. Brick masonry infill walls with reinforcement and steel frames were designed to carry lateral loads using knee bracing, belt trusses at floors to limit drift, rigid-frame moment connections using column wind-gussets, or top and bottom girder flange connections to columns. Concrete frame buildings together with shear walls emerged for industrial and lower height commercial buildings. Concrete slowly replaced with brick as a structural cladding after the 1930s and buildings commonly used light steel frame for floor support with a complete perimeter concrete wall system for lateral loads.

c. The Middle Stage (1945 – 1960)

After World War II, construction of large projects started again. New ideas were common and some refinement of framing systems for tall buildings was adopted. The transition from riveted connections to high-strength bolted joints observed in the 1950s. By 1960, another steel connection was that girder flanges welded directly to columns to create moment frame connections.

d. The Mature Stage (1960 – 1985)

The period from 1960 to 1985 represents the mature stage. In this period, plenty of projects were completed using the concepts of both ductile moment frames and concrete shear walls. Structural engineers accepted validity of ductile concrete-moment frames, ductile shear walls and ductile welded steel moment frames as the primary structural system for resisting lateral loads. Primary design activity at this stage became optimization of building systems using minimum requirements of buildings through code of practices.

e. The Creative Stage (1985 – Present)

The Loma Prieta earthquake occurred in California's Central Coast on October 17th, 1989 and the name Loma Prieta Peak is in the Santa Cruz Mountains, which lies just to the east of the main shock epicentre. Around 70 – 80 buildings were collapsed completely and also leads to lots of damage to other structures also.

Fig. 1.3 Loma Prieta earthquake, 1989

(Courtesy: Bay Area News Group, October 17, 2018)

Figure 1.3 shows the damage created at Loma Prieta due to earthquake. The 1994 Northridge earthquake occurred in San Fernando Valley region of the County of Los Angeles on January 17, 1994. Figure 1.4 shows the damage caused at California State due to earthquake. Due to the known seismic activity in California, the area building codes recommend that buildings to incorporate structural design are intended to withstand the earthquake effects. However, damage revealed that some structural specifications did not perform as intended.

Fig. 1.4 Northridge earthquake, 1994

(Source: USGS archive)

A colour-tagged structure is a structure in the United States which has been classified by colour to represent the severity of damage or overall condition of building. A "red-tagged" structure has been severely damaged to a degree that structure is too dangerous to inhabit. Similarly, a structure is "yellow-tagged", if it has been moderately damaged to the degree that its habitability is limited. A "green-tagged" structure may mean that the building is either undamaged or suffered slight damage. Many buildings are red-tagged after this earthquake even they are designed and constructed as per building code recommendations.

After the damage caused by the 1989 Loma Prieta earthquake (San Francisco Bay Area) and the 1994 Northridge earthquake (Los Angeles), .structural engineering profession began to ask itself about the actual earthquake performance. This investigative process defined many issues and one of the most important was the dissipation of seismic energy by building structure. Pursuits of this issue lead engineers to consideration of dual systems, unbounded steel bracing systems, shear wall systems and seismic isolation systems to limit the lateral displacement and energy dissipation.

This is the brief history of shear walls which become inevitable structural element in building structure nowadays.

1.3 NOMENCLATURE AND NOTATIONS

As understood, a huge horizontal shear force produces due to an earthquake and inertia of the building. This is called base shear force. A large portion of this base shear force or almost the whole is assigned to reinforced concrete walls; hence the name shear walls. The shear wall is intended for both flexure and shear strength of the building. The nomenclature arises from the force to be resisted, not from the nature and behaviour of the wall. To avoid confusion, several researchers and codes of practice use the nomenclature “Structural Wall” instead of “Shear Wall”. In this study, nomenclature “Shear Wall” has been used throughout.

Research on shear walls started in the 1950s in Japan and followed by all other parts of the world till now. Notations used by researchers and codes of practice are not uniform. Notations as per Figure 1.5 have been used throughout this study.

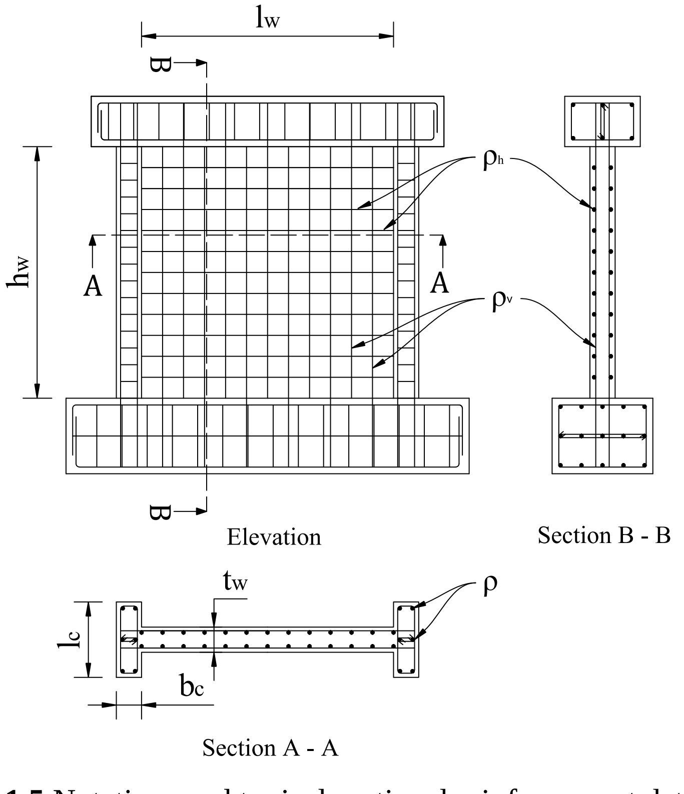

Fig. 1.5 Notations and typical sectional reinforcement details

Where, l_w - Length of shear wall; h_w - Height of shear wall;

t_w - Thickness of the wall; l_c - Length of boundary element;

b_c - Breadth of boundary element; ρ_h - Horizontal web reinforcement ratio;

ρ_v - Vertical web reinforcement ratio;

ρ - Reinforcement ratio of boundary element.

1.4 SHEAR WALL PARAMETERS

The behaviour of shear wall is different from that of the other structural elements such as beams and columns. This is due to the effect of geometric parameters, boundary conditions and loading types. The effects of these parameters on behaviour of shear wall are well studied by many researchers through experiments, which are explained in the next chapter. Here are some brief introductions for parameters of a shear wall that affect its behaviour.

a) Aspect Ratio

The governing parameter for structural response of low-rise wall is its aspect ratio. The aspect ratio is defined as the ratio of height-to-length of wall (h_w/l_w). Based on the behaviour, the shear walls can be classified as,

- Squat shear walls or Low-rise shear walls
- Slender shear walls or High-rise shear walls

Squat shear walls are the walls that predominantly fail in shear. Slender shear walls are the walls that predominantly fail in flexure. There is no definite demarcation line for dividing the walls as the squat or the slender. The aspect ratio is only the governing parameter. The experimental results on shear walls indicated that the aspect ratio greater than two, the wall behaviour is controlled by flexure (slender walls), whereas the aspect ratio less than two, it is controlled by shear (squat walls). High shear force is associated with the squat walls. Failure modes of squat shear walls include inclined web cracking, sliding along wall base and crushing of web concrete, whereas failure modes in slender walls due to development of horizontal cracks on low hinging region and yielding of vertical reinforcement. As shown in Figure 1.6, behaviour of shear wall changes from shear to flexure mode as aspect ratio increases.

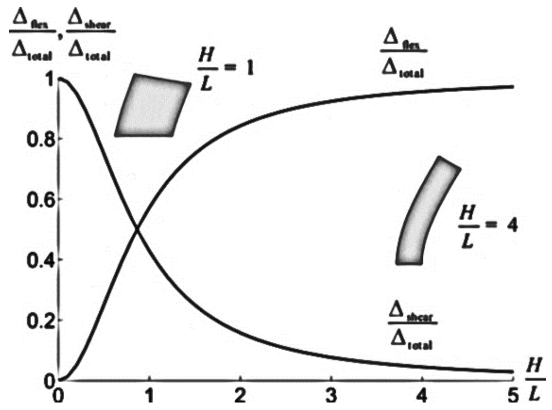

Fig. 1.**6** Relative contribution of shear and flexure deformation to total deformation (Neuenhofer, 2006)

b) Axial Compression

Gravity loads on walls increase strength and decrease deformations. Studies show that presence of moderate axial compressive load on a wall that is loaded monotonically or under reversed cyclic loading results in an increase in its flexural capacity and shear strength. Figure1.7 shows axial compressive load acting on shear wall along with lateral cyclic loading.

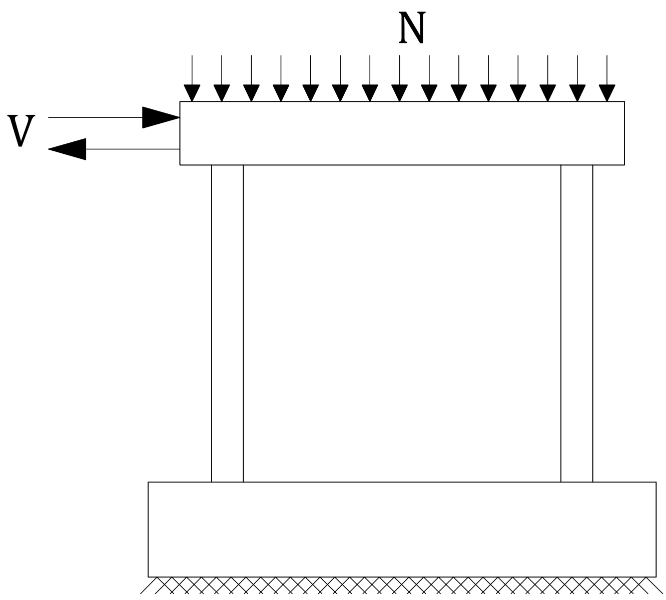

Fig. 1.7 Axial Compressive load on Shear Wall

c) Horizontal and Vertical Reinforcement

Horizontal and vertical web reinforcement, called the transverse and the longitudinal web reinforcement as synonym has significant contribution to shear wall behaviour and contribute significantly to the shear resistance. Lateral load applied on the wall will be transferred as an inclined strut action mostly in the case of squat walls. The force on an inclined strut can be resolved as vertical and horizontal forces. Horizontal bars are responsible for resisting the shear forces along the longitudinal axis i.e. vertical force. Similarly, the vertical bars are responsible for resisting the shear forces along the vertical axis i.e. horizontal force. Therefore, the amount and distribution of the horizontal and vertical web reinforcement are major parameters affecting the behaviour of shear walls. Arrangement of the horizontal and vertical web reinforcement can govern width, spacing and distribution of cracks. Many studies have been carried out for the past seven decades and many contradictory conclusions specified by researchers regarding the effect of the horizontal and vertical reinforcement. This has been explained in detail in the next chapter.

d) Top and Bottom Beam

Lateral loads on buildings due to seismic induced inertia forces act at the floor levels where there is a huge concentration of mass present. In general, load is induced along the joint between floor beam and wall or top beam and wall, as a line load. This load is transferred to the floor or foundation through diagonal compressive strut action, kinking of vertical bars at diagonal crack planes and aggregate interlock across crack surface. The top and bottom beams are usually stronger and stiffer than the wall. The top and bottom beams act like huge stirrups and restricts advancement of diagonal cracks from reaching the successive wall panels.

e) Concrete Strength

In the case of shear walls, workability becomes an important issue as concreting is done to a thin and high portion. We cannot compromise on either workability of concrete or its strength. Now much advancement has been made in construction techniques to balance the workability and strength of concrete. Strength of concrete in shear wall improves extreme fibre compression, web crushing and shear strength of concrete. A low strength results in low deformation capacity of wall.

f) Construction Joints

Construction joints between wall and beams in low-rise shear walls may become weak under inelastic load reversals during earthquakes or under cyclic loading during experimental studies. Figure1.8 shows sliding shear acting between top beam and wall and between wall and bottom beam. They may fail in shear due to sliding along construction joint before attaining full shear capacity. Therefore, construction joint is another major parameter that affects behaviour of shear walls. This problem plays a dominant role in walls with low aspect ratios.

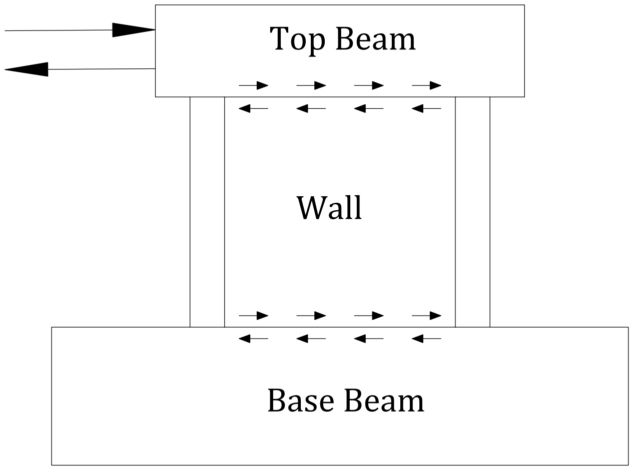

Fig. 1.8 Sliding at the construction joints in shear wall

g) Boundary elements

When wall is placed monolithically between two columns, it results in barbell shape. Columns represent boundary elements and take part an important role in shear wall behaviour. Presence of boundary element has much important role in slender shear walls. Behaviour of a short-flanged shear wall is more complex than a rectangular wall. Even a small amount of vertical reinforcement in flanges results in high flexural capacity in case of slender walls. Low-rise walls with boundary elements can support significant horizontal loads even after web has been destroyed. In general, a wall with a barbell or flanged cross-sections has a significant role in shear wall behaviour than a rectangular wall with same amount of web reinforcement. Vertical reinforcement in flange helps in lateral confining to concrete in boundary element which in turn increases crushing strain of concrete.

h) Diagonal Reinforcement

Use of diagonal reinforcement in web of walls reduces shear distortion and resists sliding shear especially in squat shear walls. It also contributes to increasing shear strength and energy dissipation capacity. Even though, this type of reinforcement arrangement is not commonly practised and recommended in codes of practices for shear walls due to some construction complications.

i) Openings in Shear wall

Presence of openings in shear walls leads the shear wall highly susceptible to earthquake loading conditions. To fulfil functional requirements such as windows, doors etc., shear wall may have openings. Behaviour of shear walls is highly affected by openings as there is a reduction in concrete area and discontinuity in reinforcement. Size and location of openings are major parameters to be considered, which in turn decides shear wall behaviour. Depending on construction, opening in shear wall is classified as,

- Existing opening
- Existing but enlarged opening
- Newly created opening

In most of cases, shear walls contain openings included in the design before construction. But in certain cases, some remodelling of existing structure may be required to fulfil functional requirements. On such occasions, demand for enlarging the existing opening or introducing new opening may arise. It is not a simple issue as importance of shear walls are well known. These openings disturb flow of forces in the wall. Analysis of shear walls with openings is very complex as stress concentration takes place near openings of wall.

1.5 MECHANISM OF SHEAR RESISTANCE IN SQUAT SHEAR WALLS

Mechanism of base shear resistance in squat wall and slender wall significantly differs. Moreover, squat wall behaviour is often correlated with deep beams as both are shear dominant in nature. Major difference between the shear wall and the deep beam comes from their boundary conditions and imposed loading on them. Apart from the lateral load, axial load in shear wall plays a major role on its behaviour. There are other significant differences between nature of deep beams and shear walls. Therefore, extensive research conducted on deep beams cannot be used directly to explain mechanism of shear resistance in low-rise walls.

Squat shear wall resists applied shear through diagonal tension and diagonal compression. Since shear capacity of concrete along a horizontal plane is much higher than diagonal tension capacity of concrete, formation of an inclined crack due to diagonal tension precede shear failure along a horizontal plane. Concrete owns responsibility of shear resistance until cracking. Beyond formation of diagonal cracks, however, mechanism of shear resistance depends on reinforcement provided in the wall. A significant portion of base shear force continues to be transmitted to the foundation or storey below through diagonal compression action. This diagonal compression is resisted by diagonal concrete struts that are formed between inclined tension cracks. Diagonal struts can be sustained only if diagonal tension is resisted by wall reinforcement during further loading and reversal loading conditions. Wall reinforcement helps in controlling crack widths, which will resist additional shear along cracked surfaces through aggregate interlock mechanism. Under cyclic loading, however, these cracks continue to be in opening and closing mode, resulting in crushing of concrete along with crack interface. Vertical reinforcement crossing inclined and horizontal cracks provide additional shear resistance through dowel action. This dowel action at many times promotes direct shear action as a potentially critical mode of behaviour, producing shear sliding along horizontal crack. Different mechanisms are involved in resistance of base shear force by squat shear walls. This section provides mechanisms involved in squat shear walls.

1.5.1 Diagonal Compression Strut Mechanism

Lateral shear force is transmitted to foundation or bottom storey through diagonal compression struts between cracks as shown in Figure 1.9. Diagonal struts can be developed only if the truss mechanism is formed. This force can be resolved into vertical and horizontal components and are equilibrated by reinforcements in wall.

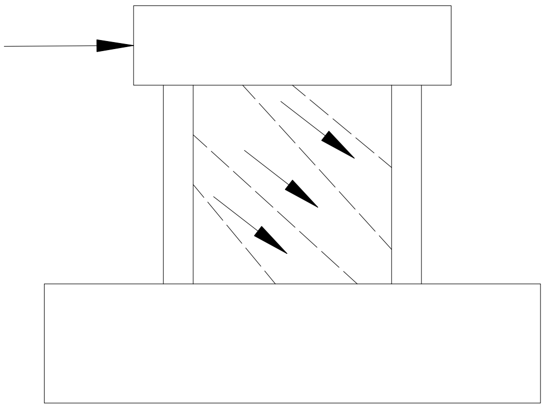

Fig. 1.9 Diagonal Compression Strut

Inclination of struts is mainly based on aspect ratio of wall. Usually, these diagonal struts are formed between diagonal corners of wall. This mechanism is almost similar to that of deep beams as truss mechanism is also developed. This mechanism is almost absent in case of slender shear walls.

1.5.2 Aggregate interlock Mechanism

Cracks formed in reinforced concrete elements are usually rough and irregular due to heterogeneity nature of concrete. Each of cracks faces contains coarse aggregate particles. On further loading, two faces of cracked surfaces will move relative to another and coarse aggregate on each face of crack are brought together. Bearing and friction action between aggregate particles resist and restrict further movement of two surfaces. This action is referred to as aggregate interlock.

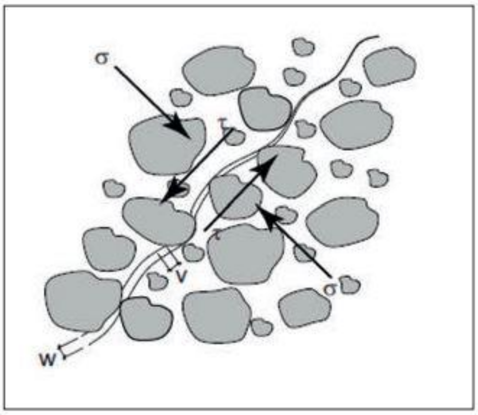

Fig. 1.10 Aggregate Interlock Mechanism

(Source: fib Bulletin No. 40)

This mechanism provides significant shear resistance, adding to other resisting mechanisms. Crack width can be controlled by providing adequate wall reinforcement and also vertical load coming from above floors. This leads to transfer of a significant amount of shear forces across crack interface and consequently, aggregate interlock mechanism comes into major action. Load reversals or cyclic loading in shear walls is also another important factor that aggravates aggregate interlock mechanism. Under inelastic load cycles, cracked surfaces slide against each other and subsequently, aggregate interlock mechanism develops.

1.5.3 Shear Friction Mechanism

Shear force resisted by friction between two cracked surfaces is the shear friction mechanism. Shear friction is mainly based on coefficient of friction between the cracked surfaces and normal force acts on this surface. This mechanism takes place when the crack width is small and crack surfaces are in contact as much as possible. Figure 1.11 shows the shear friction mechanism. Reinforcement in web and axial compressive load from the above storey helps in controlling crack width in the shear wall. This helps in enhancing mechanism of shear friction. Axial compression force from above storeys helps in increasing the shear resistance across the cracks as a portion of this force acts as normal compressive force against crack surfaces. This may cause concrete to separate slightly into two pieces. If reinforcement is present normal to the crack, slippage, and subsequent separation along the crack experience tension. This enhances the shear resistance due to friction.

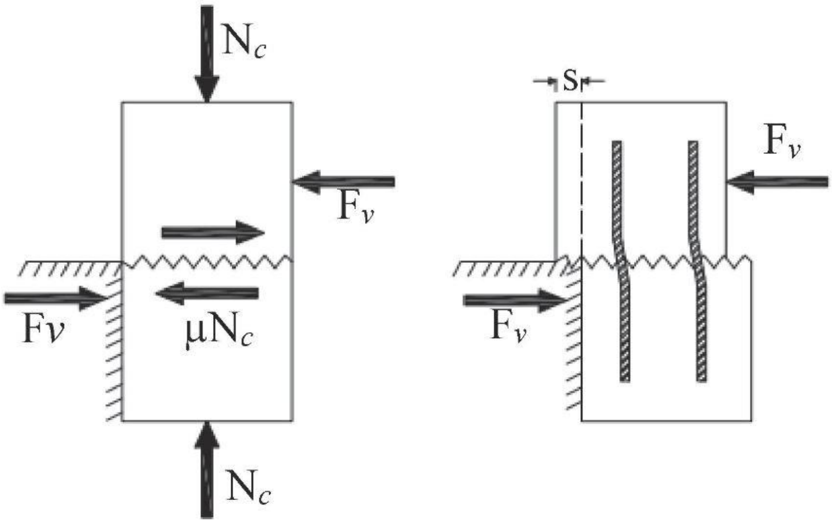

Fig. 1.11 Shear Friction Mechanism

*(**Source:** https://doi.org/10.1016/j.engstruct.2019.110122)*

1.5.4 Dowel Mechanism

A significant portion of total applied shear is resisted by wall reinforcement crossing the shear transfer planes. The shear resistance of the bars across the shear plane can be developed by one of the following three mechanisms (*Park and Pauley, 1975*).

a) Flexural deformation of reinforcement

b) Kinking of reinforcement

c) Shear stress across the bars

a. Flexural deformation of reinforcement

Vertical reinforcement crossing a shear transfer plane deforms under horizontal shear. This deflected shape is associated with bending moments imposed on reinforcement. This mechanism is utilized when full bearing exists between vertical bars and surrounding concrete. Under cyclic loading and load reversals in shear walls, concrete surrounding the vertical bars gets crushed at interface leading to loss of bearing. On further loading, reinforcement is forced to deform excessively. This leads to another mechanism called kinking of reinforcement.

b. Kinking of reinforcement

This mechanism is a major component of dowel resistance in low-rise wall under load reversals or cyclic loadings. Shear resistance provided by the kinking of reinforcement is mostly developed in the vertical reinforcement as the wall is loaded with horizontal shear force. Figure 1.12 shows the dowel action of reinforcing bars.

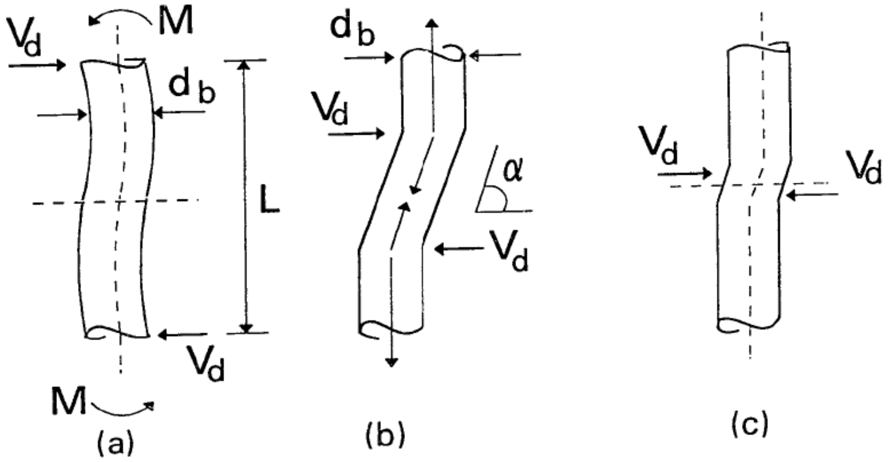

Fig. 1.12 Dowel Mechanism of reinforcement (a) Flexural Deformation, (b) Kinking, (c) Shear resistance

*(**Source**: http://hdl.handle.net/10393/9828)*

c. Shear resistance across bars

This type of dowel action is not seen often and significant as compared to the previous two types. Some amount of shear is resisted through the sheared area of reinforcement, perpendicular to the applied force. In case of small-size bars across the shear transfer planes, they may fail in shear before developing other modes of dowel action.

1.6 FAILURE MODES OF SQUAT SHEAR WALLS

Squat shear walls in a building eventually fail by diagonal tension, diagonal compression and sliding shear. In case of experimental studies, these walls may also experience uplift and overturning due to improper locking of wall at its base. With proper locking, squat shear wall will fail by one of the following modes.

1.6.1 Diagonal tension failure

This type of failure is common in squat shear walls with insufficient wall reinforcement. When horizontal shear force acts on squat shear wall, diagonal cracks are developed due to formation of truss mechanism. Reinforcement crossing these cracks provides resistance against diagonal tension on further loading. If reinforcement provided is not sufficient to resist this diagonal tension, it yields and results in diagonal tension failure. Shear walls continue resisting higher shear force with little reinforcement, as top and bottom beams, boundary elements help in controlling the diagonal cracking. This helps shear walls to observe failure at increased load. Figure 1.13 shows typical diagonal tension failure of shear wall.

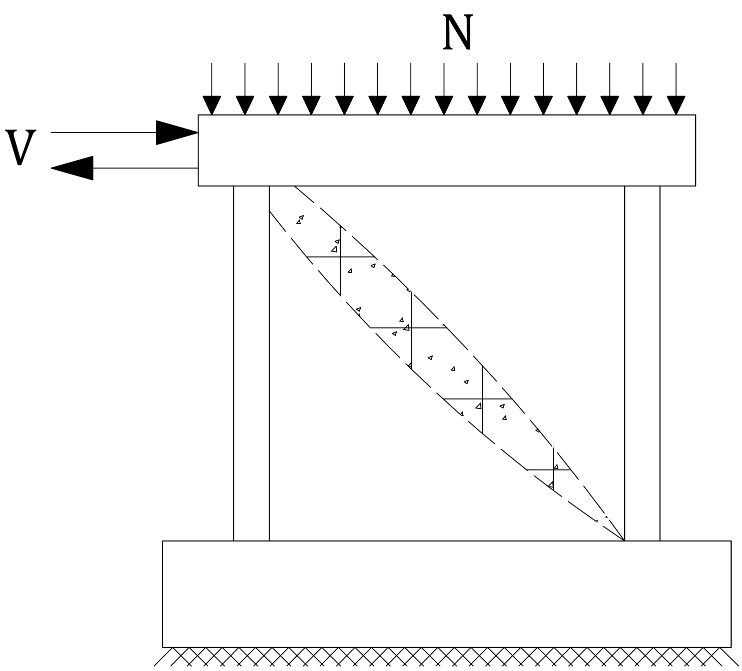

Fig. 1.13 Diagonal Tension Failure

1.6.2 Diagonal Compression Failure

Diagonal tension failure is controlled by providing adequate reinforcement in shear wall. This increases the force acting on diagonal struts as diagonal tension is prevented. Upon increasing compressive force on diagonal strut, this may lead to exceeding compression capacity of concrete. This leads to crushing of concrete. This is called diagonal compression failure. This mode of failure causes dramatic and irrecoverable loss of strength and hence highly undesirable failure mode. Figure 1.14 shows diagonal compression failure of shear wall.

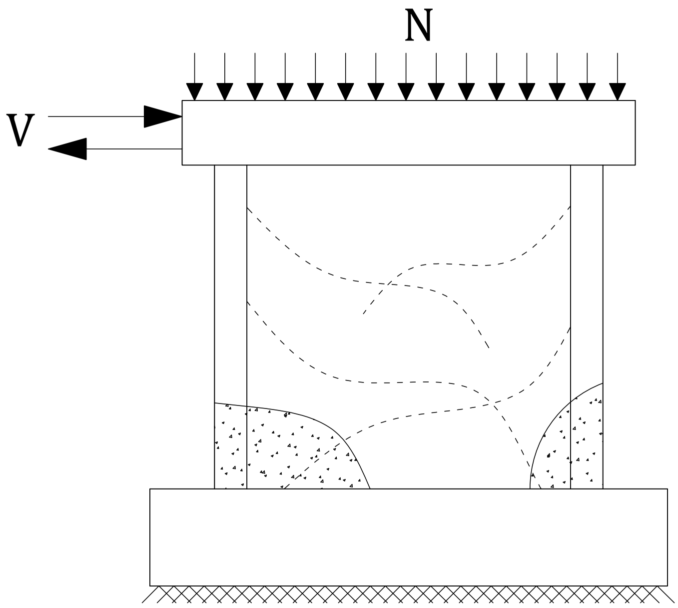

Fig. 1.14 Diagonal Compression Failure

1.6.3 Sliding shear failure

Upon avoiding diagonal tension and diagonal compression failure by providing sufficient wall reinforcement and a smaller amount of normal compressive stress, sliding shear failure may occur. Sliding shear results in sliding displacement along construction joint at the base. This sliding displacement is responsible for a considerable reduction in stiffness and pinching of hysteresis loops, reducing energy dissipation capacity of wall. Figure 1.15 shows a typical sliding shear failure.

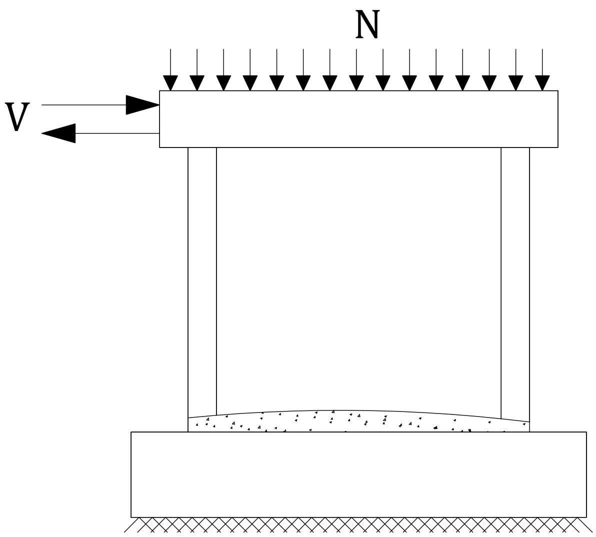

Fig. 1.15 Sliding Shear Failure

Most of squat shear walls develop significant shear sliding failure. Vertical reinforcement crossing this construction joint at the base of wall should remain elastic to avoid this failure. Simple idea is to provide additional vertical reinforcement at base of wall to avoid this failure.

1.7 MOTIVATION FOR THE PRESENT STUDY

Due to high population and infrastructures development, high-rise building constructions are inevitable. Such buildings are vulnerable for earthquake loading. So, there is a need for good lateral force resisting structural system for such buildings. Shear walls are inevitable and are easily adaptable lateral load resisting system in tall buildings. In the past, usage of shear wall is not appreciated in comparison with RC frames. Moreover, provision of openings in shear walls as doors and windows are unavoidable due to functional requirements of structure. Design standards therefore have to be competent enough to provide guidelines for design and construction of such shear walls. Provisions from various design standards differ at large and to some extent contradictory to each other.

From review of literature, as discussed in Chapter 2, it is evident that, research on solid shear walls through experimental studies has been carried out since early 1950s. The research work on shear walls with openings was initiated in the 1980s only. Many empirical and semi-empirical strength predictions have been proposed and in use. Behaviour of shear wall with openings is not explored well enough to draw guidelines for practical design in the industry. These needs performing numerous experimental and numerical studies contributing to the available data. Such a limited study on shear walls and extensive usage of shear walls in practice is motivation for this research. This study attempts to attain an understanding of the available experimental data till date and utilization of available new material like FRC to improve the behaviour of shear wall with opening.

1.8 OBJECTIVE AND SCOPE

Objective of research presented in this thesis is to study behaviour of Reinforced Concrete Squat Shear walls with and without discontinuities.

The Scope of work includes,

a) Statistical evaluation of shear strength from selected equations from the codes of practice and literature using selected experimental database from the literature to identify the best predictive equation for shear strength of shear wall.

b) Examining mode of failure, Stiffness degradation, Energy dissipation and Crack propagation of walls with and without opening using experimental studies.

c) Proposing strengthening methodologies for shear walls with openings.

d) Numerical studies on walls with and without openings to validate experimental results.

Scope of work is limited to,

a) Squat shear wall whose height is less than twice its length.

b) Single opening in the wall.

c) No eccentricity opening is considered.

d) Existing opening i.e. the opening is not newly created or enlarged.

1.9 ORGANIZATION OF THESIS

The thesis is written in seven chapters and is organized as follows.

Chapter 1 depicts a detailed introduction about the shear walls and their development over 100 years. It also includes description of parameters of shear wall, various shear resisting mechanisms by shear wall, failure modes of shear wall, motivation for present study, objective and scope of work.

Chapter 2 deals with literature review on squat shear walls. Detailed review of literature includes shear walls without opening, with opening and various recommendations provided in the codes of practice. Identification of research issues in the present study is identified.

Chapter 3 presents statistical assessment of shear strength of Reinforced Concrete squat shear walls. Sixteen empirical, semi-empirical and derived equations reported in the literature and codes of practice for predicting the shear strength of RC walls evaluated using 333 experimental data collected. Using various statistical tools, these shear strength equations are evaluated through many parametric influencing shear strength of wall by various researchers.

Chapter 4 describes details of experimental programme to accomplish the objectives of this study. In this Chapter, details on geometry of walls, design and detailing of top and bottom beams, construction, test set-up and loading protocol are described in detail. Reinforced concrete walls with and without opening were constructed and tested.

Chapter 5 discusses experimental study carried out on shear walls with and without openings to accomplish the objective. Test series includes five one-third scaled reinforced concrete squat shear walls includes without opening (SW-1.0-00-00), with concentric window opening (SW-1.0-CW-00), FRC with concentric window opening (SW-1.0-CW-FRC), with concentric door opening (SW-1.0-CD-00) and FRC with concentric door opening (SW-1.0-CD-FRC). Experimental investigations have been carried out to study the seismic performance including load-displacement response, crack and failure patterns, shear strength, ductility, shear strength degradation, lateral stiffness degradation and energy dissipation response. All these results are discussed in detail for all the five walls and also compared with each other for understanding.

Chapter 6 presents nonlinear finite element analysis (NFEA) to validate the experimental results on shear wall. With development of sophisticated numerical tools for analysis like finite element analysis programme, it is possible to model and analyse the complex reinforced concrete structures. In the present study, finite element package ANSYS 15.0 is used for modelling and analysis. The package delivers greater accuracy, fidelity, higher productivity and more computational power. Element type, Mesh convergence study, loading and boundary conditions, crack patterns and stress distribution for walls are described in detail.

Chapter 7 summarizes major conclusions drawn from the study. Recommendations for future research are also given in this chapter.

CHAPTER 2

LITERATURE REVIEW

2.1 GENERAL

In this chapter, studies carried out on shear walls with and without opening are summarised. Research on shear walls started in 1950s in Japan and US. Though it started in 1950s, many research investigations were undertaken in 1970s and later. Over the past five decades, many experimental studies reported on behaviour of shear wall by simulating monotonic and cyclic loading. This chapter deals with review on shear wall without and with opening and recommendations by important codes of practice. Behaviour of RC walls primarily depends on ratio of applied moment-to-applied shear force, which is linearly related to aspect ratio (A/R), defined as ratio of height-to-length of wall. Walls act as cantilevers similar to slender or high-rise walls with A/R ratio greater than 2.0; whereas truss action prevails in squat/short or low-rise walls with A/R ratio less than 2.0. Slender walls predominantly fail in flexure mode, while squat walls fail in shear mode. In order to remain within scope of work, reviews are mostly dealt with on squat shear walls.

2.2 EXPERIMENTAL STUDIES ON SHEAR WALLS WITHOUT OPENING

Experimental investigations on behaviour of RC walls under cyclic loading first carried out by *Badra et al. (1977)*. Prior to 1970s, research in this area is limited and efforts mainly carried out on shear in RC members. Behaviour of squat shear walls was compared with that of deep beams, which is considerably different in terms of transfer of load, load resisting and failure mechanism. Therefore, research findings from deep beam testing are not directly applicable to shear wall. After this observation, much attention has been given to shear wall investigations. The pioneers in research on RC walls are *Galletly (1952)* and *Benjamin et al. (1953)* who tested squat shear walls under monotonic loading. Experimental work carried out on shear walls is outlined in this section. Table 2.1 lists contributions by researchers around the globe on squat shear walls. Results and conclusions drawn from studies are discussed in following sections outlining all parameters of shear walls.

Table 2.1 Authors and their Contributions

S. No.	Literature	Work Contribution
1	*Galletly (1952)*	Tested six shear walls were tested with no axial load. The parameters varied are horizontal and vertical reinforcement ratios (0.79% & 1.57%) and reinforcement in boundary elements (2.76%, 4.91% & 5.51%). This is the first test conducted on shear wall with monotonic loading.
2	*Benjamin et al. (1953)*	Tested thirty one shear wall with no axial load. The parameters varied are horizontal and vertical reinforcement ratio (0.25%, 0.50% & 1.00%) and reinforcement in boundary element (1.3% to 5%).
3	*Antebi et al. (1960)*	Tested sixteen one-third shear wall with no axial load. The parameters varied are aspect ratio (0.64 & 0.34) and reinforcement ratios (0.25% & 0.5%)
4	*Alexander et al. (1973)*	Tested five half scaled shear walls. Two walls tested without axial load and three walls with axial load varying aspect ratio (0.5, 0.5 & 1.5).
5	*Hirosawa (1975)*	Tested twenty two shear walls by varying the parameters boundary element reinforcement (0.84% to 9.91%), horizontal reinforcement (0.26% to 1.28%) and axial load (ALR as 5% to 20%).
6	*Barda et al. (1977)*	Tested eight one third scaled squat shear walls were tested without axial load. The parameters varied are aspect ratio (0.25, 0.5 & 1) and web vertical reinforcement ratio (0.75%, 1.00% & 1.25%).
7	*Cardenas et al. (1978)*	Tested seven large rectangular shear walls are tested by changing both vertical and horizontal reinforcement (0%, 0.75%, 1.5% & 3%)
8	*Endo et al. (1980)*	Tested twenty shear walls. The parameters varied are web vertical and horizontal reinforcement (0.23%, 0.37% and 0.7%), boundary element reinforcement (0.22% to 1.02%), thickness (50 mm & 100 mm) and height of the walls (2 m & 3 m).
9	*Sugano et al. (1980)*	Tested eight shear wall with no axial load. The parameters varied are vertical and horizontal reinforcement ratio (0.33%, 0.66% & 0.77%).
-10	*Oesterle et al. (1984)*	Tested fourteen shear walls by varying the shape of the wall (rectangular and barbell), axial load (ALR - 0% to 12%),

		horizontal reinforcement ratio (0.3% to 1.4%) and confinement in boundary element (0.85% & 1.35%).
11	*Maier et al. (1985)*	Tested ten squat shear walls varying the parameters such as axial load (9% & 40%) and vertical reinforcement ratio (1%, 1.2%, 2% & 2.5%).
12	*Sato et al. (1989)*	Tested twenty two reinforced concrete shear wall by changing web reinforcement strength (300 MPa, 400 MPa & 500 MPa), concrete strength (24 MPa, 33 MPa & 42 MPa) and aspect ratio (0.6, 0.8 & 1.2).
13	*Lefas et al. (1990)*	Tested thirteen full-scale reinforced concrete shear walls. The parameters varied are aspect ratio (1 & 2) and axial load (0%, 10% & 20).
14	*Kabeasawa et al. (1993)*	Tested twenty one full scale shear walls using ultra high strength concrete (60 MPa, 90 MPa & 140 MPa) and varying reinforcement ratios (0.66%, 1.54% & 2.17%).
15	*Mo et al. (1993)*	Tested seventeen one-fifth scaled shear walls varying the parameters such as grades of steel (302 MPa and 443 MPa) and concrete (20 MPa, 30 MPa, 40 MPa and 60 MPa) and vertical reinforcement (0.58% & 0.72%).
16	*Pilakoutas at al. (1995)*	Tested six reinforced concrete squat shear walls. The parameters varied are by changing web horizontal and vertical reinforcements (0.25%, 0.5%, 0.75% & 1%).
17	*Gupta et al. (1998)*	Tested eight one-third scaled shear walls. The parameters varied are by varying axial load (ALR as 0%, 7%, 12% & 23%) and horizontal reinforcement ratio (0.52% & 1.06%).
18	*Salonikios et al. (1999)*	Tested eleven shear wall specimens. Six walls with aspect ratio of 1.5 and five walls with 1.0, detailed to the provisions of EC8. Horizontal and vertical reinforcement ratio as 0.3% and 0.6%.
19	*Jiang et al. (1999)*	Tested eleven one-third scaled shear walls varying the parameters such as aspect ratio (0.56 & 1.13) and axial load (ALR as 0%, 10%, 20% & 40%).
20	*Zhang et al. (2000)*	Tested four half scaled shear walls by changing transverse reinforcement (0.5%, 0.6% & 1%).
21	*Daniel et al. (2002)*	Two large-scale flanged concrete shear walls are tested with and without axial load (ALR as 0% & 23%). Both walls are retrofitted and tested.
22	*Pedro et al. (2002)*	Tested twenty six full scaled reinforced concrete shear walls are tested by changing aspect ratio (0.7, 1.00, 1.38 & 2.00) and

		web reinforcement ratios (0,0.13, 0.25 & 0.38)
23	*Christian et al. (2005)*	Tested four one third scaled lightly reinforced concrete shear walls for which the horizontal reinforcement (0 & 0.3%), and concrete compressive strength (20 MPa & 50 MPa) are varied.
24	*Dabbagh (2005)*	Tested six high-strength concrete shear walls was carried out by changing vertical reinforcement ratio (2.5% & 3%) and horizontal reinforcement ratio (0.45%, 0.75%, 0.94% & 1.34%).
25	*Su et al. (2007)*	Tested three half scaled shear walls by changing axial load (0.25% & 0.5%) and horizontal reinforcement (0.54% & 1.08%).
26	*Kuang et al. (2008)*	Tested eight full scaled shear walls. Web vertical Reinforcement with different reinforcement pattern (0.9% & 1%), and aspect ratios (1 & 1.5) of the walls are modified.
27	*Farvashany et al. (2008)*	Tested seven full-scale high-strength concrete shear walls by changing web vertical reinforcement (0.76% & 1.26%) and horizontal reinforcement (0.45% & 0.75%).
28	*Massone et al. (2009)*	Tested nine half-scaled squat shear walls by varying axial load (0%, 5% & 10%), aspect ratio (0.9% & 1%) and web vertical reinforcement (0.2% & 0.4%).
29	*Hong et al. (2015)*	Tested eight half-scaled shear wall models. The test parameters were the grade of horizontal reinforcement (0.25%, 0.5% & 0.68%), concrete strength (46.5 MPa & 70 MPa), web bar ratios and shape of cross section.
30	*Luna et al. (2015)*	Tested twelve squat shear walls by changing aspect ratio (0.33, 0.54 & 0.94), web reinforcement ratio (0.33%, 0.67%, 1.00% & 1.5%) and boundary element reinforcement ratio (0%, 1.5% & 2%).
31	*Yoshizaki et al. (2015)*	Tested fourteen one-third scaled squat shear wall with no axial load. The parameters varied are aspect ratio (0.72 & 1.08) and reinforcement ratios (0.2%, 0.4%, 0.8% & 1.2%).
32	*Rong et al. (2019)*	Tested half scaled eight shear walls varying freeze-thaw cycle, concrete strength (30, 40 and 50 MPa) and axial load ratio (0.1, 0.2 and 0.3).
33	*Christidis (2020)*	Tested half scaled four shear walls varying horizontal reinforcement ratio in shear wall (0.0, 2.5, 5.0, 10%)

ALR – Axial Load Ratio (Ratio of axial load to the uniaxial compressive strength of the wall)

2.2.1 Effect of Axial Load

Test results of *Alexander et al. (1973)* conclude that increase in axial stress reduces ductility and reduces stiffness degradation. Figure 2.1 shows that rapid loss of stiffness, which decreases with increase in axial stress.

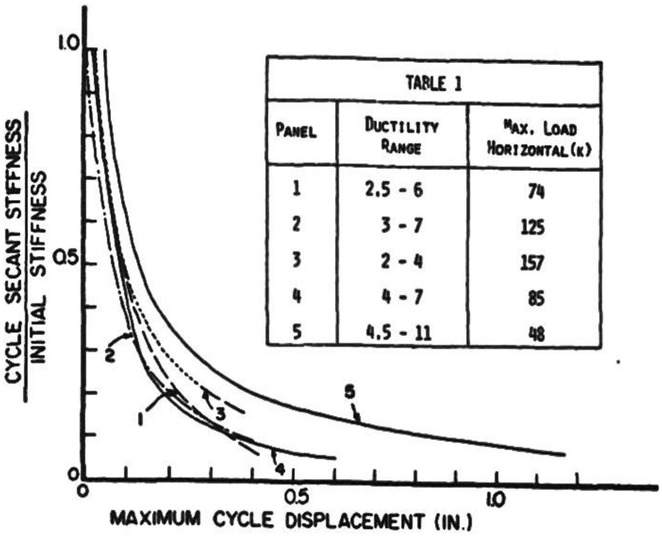

Fig. 2.1 Stiffness Degradation Curve (*Alexander et al., 1980*)

Osterley (1984) concludes that axial load is main functioning factor for web crushing of shear walls. Also found that strength limit given in ACI code is not conservative for large deflection and low axial stress. *Maier et al. (1985)* inferred from their research that axial load decreases ductility of shear walls. *Lefas et al. (1990)* recommends that axial compression reduces both horizontal and vertical displacement and plays major role in improving shear strength of shear wall as shown in Figures 2.2 and 2.3.

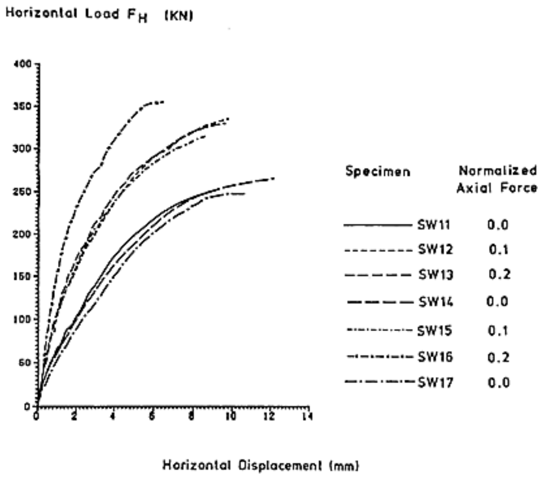

Fig. 2.2 Lateral load vs. Horizontal Displacement (*Lefas et al., 1990*)

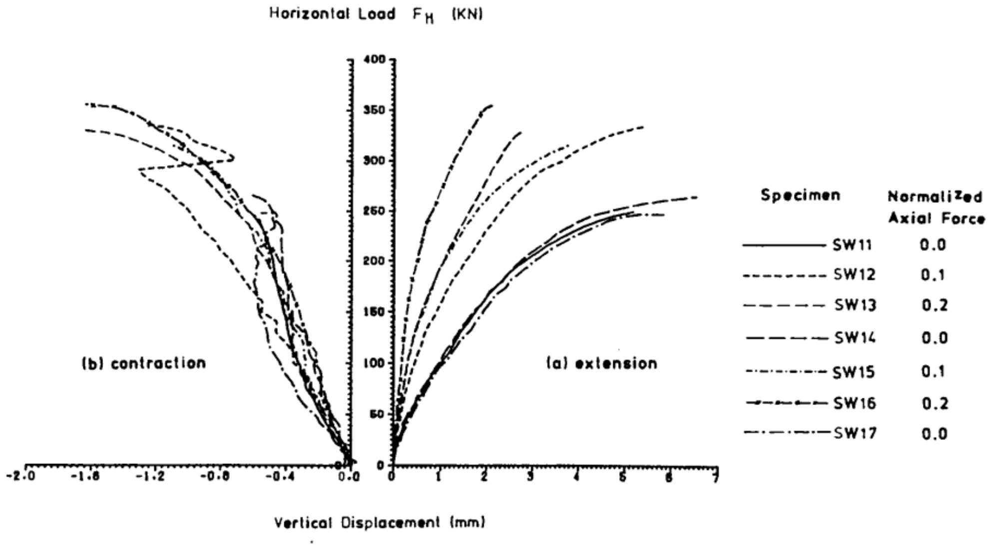

Fig. 2.3 Lateral load vs. Vertical Displacement (*Lefas et al., 1990*)

Salonikios et al. (1999) found that axial load on shear wall increases strength but reduces ductility. *Zhang et al. (2000)* reported that increase in axial-load ratio reduces ductility of walls. *Daniel et al. (2002)* reported that even light axial load has significant effect on behaviour of shear wall. *Farvashany (2004)* studied behaviour of shear wall and concluded that increase in axial load; increases shear strength but decreases ductility. *Christian et al. (2005)* reported that lower axial load does not have significant effect on behaviour of shear wall. *Dabbagh (2005)* found that axial load increases strength of wall strength but reduces ductility of walls.

Su et al. (2007) concluded that axial load has very significant effect in lowering deformability of shear wall. Figure 2.4 shows rate of axial stiffness softening given by gradient of curves. Specimens at initially higher ALR exhibited high and fast reduction as compared with smaller ratio. Reduction in ALR is an indication of drop in axial stiffness of wall. Therefore, it could be concluded that wall under high ALR experienced greater and faster deterioration of axial stiffness. *Xiang et al. (2009)* had reported from their experimental result that axial load improves energy dissipation and favours controlling pinching of hysteresis loop. *Liping et al. (2011)* found that increase in axial compression, increases shear capacity.

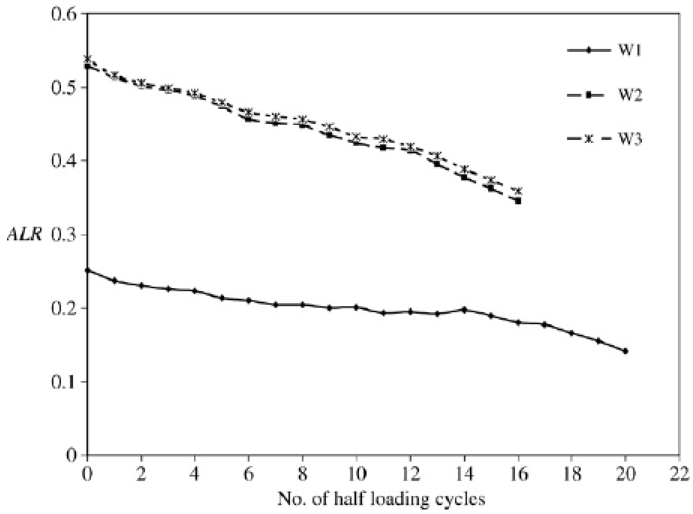

Fig. 2.4 ALR vs Number of Cycles (*Su et al., 2007*)

It has been concluded that increase in axial load on shear wall increases shear strength, decreases ductility, and stiffness degradation, improves energy dissipation capacity and also favours in controlling pinching of wall. However, *Christian et al. (2005)* reported that low axial load (below 7% ALR) does not influence behaviour of shear wall. *Rong et al. (2019)* concludes, as the axial load ratio increases, the load carrying capacity of the RC shear walls progressively increased.

2.2.2 Effect of Concrete and Strength of Reinforcement

Osterley et al. (1984) studied behaviour of shear wall and found that web crushing strength is a function of concrete strength. *Saito et al. (1989)* also found that increase in concrete strength increases shear strength of wall. *Lefas et al. (1990)* concluded that the strength and deformation capacity found to be independent of compressive strength of below 55 MPa. *Kabeyasawa et al. (1998)* suggested that high and ultra-high strength concrete can effectively be used to build ductile shear walls. However, pinching should be taken in to account during design. *Christian et al. (2005)* concluded that concrete strength plays important role in shear transfer for walls at low axial load.

It can be seen that study on effect of concrete grade on behaviour of shear wall is limited. Increase in concrete strength increases shear strength and ductility of shear walls. *Lefas et al. (1990)* suggested that strength and deformation capacity are found to be independent of strength of concrete below 55 MPa.

Studies in effect of strength of concrete are very much limited. *Hong et al. (2015)* studied shear and deformability of RC squat walls with high strength reinforcing bars of 550

MPa. Test parameters include: yield strength of horizontal reinforcement, compressive strength of concrete, web bar ratio and shape of section. Failure modes of walls with steel reinforcement with yield strength of 550 MPa are diagonal shear cracking followed by web crushing, which was similar with 420 MPa bars. Results showed that wall with moderate and high strength steel bars exhibited similar trend, but safety margin decreases with increase in strength of bars. *Rong et al. (2019)* conclude that as concrete strength increases, load carrying capacity, energy dissipation capacity, peak shear distortion and its contribution to total shear wall deformation gradually increases.

2.2.3 Effect of Horizontal Reinforcement

Barda et al. (1977) tested shear wall using cyclic loading for the first time. Failure strength of shear walls under reversed cyclic loading found approximately 10% less than that of those tested under monotonic loading. Vertical reinforcement is more effective than horizontal reinforcement. Figure 2.5 shows effect of parameters by *Badra et al. (1977).*

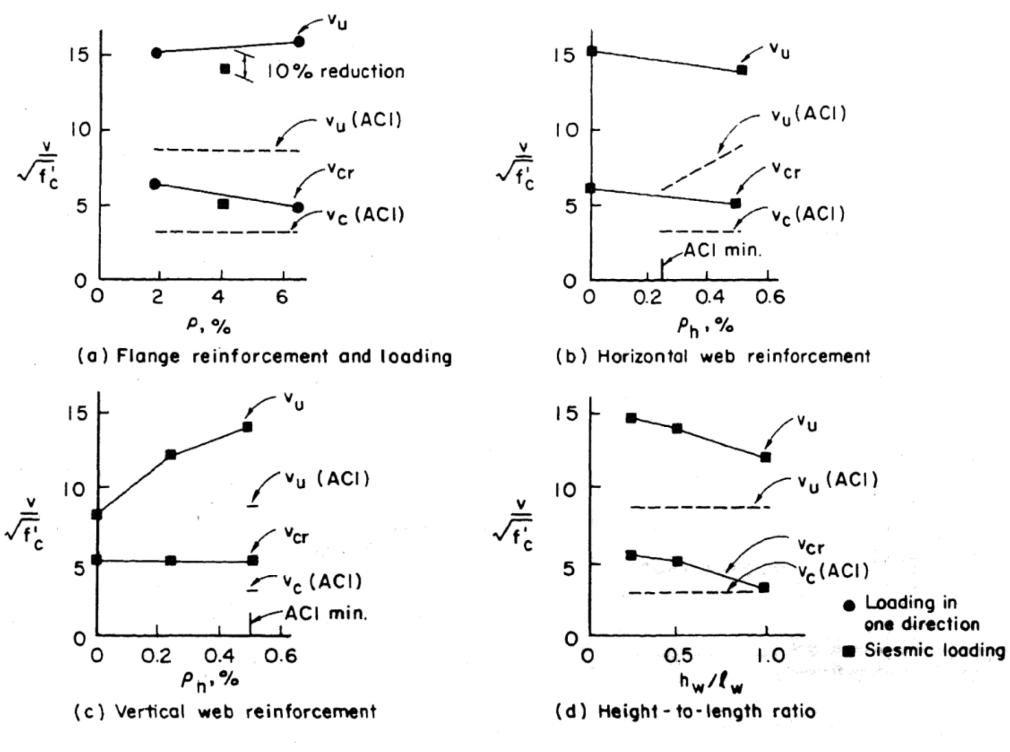

Fig. 2.5 Effect of Principle variables (*Barda et al. 1977*)

Cardenas et al. (1978) concluded that both horizontal and vertical reinforcement are effective in contributing for shear strength of squat walls. *Saito et al. (1989)* concluded that there is not much variation observed on behaviour of shear wall with horizontal reinforcement. *Lefas et al. (1990)* also concluded that horizontal reinforcement does not have significant effect on shear strength of shear wall. *Pilakoutas et al. (1995)* found from their research is that strength and deformational characteristics are not affected significantly by horizontal reinforcement in shear wall. *Pedro et al. (2002)* reported that energy absorption and dissipation of shear walls seems to be independent of both horizontal and vertical reinforcement. *Dabbagh et al. (2005)* found that increase in horizontal reinforcement ratio did not affect strength of wall considerably, but caused increase in wall deformation at failure. *Christian et al. (2005)* concluded that horizontal reinforcement does not affect behaviour of shear wall. *Su et al. (2007)* suggested that simply increasing percentage is not effective but arrangement of reinforcement influences behaviour of shear wall. *Farvashany et al. (2008)* found that horizontal steel ratio is not effective as that of vertical steel ratio. *Xiang et al. (2009)* suggested that horizontal reinforcement improves performance such as drift, ductility and energy dissipation of wall. *Luna et al. (2015)* concluded that effect of horizontal reinforcement ratio on peak shear strength of a shear-critical wall is small. *Luna et al. (2015)* concluded that effect of horizontal reinforcement is small above certain threshold value. *Christidis et al. (2020)* reported that shear walls with higher horizontal reinforcement, flexural failure dominates, whereas with inadequate reinforcement shear failure dominates.

Several research efforts have been performed on finding effect of horizontal reinforcement on behaviour of shear wall. Majority of research efforts proved that horizontal reinforcement is not effective on influencing behaviour of shear wall.

2.2.4 Effect of Vertical Reinforcement

Barda et al. (1977) suggested that vertical reinforcement is more effective than horizontal reinforcement. *Cardenas et al. (1978)* concluded that both horizontal and vertical reinforcement is effective contributing for shear strength of wall. *Wood (1990)* analysed 143 tested shear walls for evaluating effect of web and boundary reinforcement. Shear strength of walls is observed to increase with increase in amount of vertical reinforcement in web and boundary elements. *Pedro et al. (2002)* declared that behaviour of walls seems to be independent of variation of vertical reinforcement. *Dabbagh et al.* (2005) found that increase in only vertical reinforcement ratio increases wall strength. Test results indicated that an increase of 160% in longitudinal reinforcement ratio resulted in an increase of failure load of about 14%. *Farvashany et al. (2008)* concludes that increase in vertical steel ratio increases horizontal failure load.

2.2.5 Effect of Boundary Elements

Barda et al. (1977) suggested that boundary element increase ultimate load carrying capacity. *Toneo et al. (1980)* found from experimental results that boundary elements are effective to sustain horizontal loads after reaching the maximum but does not improves strength. In other words, boundary element does not improve shear strength but decreases strength degradation. Figure 2.6 shows improvement in shear strength of wall due to boundary elements.

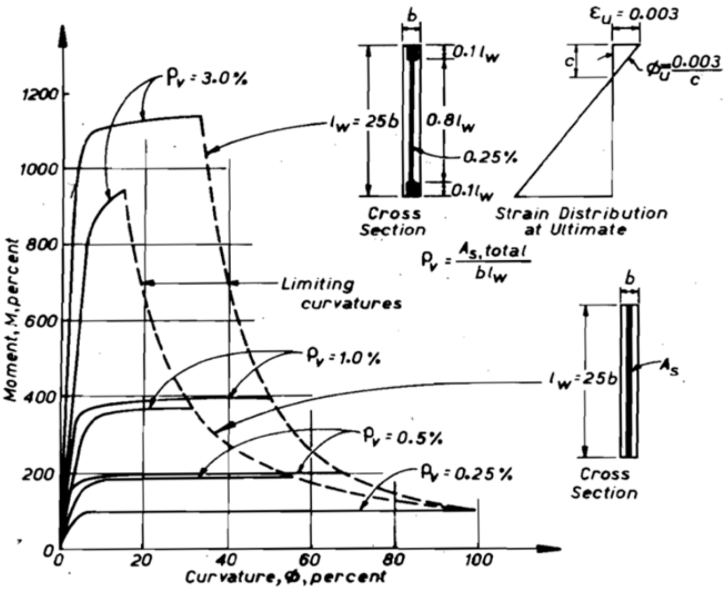

Fig. 2.6 Effect of Boundary Element (*Park & Pauley, 1974*)

Kuang et al. (2008) concluded that walls with boundary elements exhibited high deformation and energy dissipation capacity but does not improve strength. *Darani et al. (2012)* analysed 30 shear wall models for studying effect of variables such as wall aspect ratio, axial force and boundary element. They found that boundary element increases ductility and changes failure mode of wall without improving strength. *Park et al. (2015)* concluded that boundary elements improve shear strength and reduces sliding of wall.

2.3 PREDICTION OF PEAK SHEAR STRENGTH OF SHEAR WALLS

Various building standards and various researchers provided numerous empirical and semi-empirical equations for estimating ultimate shear strength of RC shear walls. Very few researchers concentrated on analytical predictions of shear strength of shear wall. In general prediction of peak shear strength of walls are only possible be means of empirical relationship. These equations are by *IS 456-2000, ACI 318-19 (Ch. 18), ASCE/SEI 43-05,*

MCBC-04, EC 08-04, AIJ-99, AS 3600-09, NZ 3101.1-06, Barda et al. (1977), Wood (1990), Hernandez et al. (1980), Sánchez et al. (2010), Gulec et al. (2009), Kaseem et al. (2010) and *Luna et al. (2019)*. They are described in following sections.

2.3.1 IS 456-2000 Equation

Section 32 in *IS 456-2000* provides recommendations for reinforced concrete walls. Horizontal shear strength for walls subjected to non-seismic lateral loads has been recommended in section 32.4.

Contribution of concrete to shear strength of wall is,

If $\frac{h_w}{l_w} \leq 1$, $$V_c = \left[\left(3 - \frac{h_w}{l_w}\right) K_1\sqrt{f_{ck}}\right](0.8 l_w t_w) \;\geq\; K_3\sqrt{f_{ck}}(0.8 l_w t_w) \tag{2.1a}$$

If $\frac{h_w}{l_w} > 1$, $$V_c = \left[K_2\sqrt{f_{ck}}\,\frac{\left(\frac{h_w}{l_w}+1\right)}{\left(\frac{h_w}{l_w}-1\right)}\right](0.8 l_w t_w) \;\geq\; K_3\sqrt{f_{ck}}(0.8 l_w t_w) \tag{2.1b}$$

Where, K_1 = 0.2 in limit state method and 0.13 in working stress method

K_2 = 0.045 in limit state method and 0.03 in working stress method

K_3 = 0.15 in limit state method and 0.10 in working stress method

Contribution of steel reinforcement to shear strength of wall is,

$$V_s = 0.87 f_y \rho_w l_w t_w \tag{2.1c}$$

Where, If $\frac{h_w}{l_w} \leq 1$, ρ_w – lower of horizontal and vertical reinforcement ratio (ρ_h and ρ_v)

If $\frac{h_w}{l_w} > 1$, ρ_w – vertical reinforcement ratio (ρ_v)

Shear strength of wall is,

$$V_n = V_c + V_s \tag{2.1d}$$

Effect of axial load and boundary element are not considered in shear capacity calculation.

2.3.2 ACI 318-14 (Ch. 11) Equation

Chapter 11 of *ACI 318 – 14*, titled “Walls”, provides recommendations for reinforced concrete walls. Horizontal shear strength for the walls subjected to non-seismic lateral loads has been recommended in section 11.5.4.4. This is semi-empirical equation based on modified truss analogy approach.

Contribution of concrete to shear strength of wall is lower of,

$$V_{c1} = 0.27\lambda\sqrt{f'_c}h_w d + \frac{N_u d}{4l_w}\ ; \tag{2.2a}$$

$$V_{c2} = \left(0.05\lambda\sqrt{f'_c} + \frac{l_w\left(0.1\lambda\sqrt{f'_c} + 0.2\frac{N_u}{l_w t_w}\right)}{\frac{M_u}{V_n} - \frac{l_w}{2}}\right)h_w d \tag{2.2b}$$

Contribution of steel reinforcement to shear strength of wall is,

$$V_s = \frac{A_v f_y d}{s} \tag{2.2c}$$

Shear strength of wall is,

$$V_n = V_c + V_s \leq 0.83\sqrt{f'_c}h_w d \tag{2.2d}$$

Upper limit for shear strength is imposed to prevent diagonal compression failure of wall as shown in Figure 2.7.

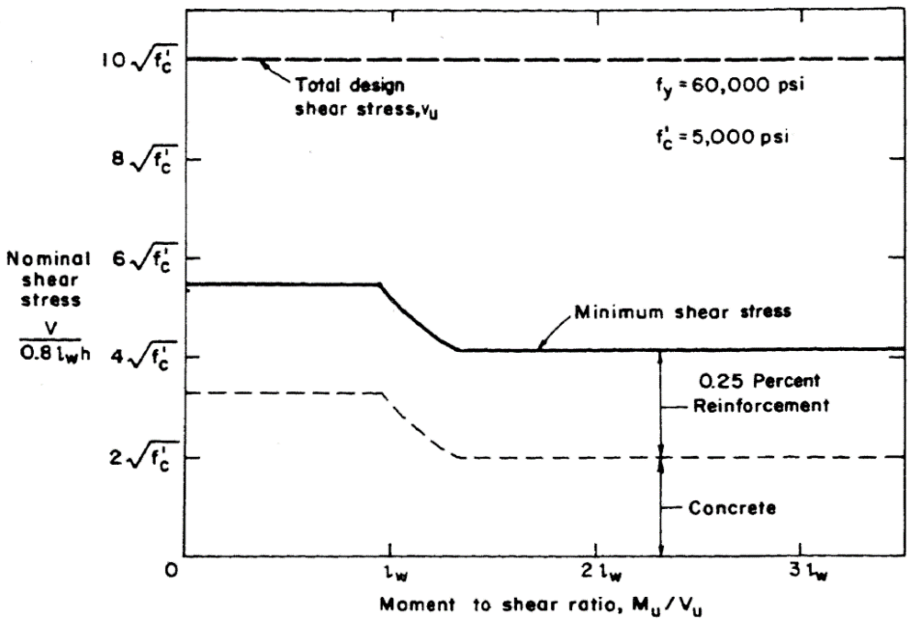

Fig. 2.7 Minimum Shear Strength of Rectangular Cross – Section (*Corley et al. 1972*)

Influence of horizontal reinforcement and boundary element are not considered for shear capacity calculation. However, this equation has been removed in ACI 318-19 due to its inconsistency nature.

2.3.3 ACI 318-19 (Ch. 18) Equation

Chapter 18 of *ACI 318-19*, titled "The Special Structural Walls", provides recommendations for reinforced concrete special structural walls. Horizontal shear strength for the walls subjected to seismic lateral loads has been recommended in section 18.12.9.1. This is a semi-empirical equation based on modified truss analogy.

Contribution of concrete to shear strength of wall is,

$$V_c = A_g \alpha_c \lambda \sqrt{f_c'} \tag{2.3a}$$

Contribution of steel reinforcement to shear strength of wall is,

$$V_s = A_g \rho_t f_y \tag{2.3b}$$

Shear strength of wall is,

$$V_n = V_c + V_s \tag{2.3c}$$

This equation does not account for influence of axial force, boundary elements and horizontal reinforcement in calculation of shear strength of shear walls.

2.3.4 ASCE/SEI 43-05 Equation

Chapter 4 of *ASCE 43-05*, titled "Capacity of low-rise concrete shear walls" provides recommendations for reinforced concrete special structural walls. Horizontal shear strength for walls subjected to seismic lateral loads has been recommended in section C4.2.3. The equation is the modified form of equation suggested by *Badra et al. (1977).*

Contribution of concrete to shear strength of wall is,

$$V_c = \left[8.3\sqrt{f_c'} - 3.4\sqrt{f_c'}\left(\frac{h_w}{l_w} - 0.5\right) + \frac{N_u}{4 l_w t_w}\right] t_w d \tag{2.4a}$$

Contribution of steel reinforcement to shear strength of wall is,

$$V_s = \rho_{se} f_y t_w d \tag{2.4b}$$

Shear strength of wall is,

$$V_n = V_c + V_s \leq 20\sqrt{f_c'}\, t_w d \tag{2.4c}$$

Badra et al. did not consider effect of horizontal web reinforcement which is taken into calculation by this equation; units are in Newton (N) and millimetre (mm).

2.3.5 MCBC-04 Equation

Chapter 4 of *Mexican City Building Code 2004 (MCBC-04)*, titled "Design for Earthquake", provides recommendations for structures subjected to effects of earthquake. Horizontal shear strength for walls subjected to seismic lateral loads has been recommended in section 6.5.2.5.

Contribution of concrete to shear strength of wall is,

If $\frac{h_w}{l_w} \leq 1.5$, $$V_c = 0.27\sqrt{f_c'}t_w l_w \quad (2.5a)$$

If $\frac{h_w}{l_w} > 1.5$ and $\boldsymbol{\rho}_v < 0.015$, $$V_c = 0.3t_w d(0.2 + 20\rho_v)\sqrt{f_c'} \quad (2.5b)$$

Else, $$V_c = 0.16t_w d\sqrt{f_c'} \quad (2.5c)$$

Contribution of steel reinforcement to shear strength of wall is,

$$V_s = \rho_h f_y t_w l_w \quad (2.5d)$$

Shear strength of wall is,

$$V_n = V_c + V_s \quad (2.5e)$$

This is an extended form of equation suggested in *ACI 318* (Ch 11). This equation did not consider effect of axial load and boundary element on shear strength of shear wall; units are in Newton (N) and millimetre (mm).

2.3.6 EC 08-04 Equation

Chapter 5 of *Eurocode 08-04 (EC 08-04)*, titled "Specific Rules for Concrete Buildings", provides recommendations for various structural elements in concrete building. Horizontal shear strength for walls subjected to seismic lateral loads has been recommended in section 5.5.3.4.

Contribution of concrete to shear strength of wall is,

$$V_c = \left\{ \text{Max}\left[180 \times (\rho_v \times 100), 35\sqrt{1 + \sqrt{\frac{0.2}{d}}}\ f_c'^{\frac{1}{6}}\right]\left[1 + \sqrt{\frac{0.2}{d}}\ \right] f_c'^{\frac{1}{3}} + 0.15 \text{ x } \frac{N_u}{A_c}\right\} t_w d$$

(2.6a)

Contribution of steel reinforcement to shear strength of wall is,

$$V_s = \rho_h f_y t_w d \quad (2.6b)$$

Shear strength of wall is,

$$V_n = V_c + V_s \tag{2.6c}$$

This is an empirical equation which did not include effect of boundary element on shear strength of shear wall; units are in Newton (N) and millimetre (mm).

2.3.7 AIJ-99 Equation

Architectural Institute of Japan, or *AIJ*, is a Japanese professional body for architects, building engineers, and researchers in architecture. Guidelines for buildings were published by them in 1999 titled "Structural Design Guidelines for Reinforced concrete Buildings". A semi-empirical equation for horizontal shear strength for walls subjected to seismic lateral loads has been recommended.

Contribution of concrete to shear strength of wall is,

$$V_c = \frac{\tan\theta\,(1-\beta)tL\vartheta f_c'}{2} \geq 0 \tag{2.7a}$$

Where, $\vartheta = 0.7 - \frac{f_c'}{2000}$; $\tan\theta = \sqrt{(\frac{h_w}{l_w})^2 + 1} - \frac{h_w}{l_w}$; $\beta = \frac{(1+\cot^2\varepsilon)\rho_h f_y}{\vartheta f_c'}$

Contribution of steel reinforcement to shear strength of wall is,

$$V_s = \rho_h f_y l_w t_w \tag{2.7b}$$

Shear strength of wall is,

$$V_n = V_c + V_s \tag{2.7c}$$

This equation does not account for influence of axial force, boundary elements and vertical reinforcement in calculation of shear strength of shear walls with units in Newton (N) and millimetre (mm).

2.3.8 AS 3600-09 Equation

Chapter 11 of *Australian Standard 3600-09 (AS 3600-09)*, titled "Design of Walls", provides recommendations for reinforced concrete walls. Horizontal shear strength for walls subjected to non-seismic lateral loads has been recommended in section 11.6.3.

Contribution of concrete to shear strength of wall is,

If $\frac{h_w}{l_w} \leq 1$, $$V_c = (0.66\sqrt{f_c'} - 0.21\frac{h_w}{l_w}\sqrt{f_c'})\,0.8 l_w t_w \tag{2.8a}$$

If $\frac{h_w}{l_w} > 1$, $$V_c = \left(0.05\sqrt{f'_c} + \frac{0.1\sqrt{f'_c}}{\left(\frac{h_w}{l_w} - 1\right)}\right) 0.8 l_w t_w \geq 0.17\sqrt{f'_c}\,(0.8 l_w t_w) \quad (2.8b)$$

Contribution of steel reinforcement to shear strength of wall is,

$$V_s = \rho_w f_y (0.8 l_w t_w) \quad (2.8c)$$

Where, If $\frac{h_w}{l_w} \leq 1$, ρ_w – lower of horizontal and vertical reinforcement ratio (ρ_h and ρ_v)

If $\frac{h_w}{l_w} > 1$, ρ_w – horizontal reinforcement ratio (ρ_h)

Shear strength of wall is,

$$V_n = V_c + V_s \leq 0.2\, f_c' (0.8 l_w t_w) \quad (2.8d)$$

This equation does not account for influence of axial force and boundary elements in calculation of shear strength of walls with units in Newton (N) and millimetre (mm).

2.3.9 NZ 3101.1-06 Equation

Chapter 11 of *New Zealand Standard 3101.1-06 (NZ 3101.1-06),* titled “Design of structural walls for strength, serviceability and ductility”, provides recommendations for reinforced concrete walls. Horizontal shear strength of walls subjected to seismic lateral loads has been recommended in section 11.3.10.

Contribution of concrete to shear strength of wall is,

$$V_c = \left[\mathrm{Min}\left\{0.17\left(\sqrt{f'_c} + \frac{N_u}{A_g}\right), 0.05\sqrt{f'_c} + \frac{l_w\left(0.1\sqrt{f'_c} + 0.2\frac{N_u}{A_g}\right)}{\frac{M_u}{V_u} - \frac{l_w}{2}}, 0.27\sqrt{f'_c} + \frac{N_u}{4A_g}\right\}\right] A_w \quad (2.9a)$$

Contribution of steel reinforcement to shear strength of wall is,

$$V_s = \rho_h f_y\, t_w (0.8 l_w) \quad (2.9b)$$

Shear strength of wall is,

$$V_n = V_c + V_s \quad (2.9c)$$

This equation does not account for influence of vertical reinforcement and boundary element in calculation of shear strength of shear walls with units are in Newton (N) and millimetre (mm).

2.3.10 Barda et al. (1977)

Barda et al. (1977) developed a semi-empirical equation for predicting the shear strength of shear walls. This equation was derived based on results from experimental tests of eight squat walls with heavily reinforced flanges.

Contribution of concrete to shear strength of wall is,

$$V_n = \left(8\sqrt{f_c'} - 2.5\sqrt{f_c'}\frac{h_w}{l_w} + \frac{N_u}{4l_w t_w}\right) t_w d \quad (2.10a)$$

Contribution of steel reinforcement to shear strength of wall is,

$$V_s = \rho_v f_y t_w d \quad (2.10b)$$

Shear strength of wall is,

$$V_n = V_c + V_s \quad (2.10c)$$

This equation does not account for influence of boundary element in calculation of shear strength of shear walls with units in Newton (N) and millimetre (mm).

2.3.11 Wood (1990)

Wood (1990) compiled peak shear strengths from 143 squat wall tests, including rectangular walls and walls with boundary elements. She developed a semi-empirical equation for nominal shear strength of squat walls.

Shear strength of wall is,

$$6\sqrt{f_c'}A_w \le V_{n10} = \frac{A_{vf} f_y}{4} \le 10\sqrt{f_c'}A_w \quad (2.11a)$$

This equation does not account for influence of height of wall, axial load and boundary element in calculation of shear strength of shear walls with units in Newton (N) and millimetre (mm).

2.3.12 Hernandez et al. (1980)

Hernandez et al. (1980) developed a semi-empirical equation for predicting shear strength of shear walls.

Contribution of concrete to shear strength of wall is,

$$V_c = V_0 \sqrt{1 + \frac{\sigma}{V_0}}; \quad (2.12a)$$

Where, $\frac{\sigma}{V_0} \leq 5$; $V_0 = \left[0.5 - 0.09\left(\frac{M_u}{V_n l_w}\right)^2\right]\sqrt{f_c'}$;

Contribution of steel reinforcement to shear strength of wall is,

If $\frac{M_u}{V_n l_w} < 0.25$, $V_s = \rho_v f_y t_w l_w$ (2.12b)

If $0.25 < \frac{M_u}{V_n l_w} < 1.25$, $V_s = \left(\rho_h f_y\left(\frac{M_u}{V_n l_w}\right) - 0.25\right) + \rho_v f_y\left(1.25 - \frac{M_u}{V_n l_w}\right) t_w l_w$ (2.12c)

If $\frac{M_u}{V_n l_w} > 1.25$; $V_s = \rho_h f_y t_w l_w$ (2.12d)

Shear strength of wall is,

$$V_n = V_c + V_s \tag{2.12e}$$

This equation does not account for influence of boundary element in calculation of shear strength of shear walls. The units are in Newton (N) and millimetre (mm).

2.3.13 Sánchez et al. (2010)

Sánchez et al. (2010) developed a semi-empirical equation for shear strength of shear wall. Methodology followed for developing equation is simplified strut-and-tie model.

Contribution of concrete to shear strength of wall is,

$$V_n = \left(\gamma\eta_v + \frac{0.04N_u}{A_w}\right)\sqrt{f_c'} \tag{2.13a}$$

Where, $\gamma = 0.42 – 0.08\frac{M_u}{V_n l_w}$; $\eta_v = 0.75+0.05\rho_v f_y$; $\eta_h = 1–0.16\rho_h f_y$

Contribution of steel reinforcement to shear strength of wall is,

$$V_s = \eta_h \rho_v f_y \tag{2.13b}$$

Shear strength of wall is,

$$V_n = V_c + V_s \tag{2.13c}$$

This equation does not account for influence of boundary element in calculation of shear strength of shear walls with units in Newton (N) and millimetre (mm).

2.3.14 Gulec et al. (2011)

Gulec et al. (2011) developed an empirical equation for shear strength of squat reinforced concrete walls using data from test results of 227 squat walls. They recommended two different equations for walls without and with boundary element for the first time.

Contribution of concrete to shear strength of wall without boundary element is,

$$V_c = \frac{1.5\sqrt{f_c'}A_w + 0.40N_u}{\sqrt{h_w/l_w}} \tag{2.14a}$$

Shear strength of wall is without boundary element is,

$$V_n = V_c + V_s \leq 10\sqrt{f_c'}A_w \tag{2.14b}$$

This equation does not account for influence of horizontal reinforcement in calculation of shear strength of shear walls. They recommended another equation for shear strength of shear wall with boundary element as follows.

Contribution of concrete to shear strength of wall with boundary element is,

$$V_c = \frac{(0.04f_c^1)A_{eff} + 0.35N_u}{\sqrt{h_w/l_w}} \tag{2.14c}$$

Contribution of reinforcement to shear strength of wall with boundary element is,

$$V_s = \frac{0.40F_{vw}+0.15F_{vbe}}{\sqrt{h_w/l_w}} \tag{2.14d}$$

Shear strength of wall is with boundary element is,

$$V_n = V_c + V_s \leq 10\sqrt{f_c'}A_g \tag{2.14e}$$

Both equations for walls with and without boundary element do not account for influence of horizontal reinforcement in calculation of shear strength of shear walls using units in Newton (N) and millimetre (mm).

2.3.15 Kassem (2010)

Kaseem et al. (2014) developed a closed form semi-empirical equation for shear strength of squat reinforced concrete walls based on softened truss model. Two different equations have been recommended for walls without and with boundary element.

Shear strength of wall without boundary element is,

$$V_n = 0.27f_c'[\psi k_s \sin(2\alpha) + 0.11\,\omega_h \frac{h_w}{d} + 0.30\,\omega_v \cot(\alpha)]t_w d \leq 0.83\sqrt{f_c'}t_w d \tag{2.15a}$$

Shear strength of wall with boundary element is,

$$V_n = 0.47f_c^1\,[\psi k_s \sin(2\alpha) + 0.15\,\omega_h \frac{h_w}{d_w} + 1.76\,\omega_v \cot(\alpha)]t_w d \leq 1.25\sqrt{f_c'}t_w \tag{2.15b}$$

Where, $\Psi = 0.95 - \frac{f'_c}{250}$; $\omega_h = \frac{\rho_h f_y}{f'_c}$; $\omega_v = \frac{\rho_v f_y}{f'_c}$; $\alpha = \tan^{-1}(h_w/d)$; $k_s = a_s/d_w$

Both equations for walls with and without boundary element do not account for influence of axial load in calculation of shear strength of shear walls using units in Newton (N) and millimetre (mm).

2.3.16 Luna et al. (2019)

Luna et al. (2019) derived an equation for the shear strength of squat reinforced concrete walls on basis of internal force resisting system. Two different equations have been recommended for walls without and with boundary elements.

Shear strength of wall without boundary element is,

$$V_n = 1.2\left(\rho_v A_{cv} f_{\bar{y}} + \frac{N_u}{l_w} l_w\right)\left(1 - 0.7\frac{h_w}{l_w} - \frac{c}{l_w}\right) + 0.25\rho_t \frac{h_w}{l_w} A_{cv} f_y + 0.5\frac{N_u}{l_w} c \leq 10\sqrt{f'_c} A_{cv} \tag{2.16a}$$

Shear strength of the wall with boundary element is,

$$V_n = 1.2\left(\rho_v A_{cv} f_y + \frac{N_u}{l_w}\right)\left(1 - 0.7\frac{h_w}{l_w} - 2\frac{l_c}{l_w}\right) + 1.7\left(\frac{N_u}{l_w} l_c + P\right) + 1.2\rho A_{BE} f_y + 0.25\rho_t A_{cv}\frac{h_w}{l_w} f_y \leq 10\sqrt{f'_c} A_{cv} \tag{2.16b}$$

Where, $c = \frac{\left(t_w \rho_v f_{\bar{y}} + \frac{N_u}{l_w}\right)(1.2 h_w)}{\left(2.4 \rho_v f_{\bar{y}} t_w - \frac{N_u}{l_w}\right)}$, $f_{\bar{y}} = 1.25 f_y$

All geometric parameters have been considered using units Newton (N) and millimetre (mm).

2.4 OTHER STUDIES ON SHEAR WALLS WITHOUT OPENING

Trevor et al. (2006) compared predicted response of shear wall under earthquake loading by macro model and with experimentally observed response from shake table tests. ANSR II programme was used for modelling. A seven storey residential building was modelled using ANSR II, constructed and tested in shake table in UCSD. Analytical studies also carried out using Newmark's beta method. Four earthquake data taken and compared with model prediction. Force-displacement relationship, peak response parameters, time history characteristics, dynamic magnification of shear compared; three procedures agree with data.

Xu et al. (2007) studied cyclic behaviour of RC shear walls using finite element software ANACAP. Results are compared with JNES/NUPEC cyclic experimental test data using shake tables. When shear deformation angle (SDA) is less than 0.002 radians, effect of multi-axial loading was found to be negligible and hence one dimensional loading can be applied. When SDA exceeds 0.002 radians, capacity of wall decreased explicitly. ANACAP concrete constitutive model is a smeared crack FEM. Computed shear capacity by ANACAP differs by 10% with test results.

Edward et al. (2009) proposed a simplified model for simulating damage of squat RC shear walls under lateral load. Model is based on damage and fracture mechanics. Analytical expressions are developed with crack resistance functions based on Griffith criterion and validated with experimental results. Proposed model does not account for combined damage due to shear and bending. However, a good correlation is found with squat shear walls.

Leonardo et al. (2009) improved modelling to capture overall flexure-shear response. Fourteen walls with aspect ratio less than 1.5 were tested. A model was formulated by modifying MVLEM (Multi Vertical Line Element Model). To represent constitutive panel behaviour, Rotating angle modelling approach was used. Results indicate that proposed model, after improvement, captures with reasonable accuracy.

Fahjan et al. (2010) studied different approaches for linear and nonlinear modelling of shear walls. Results are compared with overall behaviour of structural system. Linear model is based on frame element and shell element, and nonlinear model is based on continuum finite element, multi-layered shell element, frame element plastic hinge. Linear models overestimate capacity of shear walls. Three nonlinear models show identical results.

Musmae (2013) analysed six shear walls; one solid and five with openings, of varying height using Finite Element package ANSYS. The openings are all at the mid length. The wall was fixed at bottom and horizontal loading was applied on left edge of shear wall at each storey in accordance with IBC 2000 (International Building Code). Walls with small openings exhibited strength very close to that of solid shear walls. With larger openings, shear walls capacity is about 70% of that of solid wall. Crack initiation and propagation are also studied.

Sivakumar et al. (2014) analysed flanged shear walls using Finite element package ANSYS10.0. Analysis is done for reinforced concrete walls using smeared as well as discrete models. Slender shear walls (aspect ratio > 2.0) exhibited significant bending, while squat shear walls (aspect ratio < 2.0) failed predominantly in shear. Smeared models showed 10% higher ultimate strength compared to that of discrete models.

Many researchers reported numerical analysis results on behaviour of shear wall using various analysis packages. Main features used for modelling of shear wall by various researchers are listed in Table 2.2.

Table 2.2 Main Features of Modelling

Author	Concrete		Steel	
	Constitutive Relations	**Element used**	**Constitutive Relations**	**Element used**
Okamura et al. (1991)	Orthotropic Equivalent uniaxial strain	8-node iso parametric membrane element	Bilinear	Smeared
Sittipunt et al. (1993)	Orthotropic Equivalent uniaxial strain	4-node iso parametric Membrane element.	Bilinear	Discrete
Elmorsi et al. (1998)	Orthotropic Equivalent uniaxial strain.	12-node quadrilateral Membrane element.	Bilinear	Smeared
Palermo (2003)	Orthotropic Equivalent uniaxial strain	4-node iso parametric Membrane element.	Trilinear	Smeared
Kwak (2004)	Orthotropic Equivalent uniaxial strain.	4-node iso parametric Membrane element.	Bilinear	Smeared
Xu et al. (2007)	Orthotropic Equivalent uniaxial strain.	20 Node Brick element.	Bilinear	Smeared
Liu et al. (2011)	Multi linear Isotropic	Solid 65	Bilinear	Discrete
Merin et al. (2013)	Multi linear Isotropic	Solid 65	Bilinear	Smeared
Sivakumar et al. (2014)	Multi linear Isotropic	Solid 65	Bilinear	Discrete

2.5 STUDIES ON SHEAR WALL WITH OPENING

Many research efforts have been carried out on shear walls during past seven decades. Majority of these studies focussed on shear walls without opening. Research on shear wall with opening started four decades back but still at its early stage. *Sotomura et al. (1981)* conducted first research program on shear wall with numerous small openings for pipes and ducts which are unavoidably to be provided in shear wall of PWR nuclear power plant. They concluded that shear strength and stiffness of shear wall with numerous small openings can be restored as of wall without opening by providing diagonal reinforcement. *Lin et al. (1988)*

conducted a series of eleven shear walls with different type of opening with different reinforcement patterns around it. They concluded that reinforcement pattern around opening influences shear strength of wall.

Ali et al. (1991) performed a series of experiments to study effects of staggered door openings on the seismic behaviour of RC walls. They found that door openings located to close to edge of boundary column zone will trigger an early shear-compression failure. Moreover, walls with staggered openings could decrease energy dissipation capacity up by 29%. *Yanez et al. (1992)* tested a series of six rectangular RC walls with irregularly distributed openings. They concluded that arrangement of openings did not show significant effect on behaviour of walls under cyclic lateral loading. *Sharmin et al. (2012)* studied shear wall behaviour with openings under seismic load action by in plane and out of plane loading using ETABS. Opening in shear wall in in-plane loading is more critical than opening in shear wall in out of plane loading. *Mazen (2013)* Analysed numerically behaviour of Shear walls with small to large size openings. Cracks of large openings are near upper lintel of opening and for smaller openings near base. *Musmae (2013)* analysed six shear walls including one solid and five with openings of varying height using Finite Element package ANSYS. Walls with small openings have their capacities relatively closer to solid shear walls whereas for larger opening about 70% of that of solid wall.

Maurius et al. (2013) studied behaviour of shear wall with regular and staggered opening using experiments. They found that walls with staggered openings are more rigid than regular opening. *Vishal et al. (2015)* studied effect of opening size of RC shear wall numerically. Stiffness is highly affected when opening area is more than 20% is shear wall area. *Saeid et al. (2015)* studied effect of two regular openings in steel plate shear walls. Three one-third scaled steel plate shear walls with two rectangular opening were tested. Stiffeners were installed on steel plate. Cyclic quasi-static loading was applied. Perforation about 35% in panels leads to reduce initial stiffness and ultimate strength by 22 and 36% respectively compared to imperforated specimen.

Ayman et al. (2016) studied experimentally, performance of RC shear wall with openings and also retrofitted with by FRP laminates. FRP's are successful in enhancing strength and ductility of walls with openings. *Bing et al. (2016)* studied effect of flanges on RC walls with openings experimentally. Presence of flange significantly increases shear strength but reduces deformation capacity. *Zhang et al. (2018)* tested four shear walls with door and window opening. Influence of stress redistribution and variation of load-transfer paths in RC shear walls were explored in this study.

2.6 Code Provisions for Shear Walls

Many experiments with full and reduced scale were carried out at laboratories across the globe to study behaviour of shear walls. Results have been included in codes of practice to guide engineers. Various code reviewed in this study are: *IS 13920:2016* (Indian Standards), *ACI318-2019* (American Concrete Institute), *CSA A23.3.04* (Canadian Standards Association), *EC – 08* (Euro Code), *JSCE C15 – 07* (Japan Society of Civil Engineers), *AS3600 – 2009* (Australian Standards), *NZ3101.1 – 2006* (New Zealand Standards).

2.6.1 Shear walls without Opening

Recommendation for detailing and construction of shear walls in various codes differ from each other in terms of minimum thickness, minimum reinforcement ratios and boundary elements as listed in Table 1.

a) IS 13920:2016 (Indian Standards)

IS 13920:2016 is a code of practice titled "Ductile design and Detailing of Reinforced Concrete Structures Subjected to Seismic Forces" deals with provisions for addressing special features in design and construction of earthquake resistant RC buildings. Some important recommendations provided in this code of practice for shear walls are as follows.

- Minimum ratio of length of wall to its thickness ($\frac{l_w}{t_w}$) shall be 4.
- Depends on aspect ratio, shear wall is classified as follows.
    - $\frac{h_w}{l_w} < 1$, Squat walls
    - $1 \leq \frac{h_w}{l_w} \leq 1$, Intermediate walls
    - $\frac{h_w}{l_w} > 1$, Slender wall
- Minimum thickness of shear wall is about 150 mm.
- Reinforcement bars shall be provided in two curtains with each curtain having bars running along vertical and horizontal when factored shear stress demand in wall exceeds $0.25\sqrt{f_{ck}}$ or wall thickness is 200 mm or higher.

- Minimum horizontal reinforcement for squat walls is about $\rho_{h,min}$ = 0.25% and minimum spacing between the horizontal reinforcement is,
    - S = min($\frac{1}{5}^{th}$ of l_w; 3t; 450 mm)
- Minimum horizontal reinforcement for squat walls is about $\rho_{h,min}$ = 0.0025 + 0.5(1-$\frac{h_w}{l_w}$)(ρ_h-0.0025) and minimum spacing between horizontal reinforcement is,
    - S = min($\frac{1}{5}^{th}$ of l_w; 3t; 450 mm)
- Boundary elements shall be provided along vertical boundaries of walls, when extreme fibre compressive stress in wall exceeds $0.2f_{ck}$ due to factored gravity loads and plus earthquake loads.
- Longitudinal reinforcement in boundary elements shall not be less than 0.8 per cent and not greater than 6 per cent. Practical upper limit would be 4 per cent to avoid congestion. Special confining reinforcement throughout height and its spacing is given by,
    - $A_{sh} = 0.05\, S_v h \frac{f_{ck}}{f_y}$
    - S = min($\frac{1}{3}$ $b_c, 6\emptyset, 100$ mm)

b) ACI318-2019 (American Concrete Institute)

ACI318-2019 is a code of practice titled, "Building Code Requirements for Structural Concrete", provides minimum requirements for materials, design, and detailing of structural concrete buildings. Some important recommendations provided in this code of practice for shear walls are as follows.

- Structural element with $\frac{h_w}{l_w} \geq 2$ and $\frac{l_w}{t_w} \leq 6$, then it is called column, else called wall.
- Walls with aspect ratio $\frac{h_w}{l_w} < 2$, then it is squat wall, else it is slender walls.
- Minimum thickness of wall is,
    - $t_{w,\,min}$ = Max(100 mm, $\frac{1}{25}^{th}$ of max (h_w, l_w))
- Minimum horizontal reinforcement and its maximum spacing for squat walls are as follows,

- If, $f_y \geq 420$ MPa, $\rho_{h,min} = 0.2\%$; If, $f_y < 420$ MPa, $\rho_{h,min} = 0.25\%$;

  If, $v_n \geq 0.5\phi v_c$, $\rho_{h,min} = 0.0025$.

- S = 450 mm.

➢ Minimum vertical reinforcement and its maximum spacing for squat walls are as follows,

- If, $f_y \geq 420$ MPa, $\rho_{h,min} = 0.12\%$; If, $f_y < 420$ MPa, $\rho_{h,min} = 0.15\%$;

  If, $v_n \geq 0.5\phi v_c$, $\rho_{h,min} = = 0.0025 + 0.5\ (2.5 - \frac{h_w}{l_w})(\ \rho_h - 0.0025)$

- S = 450 mm.

➢ If boundary elements are required, then size of boundary element is given by,

- $l_{c,\,min} = \text{Max}[(c - 0.1l_w), c/2]$, $b_{c,min} = h_w/16$

➢ Minimum longitudinal and confining reinforcement in boundary elements is given by,

- $\rho = \max[0.3(\frac{A_g}{A_{ch}} - 1)\frac{f_c'}{f_y}, 0.09\frac{f_c'}{f_y}]$

- $\frac{A_{sh}}{sb_c} = \max\left[0.3\left(\frac{A_g}{A_{sh}} - 1\right)\frac{f_c'}{f_y}, 0.09\frac{f_c'}{f_y}\right]$ and spacing not to exceed 300 mm.

c) CSA A23.3.14 (Canadian Standards Association)

CSA A23.3.14 is code of practice "Design of concrete structures", provides specifies requirements, in accordance with National Building Code of Canada, for design and strength evaluation of (a) structures of reinforced and pre stressed concrete; (b) plain concrete elements; and (c) special structures such as parking structures, arches, tanks, reservoirs, bins and silos, towers, water towers, blast-resistant structures, and chimneys. Some important recommendations provided in this code of practice for shear walls are as follows.

➢ Minimum ratio of length of wall to its thickness ($\frac{l_w}{t_w}$) shall be 6 and length of wall is at least 1/3 times clear height of wall.

➢ Depends on aspect ratio, shear wall is classified as follows.

- $\frac{h_w}{l_w} < 2$, Squat wall

- $\frac{h_w}{l_w} > 2$, Slender wall

- Minimum thickness of the wall is,
    - $t_{w, min}$ = Max(150 mm, $\frac{1}{25}^{th}$ of max (h_w , l_w))
- Minimum percentage of horizontal reinforcement is 0.3% and its maximum spacing is 300 mm.
- Minimum percentage of vertical reinforcement is 0.3% and its maximum spacing is 300 mm.
- Boundary elements are not necessarily to require an increase in wall thickness. Boundary reinforcement can be confined in wall thickness itself.
- Minimum percentage of longitudinal reinforcement in boundary element is about 0.5%.

d) EC – 08 (Euro Code)

EC - 08 is a code of practice titled, “Design of structures for earthquake resistance”, applies to design and construction of buildings and civil engineering works in seismic regions. Its purpose is to ensure that in event of earthquakes, (a) human lives are protected, (b) damage is limited, and (c) structures important for civil protection remain operational. Some important recommendations provided in this code of practice for shear walls are as follows.

- Minimum ratio of length of wall to its thickness ($\frac{l_w}{t_w}$) should 4.
- Depends on aspect ratio, shear wall is classified as follows.
    - $\frac{h_w}{l_w} < 2$, Squat walls
    - $\frac{h_w}{l_w} > 2$, Slender wall
- Minimum thickness of the wall is,
    - $t_{w,,min}$ = max(150 mm, $\frac{h_w}{20}$)
- Minimum percentage of horizontal reinforcement is 0.2% and its maximum spacing is,
    - S = min(20ϕ, 300 mm)
- Minimum percentage of vertical reinforcement is 0.5% and its maximum spacing is,
    - S = min(20φ, 300 mm)

- If boundary elements are required, then size of boundary element is given by,
    - $l_{c,min} = \max[(0.2l_w), 2t_w]$
    - $b_{c,min} = \max[200 \text{ mm}, h_w/15]$
- Longitudinal reinforcement in boundary elements is 0.5% and 4%.

e) JSCE C15 – 07 (Japan Society of Civil Engineers)

JSCE C15 – 07 is a code of practice titled, "Standard Specification for Concrete Structures", applies for practical use which describes the specification during plan, design, maintenance and repair of concrete structures. Some important recommendations provided in this code of practice for shear walls are as follows.

- Minimum ratio of length of wall to its thickness ($\frac{l_w}{t_w}$) should 4.
- Minimum thickness of wall is,
    - $t_{w,,min} = \max(100 \text{ mm}, \frac{h_w}{25})$
- Minimum percentage of horizontal reinforcement is 0.15% and its maximum spacing is 300 mm.
- Minimum percentage of vertical reinforcement is 0.15% with maximum spacing is,
    - $S = \min(2t_w, 300 \text{ mm})$
- Longitudinal reinforcement in the boundary elements is 0.4% and 4%.

f) AS3600–09 (Australian Standards)

AS3600-09 is a code of practice titled, "Concrete structures". Principal objective of Standard is to provide users with nationally acceptable unified rules for design and detailing of concrete structures and members, with or without steel reinforcement or prestressing tendons, based on principles of structural engineering mechanics. Secondary objective is to provide performance criteria against which finished structure can be assessed for compliance with relevant design.

- Minimum ratio of length of wall to its thickness ($\frac{l_w}{t_w}$) shall be 4 and length of wall is at least $\frac{1}{2.5}$ times clear height of wall.
- Minimum thickness of wall is $\frac{h_w}{30}$.
- Minimum percentage of horizontal reinforcement is 0.25% and maximum spacing is,

- S = min(2.5tw, 350 mm)

- Minimum percentage of vertical reinforcement is 0.15% and its maximum spacing is,
  - S = min(2.5t_w, 350 mm)

g) NZ3101.1 – 2006 (New Zealand Standards)

NZ3101.1 – 2006 is a code of practice titled, "The Design of Concrete Structures". This Standard sets out minimum requirements for design of reinforced and pre-stressed concrete structures. Some important recommendations provided in this code of practice for shear walls are as follows.

- Depends on aspect ratio, shear wall is classified as follows.
  - $\frac{h_w}{l_w} < 2$, Squat walls
  - $\frac{h_w}{l_w} > 2$, Slender wall
- Minimum thickness of the wall is 100 mm.
- Minimum horizontal reinforcement and its maximum spacing are as follows,
  - $\rho_{h,min} = \frac{0.7 b_w S}{f_y}$; S = min($l_w$/5, 3t, 450 mm)
- Minimum vertical reinforcement and its maximum spacing for squat walls are as follows,
  - $\rho_{v,min} = \text{Max}\left(\frac{0.7}{f_y}, \frac{\sqrt{f_c'}}{4f_y}\right)$
  - S = Min(l_w/3, 3t, 450 mm)
- If boundary elements are required, then size of boundary element is given by,
  - $\frac{l_{c,min}}{b_{c,min}} = 3$
- Longitudinal reinforcement in the boundary element is,
  - $\rho = \frac{16}{f_y}$
- Longitudinal reinforcement in boundary elements shall be enclosed by lateral ties when vertical reinforcement area equals or exceeds 0.01 times gross concrete area in any locality of wall section.

Table 2.3 Code Recommendations on Shear Wall

Code No.	Aspect Ratio, AR (h_w/l_w)	Minimum Thickness (t_{min})	Horizontal Reinforcement ($\rho_{h,min}$)	Vertical Reinforcement ($\rho_{v,min}$)	Boundary Elements (BE)	BE Reinforcement (ρ_{min})
IS13920 : 2016	AR <1, Squat wall; 1<AR<2, Intermediate wall; AR>2, Slender wall.	150 mm	$\rho_{h,min}$ = 0.25%; S= min($\frac{1}{5}^{th}$ of l_w; 3t; 450 mm)	$\rho_{h,min}$ = 0.0025+0.5(1-AR)(ρ_h- 0.0025) S = min($\frac{1}{5}^{th}$ of l_w; 3t; 450 mm)	BE are provided when extreme fibre compressive stress in wall exceed $0.2f_{ck}$	ρ = 0.8 to 6 %
ACI318 : 2014	AR < 2, Squat wall; AR > 2, Slender wall.	Max (100 mm, $\frac{1}{25}^{th}$ of max (h_w , l_w))	$f_y \geq$ 420 MPa, $\rho_{h,min}$ = 0.2% ; $f_y <$ 420 MPa, $\rho_{h,min}$ = 0.25% ; $v_n \geq 0.5\phi v_c$, $\rho_{v,min}$ = 0.0025 S = 450 mm.	$f_y \geq$ 420 MPa, $\rho_{v,min}$ = 0.12% ; $f_y <$ 420 MPa, $\rho_{v,min}$ = 0.15% ; $v_n \geq 0.5\phi v_c$, $\rho_{v,min}$ = 0.0025 + 0.5 (2.5 –AR)(ρ_h – 0.0025); S = 450 mm.	L_{BE} = Max[(c – 0.1l_w), c/2] B_{BE}= Min (h_w/16)	ρ = Max [0.3($\frac{A_g}{A_{ch}}$ – 1) $\frac{f_c^1}{f_y}$, 0.09 $\frac{f_c^1}{f_y}$]
CSA A23.3	AR < 2, Squat wall; AR > 2, Slender wall.	Max (150 mm, $\frac{1}{25}^{th}$ of max (h_w , l_w))	$\rho_{h,min}$ = 0.3 %; S = 300 mm	$\rho_{v,min}$ = 0.3 %; S = 300 mm	BE do not necessarily require an increase in wall thickness.	0.5 %
EC-08	AR < 2, Squat wall; AR > 2, Slender wall.	Max(150 mm, h_w/20)	$\rho_{h,min}$ = 0.2 %; S = Min (20ϕ, 300mm)	If ε_c = 0.2% $\rho_{v,min}$ = 0.5 %; S = Min (20ϕ, 300mm)	L_{BE} = Max (0.2l_w , 2b_w) B_{BE} = Max (0.2 m, h_w/15)	ρ = 0.5 % to 4 %
JSCE C15 - 07	-	Max (100 mm, 1/25 of l_w)	$\rho_{h,min}$ = 0.15 %; S = 300 mm	$\rho_{v,min}$ = 0.15 %; S = Min(300 mm, 2t)	-	ρ = 0.4 % to 4 %
AS3600 - 2009	-	$\frac{h_w}{t_w} \leq 30$	$\rho_{h,min}$ = 0.25 %; S = Min(2.5t, 350 mm).	$\rho_{v,min}$ = 0.15 %; S = Min(2.5t, 350 mm).	-	-
NZS3101:1 - 2006	AR < 2, Squat wall; AR > 2, Slender wall.	100 mm	$A_h = \frac{0.7 b_w S}{f_y}$; S = Min($l_w$/5, 3t, 450 mm)	A_v = Max ($\frac{0.7}{f_{yn}}$, $\frac{\sqrt{f_c^1}}{4f_y}$) S = Min($l_w$/3, 3t, 450 mm)	$\frac{L_{BE}}{H_{BE}}$ = 3	$\rho < \frac{16}{f_y}$

2.6.2 Shear Walls with Openings

Shear walls with openings are recommended by codes with additional reinforcement in corners around openings, whose area is equal to interrupted bars. Some codes do not have such recommendations. Pattern of reinforcement by various codes is shown in Figure 2.8.

a) IS 13920:2016 (Indian Standards)

IS 13920:2016 recommends to provide additional reinforcement along all four edges of opening in the wall. Further,

- Area of these vertical and horizontal bars should be equal to that of respective interrupted bars, provided on either side of wall in each direction.
- These vertical bars should be extended for full height of the storey in which this opening is present.
- Horizontal bars should be provided with development length in tension beyond the edges of the opening.

b) ACI 318-2019 (American Concrete Institute)

ACI 318-19 recommends special boundary element around edges of opening where maximum extreme fibre compressive stress, corresponding to all loading combination exceeds $0.2f_c$'. This special boundary element shall be permitted to be discontinued where calculated compressive stress comes below $0.15f_c$'. Stresses shall be calculated for factored loads using a linearly elastic model and gross section properties. For shear strength of walls with opening, ACI 318 – 19 suggests same equation as that of wall without opening by changing gross area (A_{cv}) of section as section area minus area of opening. Shear strength for walls suggested in ACI 318 – 19 is shown in eq. (2.17).

$$V_n = (\alpha_c \lambda \sqrt{f_c'} + \rho_t f_{yt}) A_{cv} \tag{2.17}$$

Here, gross area (A_{cv}) is total area of defined section minus area of opening in that section.

c) JSCE C15 – 07 (Japan Society of Civil Engineers)

JSCE C15 – 07 recommends appropriate additional reinforcement around all opening in structural members to safeguard against cracks due to stress concentration. Cracks due to stress concentration tend to occur around opening. Occurrence of these cracks depends on specific local conditions, and therefore methods of reinforcement are based on available results, such as appropriate calculation, experimental tests describing actual conditions, and past cracking records. Such reinforcement should be extended to allow for appropriate development length in bars beyond corners. Primary and distribution reinforcement which cannot be provided because of openings should be arranged. Openings should be arranged that requirement for amount of reinforcement at any cross-section is satisfied.

d) CSA A23.3-14 (Canadian Standards Association)

CSA A23.3-14 recommends additional reinforcement in addition to reinforcement provided which is not less than one 15M bar per layer (bar number 15M refers to bar with cross section area 200 mm^2 corresponds to 16 mm diameter rod), or reinforcement having same area, shall be provided around all window and door or similar openings. Such bars shall extend to develop bar, but not less than 600 mm beyond each corner of opening.

e) NZ3101.1 – 06 (New Zealand Standards)

NZ3101.1 – 2006 recommends addition to minimum reinforcement as prescribed, there shall be reinforcement with yield strength equal to or greater than 600 N per mm of wall thickness, around all window or door openings. Such bars shall extend at least 600 mm beyond corners of openings.

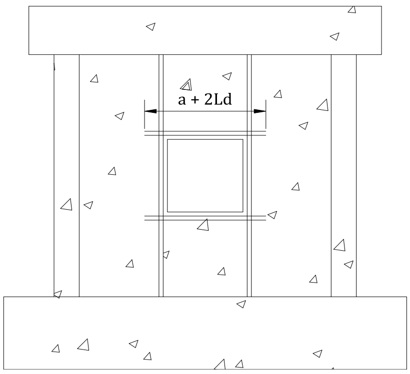

a. IS 13920 - 16

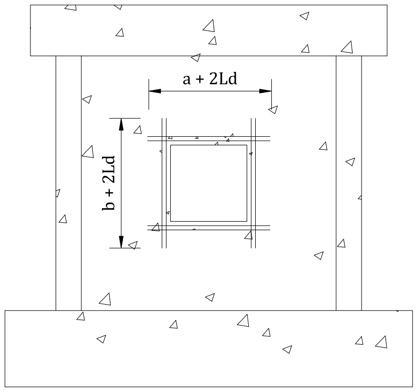

b. ACI 318 - 19

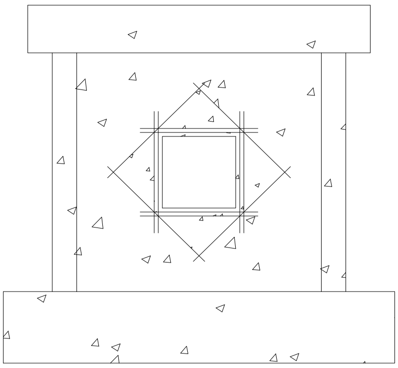

c. JSCE C15 - 07

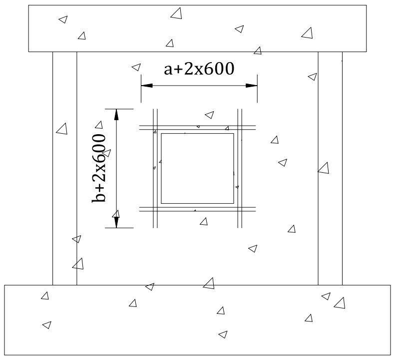

d. CSA A23.3 - 14

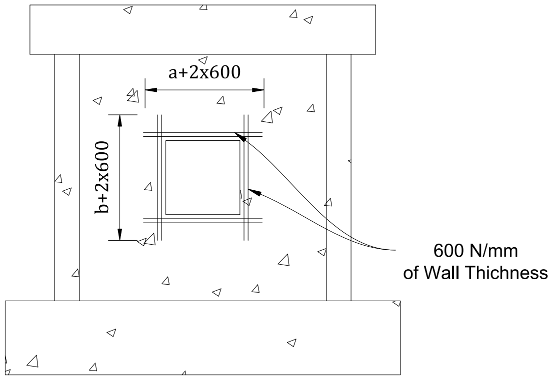

e. NZ 3101.1 - 06

Fig. 2.8 Code Recommendations for Shear wall with opening

2.7 CONCLUDING REMARKS

An overview of experimental, analytical and numerical studies carried out on reinforced concrete squat shear walls with and without openings has been discussed. Further, recommendations by various codes on shear walls have been discussed. It can be noticed that various codes of practice and researchers proposed empirical and semi-equations for predicting shear strength of RC walls. The prediction by various empirical, semi-empirical and code equations is highly deviating. Accuracy of such predictions is a great concern for designers. Such deviation in prediction needs to be addressed. From the literature in shear wall with openings, only few authors have done experimental work on walls with openings. Other researchers using numerical studies on walls with openings showed contradictory and deviating conclusions. Experimental studies performed with varying parameters result in no common conclusion on walls with opening. This understands behaviour of RC walls with openings is least known. Similarly, study on walls without openings also differ at large amongst authors which has been explained in detail. Performance of shear wall seems to be significantly influenced by shape of opening, its dimensions and location in walls. Even several national codes do not include provisions for detailing of reinforcement in shear walls with openings, but few national codes recommend additional corner reinforcement around openings. Further, strengthening of shear wall with openings also need to be addressed.

CHAPTER 3

ASSESSMENT OF SHEAR STRENGTH OF RC SQUAT SHEAR WALLS

3.1 GENERAL

Prediction of shear strength of RC walls according to various empirical, semi-empirical and codes of practice is highly deviating from each other. Accuracy of such predictions is a major concern for designers. Though several factors influence shear strength of RC walls, influence of important parameters such as vertical and horizontal reinforcement, axial load, and boundary elements is still debatable. Such deviation in prediction of shear strength of RC walls needs to be addressed due to this deviation. Several predicting equations proposed and reported prominently in various sources have been assessed through statistically based 333 selective experimental data points. Variation of predicted shear strength of RC walls as per existing equations has been inferred. Prediction of shear strength of RC shear wall by few equations and codes of practice are in proximity with statistical experimental data. Selective main factors influencing shear strength of RC walls have been emphasised.

3.2 SELECTED EXPERIMENTAL DATABASE

Research efforts on squat RC walls with several influencing parameters have been reported from the 1950s to till date. Data base on RC squat shear walls from 333 experimental results have been selected carefully from sources by *Galletly (1952), Benjamin et al. (1953), Muto et al. (1953), Antebi et al. (1960), Ryo (1963), Tsuboi et al. (1967), Alexander et al. (1973), Hirosawa (1975), Barda et al. (1977), Cardenes et al. (1978), Sugano et al. (1980), Pauley et al. (1992), Aoyagi et al. (1984), Maier et al. (1985), Wiradinata et al. (1986), Tanabe et al. (1987), Fukuzawa et al. (1988), Lefas et al. (1990), Kabeasawa et al. (1992), Mo (1993), Gupta et al. (1998), Jiang et al. (1999), Salonikios et al. (1999), Pedro et al. (2002), Dabbage (2005), Farvashany et al. (2008), Kuang et al. (2008), Massone et al. (2009), Luna et al. (2015), Yoshizuaki et al. (2015).* The selected data points are shown in Table A-1. All standards and researchers agreed up on that walls with aspect ratio less than two are squat walls. Hence, database assessed has been selected from tests on walls with aspect ratio less than two.

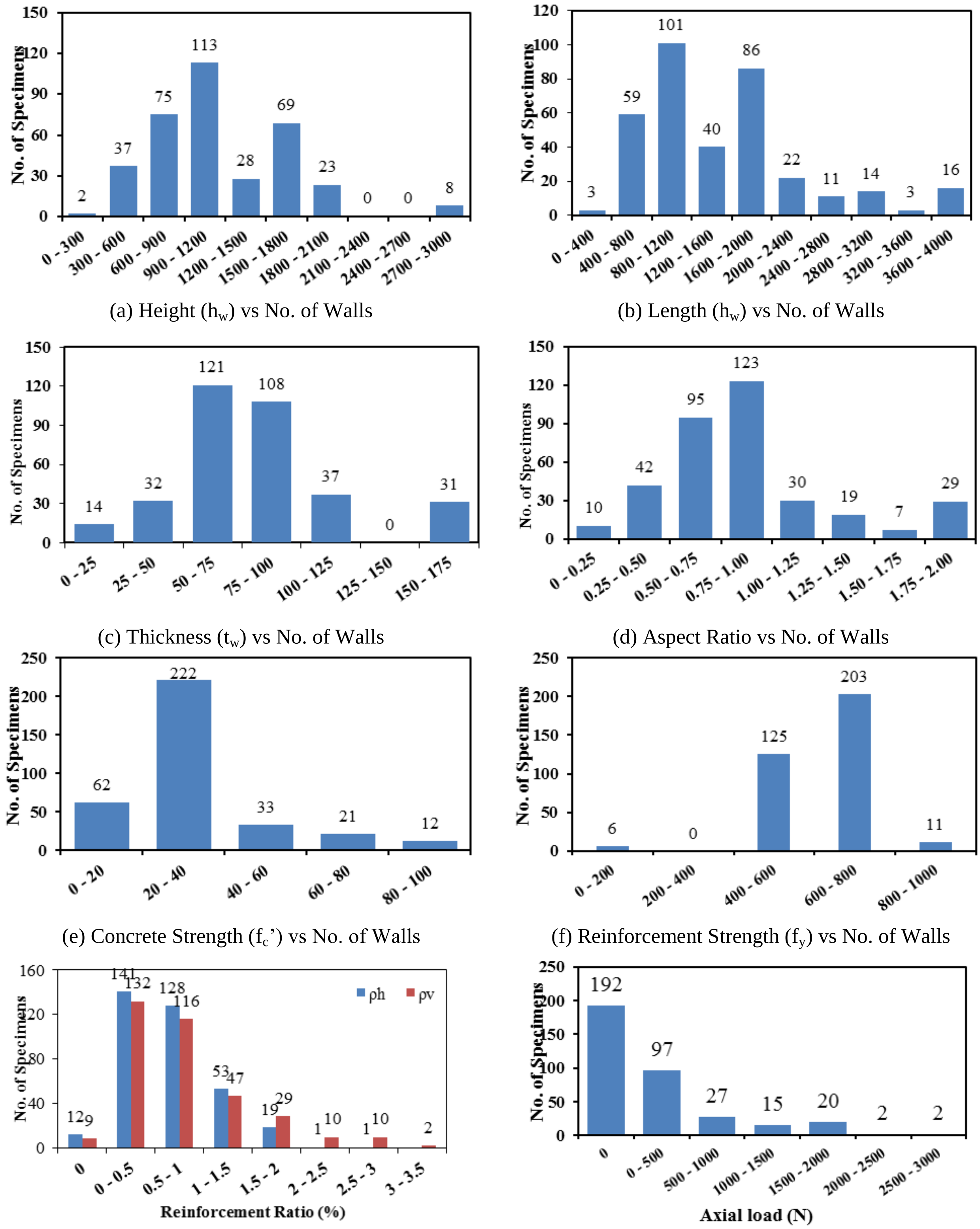

(a) Height (h_w) vs No. of Walls

(b) Length (h_w) vs No. of Walls

(c) Thickness (t_w) vs No. of Walls

(d) Aspect Ratio vs No. of Walls

(e) Concrete Strength (f_c') vs No. of Walls

(f) Reinforcement Strength (f_y) vs No. of Walls

(g) Reinforcement Ratio (ρ_h & ρ_v) vs No. of Walls

(h) Axial Load (N) vs No. of Walls

Fig. 3.1 Frequency Distribution of Collected Database

Frequency distribution of selected database is shown in Figure 3.1. Many details of geometric parameters of shear wall for experimental purpose can be inferred. Almost 300 shear walls out of 333 shear walls have their lengths and heights are less than 2.0m. Most tested walls are scaled down for easy handling in laboratories. Many researchers used aspect ratio less than 1.0 for pure shear failure of wall. Low to medium strength concrete has been used in many experimental walls as in plane strength of wall is very high. Reinforcement ratio used was 1.0 % or below in most cases. Almost 60% of walls were tested without axial load implying single storey building.

Scatter has been plotted for each geometrical parameter from experimental database where shear strength is normalized with concrete strength (f_c'). It gives some rough idea for behaviour of shear wall with parameters. Shear strength increases with increase in length, height, and thickness of wall. Shear strength of wall is high with low aspect ratio. It can also infer that walls with boundary elements show increased shear strength than rectangular shear walls. Scatter of data points is shown in Figure 3.2.

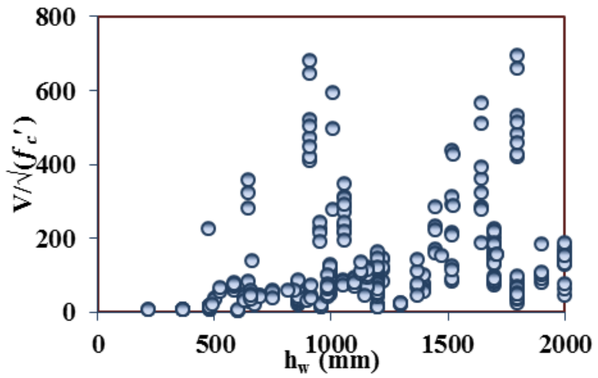

h_w vs $V/\sqrt{(f_c')}$

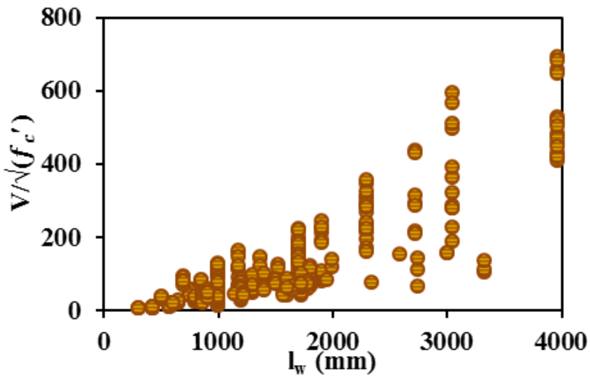

l_w vs $V/\sqrt{(f_c')}$

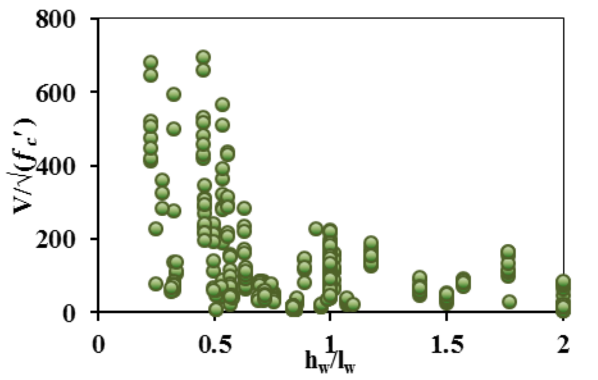

h_w/l_w vs $V/\sqrt{(f_c')}$

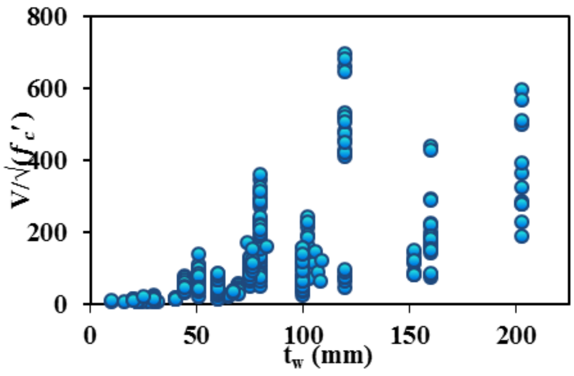

t_w vs $V/\sqrt{(f_c')}$

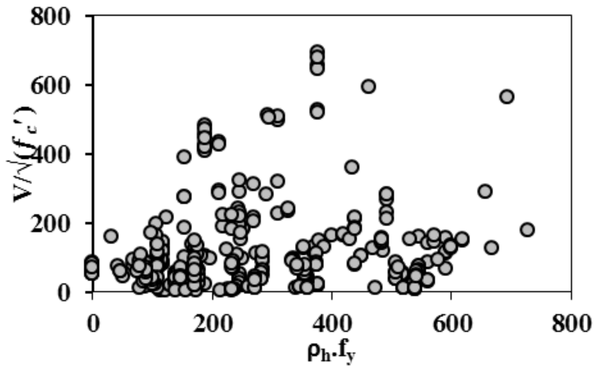

$\rho_h.f_y$ vs $V/\sqrt{(f_c')}$

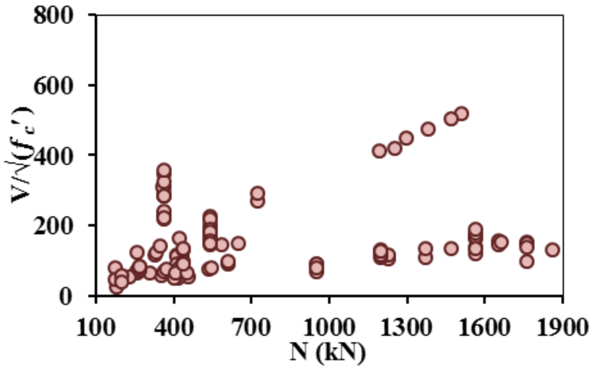

N vs $V/\sqrt{(f_c')}$

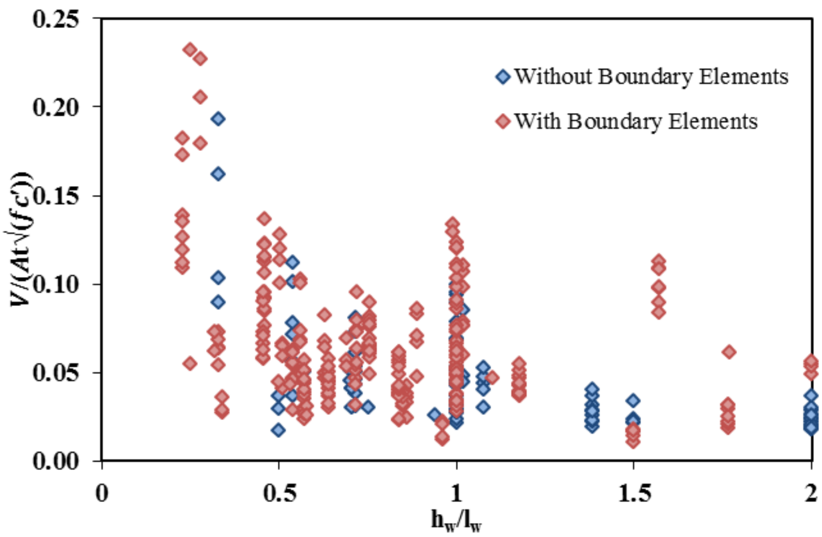

h_w/l_w vs $V/(A_t\sqrt{(f_c')})$

Fig. 3.2 Scatter of shear wall Parameters in Database

3.3 Predictive Equation for Shear Strength of RC Walls

Sixteen equations identified for predicting shear strength of RC squat shear walls by codes of practice and researchers are summarised in Table 3.1. All these sixteen equations have been described in detail in Section 2.3 of Chapter 2. Predictive equations by *IS 456-2000, ACI 318-14, ACI 318-19, ASCE/SEI 43-05, MCBC-04, EC 08-04, AIJ-99, AS 3600-09, NZ 3101.1-06, Barda et al. (1977), Wood (1990), Hernandez et al. (1980), Sánchez et al. (2010), Gulec et al. (2009), Kaseem et al. (2010), Luna et al. (2019).* Except the prediction by *Gulec et al. (2009), Kaseem et al. (2010),* and *Luna et al. (2019),* predictive equations by others on shear strength of squat RC walls do not account for influence of boundary elements. *Kaseem et al. (2010)* proposed two distinct equations for predicting shear strength of walls with and without boundary elements. Influence of vertical and horizontal reinforcement and axial load on walls differs from each other. Confusion aroused due to different notations used to denote various parameters in shear wall by codes and researchers, following notations demonstrated Figure 3.3 are adopted in this study.

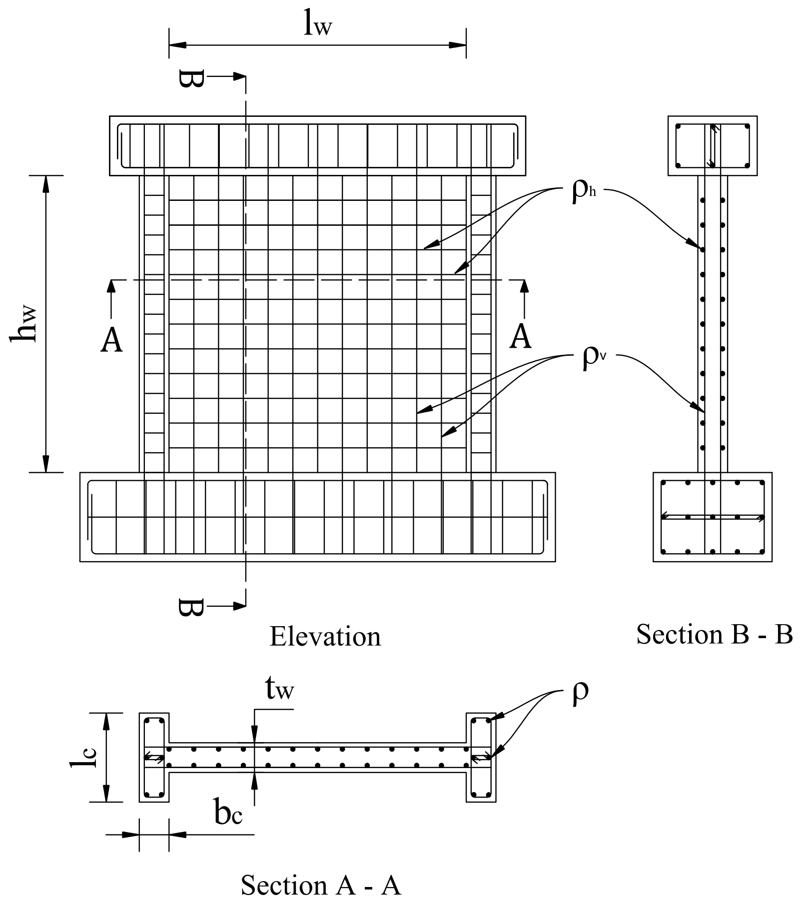

Fig. 3.3 Notations and typical sectional reinforcement details of a shear wall

Table 3.1 Predictive equation for Shear Strength of RC walls

Eq. No.	Standard/ Literature	Peak Shear Strength expression	Unit
1	*ACI 318–14 (Ch. 11 – Walls)*	**Concrete Contribution, V_c (Lower of)** **Steel Contribution, V_s** $V_c = 0.27\lambda\sqrt{f_c'}h_w d + \frac{N_u d}{4l_w}$; $V_c = \left(0.05\lambda\sqrt{f_c'} + \frac{l_w\left(0.1\lambda\sqrt{f_c'} + 0.2\frac{N_u}{l_w h}\right)}{\frac{M_u}{V_n} - \frac{l_w}{2}}\right)h_w d$ $\quad V_s = \frac{A_v f_y d}{s}$ $\boldsymbol{V_{n1} = V_c + V_s} \leq 0.83\sqrt{f_c'}h_w d$	N
2	*ACI 318–19 (Ch. 18–Sp. St. walls)*	**Concrete Contribution, V_c** **Steel Contribution, V_s** $V_c = A_g\alpha_c\lambda\sqrt{f_c'}$; $\quad V_s = A_g\rho_t f_y$ $\boldsymbol{V_{n2} = V_c + V_s}$	N
3	*ASCE/SEI 43-05*	$\boldsymbol{V_{n3}} = v_n\, d\, t_w$; Where, $v_n = 8.3\sqrt{f_c'} - 3.4\sqrt{f_c'}\left(\frac{h_w}{l_w} - 0.5\right) + \frac{N_u}{4l_w t_w} + \rho_{se}f_y \quad \leq \quad 20\sqrt{f_c'}$	lb
4	*MCBC–04*	**Concrete Contribution, V_c** **Steel Contribution, V_s** *If* $h_w/l_w \leq 1.5$, $V_c = 0.27\sqrt{f_c'}t_w l_w$; $\quad V_s = \rho_h f_y t_w l_w$ *If* $h_w/l_w > 1.5$, $\boldsymbol{\rho_v} < 0.015$, $V_c = 0.3t_w d(0.2 + 20\rho_v)\sqrt{f_c^1}$; *Else*, $V_c = 0.16t_w d\sqrt{f_c^1}$. $\boldsymbol{V_{n4} = V_c + V_s}$	N
5	*EC 08-04*	**Concrete Contribution, V_c** **Steel Contribution, V_s** $V_c = \{ Max\ [180\ x\ (\rho_v\ x\ 100)^{1/3}, 35\sqrt{1 + \sqrt{\frac{0.2}{d}}\ f_c'^{1/6}}][1 + \sqrt{\frac{0.2}{d}}\ ]\ f_c'^{1/3} + 0.15\ x\ \frac{N_u}{A_c}\}t_w d$ $\quad V_s = b_w(0.8l_w)\,\rho_h f_y$ $\boldsymbol{V_{n5} = V_c + V_s}$	N
6	*AIJ-99*	**Concrete Contribution, V_c** **Steel Contribution, V_s** $V_c = \frac{\tan\theta\,(1-\beta)tL\vartheta f_c'}{2} \geq 0$;Where, $\vartheta = 0.7 - \frac{f_c'}{2000}$; $\tan\theta = \sqrt{(\frac{h_w}{l_w})^2 + 1} - \frac{h_w}{l_w}$; $\beta = \frac{(1+\cot^2\varepsilon)\rho_h f_{yh}}{\vartheta f_c^1}$ $\quad V_s = \rho_h f_{yh} tl$ $\boldsymbol{V_{n6} = V_c + V_s}$	N
7	*AS 3600-09*	**Concrete Contribution, V_c** **Steel Contribution, V_s** If $h_w/l_w \leq 1$, $V_c = (0.66\sqrt{f_c'} - 0.21\frac{h_w}{l_w}\sqrt{f_c'})\ 0.8l_w t_w$ $\quad V_s = \rho_w f_y(0.8l_w t_w)$ If $h_w/l_w > 1$, $V_c = \left(0.05\sqrt{f_c'} + \frac{0.1\sqrt{f_c'}}{\left(\frac{h_w}{l_w} - 1\right)}\right)0.8l_w t_w \geq 0.17\sqrt{f_c'}\ (0.8l_w t_w)$ $\boldsymbol{V_{n7} = V_c + V_s} \leq 0.2\ f_c^1(0.8l_w t_w)$	N

8	*NZ 3101.1-06*	**Concrete Contribution, V_c** **Steel Contribution, V_s** $V_c = [Min\{0.17(\sqrt{f_c'} + \frac{N_u}{A_g}), 0.05\sqrt{f_c'} + \frac{l_w(0.1\sqrt{f_c'}+0.2\frac{N_u}{A_g})}{\frac{M_u}{V_u} - \frac{l_w}{2}}, 0.27\sqrt{f_c'} + \frac{N_u}{4A_g}\}]A_w$ $V_s = t_w(0.8l_w)\rho_h f_y$ $\boldsymbol{V_{n8} = V_c + V_s}$	N
9	*Barda et al. (1977)*	**Concrete Contribution, V_c** **Steel Contribution, V_s** $V_n = \left(8\sqrt{f_c'} - 2.5\sqrt{f_c'}\frac{h_w}{l_w} + \frac{N_u}{4l_w t_w}\right)t_w d;$ $V_s = \rho_v f_y t_w d$ $\boldsymbol{V_{n9} = V_c + V_s}$	lb
10	*Wood (1990)*	$6\sqrt{f_c'}A_w \le \boldsymbol{V_{n10}} = \frac{A_{vf} f_y}{4} \le 10\sqrt{f_c'}A_w$	lb
11	*Hernandez et al. (1980)*	**Concrete Contribution, V_c** **Steel Contribution, V_s** $V_c = V_0\sqrt{1 + \frac{\sigma}{V_0}}; \quad \frac{\sigma}{V_0} \le 5;$ If $\frac{M_u}{V_n l_w} < 0.25$, $V_s = \rho_v f_y t_w l_w$; If $\frac{M_u}{V_n l_w} > 1.25$; $V_s = \rho_h f_y t_w l_w$; $V_0 = \left[0.5 - 0.09\left(\frac{M_u}{V_n l_w}\right)^2\right]\sqrt{f_c'};$ If $0.25 < \frac{M_u}{V_n l_w} < 1.25$, $V_s = (\rho_h f_y\left(\frac{M_u}{V_n l_w}\right) - 0.25) + \rho_v f_y\left(1.25 - \frac{M_u}{V_n l_w}\right)t_w l_w$. $\boldsymbol{V_{n11} = V_c + V_s}$	N
12	*Sánchez et al. (2010)*	**Concrete Contribution, V_c** **Steel Contribution, V_s** $V_c = \left(\gamma\eta_v + \frac{0.04N_u}{A_w}\right)\sqrt{f_c'}$; Where $\gamma = 0.42 - 0.08\frac{M_u}{V_n l_w}$; $\eta_v = 0.75 + 0.05\rho_v f_y$; $\eta_h = 1 - 0.16\rho_h f_y$ $V_s = \eta_h\rho_v f_y$ $\boldsymbol{V_{n12} = V_c + V_s}$	N
13	*Gulec et al. (2011)*	$(\boldsymbol{V_{n13}})_{rec} = \frac{1.5\sqrt{f_c^1}A_w + 0.25F_{vw} + 0.20F_{vbe} + 0.40N_u}{\sqrt{h_w/l_w}} \le 10\sqrt{f_c'}A_w$ $(\boldsymbol{V_{n13}})_{BE} = \frac{(0.04f_c^1)A_{eff} + 0.40F_{vw} + 0.15F_{vbe} + 0.35N_u}{\sqrt{h_w/l_w}} \le 15\sqrt{f_c'}A_g$	lb
14	*Kassem et al. (2010)*	$(\boldsymbol{V_{n14}})_{rec} = 0.27f_c'[\psi k_s \sin(2\alpha) + 0.11\,\omega_h\frac{h_w}{d} + 0.30\,\omega_v \cot(\alpha)] \le 0.83\sqrt{f_c'}$ $(\boldsymbol{V_{n14}})_{BE} = 0.47f_c^1[\psi k_s \sin(2\alpha) + 0.15\,\omega_h\frac{h_w}{d_w} + 1.76\,\omega_v \cot(\alpha)] \le 1.25\sqrt{f_c'}$ Where, $\Psi = 0.95 - \frac{f_c'}{250}$; $\omega_h = \frac{\rho_h f_y}{f_c^1}$; $\omega_v = \frac{\rho_v f_y}{f_c^1}$; $\alpha = tan^{-1}(h_w/d)$; $k_s = a_s/d_w$	N
15	*Luna et al. (2019)*	$(\boldsymbol{V_{n15}})_{rec} = 1.2\left(\rho_l A_{cv} f_{\bar{y}} + \frac{N_u}{l_w}l_w\right)\left(1 - 0.7\frac{h_w}{l_w} - \frac{c}{l_w}\right) + 0.25\rho_t\frac{h_w}{l_w}A_{cv}f_y + 0.5\frac{N_u}{l_w}c \le 10\sqrt{f_c'}A_{cv}$ $(\boldsymbol{V_{n15}})_{BE} = 1.2\left(\rho_l A_{cv} f_y + \frac{N_u}{l_w}\right)\left(1 - 0.7\frac{h_w}{l_w} - 2\frac{l_{BE}}{l_w}\right) + 1.7\left(\frac{N_u}{l_w}l_{BE} + P\right) + 1.2\rho_{BE}A_{BE}f_y + 0.25\rho_t A_{cv}\frac{h_w}{l_w}f_y \le 10\sqrt{f_c'}A_{cv}$ *Where,* $c = \frac{\left(\rho_l t_w(1.2f_y) + \frac{N_u}{l_w}\right)(1.2h_w)}{(2.4\rho_l(1.2f_y)t_w - \frac{N_u}{l_w})}$	lb

3.4 INFLUENCING PARAMETERS IN RC SHEAR WALLS

In general, performance of RC walls is influenced by its aspect ratio, slenderness ratio, quantity of flexural reinforcement, quantity and distribution of vertical, and horizontal reinforcement and axial load, compressive strength of concrete, and yield strength of reinforcement. However, all predictive shear strength equations in codes and by researchers have not accounted for all influencing factors. Geometric dimensions of wall such as height, h_w, length, l_w and thickness, t_w and ratio of height-to-length (h_w/l_w) known as aspect ratio, play a major role on its structural response. Slenderness ratio is the ratio of height-to-thickness, (h_w/t_w) influences lateral buckling strength of wall. Boundary element may be in form of enlarged cross-section at ends, provided with and without longitudinal reinforcement or end zones of wall provided with special reinforcement. Strength and stiffness of RC walls are influenced by characteristics of boundary elements i.e. length, l_c and thickness, t_c, and their ratio l_c/t_c. Compressive strength of concrete, f'_c and yield strength of reinforcement, f_y also influence behaviour and strength of RC walls. Quantity of flexural reinforcement, ρ_t, quantity of vertical reinforcement, ρ_v and horizontal reinforcement, ρ_h, and their distribution play significant role on shear strength, cracking resistance, and ductility of RC shear walls. Axial load, N_u also influences strength, stiffness, and stability of RC walls. Accuracy of prediction of shear strength depends up on form of equation and factors. All influencing parameters need to be judiciously identified through an appropriate form for better prediction. Hence, an attempt has been made to assess influence of factors in various predictive equations through statistical analysis. Table 1 shows parameters in various shear strength predictive equations of RC walls.

Table 3.2 Summary of parameters adopted in various shear strength equations of shear walls

Eq. No.	Standards/Literature	Parameters Considered										
		h_w	l_w	t_w	l_c	b_c	f_c'	f_y	ρ_v	ρ_h	ρ	N_u
1	*IS 456-2000*	✓	✓	✓	×	×	✓	✓	✓	✓	×	×
2	*ACI 318-14 (Ch. 11)*	✓	✓	✓	×	×	✓	✓	✓	×	×	✓
3	*ACI 318-19 (Ch.18)*	✓	✓	✓	×	×	✓	✓	✓	×	×	×
4	*ASCE/SEI 43-05*	✓	✓	✓	×	×	✓	✓	✓	✓	×	✓
5	*MCBC-04*	✓	✓	✓	×	×	✓	✓	✓	✓	×	×
6	*EC 08-04*	✓	✓	✓	×	×	✓	✓	✓	✓	×	✓
7	*AIJ-99*	✓	✓	✓	×	×	✓	✓	×	✓	×	×
8	*AS 3600-09*	✓	✓	✓	×	×	✓	✓	✓	✓	×	×
9	*NZ 3101.1-06*	✓	✓	✓	×	×	✓	✓	×	✓	×	✓
10	*Barda et al. (1977)*	✓	✓	✓	×	×	✓	✓	✓	×	×	✓

11	*Wood (1990)*	✗	✓	✓	✗	✗	✓	✓	✓	✗	✗	✗
12	*Hernandez et al. (1980)*	✓	✓	✓	✗	✗	✓	✓	✓	✓	✗	✓
13	*Sánchez et al. (2010)*	✓	✓	✓	✗	✗	✓	✓	✓	✓	✗	✓
14	*Gulec et al. (2011)*	✓	✓	✓	✓	✓	✓	✓	✓	✓	✓	✓
15	*Kassem et al. (2010)*	✓	✓	✓	✗	✗	✓	✓	✓	✓	✗	✗
16	*Luna et al. (2019)*	✓	✓	✓	✓	✗	✓	✓	✓	✓	✓	✓

3.5 STATISTICAL ASSESSMENT OF THE SHEAR STRENGTH

Empirical and semi-empirical equations proposed for predicting shear strength of RC shear walls have been assessed for accuracy of prediction using selected 333 experimental test data on RC squat shear walls. Experimental results in various sources are tabulated in Table A - 1.

Statistical assessment of predicted shear strength is an appropriate and easier way to describe strengths and weaknesses of such predictive equations and enables in identifying parameters to be retained and allows formulating another refined equation with improved accuracy in agreement with experimental database. Shear strength ratio is defined as the ratio of predicted shear strength from proposed equations-to-experimental shear strength. A statistical representation of ratios of shear strength with reference to selected 333 data points from RC squat shear wall tests is shown in Table 3.3. If mean of shear strength ratio, as shown in Table 3.3, is greater than 1.0, prediction from such equations overestimates shear strength and vice-versa.

Median in Table 3.3 denotes central scattering of all data points predicted using corresponding shear strength equation. Coefficient of variation (CoV) describes dispersion of data points around the mean. Lower value of CoV indicates lower dispersion of data points around the mean. Coefficient of determination (R2) quantifies variance of predicted equations from experimental results. Higher R^2 value indicates lower error between strength using predicted equations and experimental results. Percentage predictor quantifies error of individual data points with predicted equation. If percentage predictor error is positive, then it represents percentage overestimation by corresponding equation and vice-versa. Graphic presentation is another way of analysing numerical data points. This is an effective method of understanding and interpretation of analysing data points. Ratio of predicted-to-measured shear strength vs. aspect ratio is shown as scatter diagram in Figure 3.4.

Table 3.3 Statistics of the ratio of predicted to experimental shear strength

Ratio	Equation	Mean	Median	SD	CoV	R^2	% Predictor Error
V_{n1}/V_{exp}	*IS 456-2000*	1.18	1.06	0.54	0.46	0.71	18
V_{n2}/V_{exp}	*ACI 318-14 (Ch.11)*	0.77	0.71	0.29	0.38	0.64	23
V_{n3}/V_{exp}	*ACI 318-19 (Ch.18)*	1.03	0.94	0.48	0.47	0.68	03
V_{n4}/V_{exp}	*ASCE/SEI 43-05*	0.94	0.89	0.38	0.40	0.77	-06
V_{n5}/V_{exp}	*MCBC-04*	1.05	0.97	0.48	0.46	0.68	05
V_{n6}/V_{exp}	*EC 08-04*	0.75	0.65	0.40	0.54	0.62	-25
V_{n7}/V_{exp}	*AIJ-09*	1.39	1.17	0.80	0.58	0.63	39
V_{n8}/V_{exp}	*AS 3600-09*	0.97	0.92	0.38	0.39	0.70	03
V_{n9}/V_{exp}	*NZ 3101.1-06*	1.00	0.86	0.53	0.53	0.70	01
V_{n10}/V_{exp}	*Barda et al. (1977)*	1.27	1.14	0.54	0.43	0.63	27
V_{n11}/V_{exp}	*Wood (1990)*	0.74	0.69	0.32	0.43	0.45	-26
V_{n12}/V_{exp}	*Hernandez et al. (1980)*	1.26	1.14	0.53	0.42	0.59	26
V_{n13}/V_{exp}	*Sánchez et al. (2010)*	0.87	0.84	0.29	0.34	0.76	-13
V_{n14}/V_{exp}	*Gulec et al. (2011)*	0.70	0.68	0.26	0.38	0.77	-30
V_{n15}/V_{exp}	*Kassem (2010)*	1.28	1.19	0.55	0.43	0.69	28
V_{n16}/V_{exp}	*Luna et al. (2019)*	1.07	1.03	0.53	0.49	0.73	07

Graphic presentation is another way of analysing numerical data points. This is a very effective way of understanding and interpretation of analysing the data points. The ratio of predicted-to-measured shear strength vs. aspect ratio is shown in the form of a scatter plot in Figure 3.4.

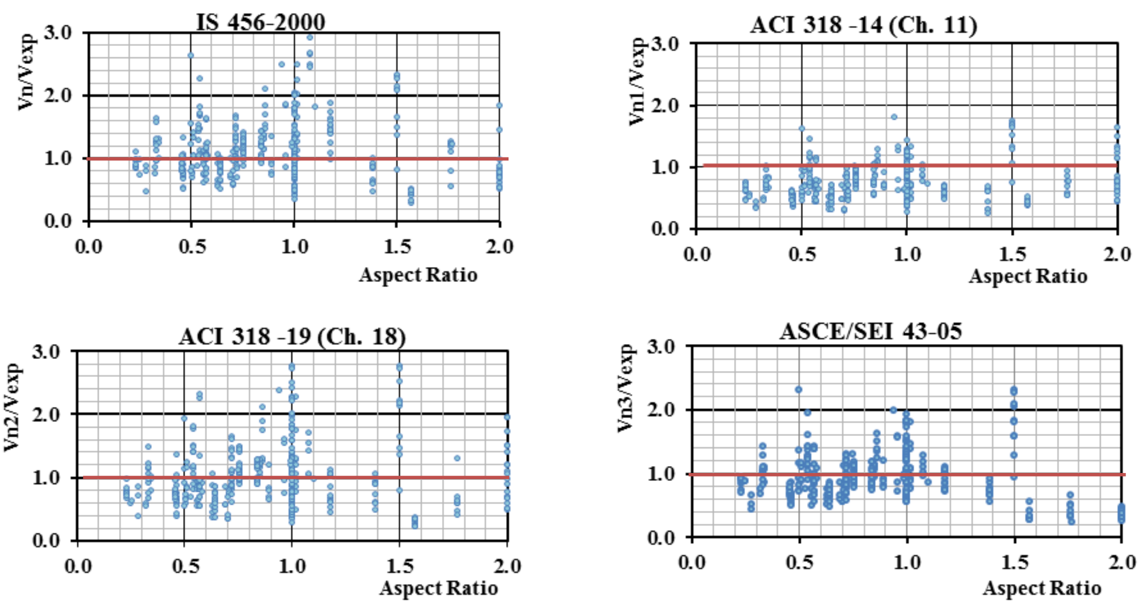

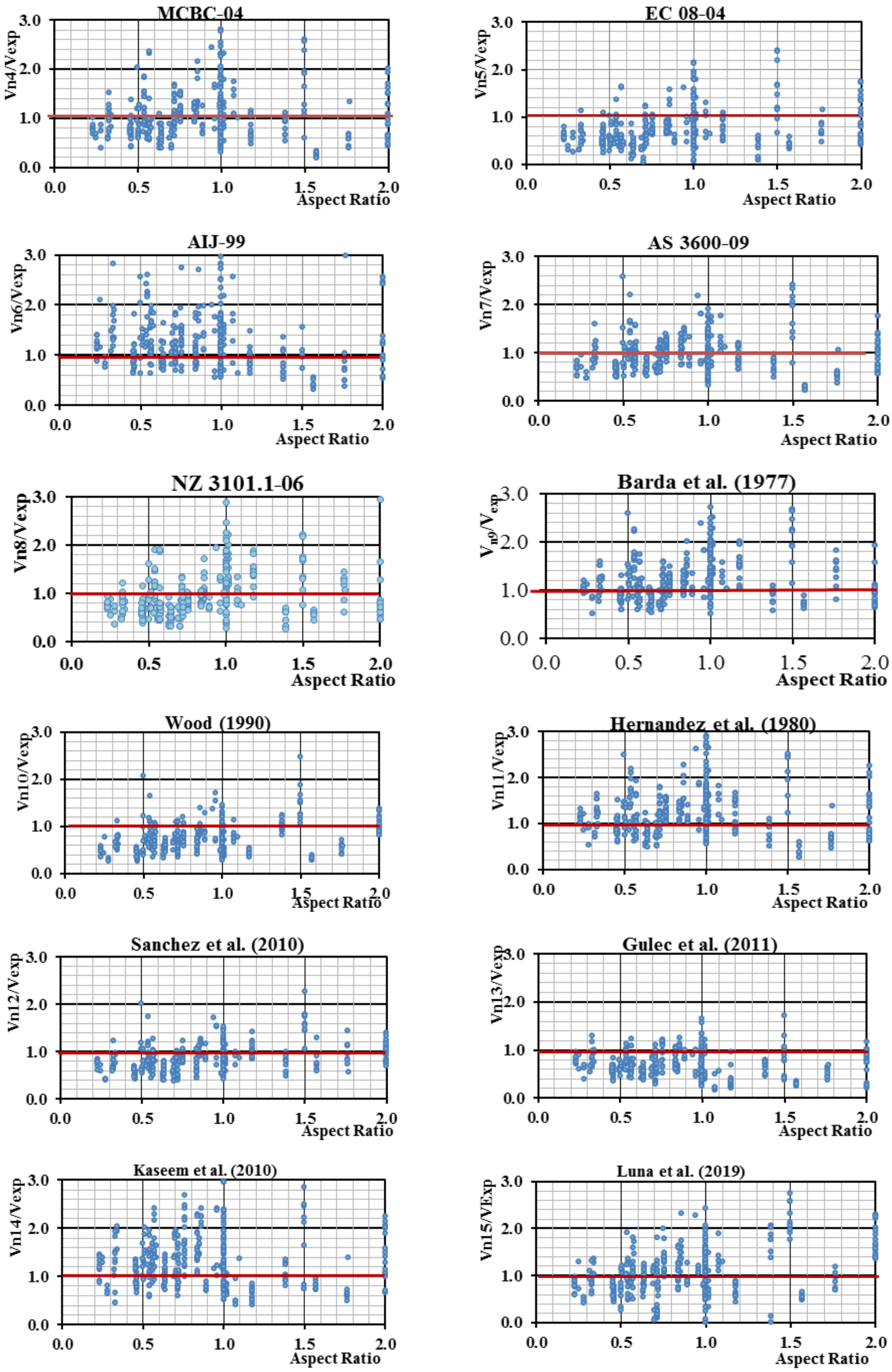

Fig. 3.4 Scatter of V_{pre}/V_{exp} vs. Aspect Ratio

Frequency distribution diagrams as shown in Figure 3.5 display number of observations within a particular interval of ratio of predicted-to-measured shear strength. This is a typical representation showing distribution of different ranges among all observations in a quantitative dataset. It is advantageous for describing shape, centre and spread for better understanding distribution of dataset. One of challenges in constructing histograms is selecting optimal number of bins. To determine a reasonable bin width, Freedman-Diaconis rule is used here, which was designed to minimize difference between area under empirical probability distribution and area under theoretical probability distribution. Formally, rule takes as input interquartile range (IQR) and number of observations n in empirical dataset, and returns a bin width estimate. The rule can be expressed as follows.

$$\text{Bin width} = \frac{2(\mathrm{IQR})}{\sqrt[3]{n}}$$

Where, IQR - Difference between largest and smallest values in middle 50% of an empirical dataset;

n – Total number of dataset

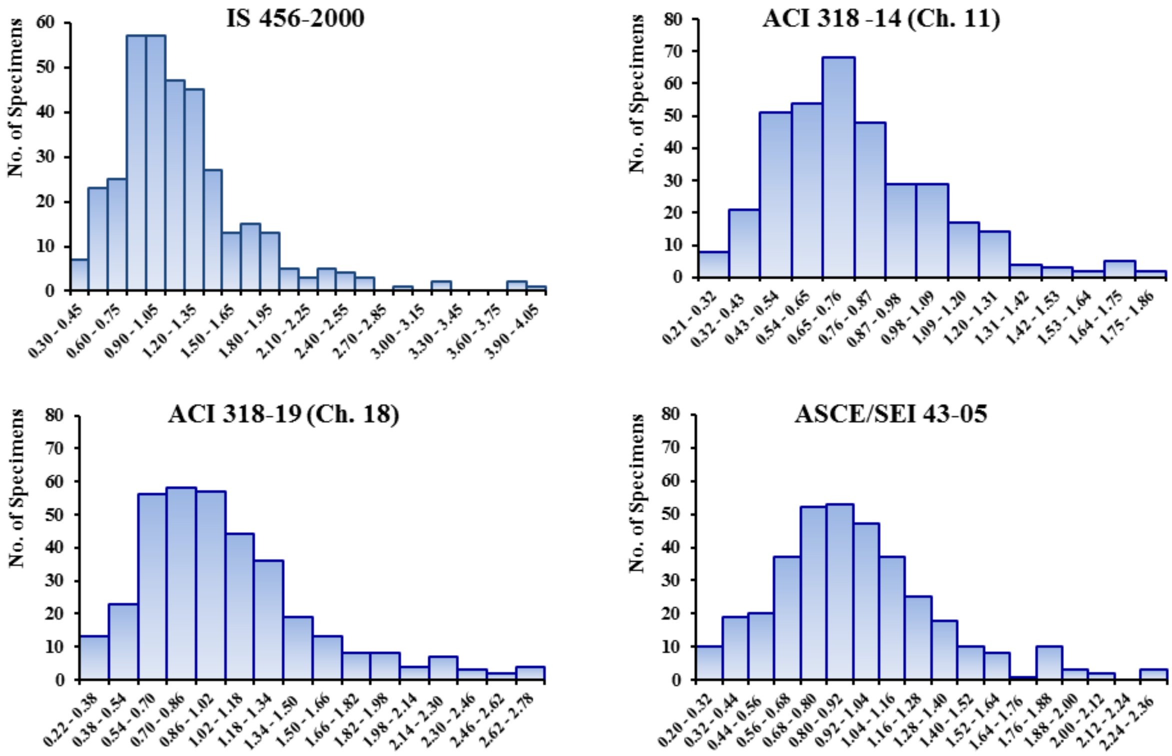

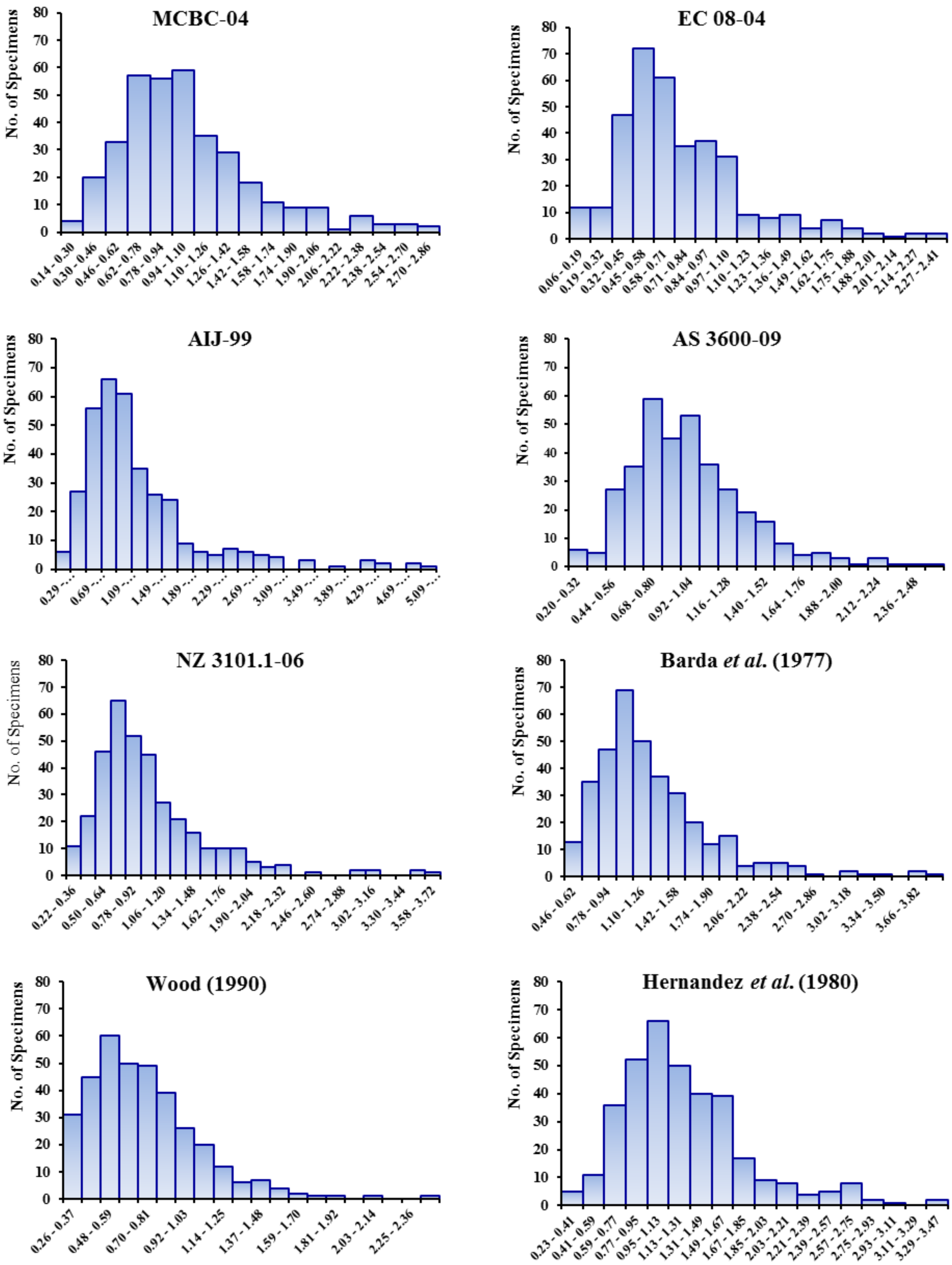
MCBC-04
EC 08-04
AIJ-99
AS 3600-09
NZ 3101.1-06
Barda *et al.* (1977)
Wood (1990)
Hernandez *et al.* (1980)
No. of Specimens

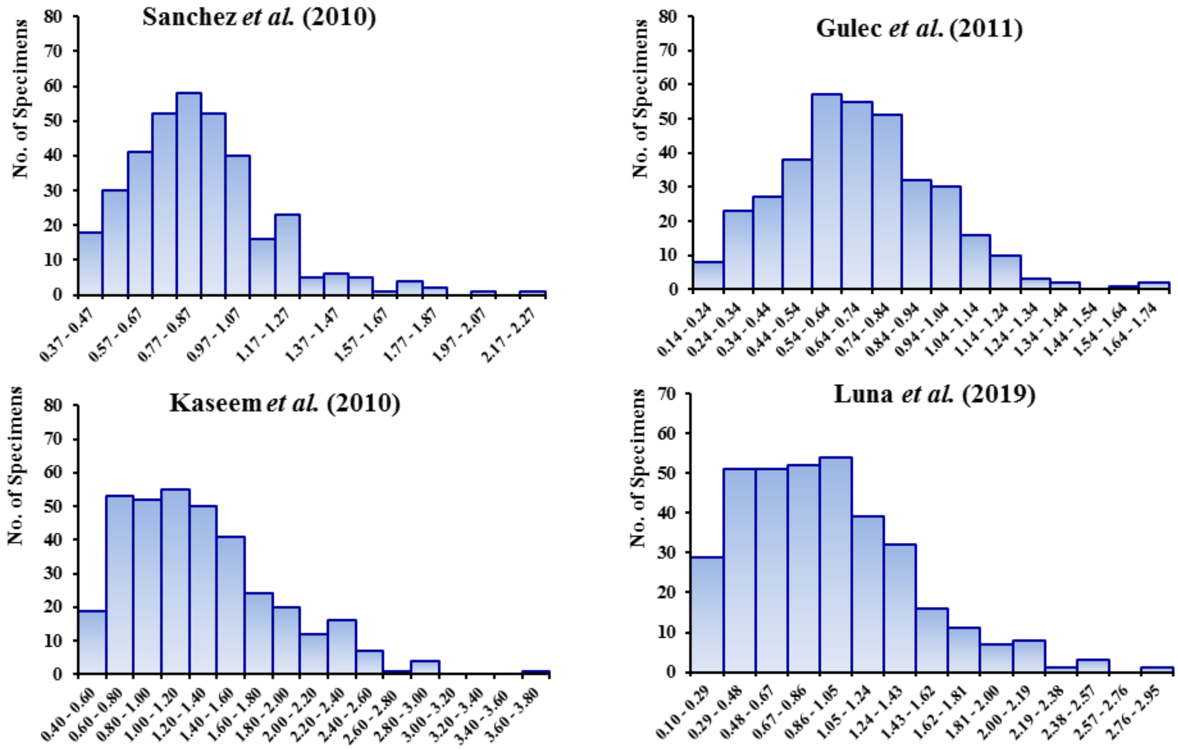

Fig. 3.5 Frequency Distribution of V_{pre}/V_{exp}

A box and whisker plot is a graphical representation that informs five-number summary, i.e. lower extreme, lower quartile, median, upper quartile, and upper extreme. This box and whisker plots indicate whether a distribution is skewed or not, and whether there are potential unusual observations in the data points or not. The box and whisker plot, as shown in Figure 3.6, is plotted for points of ratio of predicted shear strength-to-measured shear strength against all predictive equations.

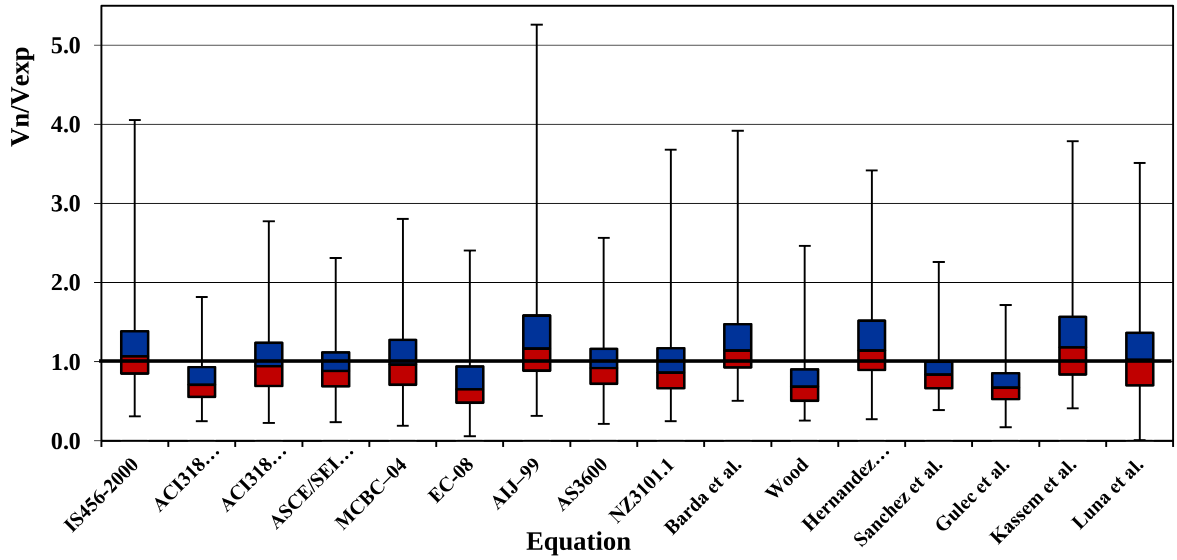

Fig. 3.6 Whisker Plots of V_{pre}/V_{exp}

3.6 Results and Discussion

Statistical assessment of accuracy of prediction of shear strength of RC squat walls by various proposals has been verified. The descriptive statistics have been discussed. Shear strength predictions by *ACI 318-19, MCBC–04, AS3600-09, NZ 3101.1-06* and *Luna et al. (2019)* result in mean shear strength ratios of 1.03, 1.05, 0.97, 1.00 and 1.07 respectively. Prediction seems to be in proximity with mean shear strength ratio. Shear strength predictions by *IS 456-2000, ACI 318-19 (Ch. 18), MCBC-04* and *Luna et al. (2019)* show comparatively better median of 1.06, 0.94, 0.97 and 1.03 respectively. Shear strength equation proposed by *Sánchez et al. (2010)* exhibits best prediction of ultimate shear strength with a coefficient of variation (CoV) of 0.34. Both *ACI 318-19* and *Sánchez et al. (2010)* equations are semi-empirical based on the truss analogy and do not consider influence of boundary elements.

Highest CoV of 0.58 is associated with AIJ-09 prediction. Shear strength equations by *ASCE/SEI 43-05, Sánchez et al. (2010)* and *Gulec et al. (2009)* show better prediction with a coefficient of determination of about 0.77. Lowest coefficient of determination is 0.45, associated with Wood's equation.

Shear strength equation by *AIJ-09* observes highest overestimate of percentage peak shear strength of 39%. Gulec et al. (2009) equation yields highest underestimate percentage shear strength of 30%. Shear strength equations by *ACI 318-19, AS3600-09* and *NZ 3101.1-06* observe lowest overestimate of peak shear strength of 3.0, 3.0, and 1.0% respectively.

Scatter diagrams of V_{pre}/V_{exp} vs. Aspect Ratio are shown in Figs. 3.4. Substantial scatter of data points can be seen from distribution diagram using all sixteen shear strength equations. Points above 1.0 of horizontal axis indicate that predicted shear strength using equations are higher than experimental results, which are not satisfactory for designing walls. Equations by *ACI 318-14, Sánchez et al. (2010)* and *Gulec et al. (2009)* show comparatively least scatter with minimum deviation from mean. Shear strength equation by *Hernandez et al. (1980)* and *Sánchez et al. (2010)* show better frequency distribution, in Figure 3.5, comparing with other equations.

A box and whisker plot, as shown in Figure 3.6, is useful in indicating skewness of scatter data distribution. Shear strength prediction by AIJ-09 shows lengthiest upper whisker among all predictions. It can be noticed that interquartile range box (IQR) using *wood's equation* and *Gulec et al. (2009)* is skewed high, which doesn't cross mean line of V_n/V_{exp}

equals to 1.0. Predictions by *ACI 318-19, MCBC-04, AS 3600-09* and *Luna et al. (2019)* show relatively least skewness as mean line crosses almost centre of interquartile range box (IQR) in the distribution. These shear strength predictions incorporated all influencing parameters on shear strength of RC walls. Some equations are more empirical may be useful for more safe and conservative designs. Table 3.4 shows performance in terms of different aspects of design.

Table 3.4 Equations with the Best performance

Statistical Parameter	Equation with Best performance
Mean	*ACI 318-19, AS3600-09, NZ 3101.1-06* and *Luna et al. (2019)*
Median	*IS 456-2000, ACI 318-19, MCBC-04* and *Luna et al. (2019).*
Coefficient of variation	*Sánchez et al. (2010)*
Coefficient of Determination	*ASCE/SEI 43-05, Sánchez et al. (2010)* and *Gulec et al. (2011)*
Predictor Error	*ACI 318-19, AS 3600-09* and *NZ 3101.1-06*
Scatter Plot	*ACI 318-14, Sánchez et al. (2010)* and *Gulec et al. (2011)*
Frequency Distribution	*Hernandez et al. (1980)* and *Sánchez et al. (2010)*
Box and Whisker Plot	*ACI 318-19, MCBC-04, AS 3600-09* and *Luna et al. (2019)*

Predictions by best equations shall be validated with acceptable experimental results for accepting such equations for accurate designs. Prediction of shear strength of RC walls has been validated with experimental findings of *Lefas et al. (1990)*, which was widely referred. Shear walls were tested under constant axial load with monotonically increasing horizontal loading, to investigate influence of axial load, compressive strength of concrete and web reinforcement. Squat shear wall with low aspect ratio has been considered as they predominantly fail by shear action. All equations referred are applicable only to squat RC walls. Geometric and material properties adopted for their experimental investigation are given in Table 3.5. Hence, these experimental observations are considered for validation of predicted shear strength by *ACI 318-19* and *Sánchez et al. (2010)*. Comparison of prediction is shown in Figure 3.7. Ratios of predicted shear strength -to-observed shear strength in various shear walls tested are shown in Figure 3.8.

Table 3.5 Geometric and Reinforcement Details of Walls and results (*Lefas et al.,1990*)

S. No.	Wall Designation	Geometrical Properties				Material Properties				Axial Load, N (kN)	Shear Strength, kN
		h_w (mm)	l_w (mm)	h_w/l_w	b_w (mm)	f_c' (MPa)	f_y (MPa)	ρ_v (%)	ρ_h (%)		
1	SW11	750	750	1.00	70	45	470	2.49	1.10	0	260
2	SW12	750	750	1.00	70	46	470	2.49	1.10	230	340
3	SW13	750	750	1.00	70	35	470	2.49	1.10	355	330
4	SW14	750	750	1.00	70	36	470	2.49	1.10	0	265
5	SW15	750	750	1.00	70	37	470	2.49	1.10	185	320
6	SW16	750	750	1.00	70	44	470	2.49	1.10	460	355
7	SW17	750	750	1.00	70	41	470	2.49	0.37	0	247

Note. ρ, l_c & b_c are zero

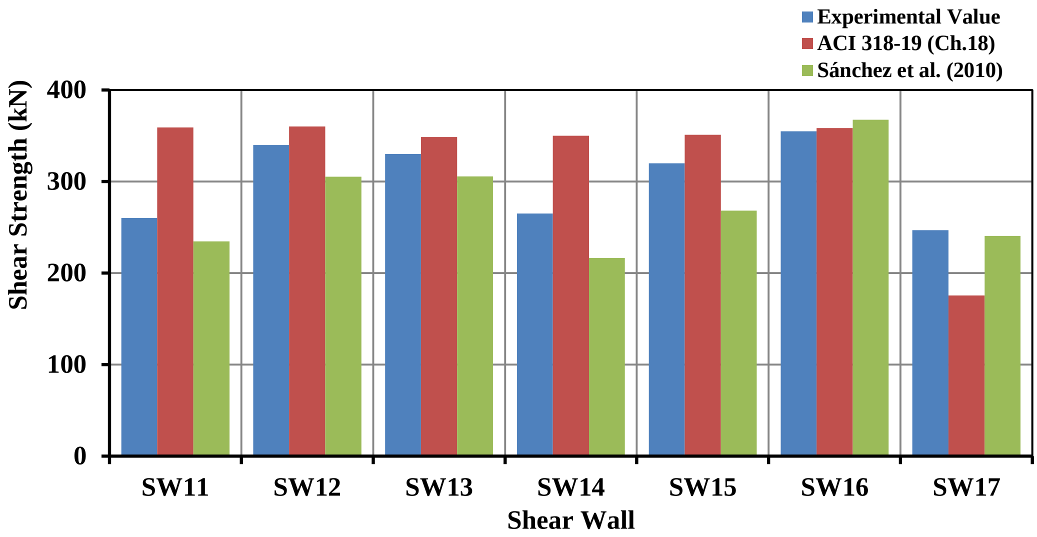

Fig. 3.7 Comparison of predicted shear strength with the observed strength (*Lefas et al., 1990*) of RC Squat shear walls

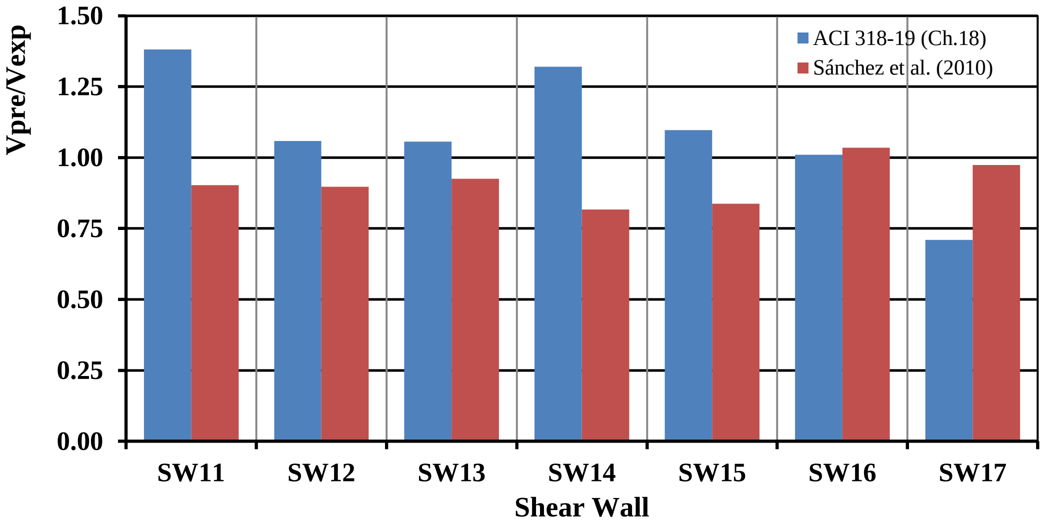

Fig. 3.8 Ratio of Predicted-to-experimental, V_{pre}/V_{exp} of squat shear walls

3.7 CONCLUDING REMARKS

Statistical assessment of prediction of shear strength of RC squat walls by various equations has been discussed.

1. All these predicting equations show entirely different scatter due to their form and level of influence of parameters selected.
2. Shear strength predictions by *ACI 318-19* and *Sánchez et al. (2010)* are closely agreeable with experimental results.
3. Prediction by *ACI 318-14* based on semi-empirical modified truss analogy performing relatively unsatisfactory.
4. Improvement of shear strength prediction needs to be attempted incorporating all parameters including influence of boundary elements.

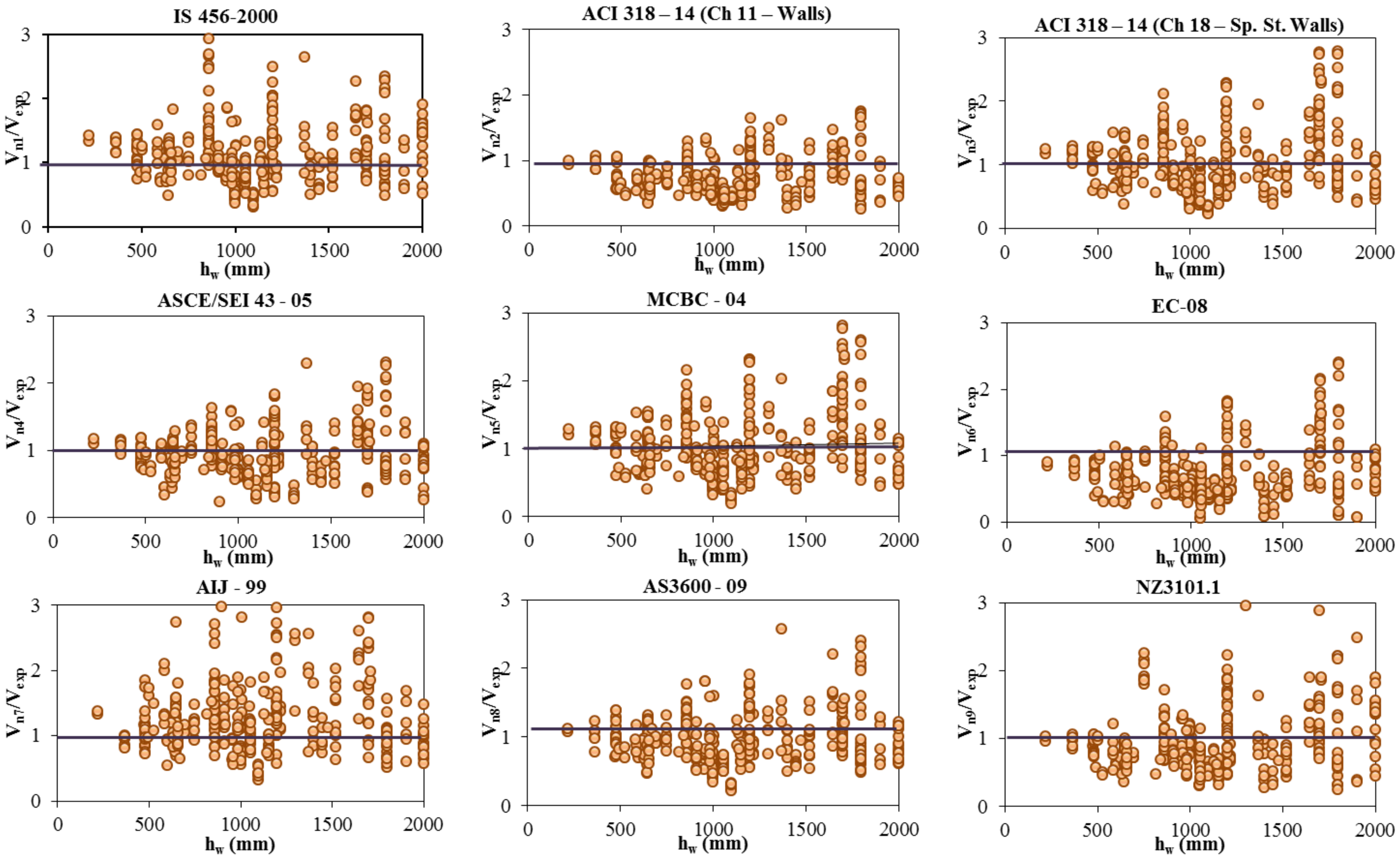

IS 456-2000
ACI 318 – 14 (Ch 11 – Walls)
ACI 318 – 14 (Ch 18 – Sp. St. Walls)
ASCE/SEI 43 - 05
MCBC - 04
EC-08
AIJ - 99
AS3600 - 09
NZ3101.1
V_{n1}/V_{exp}
V_{n2}/V_{exp}
V_{n3}/V_{exp}
V_{n4}/V_{exp}
V_{n5}/V_{exp}
V_{n6}/V_{exp}
V_{n7}/V_{exp}
V_{n8}/V_{exp}
V_{n9}/V_{exp}
h_w (mm)
0
500
1000
1500
2000
0
1
2
3

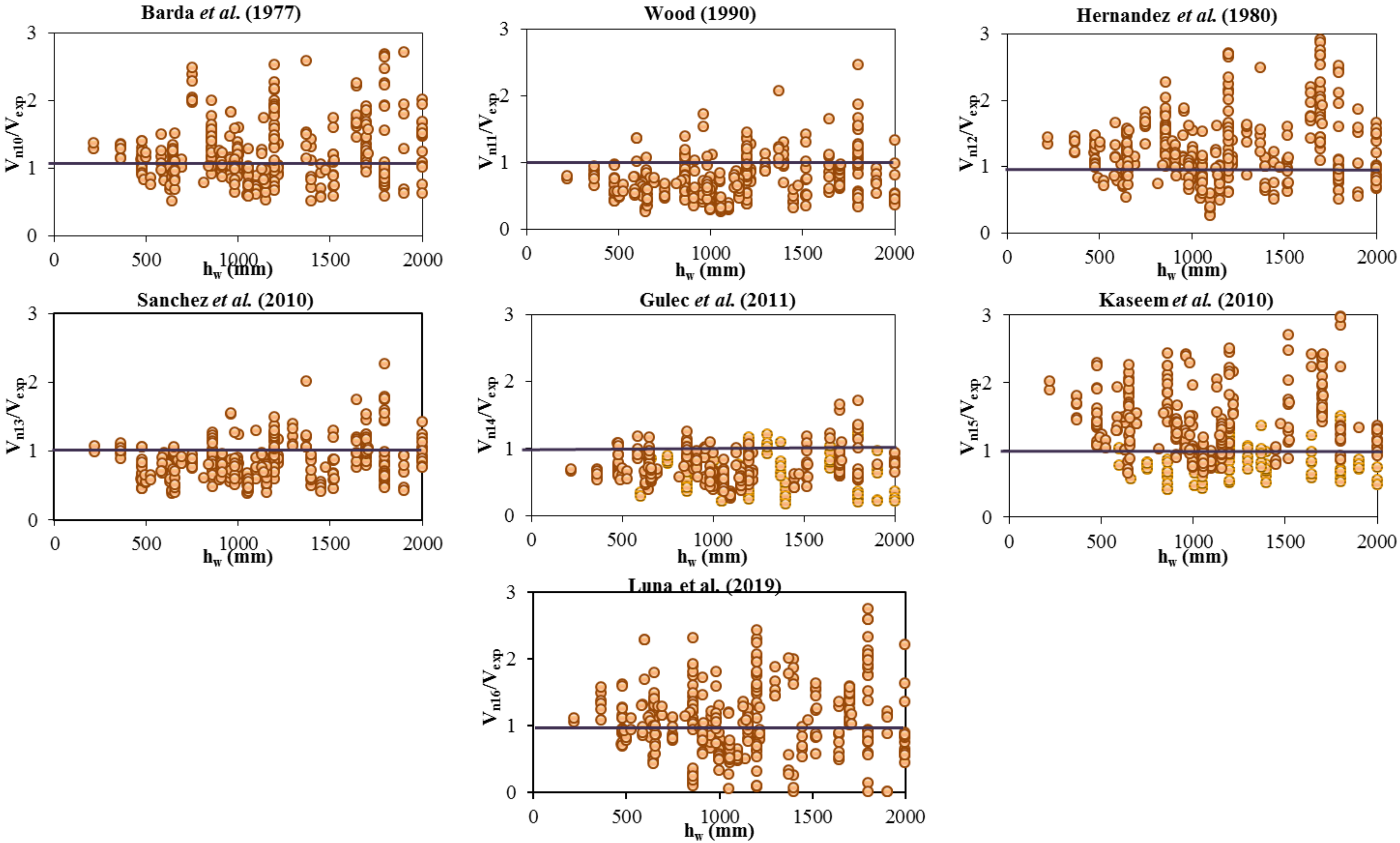

Fig. 3.9 Scatter Plot for V_{pre}/V_{exp} vs. Height of the Shear Wall

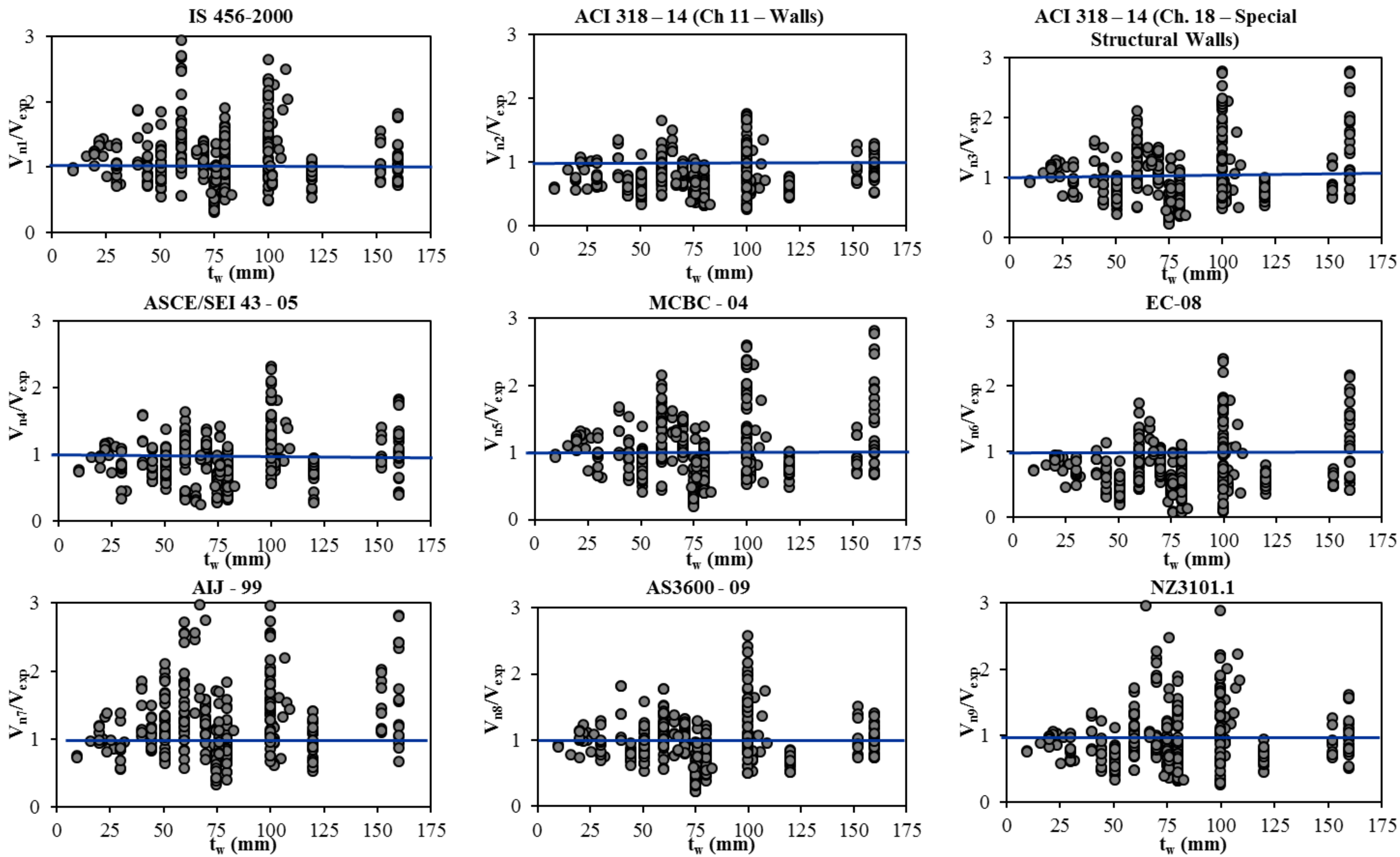
IS 456-2000
ACI 318 – 14 (Ch 11 – Walls)
ACI 318 – 14 (Ch. 18 – Special Structural Walls)
ASCE/SEI 43 - 05
MCBC - 04
EC-08
AIJ - 99
AS3600 - 09
NZ3101.1
V_{n1}/V_{exp}
V_{n2}/V_{exp}
V_{n3}/V_{exp}
V_{n4}/V_{exp}
V_{n5}/V_{exp}
V_{n6}/V_{exp}
V_{n7}/V_{exp}
V_{n8}/V_{exp}
V_{n9}/V_{exp}
t_w (mm)

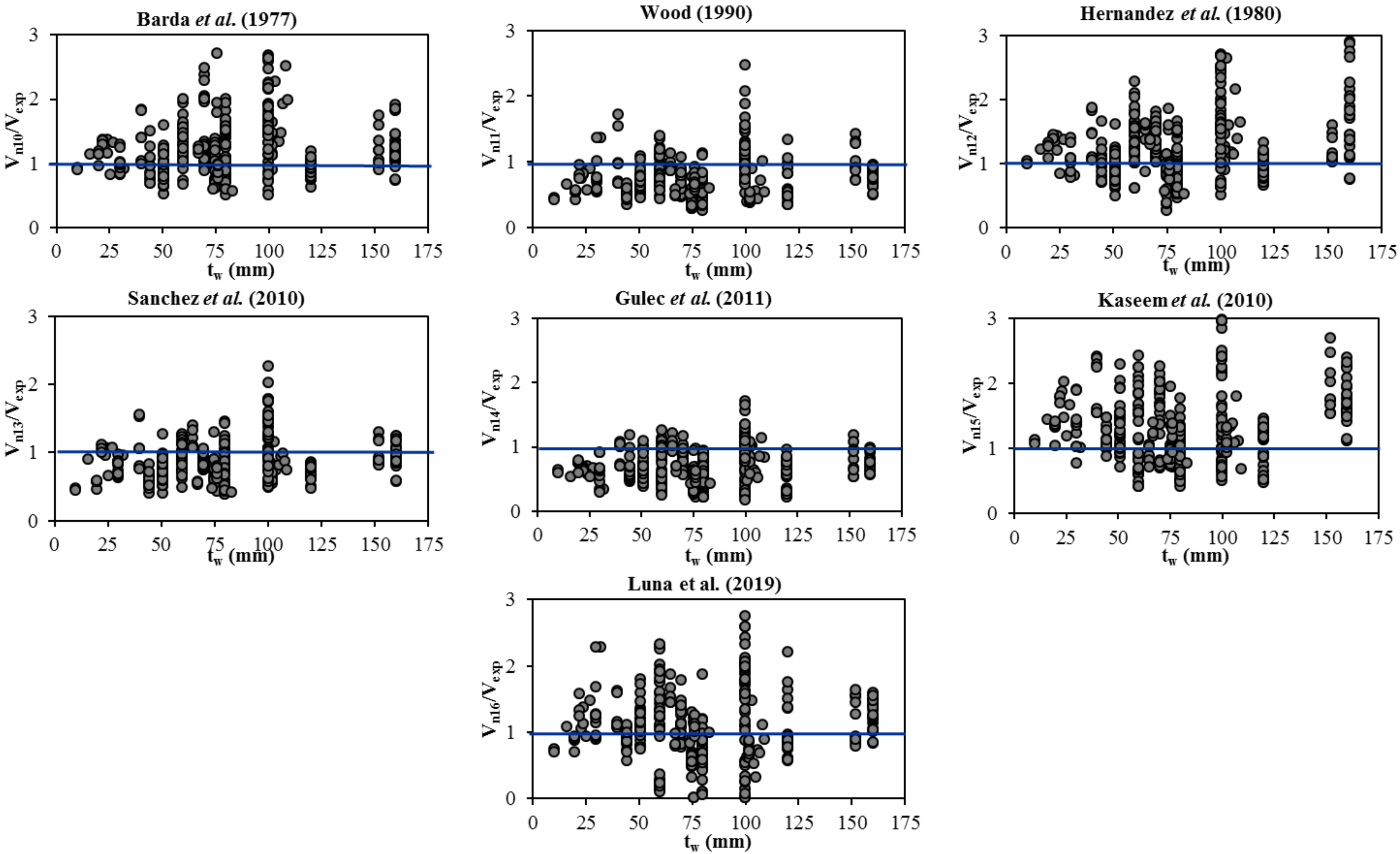

Fig. 3.10 Scatter Plot for V_{pre}/V_{exp} vs. Thickness of the wall

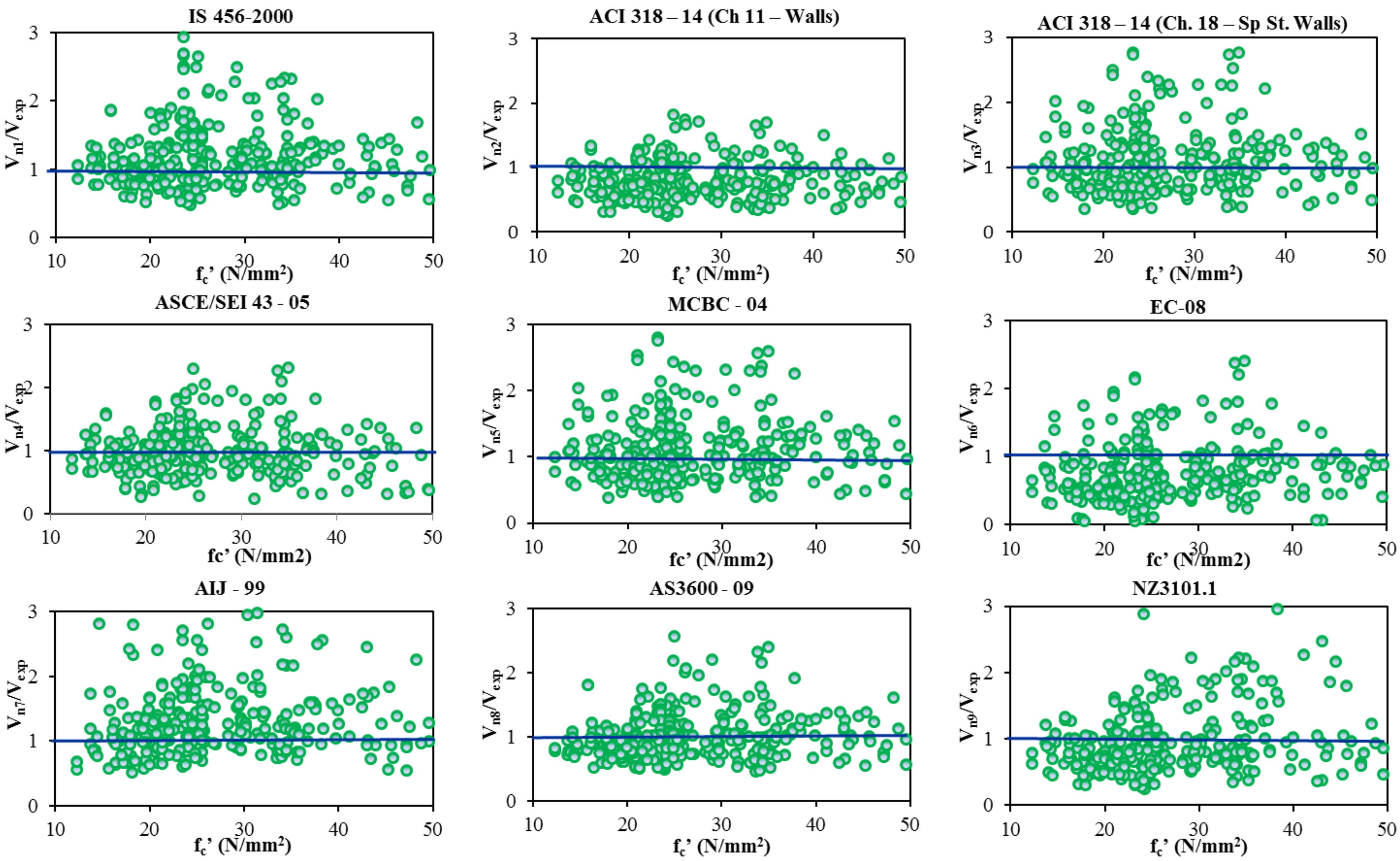
IS 456-2000
Vn1/Vexp
fc' (N/mm²)
ACI 318 – 14 (Ch 11 – Walls)
Vn2/Vexp
fc' (N/mm²)
ACI 318 – 14 (Ch. 18 – Sp St. Walls)
Vn3/Vexp
fc' (N/mm²)
ASCE/SEI 43 - 05
Vn4/Vexp
fc' (N/mm2)
MCBC - 04
Vn5/Vexp
fc' (N/mm2)
EC-08
Vn6/Vexp
fc' (N/mm2)
AIJ - 99
Vn7/Vexp
fc' (N/mm²)
AS3600 - 09
Vn8/Vexp
fc' (N/mm²)
NZ3101.1
Vn9/Vexp
fc' (N/mm²)

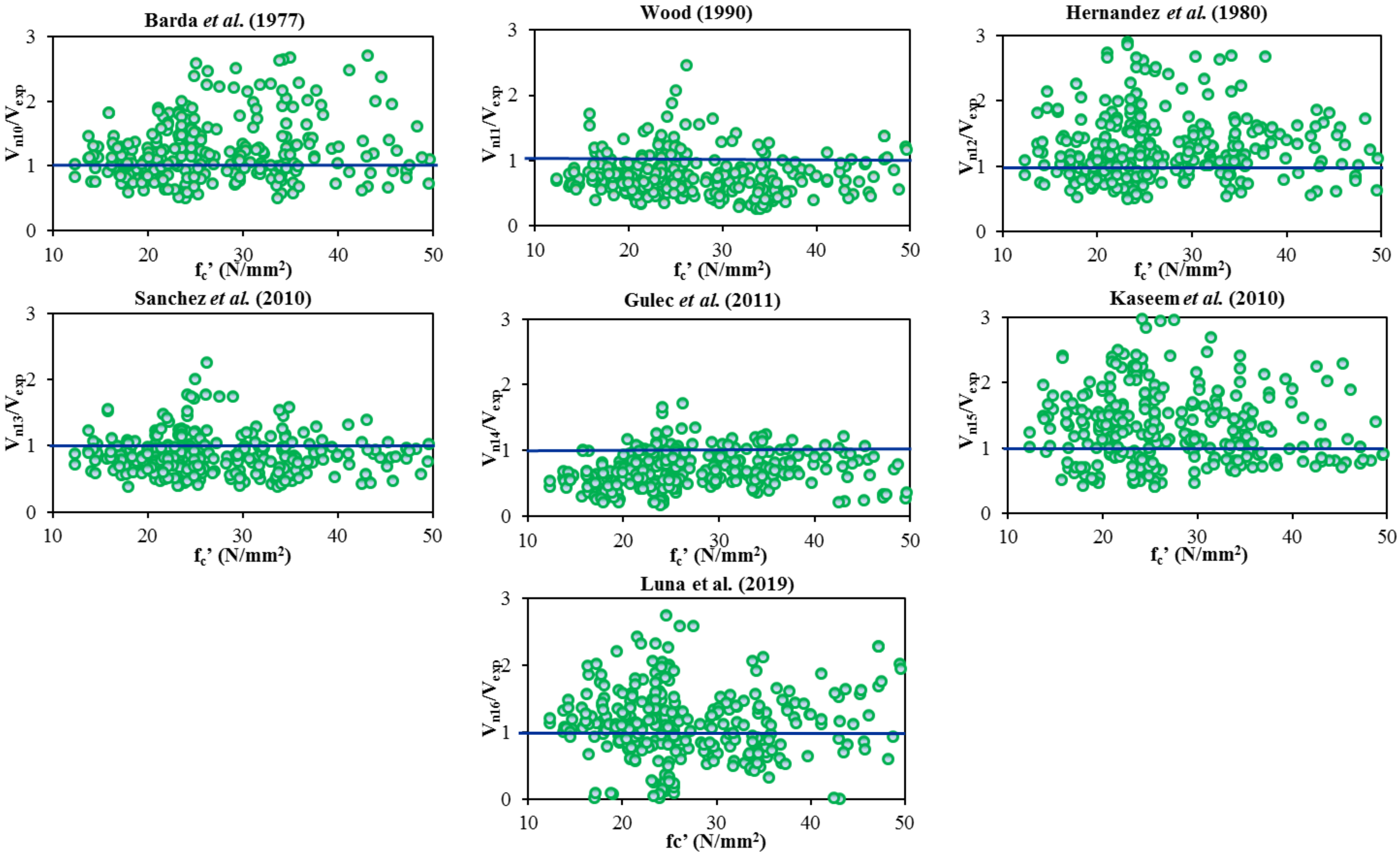

Fig. 3.11 Scatter Plot for V_{pre}/V_{exp} vs. f_c'

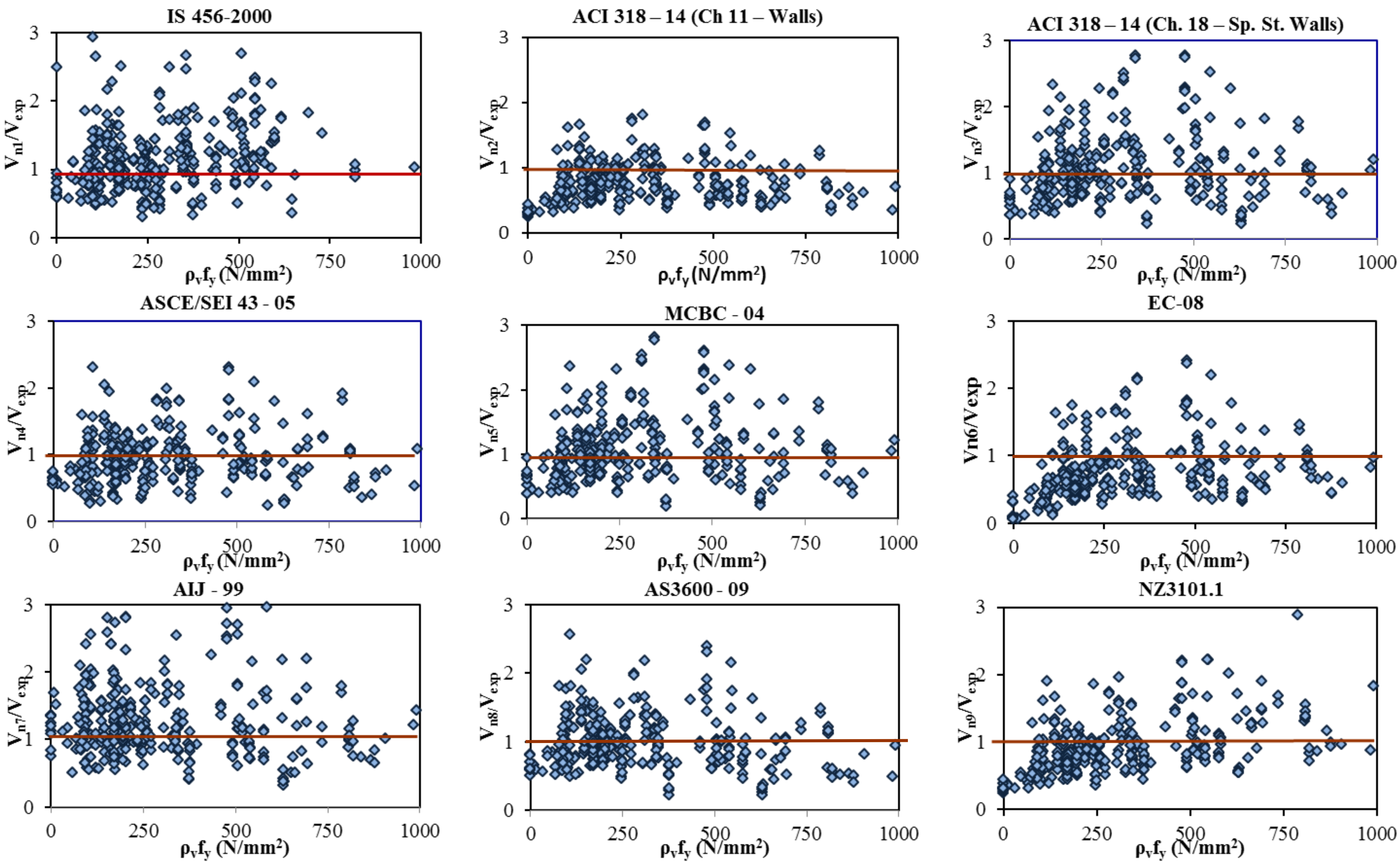

IS 456-2000
ACI 318 – 14 (Ch 11 – Walls)
ACI 318 – 14 (Ch. 18 – Sp. St. Walls)
ASCE/SEI 43 - 05
MCBC - 04
EC-08
AIJ - 99
AS3600 - 09
NZ3101.1
V_{n1}/V_{exp}
V_{n2}/V_{exp}
V_{n3}/V_{exp}
V_{n4}/V_{exp}
V_{n5}/V_{exp}
Vn6/Vexp
V_{n7}/V_{exp}
V_{n8}/V_{exp}
V_{n9}/V_{exp}
$\rho_v f_y$ (N/mm^2)
0
1
2
3
0
250
500
750
1000

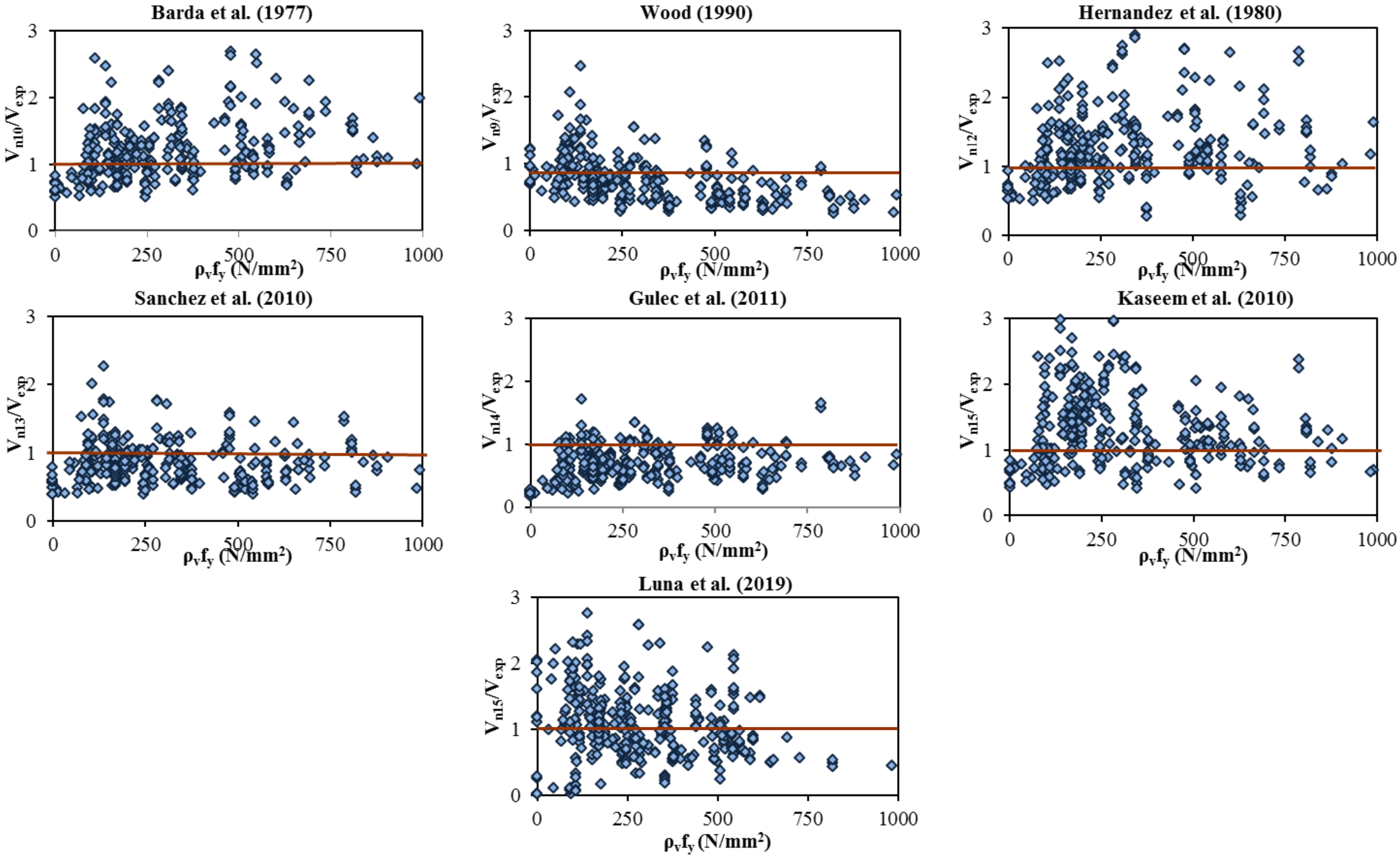

Fig. 3.12 Scatter Plot for V_{pre}/V_{exp} vs. $\rho_v f_y$

CHAPTER 4

EXPERIMENTAL PROGRAMME

4.1 GENERAL

To achieve the objective of the study, as mentioned in the methodology, experimental investigations carried out on shear walls. In this section, details on geometry, design and detailing of other structural elements such as top and bottom beam which are involved in experiment, construction, test set-up and loading protocol are described in detail. Reinforced concrete walls with and without opening were constructed and tested.

4.2 DESCRIPTION OF TEST SPECIMENS

Test series includes five one-third scaled reinforced concrete squat shear wall with and without opening. It is presumed that tested cantilever wall subjected to constant vertical load and static cyclic lateral load exhibits similar behaviour of shear wall under earthquake loading. Shear wall consists of three components. First component is top beam through which vertical and lateral loads are transferred to wall. Second component is wall web which is the test element in specimen. Third component is bottom beam which anchors to a strong floor for fixity. Five shear walls that are designed for this study includes, shear wall without opening (SW-1.0-00-00), shear wall with concentric window opening (SW-1.0-CW-00), FRC shear wall with concentric window opening (SW-1.0-CW-FRC), shear wall with concentric door opening (SW-1.0-CD-00) and FRC shear wall with concentric door opening (SW-1.0-CD-FRC). Geometric details of shear walls for experimentation are shown in Table 4.1.

All shear walls possess same geometric dimension. Wall portion has a length of 1000 mm, height of 1000 mm for revealing one-third scale with actual wall in structure. Thickness of wall is 125 mm. length and breadth of boundary elements are 300 mm and 150 mm respectively. Design and detailing of bottom and top beams are explained below. Figure 4.1 shows five shear walls considered for experimental programme.

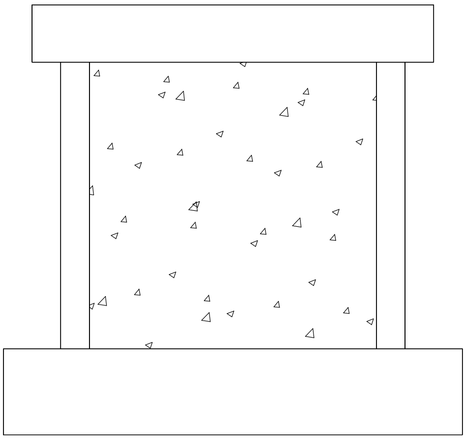

(a) SW-1.0-00-00

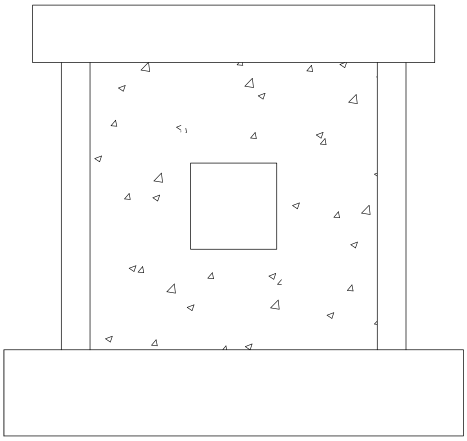

(b) SW-1.0-CW-00

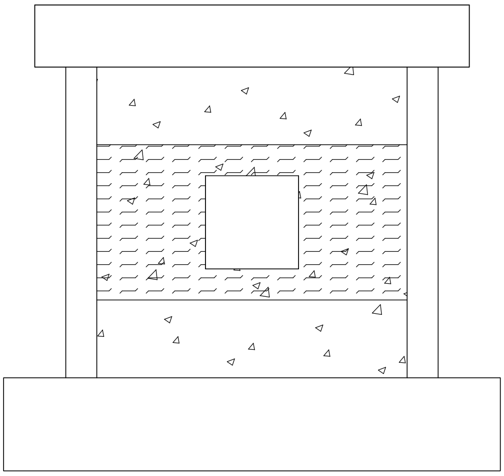

(c) SW-1.0-CW-FRC

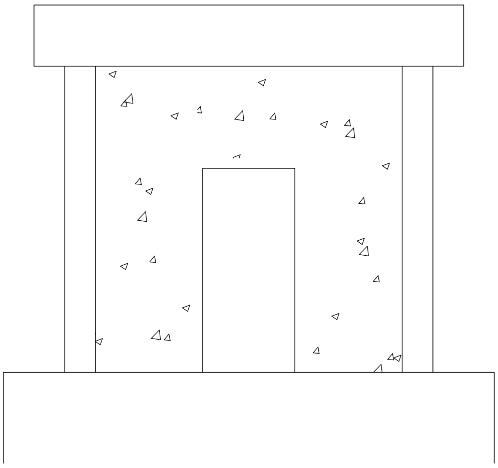

(d) SW-1.0-CD-00

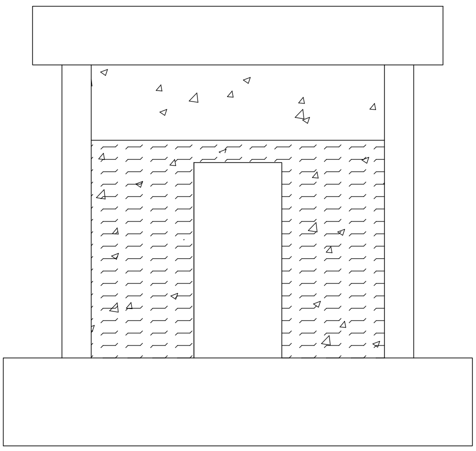

(e) SW-1.0-DO-FRC

Fig. 4.1 RC Shear walls adopted for experimental study.

Table 4.1 Geometrical details of RC shear walls adopted for experimental study

S. No	Specimen ID	l_w mm	h_w mm	t_w mm	Boundary Elements		Opening		ρ_l %	ρ_h %	ρ %	f_{ck} MPa	f_y MPa	N kN
					l mm	h mm	a mm	b mm						
1	SW-1.0-00-00	1000	1000	125	300	150	-	-	0.4	0.4	1	500	24	250
2	SW-1.0-CW-00	1000	1000	125	300	150	300	300	0.4	0.4	1	500	26	250
3	SW-1.0-CW-FRC	1000	1000	125	300	150	300	300	0.4	0.4	1	500	23	250
4	SW-1.0-CD-00	1000	1000	125	300	150	300	700	0.4	0.4	1	500	26	250
5	SW-1.0-CD-FRC	1000	1000	125	300	150	300	700	0.4	0.4	1	500	24	250

Reinforcement details listed in Table 4.1 are provided as per requirements of IS13920-16. Web reinforcement in wall comprises of 8 mm diameter bars with 200 mm spacing c/c in two layers. Web reinforcement ratio is kept constant, i.e 0.4% on both vertical and horizontal directions (Pilakoutas, 1995) and conforms to IS 13920-16 provisions. All walls cast with boundary elements play a major role on their behaviour (Kuang, 2008). Moreover, in case of walls with openings, boundary elements increase ultimate strength of wall to a larger extent (Bing, 2016). Here, boundary element comprises of 4 numbers of 12 mm diameter bars as longitudinal reinforcement and 8 mm diameter reinforcement with 100 mm c/c as ties on either face of wall.

In this study, adopted reinforcement was Fe500 grade conforming to IS 1786:2008. For walls with opening, additional reinforcements were provided as recommended by IS 13920-16. As per code, area of additional reinforcement to be provided is the area of interrupted bars due to openings, in two layers. For walls with window opening, two numbers of 8 mm diameter bar in two layers were provided as both longitudinal reinforcement and transverse reinforcement in two layers around opening. For walls with door opening, two numbers of 8 mm diameter bar in two layers as longitudinal reinforcement and two numbers 12 mm diameter bars in two layers as transverse reinforcement are provided around opening. Details of reinforcement in shear wall are illustrated in Figure 4.2.

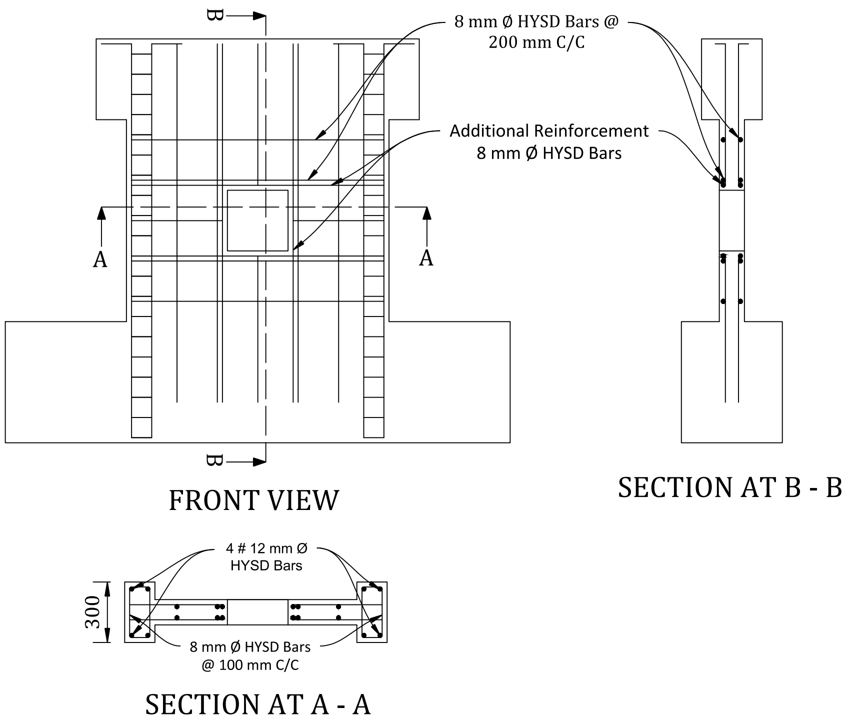

a. Shear wall with window opening

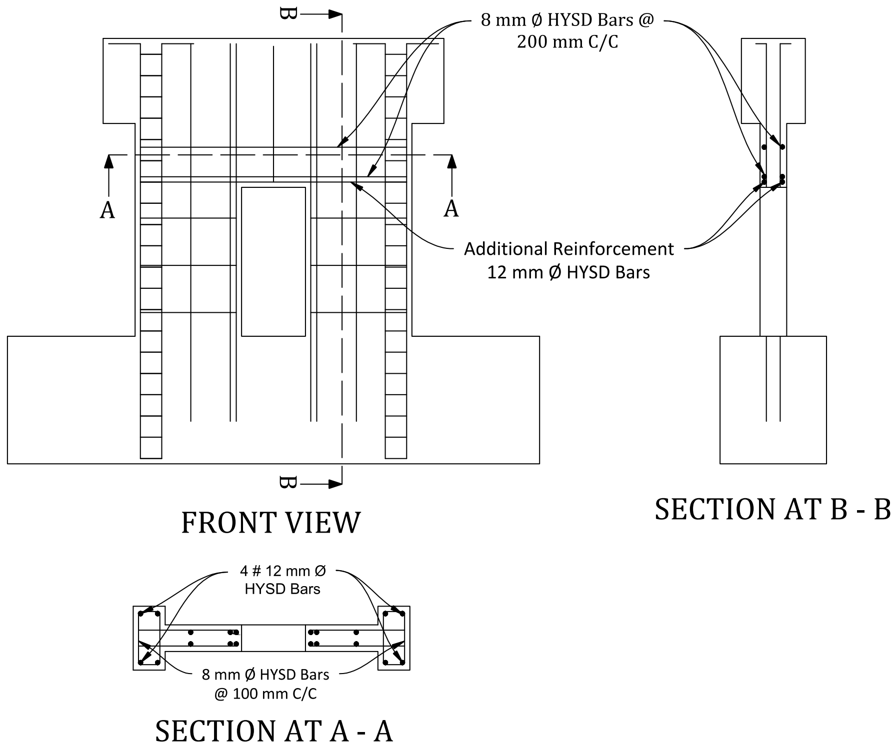

b. Shear wall with door opening

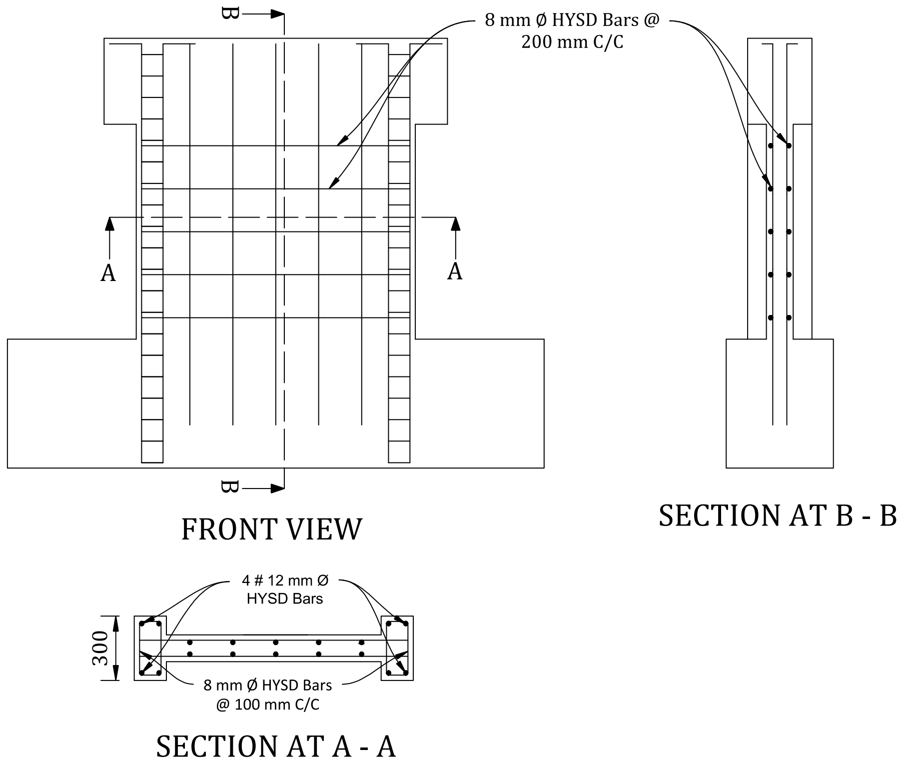

c. Shear wall without opening

Fig. 4.2 Detailing of walls with and without opening

4.3 DESIGN AND DETAILING OF ELEMENTS IN TEST SPECIMEN

As discussed earlier, shear wall consists of three major components, top beam, wall and bottom beam. For successful testing of wall element, bottom beam and top beams should possess sufficient stiffness to bear and transfer forces with negligible deformation. Moreover, locking of shear wall should be appropriate to prevent overturning and sliding. These issues are discussed in this section.

4.3.1 Axial load ratio (ALR)

Axial load on shear wall was kept constant throughout testing. Axial load ratio (ALR) is the ratio of axial load applied on wall-to-its uniaxial compressive strength. As per Lefas et al. (1990), walls with ALR as 0.0%, without axial load represents single-storey structure, walls with ALR of 10% represents medium-rise buildings and walls with ALR as 30% and more represents high-rise buildings. In this study, medium-rise building conditions were considered as it is huge in number. Hence, axial load ratio (ALR) considered as 10% i.e. 0.1 times of uniaxial compressive strength of wall.

Considering Axial Load Ratio (ALR) of 10%, then, Axial Load = $\mathrm{ALR} \times f_c' \times l_w \times t_w$

$$= \frac{10}{100} \times 0.8 \times 25 \times 1000 \times 125$$

$$N = 250 \text{ kN}$$

4.3.2 Predicted shear strength for SW-1.0-00-00

Empirical and semi-empirically derived equations for predicting shear strength of shear walls in codes and literature have been collected and described in Chapter 3. These equations are applicable for only walls without opening. In the present case, only one wall without opening is considered for testing (SW-1.0). Shear strength of shear wall is calculated from these equations for preliminary calculations. Moreover, shear strength for this shear wall is found using numerical analysis using ANSYS 15.0 also are described in Chapter 6. These calculated shear strength for SW-1.0 wall by various equations and numerical analysis are tabulated in Table 4.2.

Table 4.2 Calculated shear strength of wall SW-1.0-00-00

Eq. No.	Code/ Literature	Shear Strength (kN)
1	IS 456-2000	485
2	ACI 318 – 14 (Ch 11 – Walls)	372
3	ACI 318 – 14 (Ch. 18 – Sp. St. walls)	440
4	ASCE/SEI 43-05	409
5	MCBC – 04	495
6	EC8	335
7	AIJ – 99	367
8	AS3600 - 2009	400
9	NZ3101.1	400
10	Barda et al. (1977)	495
11	Wood (1990)	279
12	Hernandez et al. (1980)	566
13	Sanchez et al. (2010)	395
14	Gulec et al. (2011)	218
15	Kassem et al. (2010)	653
16	Luna et al. (2019)	519
17	Numerical Study	462

It can be observed that shear strength is dispersed largely ranging from 218 to 653 kN. Reason for such dispersion is discussed in Chapter 3. For preliminary calculations, shear strength of shear wall SW-1.0-00-00 adopted was 660 kN for the worst-case in Table 4.2.

4.3.3 Design of the top and bottom beam

In general, load is applied along the junction between floor beam and wall or top beam and wall, as a line load. Top and bottom beams are usually stronger and stiffer than wall. This is to resemble in experimentation also. Hence, bottom and top beams should be designed to possess sufficient stiffness to bear and transfer forces with negligible deformation. Taking predicted shear strength as 660 kN and axial load as 250 kN, design the top and bottom beams has been done. Here, beams are analysed through modelling using ANSYS and also without modelling using free-body analysis.

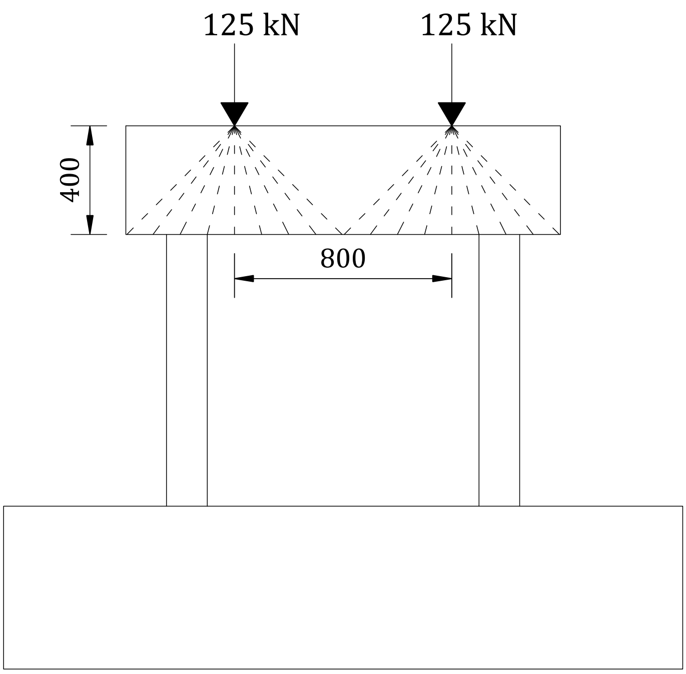

Fig. 4.3 Axial load dispersion

a) Beam analysis from Numerical Study

In the present study, finite element package ANSYS 15.0 Multiphysics (ANalysis SYStem 15.0) is used for modelling, which delivers greater accuracy, fidelity, higher productivity and more computational power. For preliminary works, beams and wall are modelled using Beam and Shell element. Three-dimensional modelling using SOLID65 element of shear wall is carried out and detailed analysis are described in Chapter 6.

Top and bottom beams are modelled using BEAM188 element. BEAM188 is a linear (2-node) beam element in 3-D with six degrees of freedom at each node. Degrees of freedom at each node include translations in x-, y- and z-directions, and rotations about the x-, y- and z-directions. Warping of cross-sections is assumed to be unrestrained. BEAM188 element is suitable for analysing slender to moderately stubby/thick beam structures. This element is based on Timoshenko beam theory. Shear deformation effects are included in this beam element. Beam elements are well-suited for linear, large rotation, and/or large strain nonlinear applications.

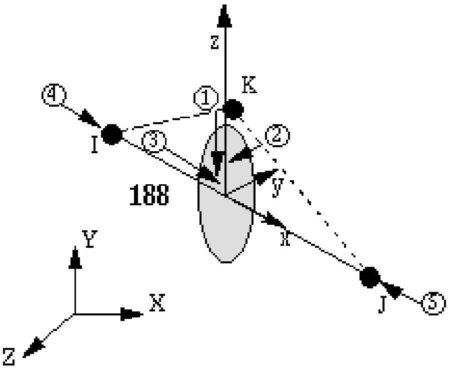

a. BEAM188 Element

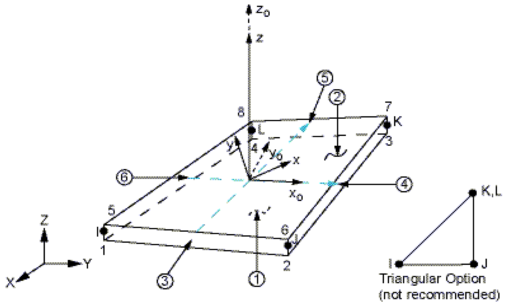

b. SHELL281 Element

Fig. 4.4 Beam and Shell Elements

Wall portion is modelled using SHELL281 element. It is a four-node element with six degrees of freedom at each node: translations in x-, y-, and z-directions, and rotations about x-, y-, and z-axes. SHELL281 is well-suited for linear, large rotation, and large strain nonlinear applications. The element formulation is based on logarithmic strain and true stress measures. This element is based on Mindlin–Reissner plate theory.

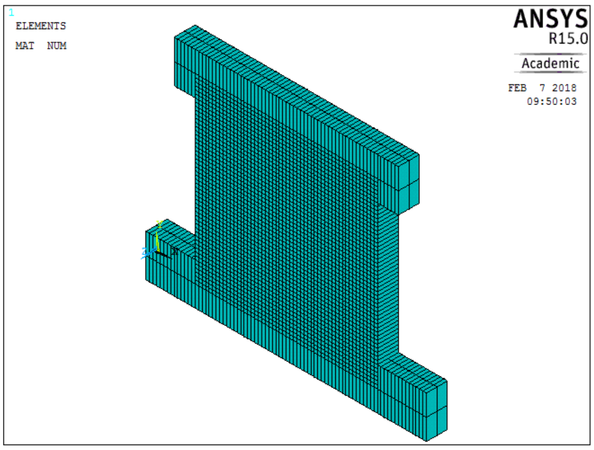

Fig. 4.5 Model rendered view

Above figure shows a rendered view of beam and shell element of wall for preliminary works. Arbitrary sizes were given for beams for initial analysis. Analysis is carried out for two cases. In first case, only lateral load has been applied. Bending moment and shear force diagrams obtained from this case are shown in Figure 4.6.

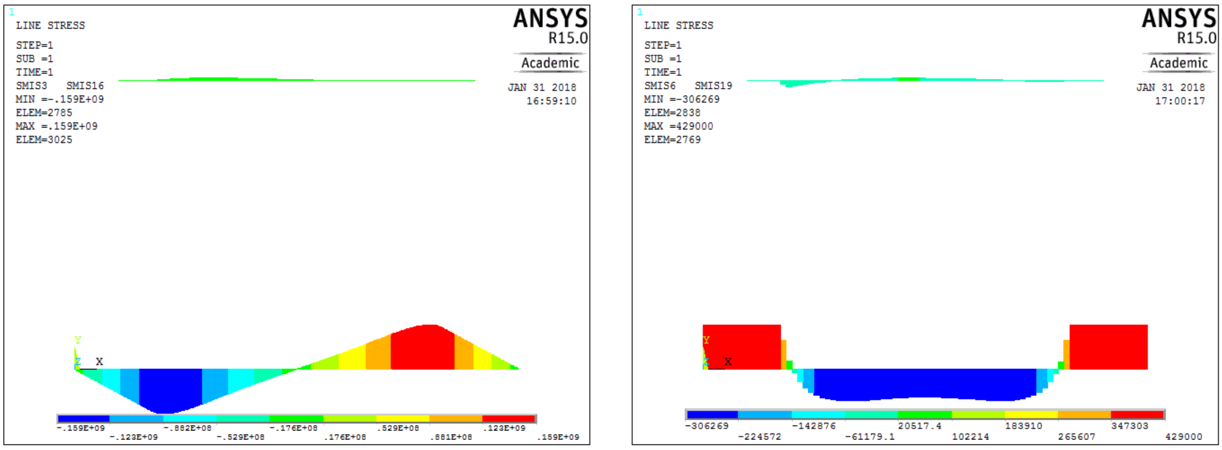

a. Bending Moment Diagram b. Shear Force Diagram

Fig. 4.6 BMD and SFB without axial load

The maximum bending moments and maximum shear force obtained from the ANSYS15.0 when the only lateral load is applied are as follows.

- Top Beam: M = 17.6 kNm; V = 20.5 kN.
- Base Beam: M = 159 kNm; V = 429 kN.

In second case, both vertical load and lateral load are applied. Bending moments and shear force diagrams obtained for this case are shown in Figure 4.7.

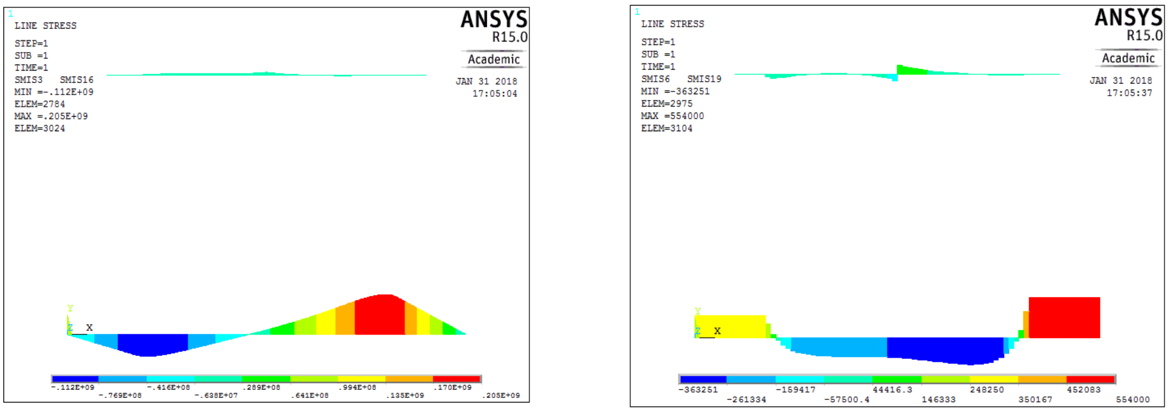

a. Bending Moment Diagram b. Shear Force Diagram

Fig. 4.7 BMD and SFB with axial load case

Maximum bending moment and maximum shear force obtained from ANSYS15.0 when both lateral and vertical loads are applied are as follows.

- Top Beam: M = 28.9 kNm; V = 142.5 kN.
- Base Beam: M = 205 kNm; V = 554 kN.

b) Beam analysis using free-body analysis

Free body diagrams are used to visualize forces and moments applied to a body and will help in making comfort to calculate resulting reactions. Top beam and bottom beams are analysed by simple free body beam analysed here.

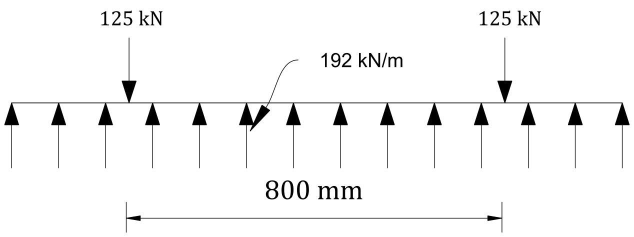

Fig. 4.8 Free body diagram for top beam

As stated earlier, axial load over shear to be applied is about 250 kN in compression. It is planned to apply two 125 kN using two hydraulic jacks. Jacks were spaced 800 mm for uniform dispersion of load over width of wall. Point loads applied from jacks will attain uniformly distributed after a certain depth of top beam. Assuming dispersion at 45°, load attain uniformly distributed at depth of 400 mm from application of point load. In this case, free body diagram of top beam is as shown. Maximum bending moment and maximum shear force of top beam from free body analysis are 25 kNm and 125 kN respectively.

In case of bottom beam, it is subjected to a concentric moment due to applied lateral force as shown if Figure 4.9. Strong floor consists of provision for locking at every 1.0 m intervals. Hence, support for bottom beam is at a distance of 2.0 m. Free-body analysis for bottom beam is as follows.

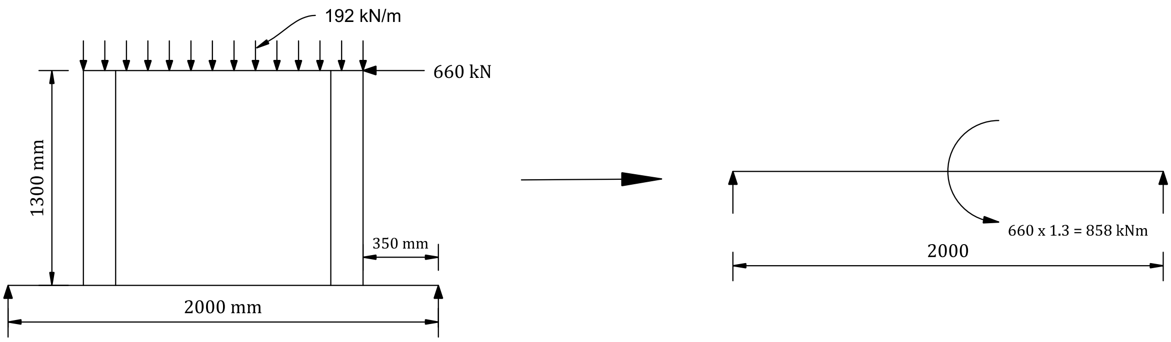

Fig. 4.9 Free body Diagram for bottom beam

At left support,

Reaction at support due to applied moment	=	429 kN
Reaction at support due to Vertical Load	=	125 kN
Total Reaction, V	=	429 + 125 = 554 kN
Moment at Face of Wall, M	=	554 × 0.35 = 194 kNm

Considering all cases and results from numerical and free body analysis, critical moments and shear forces have been adopted for design of top and bottom beams. Hence design is carried out for moment and shear forces as below.

- Top Beam, M = 31.25 kNm; V = 142.5 kN;
- Bottom Beam, M = 205 kNm; V = 554 kN.

Design is carried out using IS 456-2000 by neglecting safety factors on materials. Design output is as follows,

Top Beam:	Cross-section	-	300 mm × 400 mm
	Main reinforcement	-	2 # 16 mm φ Bars
	Shear reinforcement	-	2 legged 8 mm Stirrups @ 100 mm C/C

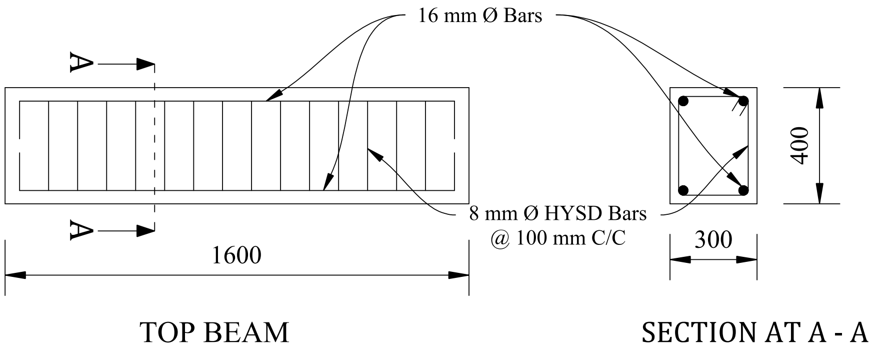

Fig. 4.10 Reinforcement Details of top beam

Bottom Beam: Cross-section - 500 mm × 600 mm

Main reinforcement - 4 # 20 mm φ Bars

Shear reinforcement - 4 legged 8 mm Stirrups @ 75 mm C/C

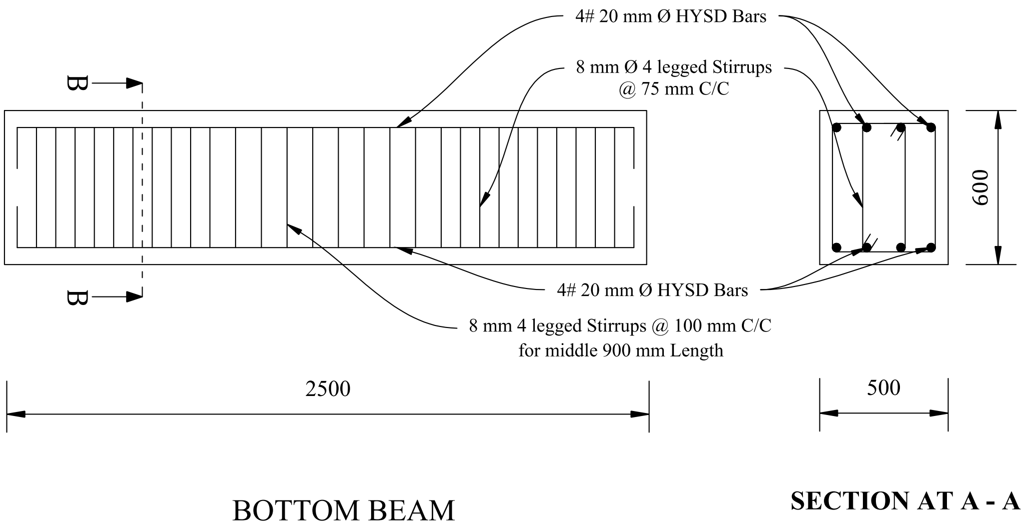

Fig. 4.11 Reinforcement Details of Bottom beam

4.3.4 Bolt Capacity

Locking of wall is as shown in Figure 4.12, at 2.0 m intervals as discussed earlier. At each level, 2 bolts of 30 mm diameter and 2.3 m length bolts were adopted. A strong built-up section is used at each locking location through which these two bolts were attached at one end while other end of the bolts was in the strong floor. This strong beam runs over the overhang portion of bottom beam for holding it firmly.

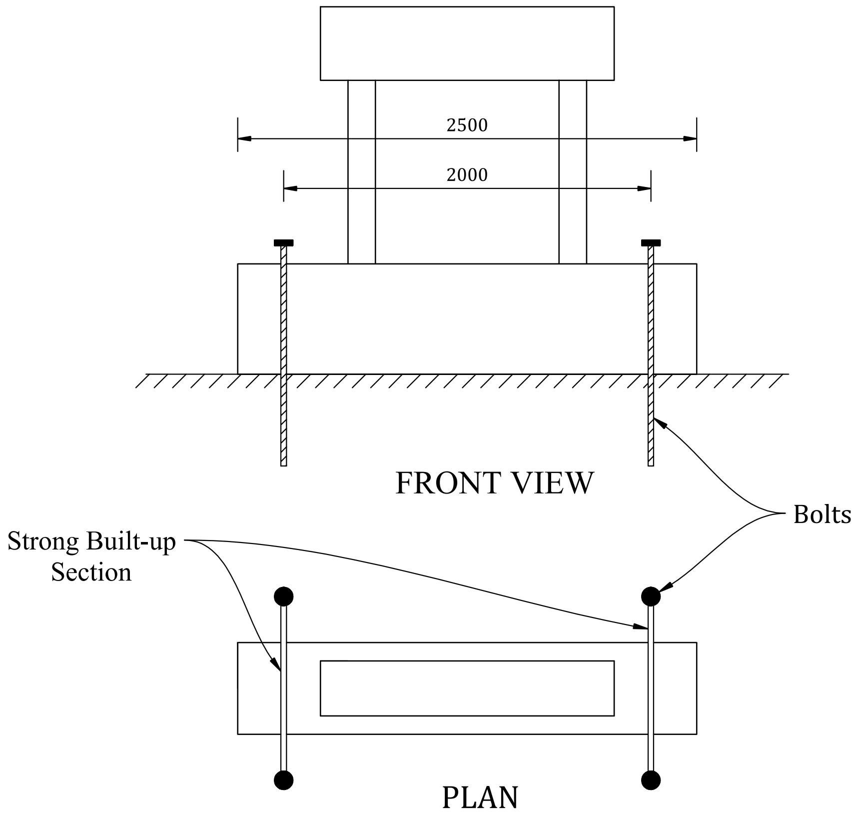

Fig. 4.12 Locking of the specimen

The anchor bolts are subjected to tension and shear due to lateral cyclic loads. Hence, bolts should be checked for shear and tension capacity. Bolts are subjected to single shear at the juncture of bottom beam and floor to be checked.

As per IS 800-2007, shear capacity of bolt is given by,

$$V_{dsb} = \frac{f_u}{\sqrt{3}}(nA_{nb})\frac{1}{\gamma_{mb}} = \frac{700}{\sqrt{3}}\left(4 \times \frac{\pi}{4} \times 32^2\right)\frac{1}{1.25}$$

$$V_{dsb} = 1040 \text{ kN} > 660 \text{ kN}$$

Combined designed shear strength of four bolts is higher than predicted lateral shear strength. Hence, bolts are safe in case of sliding shear between bottom beam and floor. It should be checked for tension as a reaction at one end may experience up to 429 kN as seen earlier in section 4.3.3 (b).

As per IS 800-2007, Tension Capacity of Bolt is given by,

$$T_b \leq \frac{T_{nb}}{\gamma_{mb}}, \qquad \gamma_{mb} = 1.25$$

$$T_{nb} = 0.9 f_{ub} A_n < f_{yb} A_{sb} \frac{\gamma_{mb}}{\gamma_{ml}}$$

`

$T_{nb} = 0.9 \times 700 \times 0.78 \times \frac{\pi}{4} \times 32^2 < 500 \times \frac{\pi}{4} \times 32^2$

$T_{nb} = 395$ kN

$T_b = 395/1.25 = 316$ kN

Two Bolt Capacity $= 2 \times 316 = 632$ kN > 429 kN

Combined design tensile strength of two bolts is higher than prediction reaction in the bolts. Hence bolts are safe in case of tension also.

4.3.5 Check for Sliding at Wall and Beam

Construction joints between wall and beams are the weak points under inelastic load reversals during application of cyclic loading. Figure 4.13 shows sliding shear acting between top beam and wall and also between wall and bottom beam. There was also a chance that wall may fail in shear sliding along construction joint before attainment of full shear capacity. Therefore, sliding shear capacity at these joints should be checked as it should not affect experimentation.

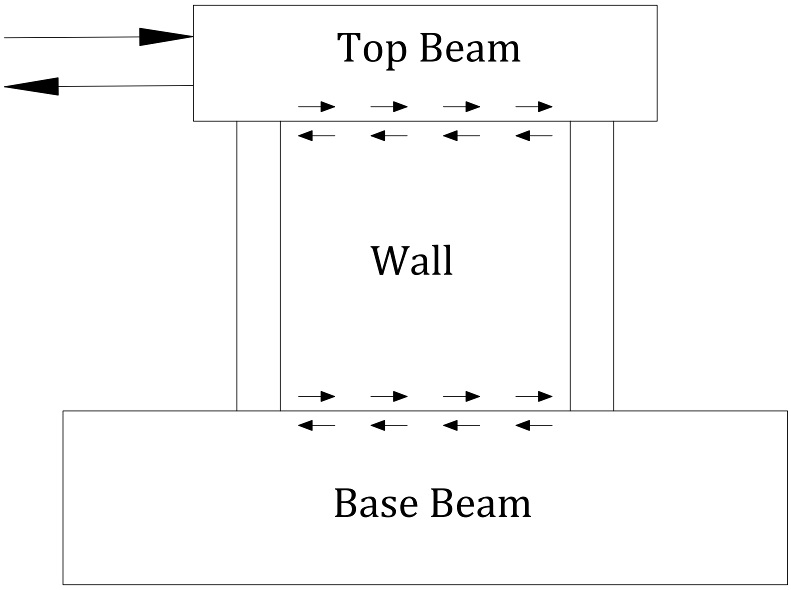

Fig. 4.13 Sliding between Wall and Beam

Shear stresses developed at the junction of wall and beam are,

$$\tau = \frac{V_u}{(l_w t_w + 2 \times l_c b_c)}$$

$$\tau = \frac{660 \times 10^3}{(1000 \times 125 + 2 \times 300 \times 150)} = 3.069 \text{ N/mm}^2 < \tau_{c,max}$$

Code IS 456-2000 does not give any guidance related to these shear-friction concepts. Canadian standard CSA A23.3.04 recommends following formula for determining factored interface shear resistance, γ_r, based on shear-friction concept.

$$\gamma_r = \lambda\, \phi_c\, (c + \mu\, \sigma) + \phi_s\, \rho_v\, f_y \cos \alpha_f$$

Where,

$\sigma = \rho_v f_y \sin\alpha_f + N/A_g$; A_{cv} = area of concrete section resisting shear

A_g = gross area of section; A_{vf} = area of shear-friction reinforcement

c = resistance due to cohesion; f_y = yield stress of shear-friction reinforcement

N = unfactored permanent compressive load perpendicular to the shear plane

$\gamma_r = V_r / A_{cv}$ = factored shear stress resistance

α_f = inclination of shear-friction reinforcement with shear plane

$\rho_v = A_{vf} / A_{cv}$ = ratio of shear-friction reinforcement; μ = coefficient of friction

φ_c, φ_s = material resistance factors for concrete and steel reinforcement

λ = factor to account for low density concrete.

Table 4.3 Values of c and μ (CSA A23.3 - 04, Cl. 11.5.2)

S. No.	Fresh Concrete Placed Against	c (MPa)	μ
1	Hardened concrete	0.25	0.6
2	Hardened concrete, clean and intentionally roughened	0.50	1.0
3	Monolithic construction	1	1.4
4	As-rolled structural steel and anchored by headed studs or reinforcing bars	0	0.6

From above equation, factored interface shear resistance calculated to be 3.3 N/mm^2 which is higher than shear stress developed at the junction. Hence sliding shear capacity of wall is adequate to resist predicted shear strength of wall. Complete geometric details of walls for testing are shown in Figure 4.14.

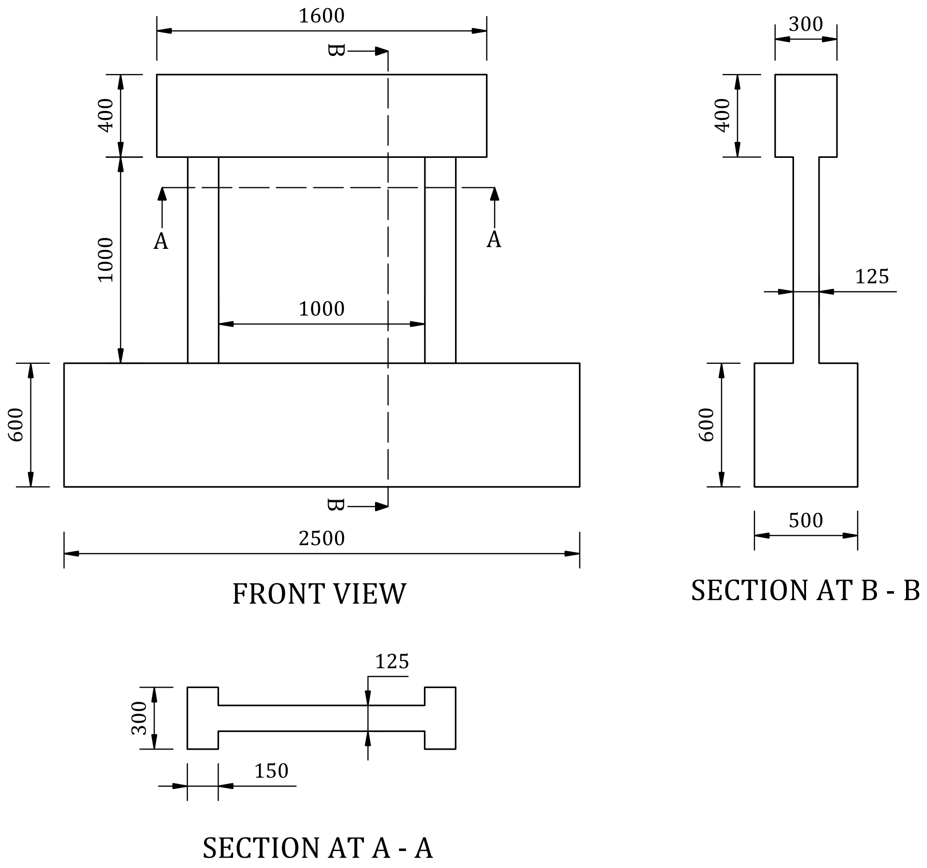

a. Geometric details of SW-1.0-00-00

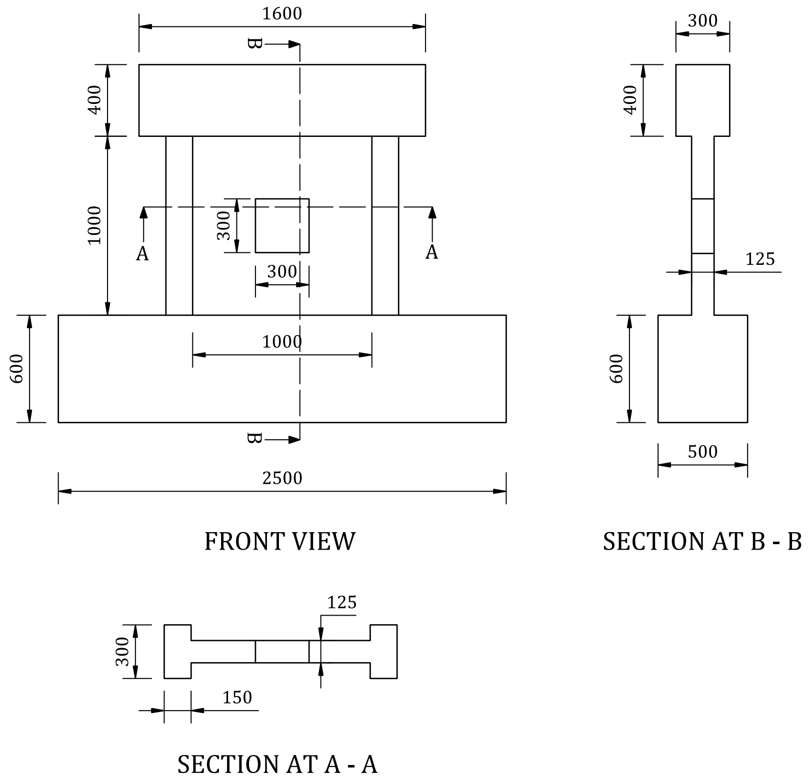

b. Geometric details of SW-1.0-CW-00
and SW-1.0-CW-FRC

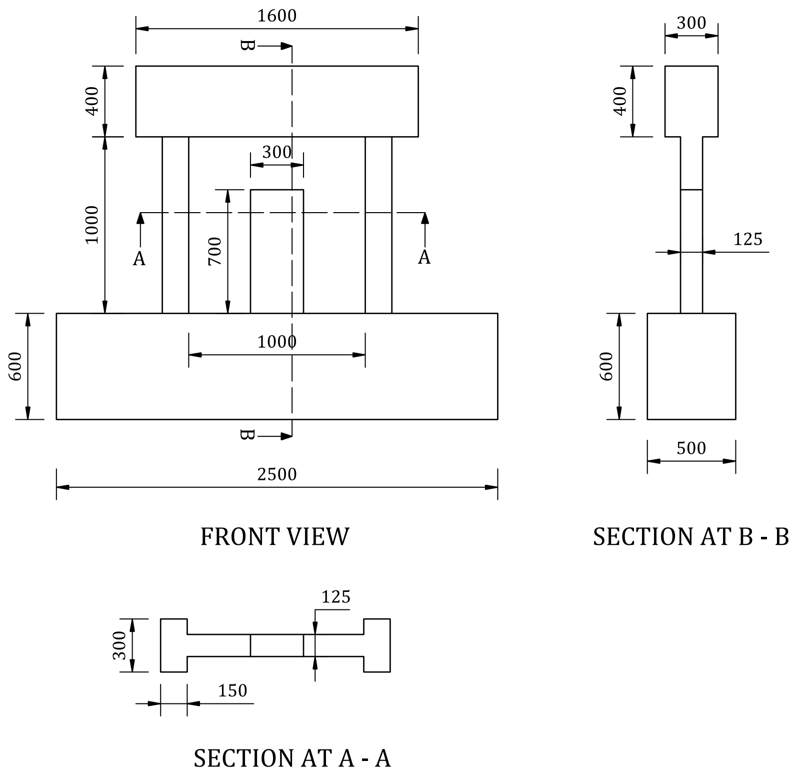

c. Geometric details of SW-1.0-CD-00
and SW-1.0-CD-FRC

Fig. 4.14 Complete Geometric details of walls for Experimental Programme

4.4 CONSTRUCTION OF TEST SPECIMENS

All shear walls were constructed in casting yard. To ensure realistic site conditions, all test walls were built in fully upright position. However, casting of walls was somewhat challenging in some cases due to small wall web thickness and congestion of reinforcement in boundary elements.

A wooden formwork made of plywood and silver wood was prepared for wall portion and top beam. A steel formwork made for bottom beam using channel sections available in the laboratory. However, for all the specimens, reinforcement cage for bottom block and wall are erected as single unit. Caging for top beam has been done separately. This cage unit was placed in the formwork for bottom beam using the forklift. Two hooks using 20 mm diameter rods bound to bottom block cage for lifting walls.

b. Specimen Mould

a. Concreting of Bottom Beam

c. Concreting of Wall

d. Preparation of wall Specimen

Fig. 4.15 Construction of Test Specimens

All walls were cast in three stages in three consecutive days. In first stage, bottom block was concreted fully. In second stage, wall formwork has been inserted using forklift into caging. Concreting was done fully for wall in second stage. In third stage, e top reinforcement cage was inserted with top beam cage. Concreting was done for top beam. All three stages have been carried out on three consecutive days for each wall. Formwork was removed on fourth day and left for curing for 28 days. Each wall weighs around 2.8 tons. A forklift was used comfortably for shifting. Figure 4.16 shows walls ready for testing.

a. Wall with Window Opening

b. Wall with Door Opening

c. Wall without Opening

Fig. 4.16 Specimens for Testing

4.5 TEST SET UP

Walls were tested as per set-up illustrated in Figure 4.17 and 4.18. Bottom beam anchored to strong floor rigidly to prevent rocking of wall. Bottom beam also restrained horizontally to prevent sliding of wall. A hydraulic actuator with 1000 kN capacity was fixed to a reconfigurable reaction wall in the lateral direction.

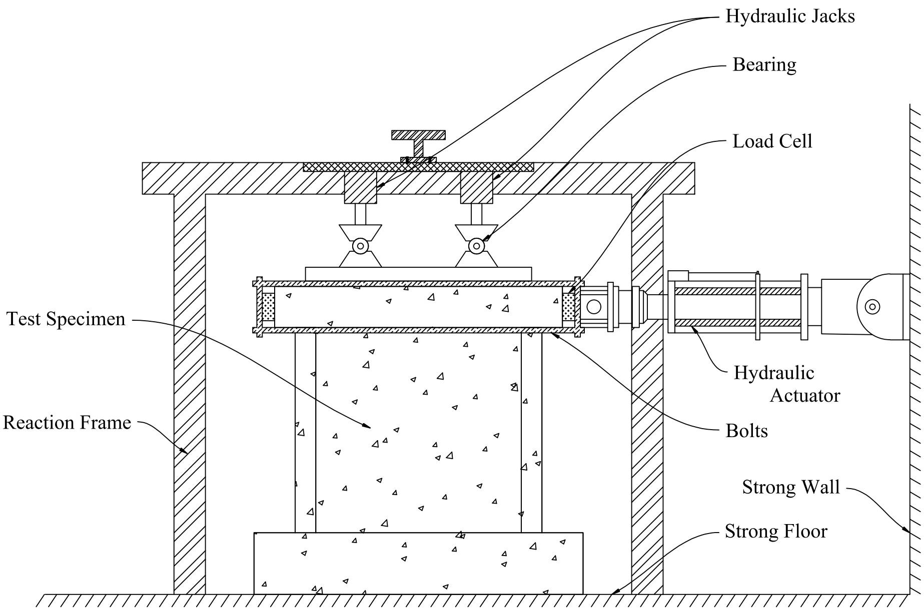

Fig. 4.17 Test Set up Model

Vertical load was applied vertically using a loading frame through two hydraulic jacks each with 300 kN capacity. Hydraulic jacks were connected to a stiff beam for transferring load from two jacks and a stiff beam was placed over two hinges. In addition to that, a spreader beam was placed on top of wall to make sure that vertical load was applied uniformly to the wall.

Fig. 4.18 Test Setup for shear wall

4.6 INSTRUMENTATION

Linear variable differential transformer (LVDT) (also called linear variable displacement transformer) is a type of electrical transformer used for measuring linear displacement. These LVDTs are positioned horizontally, vertically and diagonally to monitor displacements for all components as shown in Figure 4.19. Sliding and overturning of each wall monitored using LVDTs connected to bottom beam. An actuator was fixed with a load cell to monitor applied load to the wall.

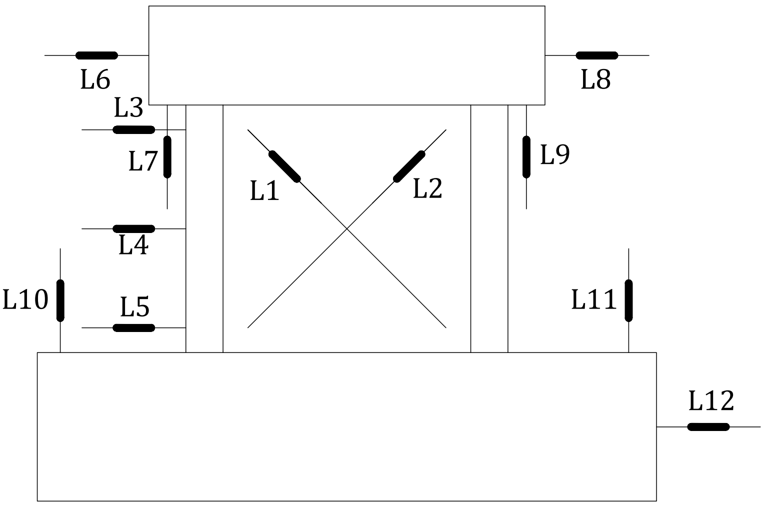

a. LVDT Positions for SW-1.0-00-00

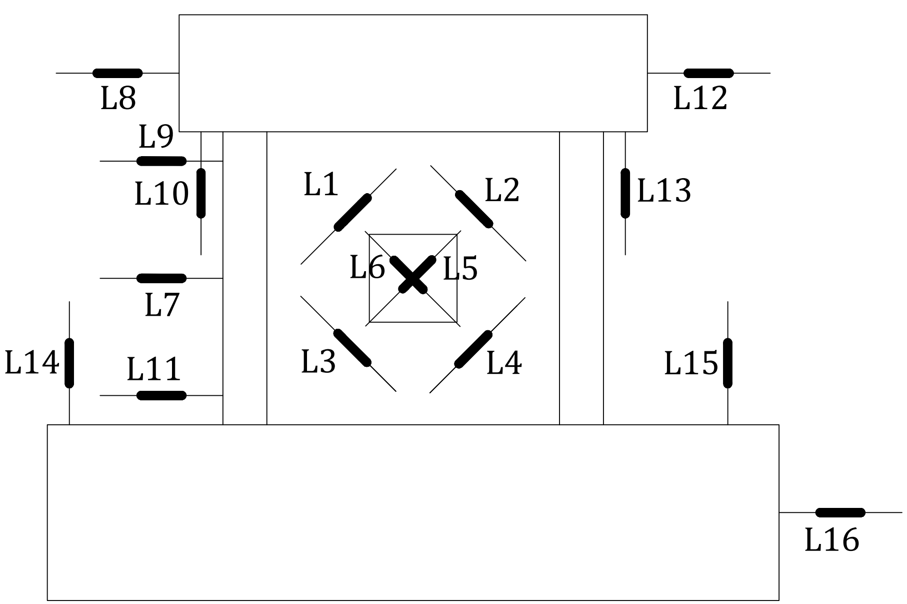

b. Position of LVDTs for SW-1.0-CW-00
and SW-1.0-CW-FRC

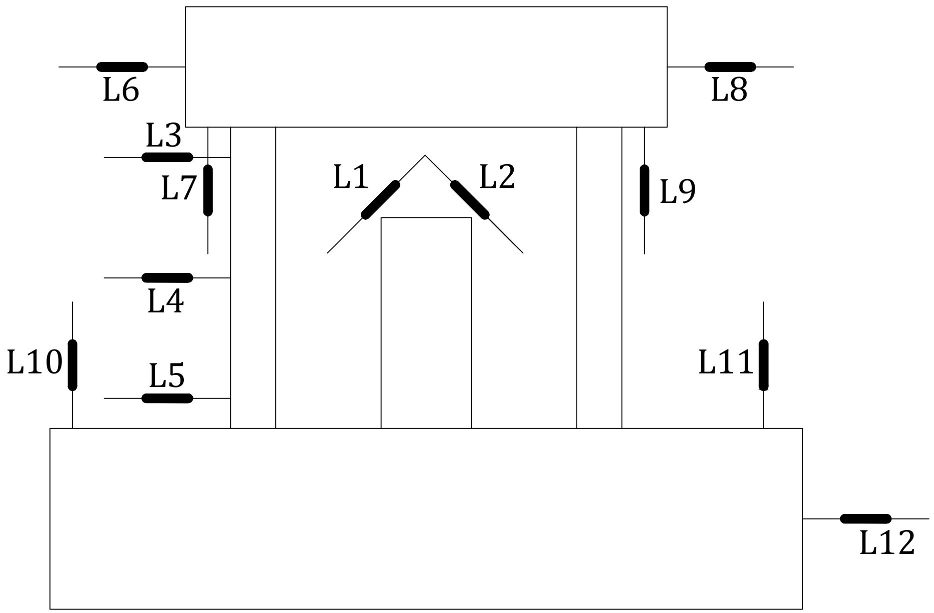

c. Position of LVDTs for SW-1.0-CD-00
and SW-1.0-CD-FRC

Fig. 4.19 Position of LVDTs

A strain gauge is a device used to measure strain on an object. The gauge was attached to reinforcement by an adhesive acrylate. In this experiment, 5 mm strain gauge is used for measuring strains in reinforcement. As reinforcement is deformed, it causes electrical resistance to change. This resistance change, usually measured using a Wheatstone bridge, is converted to strain quantity at that location of 5 mm gauge length by quantity known as gauge factor. These strain gauges attached to reinforcing bars at several locations. Locations of strain gauges are shown in Figure 4.20

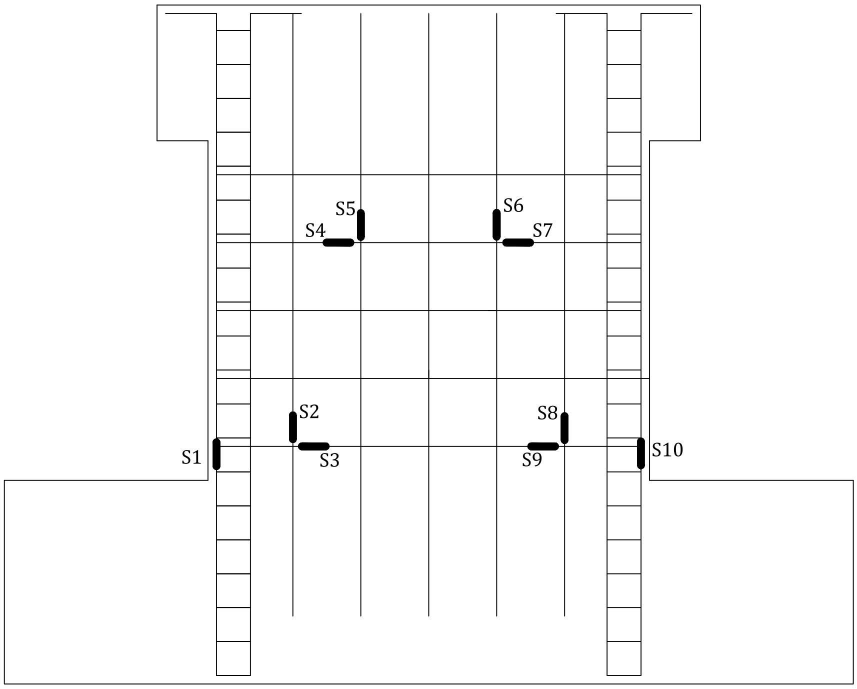

a. Position of Strain gauge for SW-1.0-00-00

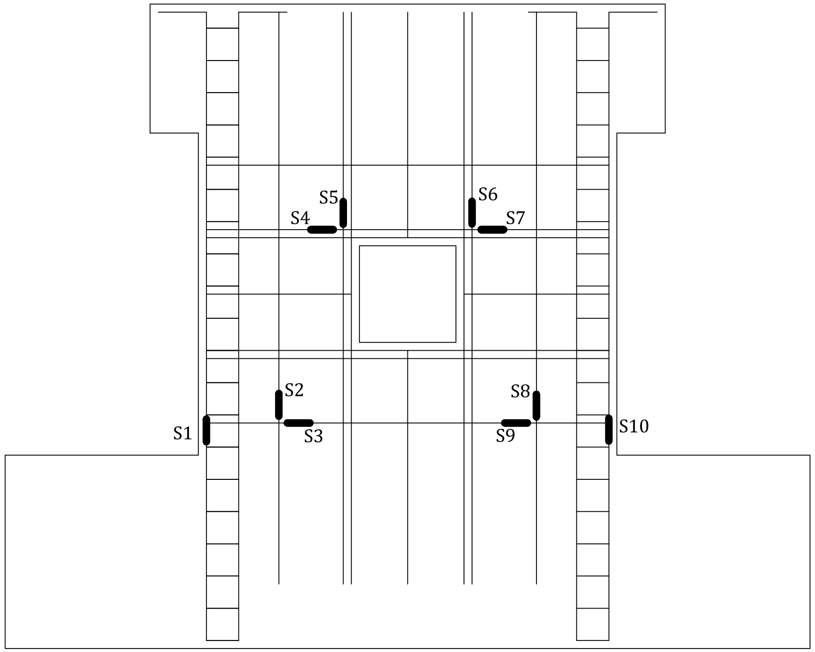

b. Position of Strain gauge for SW-1.0-CW-00
and SW-1.0-CW-FRC

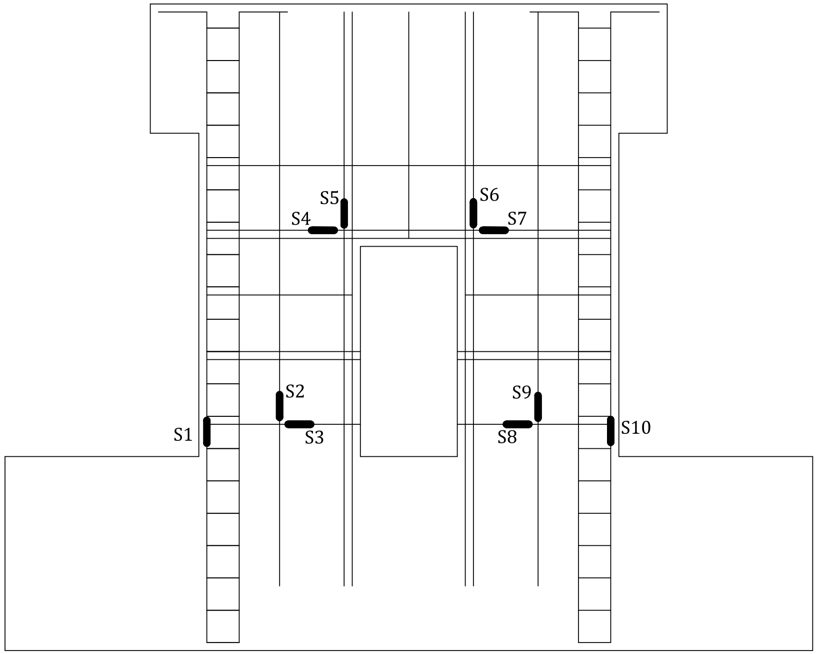

c. Position of Strain gauge for SW-1.0-CD-00
and SW-1.0-CD-FRC

Fig. 4.20 Position of Strain gauges

4.7 LOADING PROCEDURE

Vertical load was kept constant throughout testing maintaining axial load ratio (ALR) as 10% i.e. 0.1 times of uniaxial compressive strength of wall. This load level is considered to be representative of a medium-rise building (Lefas, 1990). Cyclic lateral loading was accompanied by a displacement control system as per ASTM E2126-11. As per ASTM E2126-11, first displacement pattern comprises of five single cycles at displacements of 1.25, 2.5, 5, 7.5 and 10% of lateral drift (10 mm), and second displacement pattern comprises of three fully reversed cycle starting from 20, 40, 60, 80,100, 120% of lateral drift and so on as illustrated in Figure 4.21, until failure or up to 10% lateral drift.

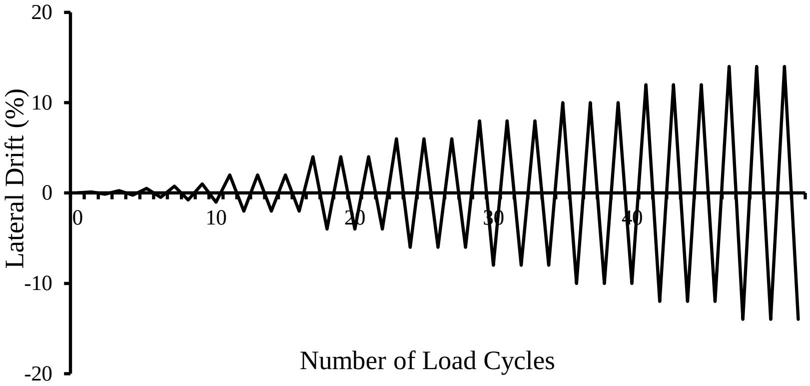

Fig. 4.21 Loading Protocol

4.8 CONCLUDING REMARKS

Experimental programme includes the selection and processing of materials, dimensions and preparation of walls, reinforcement detailing, test set-up, loading protocol and testing to understand horizontal strength and behaviour of reinforced concrete shear walls with and without openings. The shape, dimensions and location of openings influence performance of RC shear walls. The experimental investigations reveal influence of opening and fibres in reinforced concrete for improving structural performance under horizontal cyclic loading and are discussed in next chapter.

CHAPTER 5

BEHAVIOUR OF RC SQUAT SHEAR WALLS WITH OPENINGS UNDER CYCLIC LOADING

5.1 GENERAL

Reinforced concrete shear walls are adopted in high-rise buildings to resist lateral forces generated by effects of earthquake and wind loads. Shear walls can efficiently control performance and damage in buildings. During past few decades, a considerable development has been made in design and detailing of reinforced concrete walls. Behaviour of RC walls primarily depends on ratio of applied moment-to-applied shear force, which is linearly related to aspect ratio (A/R), defined as the ratio of height-to-length of the wall. Walls exhibit cantilever behaviour similar to slender or high-rise walls with A/R ratio greater than 2.0, and truss action prevails in squat/short or low-rise walls with A/R ratio less than 2.0. Slender walls predominantly fail in flexure mode, while squat walls fail in shear mode. Local buckling of web of RC walls is effectively prevented by providing RC boundary elements with minimum web thickness. Parameters such as the boundary elements, aspect ratio, wall thickness, reinforcement ratio, yield strength of reinforcement, compressive strength of concrete, and applied axial stress influence the strength, stiffness degradation, energy dissipation, crack pattern and modes of failure under seismic loading. Practically, openings in the shear walls are inevitable for various functional requirements. Not much study has been reported on behaviour of shear walls with openings under seismic loading. Even several national codes do not include provisions for detailing of reinforcement in shear walls with openings, but few national codes recommend additional corner reinforcement around openings.

5.2 EXPERIMENTAL RESULTS

Five reinforced concrete shear walls, designed with and without openings, tested as per standard loading protocol under reverse cyclic loading. Performance parameters include load vs. displacement response, cracking and failure pattern, shear strength, ductility, shear strength degradation, lateral stiffness degradation and energy dissipation in shear walls.

5.2.1. Load vs. Displacement Response and Crack Pattern

Lateral load vs. displacement response and crack pattern after testing under designed cyclic loading in all three walls are discussed hereunder. Lateral displacement is the net displacement after corrections due to sliding of shear wall during experimentation.

A. Shear Wall without opening, SW–1.0-00-00

First crack formed in upper half of boundary element at a drift ratio of 0.4%. During subsequent increments of displacement, a horizontal crack originated at boundary element inclined towards toe in opposite end of web wall. Several such small inclined cracks also formed and propagated in web wall. Crack pattern in web wall, at peak load and at failure, is shown in Figure 5.1. Failure occurred by crushing of concrete in both toes of boundary elements due to reversed cyclic displacements.

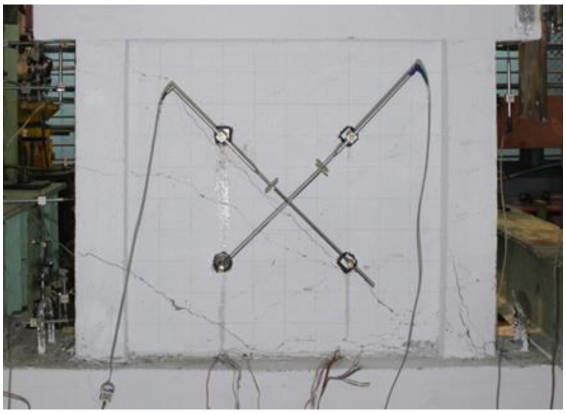

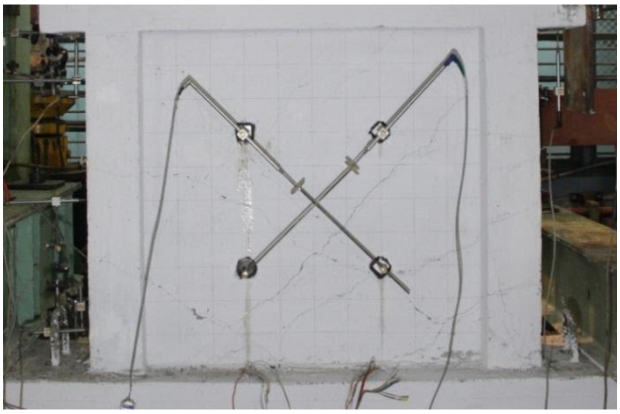

Positive Cycle Negative Cycle

a. At Peak load

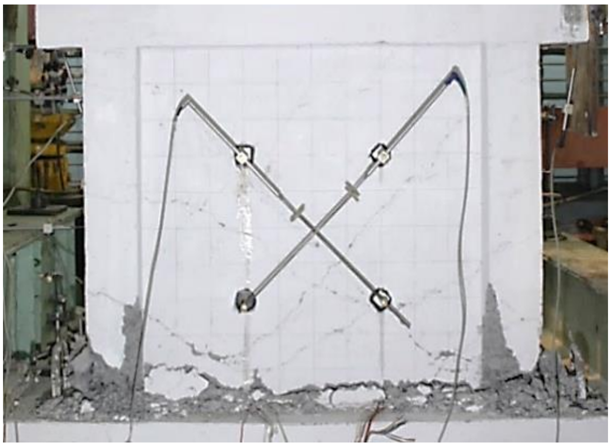

b. At Failure Stage

Fig. 5.1 Crack pattern at Peak and ultimate failure load for SW-1-00-00

Hysteresis loops and backbone envelope curves have been developed for shear walls as shown in Figure 5.2. Backbone curve corresponding to first cycle of each displacement amplitude has been constructed by joining points of peak loads of recorded hysteresis loops.

Response of shear wall under lateral loading is linear up to +387 and -345 kN at drift ratios of +0.32 and -0.34% respectively. On further increasing load, slope of response changes significantly. Peak loads of +462 and -393 kN were observed at drift ratios of +0.88 and -0.68% respectively. Failure occurred in wall at drift ratio of +2.19 and -2.07% respectively. Hysteresis loops also exhibit alteration of slope during reverse cyclic loading, resulting in significant decrease in stiffness of wall. This phenomenon, known as pinching effect, is primarily caused by closing previously formed cracks during reversed loading and hence leads to reduction of dissipated energy.

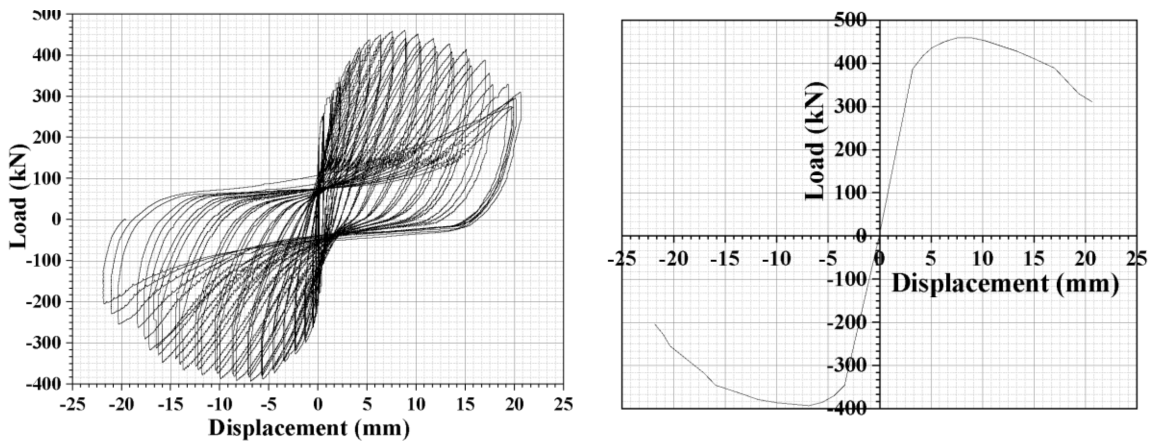

a. Hysteresis Curve

b. Backbone Envelope

Fig. 5.2 Lateral Load vs. Displacement at Top in SW-1.0-00-00

In shear walls failing in flexure, deformation along diagonal of web wall is usually high with respect to top lateral displacement. In shear walls failing in shear, deformation measured along diagonal of web of wall is very small due to shear. Figure 5.3 shows lateral load vs. deformation along diagonal of web. It can be seen from Figure 5.3 that maximum deformation along diagonal of web is less than 2.0 mm, while maximum top lateral displacement is observed to be 22.0 mm. Mode of failure is primarily in shear with significant holding capacity and integrity of two-dimensional grid reinforcement in walls. Rotation of top beam is shown in Figure 5.4.

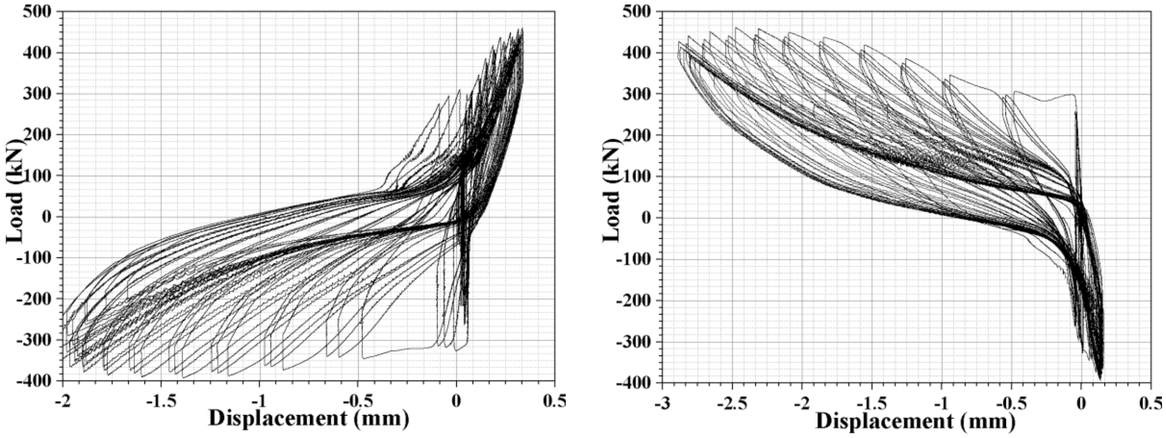

a. Diagonal 1 b. Diagonal 2

Fig. 5.3 Lateral Load vs. Diagonal Displacement in web in SW-1.0-00-00

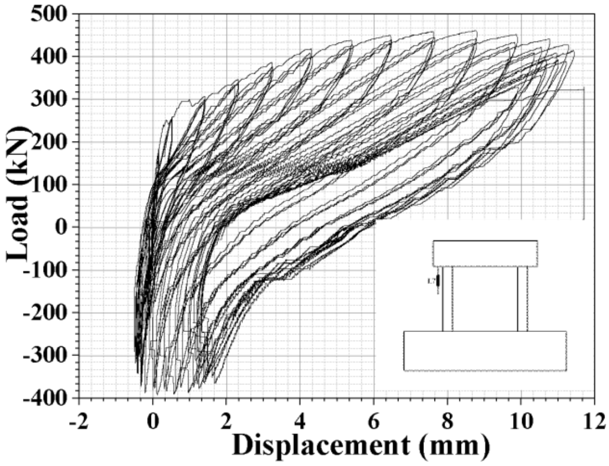

Fig. 5.4 Lateral Load vs. Vertical Displacement of Top Beam in SW-1.0-00-00

B. Wall with window opening (SW-1.0-CW-IS)

First crack observed at top corner of opening and develops diagonally towards top corner of wall during 0.2% drift cycle shown in Figure 5.5.

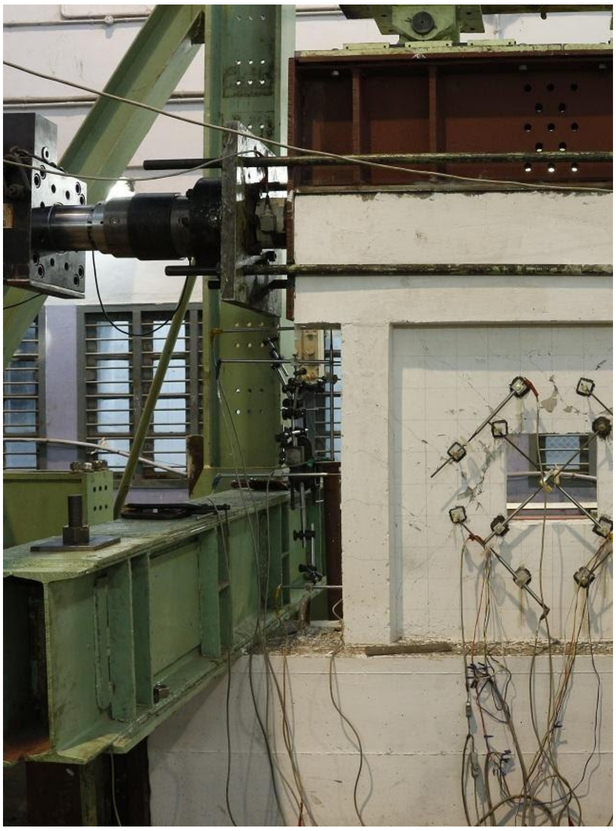

Positive Cycle Negative Cycle

a. At Peak load

b. At Failure Stage

Fig. 5.5 Crack pattern at Peak and Ultimate failure load for SW-1.0-CW-00.

On further loading, cracks at all four corners of opening were formed and developed towards nearest corners of wall. Response of shear wall under lateral loading is linear up to +180 and -173 kN at drift ratios of +0.4 and -0.4% respectively. On further increasing load, slope of response changes significantly. At failure load, weak plane near opening was sheared off horizontally. Peak loads of +292.65 and -289.38 kN were observed at drift of +2.00 and -2.05% respectively.

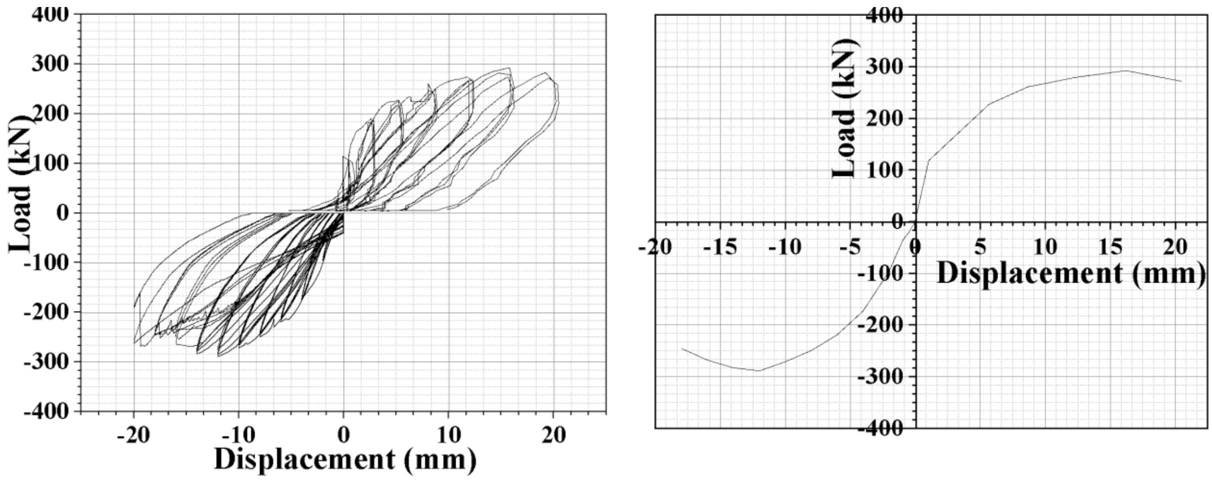

a. Hysteresis Curve b. Backbone Envelope

Fig. 5.6 Lateral Load vs. Displacement at Top in SW-1.0-CW-00

C. Wall with window opening (SW-1.0-CW-IS)

This wall was designed with FRC around opening, is highly prone to stress concentration. First cracking observed at top corner of opening and developed diagonally towards top corner of wall at 0.2% drift. Almost same crack pattern was observed similar to wall with window opening without FRC at initial stages. On loading, cracks from all four corners of opening were formed and developed towards nearest corners of wall. Crack pattern of wall at peak and failure load is shown in Figure 5.7. At failure load, crushing of concrete in both left and right toes of boundary elements was observed in both positive and negative cycles as observed in wall without opening.

Positive Cycle

Negative Cycle

a. At Peak load

b. At Failure Stage

Fig. 5.7 Crack pattern at Peak and Ultimate failure load for SW-1.0-CW-FRC.

Response of shear wall under lateral loading is linear up to +283 and -208 kN at drift ratios of +0.3 and -0.45% respectively. On further increasing load, slope of response changes slightly. Peak loads of +476 and -349 kN were observed at drift ratios of +1.6 and -1.4% respectively. Failure occurred in wall at drift ratio of +2.92 and -2.5% respectively.

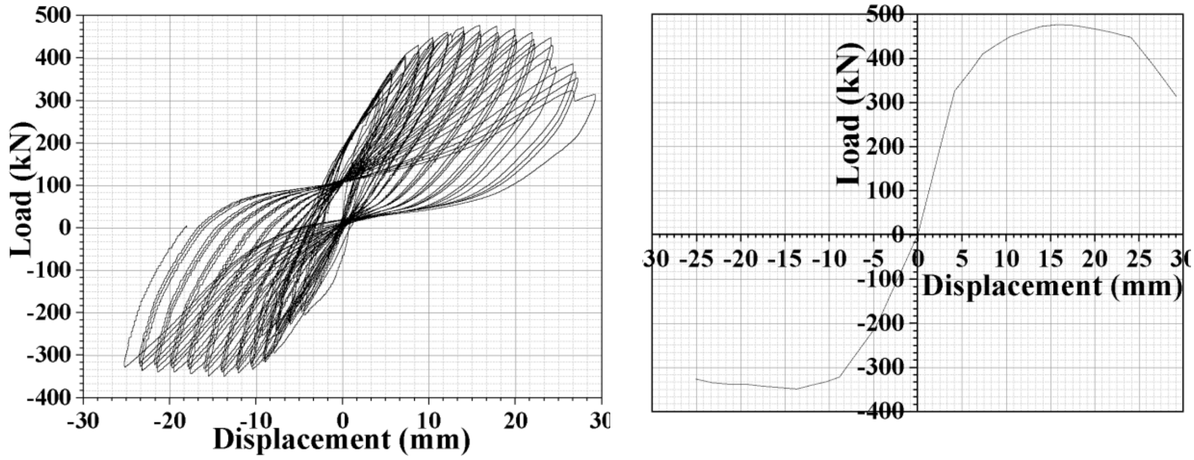

a. Hysteresis Curve b. Backbone Envelope

Fig. 5.8 Lateral Load vs. Displacement at Top in SW-1.0-CW-FRC

Two LVDTs were inclined at top corner of opening expecting stress concentration. Though first crack started at corner of opening, however, failure was not observed through that path. It can be seen from Figure 5.9 that maximum displacement around corners of opening is less than 4 mm. Total lateral displacement was 29 mm. Hence, in this case, stress concentration path is not the failure path of shear wall.

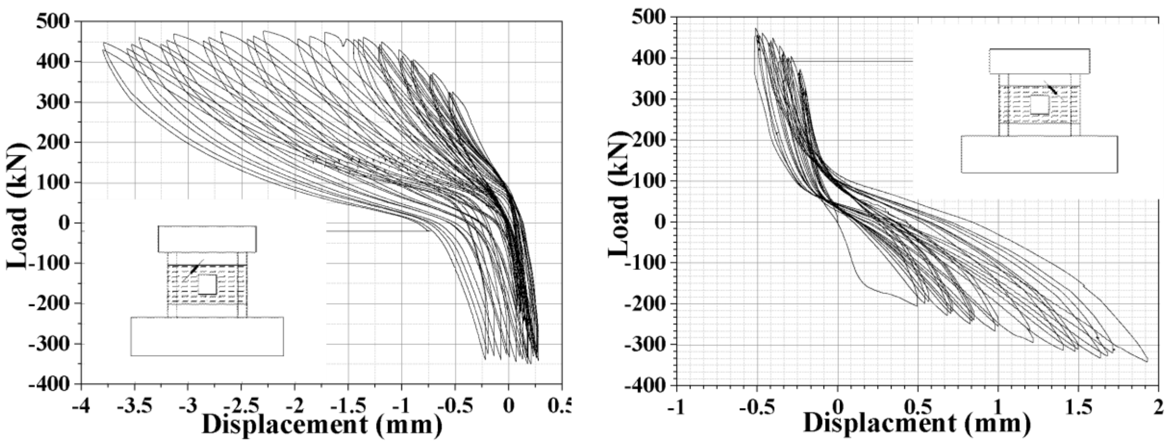

a. Diagonal 1 b. Diagonal 2

Fig. 5.9 Lateral Load vs. Displacement around corners of opening in SW-1.0-CD-00

In shear walls failing in flexure, deformation along diagonal of web wall is usually high with respect to top lateral displacement. In walls failing in shear, deformation measured along diagonal of web of wall is very small due to shear. In this case, diagonal displacement is about 9 mm while top lateral displacement is about 29 mm. In case of wall without opening, this value is less than 2 mm. In this case, it seems to be a significant value. This infers that demarcation line that divides wall as squat or slender is low in case of wall with openings i.e wall with opening becomes slender even with lower aspect ratio.

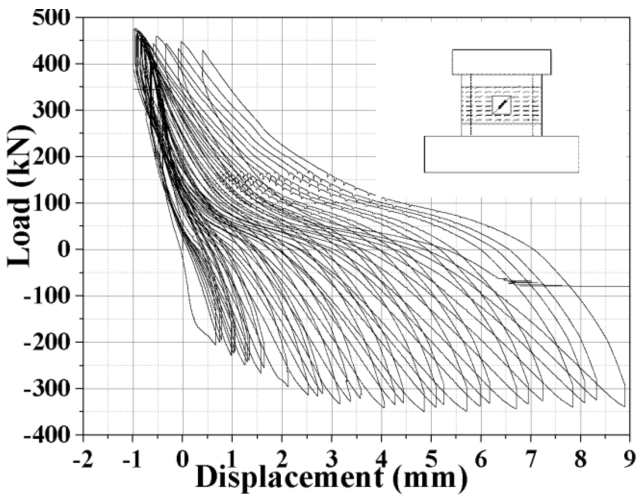

Fig. 5.10 Lateral Load vs. Diagonal Displacement in the web in SW-1.0-CW-FRC.

D. Wall with Door Opening, SW-1.0-CD-00

In this squat wall, a central opening was provided symmetrically. First crack originated at top corner of utility opening and progressed diagonally towards upper corner of wall at a drift ratio of 0.2%. On further lateral loading, more cracking initiated near toe of boundary element and progressed towards topmost corner of utility opening. On other hand, crack originated from bottom most corner of opening progressed towards boundary element up to top of utility opening. During reversed loading cycle, similar cracking observed on reverse corners of utility opening. These reverse cracks frame at a junction. Crack pattern in wall, at peak load and at stage of failure are shown in Fig. 5.11. Unlike in solid wall, weak plane does not coincide any horizontal plane passing through walls with opening.

Positive Cycle　　　　　　　　　　Negative Cycle

a. At Peak load

b. At Failure stage

Fig. 5.11 Crack pattern at Peak Load and Failure stage for SW-1.0-CD-00

Hysteresis loop and backbone envelope curves developed for shear wall, SW-1.0-CD-00 are shown in Figure 5.12. Wall behaves linearly up to load of +179 and -246 kN at drift ratios of +0.15 and -0.29% respectively. On further loading, slope of curve changes significantly. Peak loads of +242 and -269 kN observed at drift ratios of +0.93 and -0.62% respectively. Failure occurred at drift ratios of shear wall of +1.63 and -2.00% respectively under reverse cycles. A mild pinching of hysteresis loop has been observed in shear wall, SW-1.0-CD-00, with central opening as shown in Figure 5.12 due to closing and opening of cracks during reverse cyclic loading.

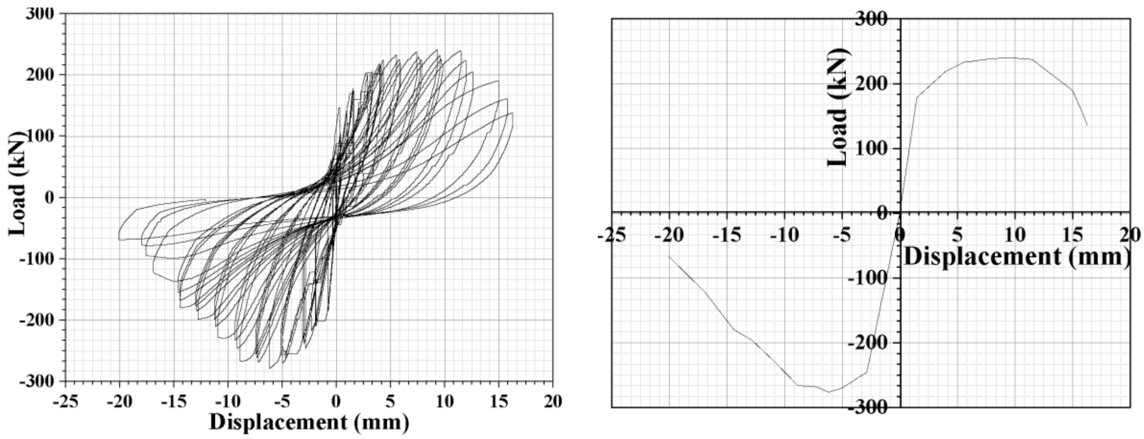

a. Hysteresis Curve   b. Backbone Envelope

Fig. 5.12 Lateral Load vs Top Displacement relationship for SW-1.0-CD-00

In structural member with discontinuities like openings, upon far field load application, stress concentration occurs at corners. Due to stress concentration, cracks can initiate and progress from corners of utility opening very easily. Figure 5.13 shows lateral load and web displacement measured at corners of utility opening in shear wall. Though first crack formed at corners of opening, major crack and failure plane does not pass through the corner as shown in Figure 5.11. It can be observed that the maximum deformation of web around corners of opening is less than 4.0 mm, while the maximum lateral displacement at top of web of wall is 20 mm.

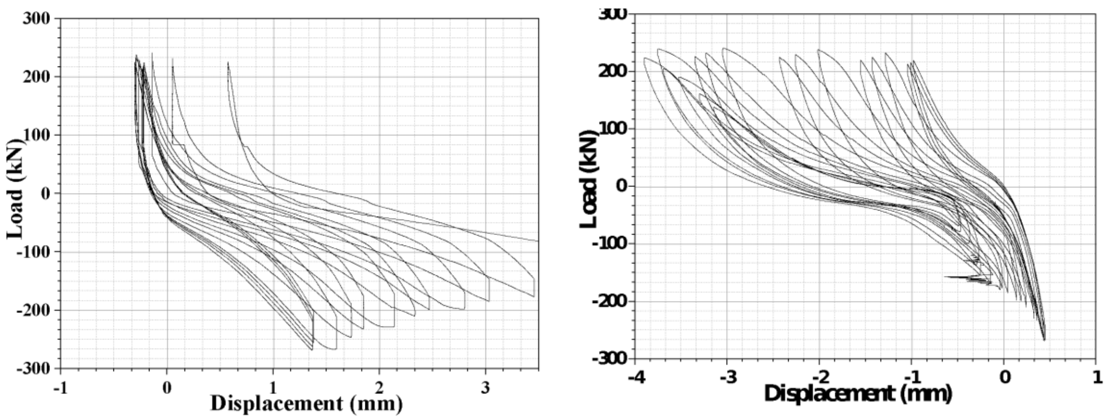

a. Diagonal 1 b. Diagonal 2

Fig. 5.13 Lateral Load vs. Displacement around corners of opening in SW-1.0-CD-00

E. Shear Wall using FRC with Door Opening, SW-1.0–CD–FRC

This squat wall was designed with a central opening. Concrete used for construction of this wall was randomly distributed with 1.0% steel fibres by weight. Crack pattern and mode of failure of shear wall using FRC with opening observed to be similar to wall with opening, SW-1.0-CD-00 cast with same grade of normal concrete. Crack pattern in wall at peak and failure loads are shown in Figure 5.14. In this wall, weak plane with opening did not coincide with horizontal, unlike in wall without opening.

Positive Cycle Negative Cycle

a. At the Peak load

b. At the Failure load

Fig. 5.14 Crack pattern at Peak Load and Failure load for SW-1.0-CD-FRC

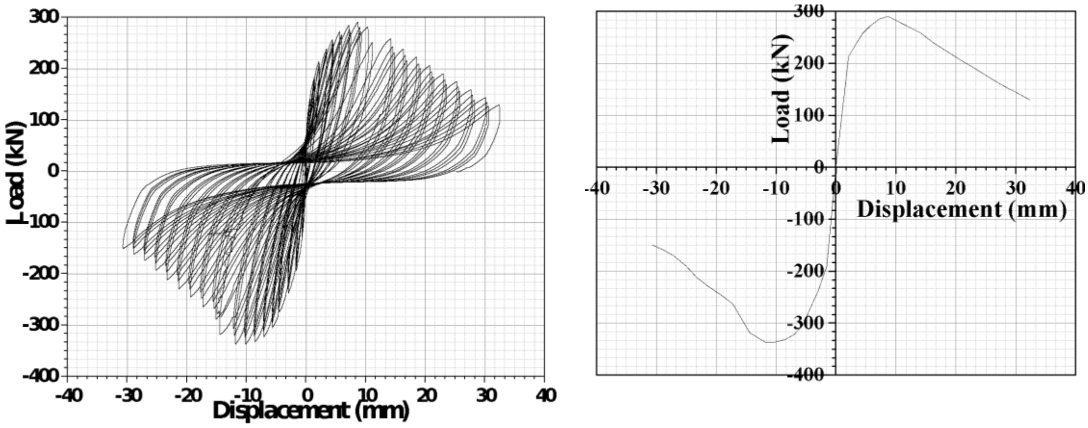

a. Hysteresis loops

b. Backbone Envelope curve

Fig. 5.15 Lateral Load vs. Displacement at top of the web in SW-1.0-CD-FRC.

Hysteresis loop and backbone envelope curves developed in shear wall, SW-1.0-CD-FRC, are shown in Figure 5.15. Behaviour of wall is linear up to loads +238.7 and -190 kN at drift ratios of +0.34 and -0.16% respectively. On further loading, slope of response changes gradually. Peak loads of +290 and -336 kN observed at drift ratios of +0.86 and -1.01% respectively. Drift ratios at failure were +3.25 and -3.07%. Significant hysteresis pinching has been observed, Figure 5.15, due to closing and opening of cracks during reverse cyclic loading. Figure 5.16 shows vertical displacement of extreme fibre of wall.

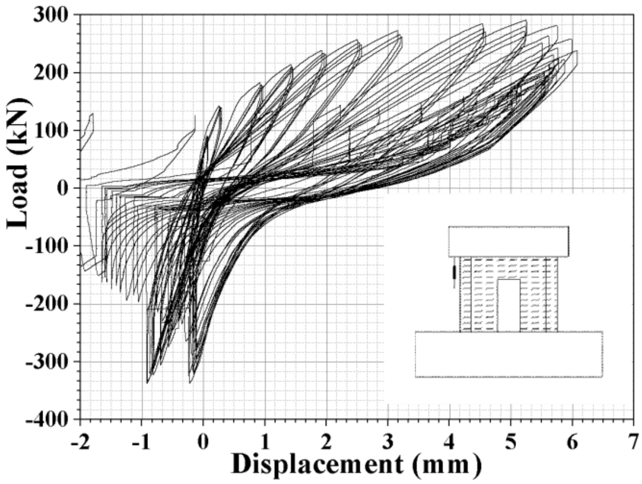

Fig. 5.16 Lateral Load vs. Vertical Displacement at top Beam in SW-1.0-CD-FRC.

Fig. 5.17 Failure Stages for SW-1.0-00-00

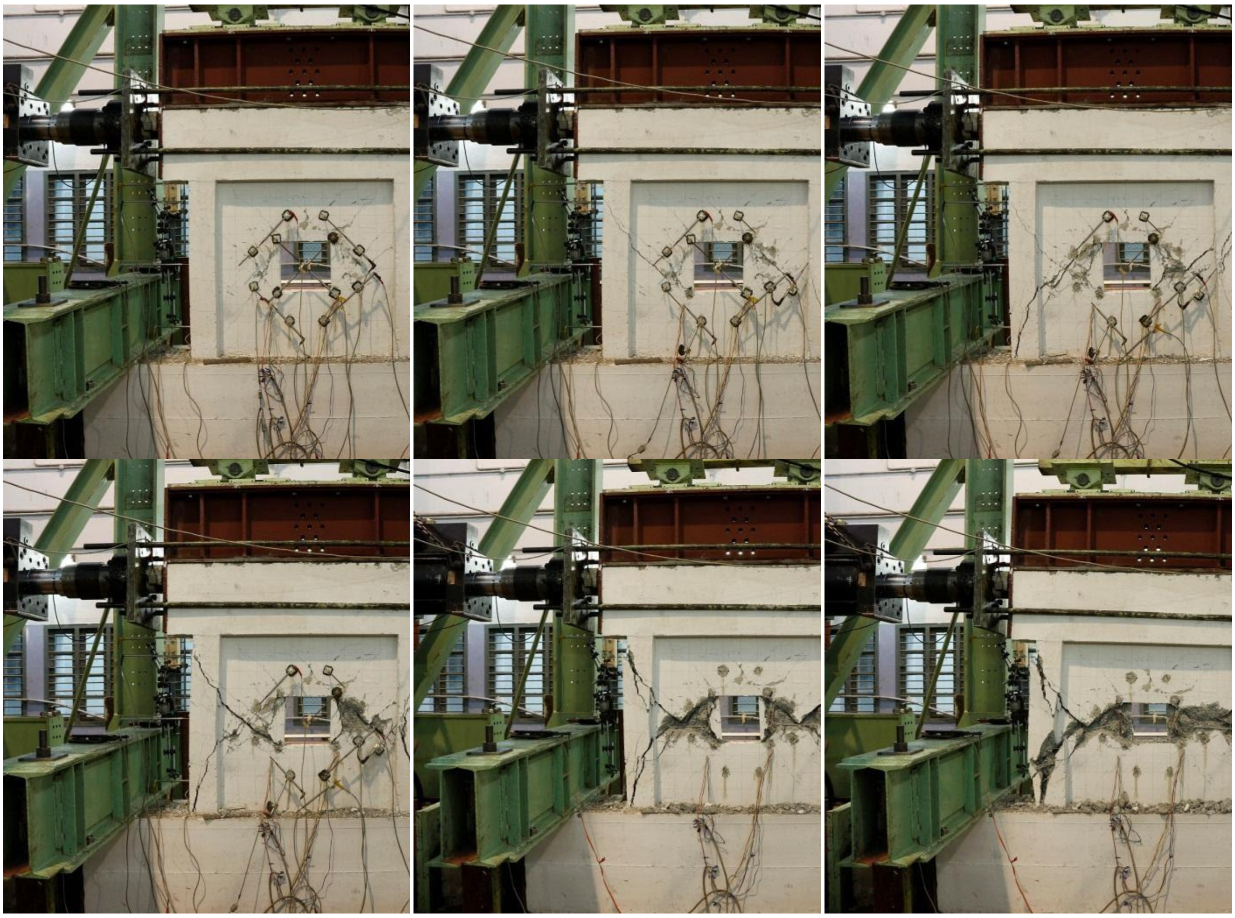

Fig. 5.18 Failure Stages for SW-1.0-CW-00

Fig. 5.19 Failure Stages for SW-1.0-CW-FRC

Fig. 5.20 Failure Stages for SW-1.0-CD-00

Fig. 5.21 Failure Stages for SW-1.0-CD-FRC

5.2.2. Shear Strength

For estimation of shear strength and ductility, backbone load vs. displacement envelopes have been constructed and compared in all three squat walls as shown in Figure 5.22 shows comparative back bone envelopes for window opening and Figure 5.23 shows comparative backbone envelope with door opening.

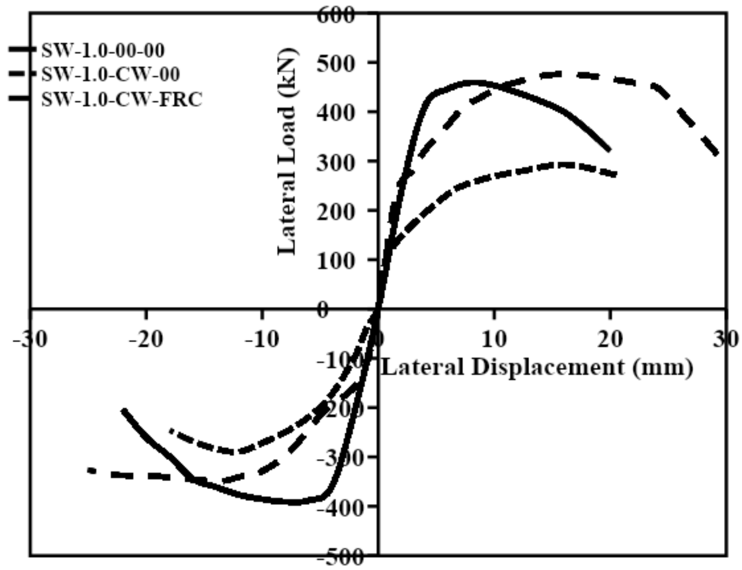

Fig. 5.22 Comparison of Load-Displacement Envelope for Door Opening

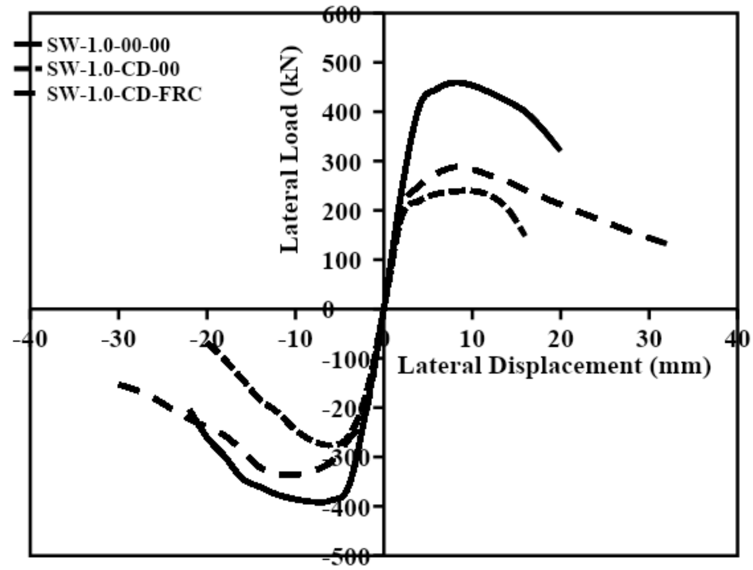

Fig. 5.23 Comparison of Load-Displacement Envelope for Window Opening

Shear strength, displacement at various stages and ductility factors in all three shear walls are shown in Table 5.1. Shear strength at a given lateral drift ratio of squat wall with opening has been found to be lesser than that without opening. Shear strength of squat wall has been found to be reduced significantly with opening. However, shear strength has been increased by adding steel fibres in concrete around corners of opening.

Table 5.1 Shear strength in squat shear walls.

Specimen	V_{peak^+} (kN)	V_{peak^-} (kN)	V_{Peak} (kN)	$(V_{peak})_{sw-1.0}/V_{peak}$	τ_{max} (MPa)
SW-1.0-00-00	462	-393	428	-	1.99
SW-1.0-CW-00	293	289	291	68%	1.35
SW-1.0-CW-FRC	476	349	413	97%	1.92
SW-1.0-CD-00	242	-269	259	60%	1.20
SW-1.0-CD-FRC	292	-338	315	74%	1.75

Shear strength of squat wall without opening has been found to be 428 kN, whereas in squat wall with window opening, it has been reduced to 283 kN and for door opening, it has been reduced to 259 kN. There has been a 32 and 40% reduction in strength of shear wall with window and door opening respectively. Shear strength of squat wall cast with FRC with opening has been observed to be 413 kN and 315 kN for walls with window and door opening respectively. Wall with window opening cast wit FRC has almost reached capacity of wall without opening. In case of door opening cast with FRC its capacity is only 73.6% of that of wall without opening. There has been a reduction of 26.4% in shear strength of FRC squat walls with door opening. Figure 5.24 shows comparison of lateral load capacity of three shear walls.

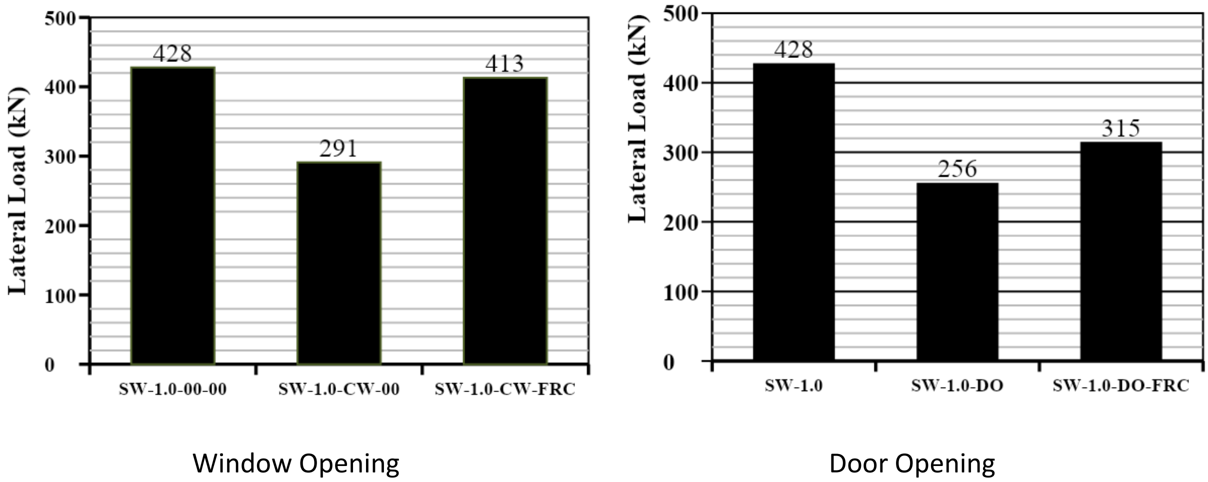

Fig. 5.24 Comparison of Average Lateral Load Capacity of the squat walls

5.2.3. Ductility Factor

The ductility factor is calculated using equivalent energy elastic-plastic (EEEP) curve principle. This EEEP curve is a perfectly elastic-plastic representation of the actual response of the specimen. This bilinear EEEP curve is plotted such that it equals the area under the load-deflection curve until failure i.e. the energy dissipation capacity is equal. Fig. 4 shows the various points of interest used to derive the EEEP curve.

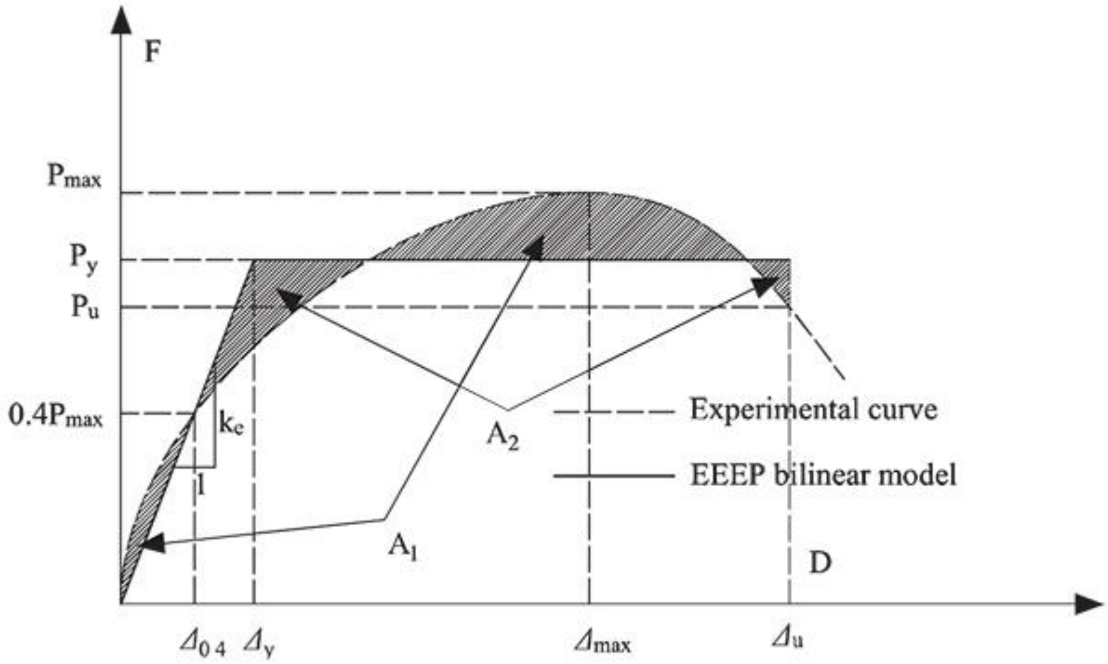

Fig. 5.25 EEEP Curve

The salient features of the EEEP bilinear curve are,

k_e – Secant Stiffness at the point corresponding to 40% of the maximum load

P_y – Yield strength as per EEEP curve

Δ_y – Yield Displacement corresponds to P_y

Δ_u – Ultimate displacement which corresponds $0.8P_{max}$ at post peak

The area (energy) under the backbone curve was then calculated up to the post-peak displacement that corresponds to the EEEP curve up to the lateral displacement Δ_u. The slope of inclined portion of the EEEP curve corresponds to the Secant Stiffness at 40% of the maximum load in backbone curve. A horizontal line depicting the plastic portion of the EEEP curve was then positioned so that the area bounded by the EEEP curve and the back bone are equal. Thus the value of yield strength and yield displacement is calculated.

Table 5.2 Ductility factors in squat shear walls.

	P_{max} (kN)	40% P_{max} (kN)	40% Δ_{max} (mm)	80% P_{peak} (kN)	Δ_u (mm)	k_e (kN/mm)	Total Energy E (kNmm)	P_y (kN)	Δ_y (mm)	μ
SW-1.0-00-00	459	184	1.53	367	17.8	120	7582	480	4.0	4.43
SW-1.0-CW-00	293	117	1.02	234	18.1	114	4896	291	2.5	7.06
SW-1.0-CW-FRC	476	190	1.25	381	26.8	152	11714	464	3.1	8.76
SW-1.0-CD-00	239	95	1.73	191	14.4	55	3095	256	4.6	3.10
SW-1.0-CD-FRC	288	115	1.14	230	17.5	100	5586	356	3.5	4.92

Ductility factors are 4.43, 7.06, 8.76, 3.10 and 4.92 respectively in five walls SW-1.0-00-00, SW-1.0-CW-00, SW-1.0-CW-FRC, SW-1.0-CD-00 and SW-1.0-CD-FRC as shown in Table 5.2. Ductility factor in wall made with same concrete with opening has been observed to be 59% increase in case of wall with window opening and 30% decrease in case of wall with door opening. Ductility factor in wall cast with FRC with opening has been observed to increase about 24% and 58% of that of wall with opening in respective of window and door opening. This indicates that wall with FRC exhibited better ductility than shear wall without opening. Shear wall without opening failed in a horizontal plane. Figure 15 shows bar chart for better understanding.

5.2.4. Horizontal Strength Degradation

Walls should ensure minimum strength under multiple cycles of loading after reaching a maximum peak load in a cycle for safety of structures. Generally, reinforced concrete walls exhibit rapid strength loss during subsequent repeated cycles of loading (Luna[28]). To assess strength of squat walls with openings and cast with different concretes, strength endured during subsequent cycles of loading after cycle with maximum peak load in all three walls have been compared. Shear strength of a wall is V_1, corresponding to highest peak load in a cycle, and maximum peak loads in consecutive two cycles are V_2 and V_3. Maximum loads V_1, V_2, V_3 correspond to three consecutive hysteresis loops extracted from first and third quadrants independently in all three shear walls. Three peak loads V_1, V_2, and V_3 have been extracted independently in all shear walls SW-1.0-00-00, SW-1.0-CW-00, SW-1.0-CW-FRC, SW-1.0-CD-00 and SW-1.0-CD-FRC. These three peak loads in three consecutive loops in a shear wall are shown in circles in Figure 5.26. Tables 5.3 and 5.4 show peak loads, V_1, V_2, and V_3 observed in three consecutive cycles in all three shear walls. Ratios of highest peak load observed in loop-to- peak load in two subsequent cycles observed i.e. V_2/V_1, V_3/V_1 have been calculated in all three shear walls.

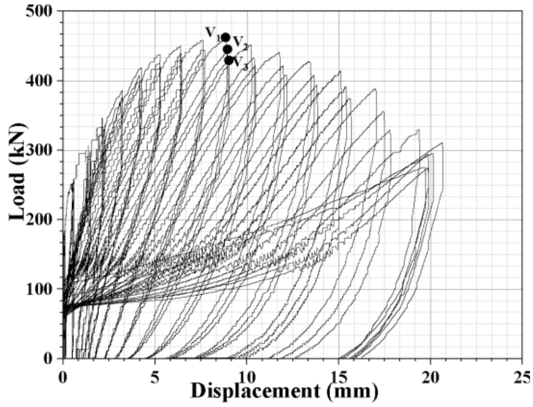

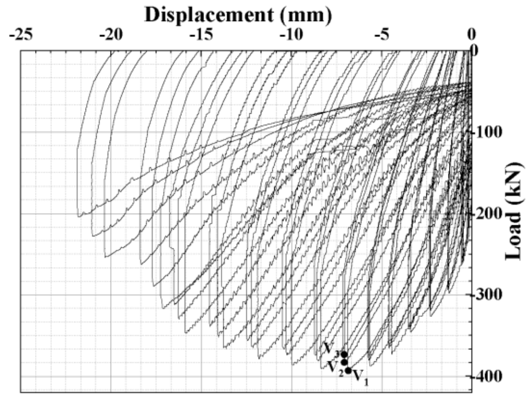

a. First Quadrant Hysteresis of SW-1.0-00-00 b. Third Quadrant Hysteresis of SW-1.0-00-00

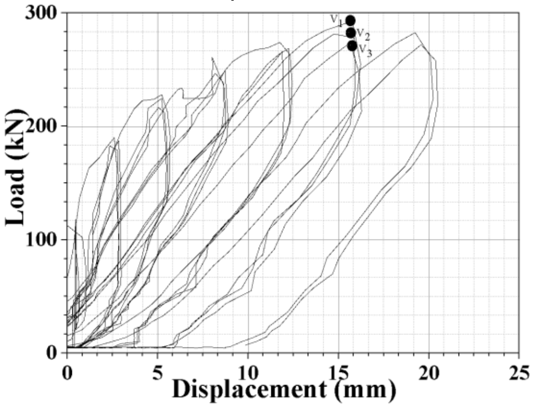

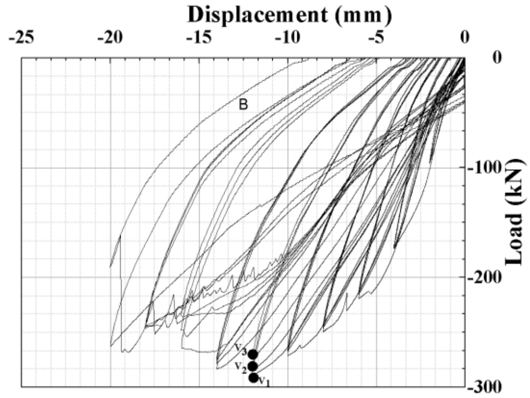

a. First Quadrant Hysteresis of SW-1.0-CW-00 b. Third Quadrant Hysteresis of SW-1.0-CW-00

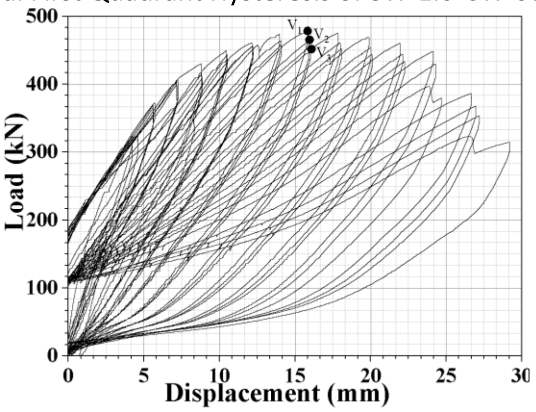

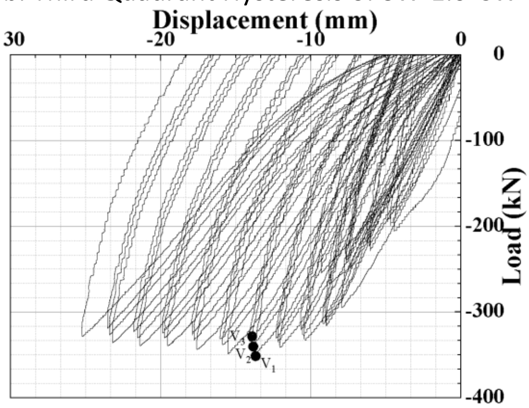

c. First Quadrant Hysteresis of SW-1.0-CW-FRC d. Third Quadrant Hysteresis of SW-1.0-CW-FRC

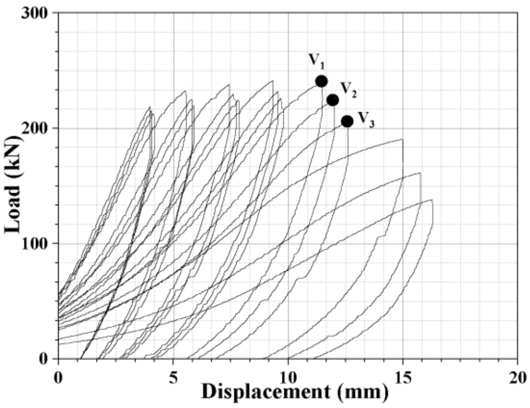

e. First Quadrant Hysteresis of SW-1.0-CD-00

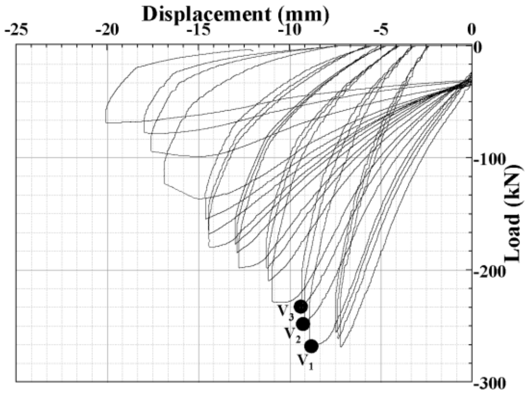

f. Third Quadrant Hysteresis of SW-1.0-CD-00

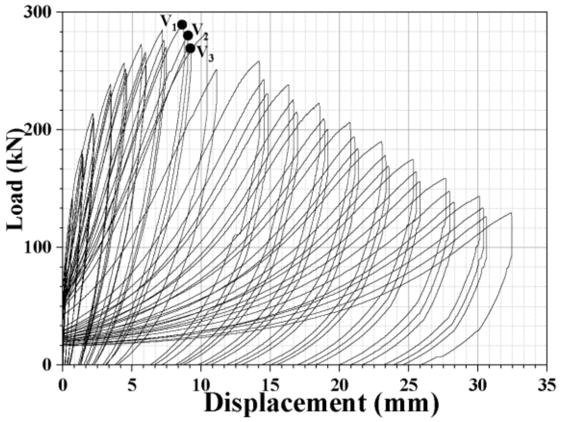

g. First Quadrant Hysteresis of SW-1.0-CD-FRC

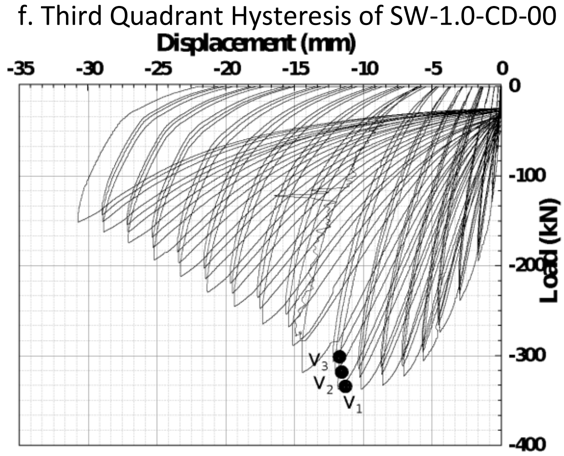

h. Third Quadrant Hysteresis of SW-1.0-CD-FRC

Fig. 5.26 First and Third Quadrant Hysteresis Loops

Ratios of peak loads observed in walls during second and third consecutive cycles after highest peak load divided by that in previous cycle. This ratio indicates strength loss in subsequent cycles in shear walls. It is evident from shear strength ratios in Table 5.3 that strength degradation varies for wall with window opening. It has been observed that wall with window opening shows similar trend as that of wall without opening. Addition of steel fibers decreases loss to a small extent. In wall without opening, residual strength during second and third consecutive cycles are 96 and 93% respectively beyond highest peak load. In squat wall with window opening cast in normal concrete, residual strengths are similar about 96 and 93% respectively. However, in squat wall with opening cast with FRC exhibited residual strength of 97 and 96% respectively. This infers that, the residual strengths being increased marginally in case of wall with window opening using FRC. Steel fibers improve the cracking resistance and ductility more then the strength.

Table 5.3 Shear Strength and its Degradation for Window opening

	Wall ID	SW-1.0-00-00	SW-1.0-CW-00	SW-1.0-CW-FRC
Positive Cycle	**V_1 (kN)**	462	293	477
	V_2 (kN)	442	281	465
	V_3 (kN)	429	273	457
	V_2/V_1	**0.96**	**0.96**	**0.97**
	V_3/V_1	**0.93**	**0.93**	**0.96**
Negative Cycle	**V_1 (kN)**	393	289	349
	V_2 (kN)	383	284	340
	V_3 (kN)	377	274	334
	V_2/V_1	**0.97**	**0.98**	**0.97**
	V_3/V_1	**0.96**	**0.95**	**0.96**

Table 5.4 shows strength degradation variation for wall with door opening. It is observed that shear walls with door openings exhibited rapid loss of strength in subsequent cyclic loading beyond maximum peak load. However, wall without opening and wall cast with FRC with opening exhibited moderate loss of strength during subsequent cycles of loading beyond highest peak load. This ensures, in reality, better performing of shear walls with FRC during an event of Earthquake.

Table 5.4 Shear Strength and its Degradation for Door opening

	Wall ID	SW-1.0-00-00	SW-1.0-CD-00	SW-1.0-CD-FRC
Positive Cycle	**V_1 (kN)**	462	242	292
	V_2 (kN)	442	223	280
	V_3 (kN)	429	205	271
	V_2/V_1	**0.96**	**0.92**	**0.96**
	V_3/V_1	**0.93**	**0.85**	**0.93**
Negative Cycle	**V_1 (kN)**	393	269	338
	V_2 (kN)	383	246	320
	V_3 (kN)	377	232	307
	V_2/V_1	**0.97**	**0.91**	**0.95**
	V_3/V_1	**0.96**	**0.86**	**0.91**

In wall without opening, residual strength during second and third consecutive cycles are 97 and 96% respectively beyond the highest peak load. In squat wall with opening cast in normal concrete, residual strengths are 91 and 86% respectively. However, in squat wall with opening cast with FRC exhibited residual strength of 95 and 91% respectively. This shows that fibers in concrete in walls with opening prevent sudden failures as well as improve the integrity of concrete under cyclic loading.

5.2.5. Lateral Stiffness

Shear walls are primary lateral load resisting elements adopted in tall buildings in high seismic prone areas due to their inherent high lateral stiffness. Table 5.5 shows the initial and secant stiffness observed in five RC walls. Initial stiffness has been calculated from first cycle at 1.25% drift ratio in all three-shear walls. Secant stiffness has been calculated corresponding to maximum peak load in first quadrant.

Table 5.5 Initial and Secant Stiffness

Wall ID	Initial Stiffness (kN/mm)	Secant Stiffness at Peak load (kN/mm)
SW-1.0-00-00	202	57
SW-1.0-CW-00	114	18
SW-1.0-CW-FRC	150	30
SW-1.0-CD-00	120	26
SW-1.0-CD-FRC	129	34

As shown, shear wall without opening exhibited high initial stiffness than those with openings. Initial stiffness of wall with opening has been observed to be about 60% of that of wall without opening cast with same concrete. Both shear walls with openings but cast with different concretes exhibited different initial stiffness. Additional reinforcement detailing adopted around corners of opening effectively counteracts without much reduction of initial stiffness of shear walls. Walls with opening were provided with corner reinforcement as discussed above. Initial stiffness would have been reduced further if there was no additional reinforcement in wall around corners. Wall with opening and also provided with additional reinforcement, cast with FRC exhibited higher stiffness. In other words, walls cast with FRC exhibited slightly increased initial stiffness compared with that of wall cast in normal concrete. This implies that FRC in shear walls increases initial stiffness.

Variation of secant stiffness (corresponding to first cycle at each drift ratio as per loading protocol) with displacement measured at top of web and comparison of normalized stiffness (calculated as secant stiffness of cycle 1 with secant stiffness of consecutive cycles) with lateral displacement at top of shear walls are shown in Figure 5.27 and Figure 5.28 for wall with window and door openings respectively.

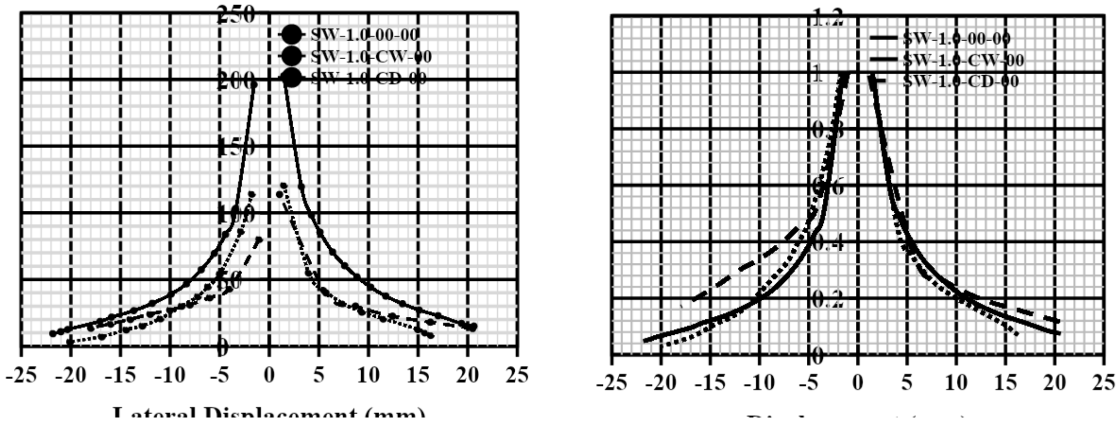

Fig. 5.27 Stiffness Degradation of Shear Walls with Window Opening

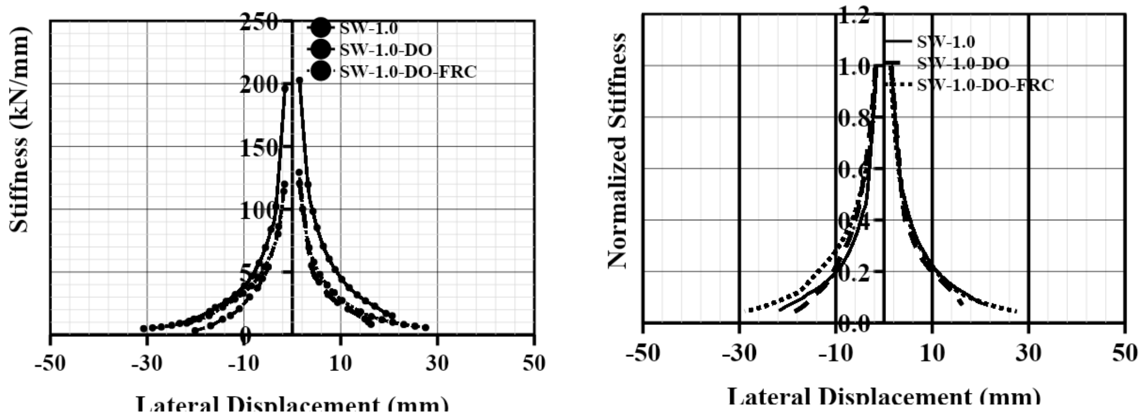

Fig. 5.28 Stiffness Degradation of Shear Walls with Door Opening

It can be noticed that stiffness of walls decreases with increase in subsequent cycles of loading. Reduction in stiffness of wall is due to the fact that cracking under reverse cycles increases cracking in concrete and deterioration of properties of reinforcement. Stiffness degradation in shear walls with opening has been observed to be rapid. Stiffness degradation in wall with opening and cast with FRC is very minimal than other two walls.

5.2.6. Energy Dissipation

Energy dissipation during each cycle has been calculated from area under load-displacement hysteresis curve. Variation of energy dissipation at three consecutive cycles of lateral displacement of wall at top of web is shown in Figure 5.29. There has been a considerable reduction in energy dissipation in consecutive cycles at same drift ratio.

Normalized energy dissipation is calculated as the ratio of energy dissipated in each cycle at onward displacement to product of $0.5V_y\Delta_y$, where V_y and Δ_y are horizontal load and displacement respectively at time of yielding. Energy dissipated in wall without opening has been observed to be greater than that of walls with opening. Post-peak response is not gradual in walls with normal concrete. Wall cast with FRC with opening showed ductile post-peak response. In walls with opening, energy dissipation in both walls with openings has been observed to be similar. But post-peak response has been found to be more ductile in wall cast with FRC. Main reason for this response is addition of fibres in concrete, which improved ductility of concrete. It can be seen from normalized energy dissipation response (Figs. 5.30 and 5.31) that response of all walls with respect to energy dissipation is similar in shape.

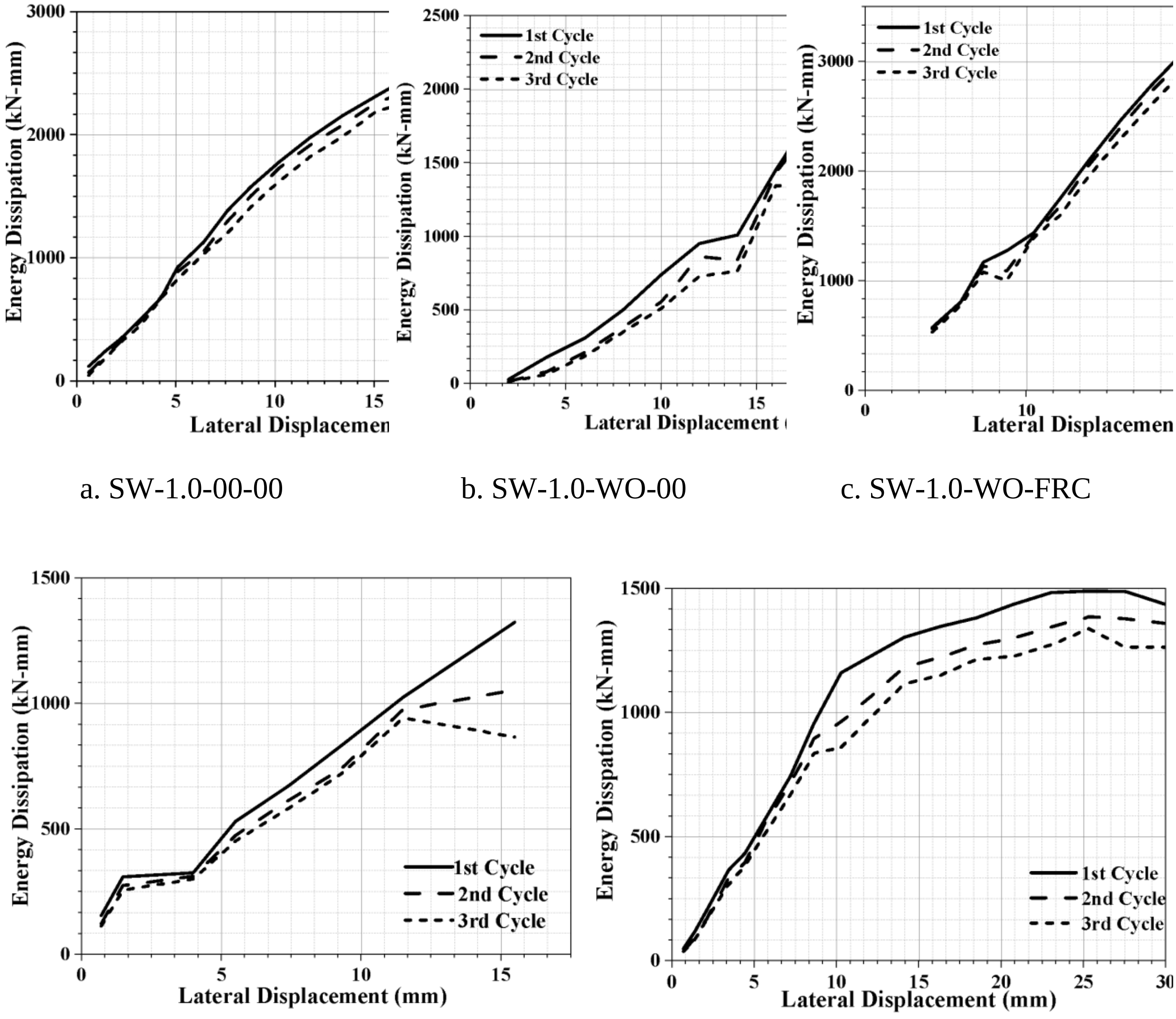

a. SW-1.0-00-00 b. SW-1.0-WO-00 c. SW-1.0-WO-FRC

d. SW-1.0-DO-00 e. SW-1.0-DO-FRC

Fig. 5.29 Energy Dissipation vs. Lateral Displacement.

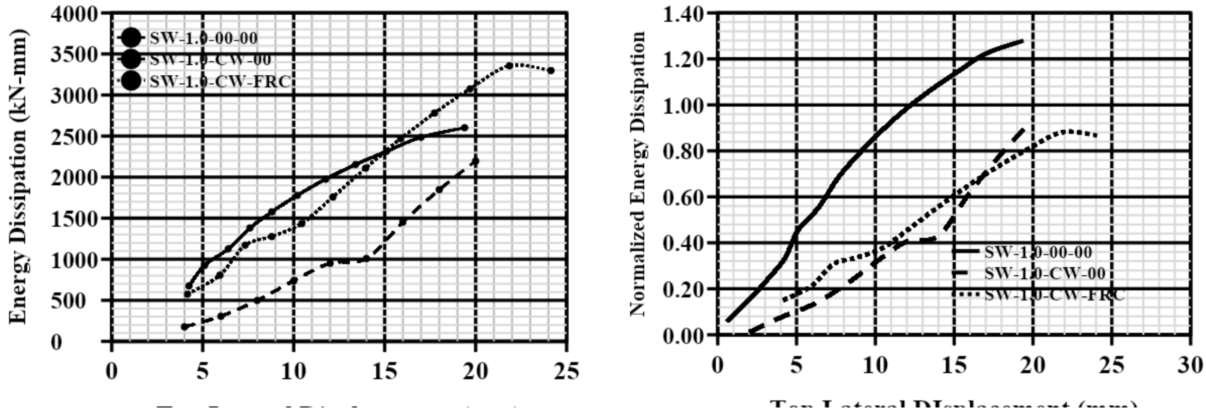

a. Energy Dissipation vs. Displacement

b. Normalized Energy Dissipation vs. Displacement

Fig. 5.30 Comparison of Energy Dissipation of walls with window opening

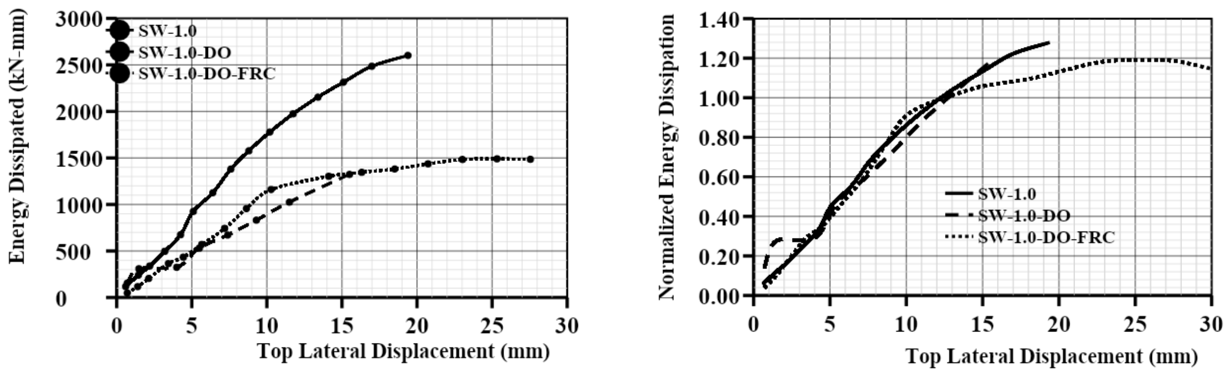

a. Energy Dissipation vs. Displacement

b. Normalized Energy Dissipation vs. Displacement

Fig. 5.31 Comparison of Energy Dissipation of walls with door opening

5.3 Prediction of Strength of RC Walls With and Without Openings

Various equations reported for predicting shear strength of shear walls with and without openings by design codes and literature have been reviewed and predicted results from such equations are compared.

5.3.1. Shear Strength of Wall without Opening

Shear strength of walls estimated by various equations is shown in Table 5.6. It is evident that there is an appreciable deviation of shear strength of RC wall predicted by various equations. Shear strength of RC wall observed in this experimental study has been found to be agreeable with predictions by *ACI 318–19, ASCE/SEI 43-05, MCBC–04, AS3600–2009* and *Sanchez et al. (2010).*

Table 5.6 Comparison of Shear Strength of Shear Wall without Opening

S. No.	Code/ Literature	Eq. No.	Shear Strength (kN)
1	*ACI : 318 (2014) (Ch 11 – Walls)*	1	383
2	*ACI : 318 (2014) (Ch. 18 – Special St. walls)*	2	**404**
3	*ASCE/SEI 43 (2005)*	3	**396**
4	*IS : 456 (2000)*	4	485
5	*MCBC (2004)*	5	**416**
6	*EC8 (2004)*	6	295
7	*AIJ (1999)*	7	324
8	*AS : 3600 (2009)*	8	**421**
9	*NZ : 3101.1 (2006)*	9	303
10	*Barda et al. (1977)*	10	473
11	*Wood (1990)*	11	306
12	*Hernandez et al. (1980)*	12	534
13	*Sanchez et al. (2010)*	13	**396**
14	*Gulec et al. (2011)*	14	225
15	*Kassem et al. (2010)*	15	708
16	*Luna et al.(2019)*	16	509
17	*Present Study*	17	**428**

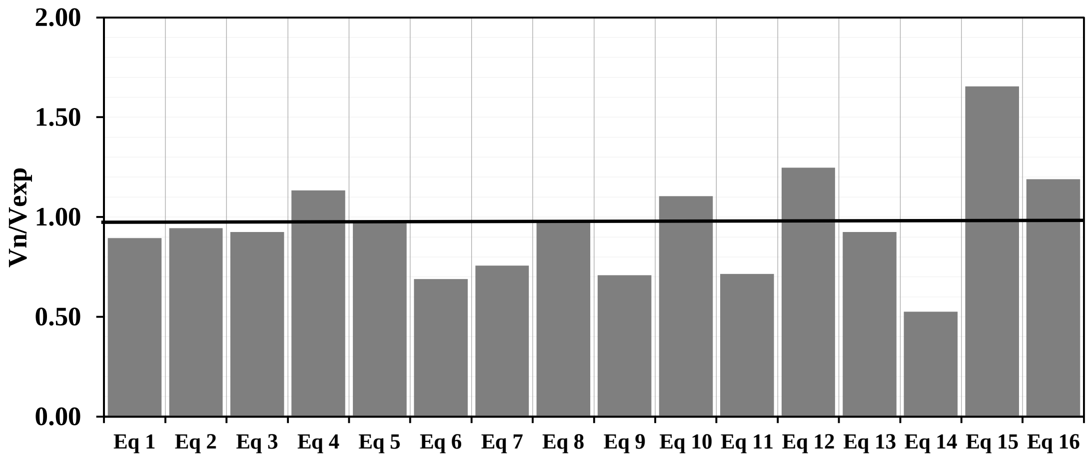

Fig. 5.32 Bar Chart showing the ratio V_n/V_{exp} estimated from various equations.

5.3.2. Shear Strength of wall with Opening

Horizontal strength of walls with opening is described in *ACI 318–2019*. Unlike in RC walls without openings, prediction of horizontal strength of walls with openings is not commonly encountered due to lack of investigations. For RC walls with opening, *ACI 318–2019* recommends an equation for predicting strength RC wall with opening by replacing gross area (A_{cv}) of section with section area less area of opening. Horizontal strength of RC walls prescribed by *ACI 318* is.

$$V_n = (cf_c' + tf_{yt})A_{cv} \tag{5.1}$$

Here, gross area (A_{cv}) is total area of defined section minus area of the utility opening in that section. Shear strength of the wall with window opening is 291 kN from experimental result. This is closely in accordance with ACI 318 prediction value of 287 kN. The shear strength of wall with door opening is 255 kN from experimental result, whereas, same with ACI 318 prediction is 287 kN. ACI 318 prediction for door opening is unconservative due to the fact that ACI 318 does not account for the shape of opening. Rather it accounts only for width of opening in wall. As suggested by *ACI 318* that weak plane coincides with horizontal in opening, which does not seem to be observed in experimental investigations.

5.4 CONCLUDING REMARKS

Based on experimental investigations on squat shear walls with openings, and estimation of strength of RC walls using various equations specified by codes and research studies, following conclusions have been drawn.

- Wall without opening failed by crushing of concrete in both toes of boundary elements and sheared off horizontally due to reversed cyclic displacements. For wall with window opening, failure mode has been due to shearing off weaker plane of wall (i.e) across opening. For wall without opening and with window opening with addition of FRC, failure mode occurred due to crushing of concrete at both left and right toes of boundary elements. Interestingly, addition of FRC around window opening alters cracking pattern of wall. In case of door opening, cracking and failure have been similar in RC squat walls cast with normal concrete and fiber reinforced concrete.
- Shear strength of RC walls with opening has been rapidly reduced, which is about 68% in case of window opening and 61% in case of door opening of that of RC squat wall without opening. Steel fibres used in concrete in and around corners of opening has improved shear strength by above 29 and 14% respectively as compared with RC squat wall cast with normal concrete with opening.
- Ductility of RC walls with opening has been reduced significantly, which is about 51% in case of window opening and 70% in case of door opening of that of RC squat wall without opening. Steel fibres used in concrete in and around corners of opening has

improved shear strength by above 23 and 40% respectively as compared with RC squat wall cast with normal concrete with opening.

- Reduction of shear strength of RC wall with opening is rapid during subsequent consecutive cycles after cycle in which highest peak load was observed. Addition of FRC in wall with opening minimizes loss of strength in comparison with that of wall without opening.
- Initial stiffness of walls with openings has been found to be 60% of that of wall without opening. Stiffness degradation has been rapid in walls with normal concrete, showing gradual reduction in wall cast with FRC.
- Addition of FRC with openings improved ductility. Energy dissipation capacity has been found to be significantly reduced by openings. However, addition of fibres in concrete compensated to improve energy dissipation in wall with opening.
- Observed shear strength of squat wall has been agreeable with shear strength predicted by *ACI 318–19, ASCE/SEI 43-05, MCBC–04, AS3600–2009* and *Sanchez et al. (2010).* Though shear strength predicted by *ACI 318* equations in walls with openings is closely agreeable with test results, it does not state shape of opening. Moreover, as suggested by *ACI 318* that weak plane coincides with horizontal in opening, which does not seem to be observed from experimental investigations.

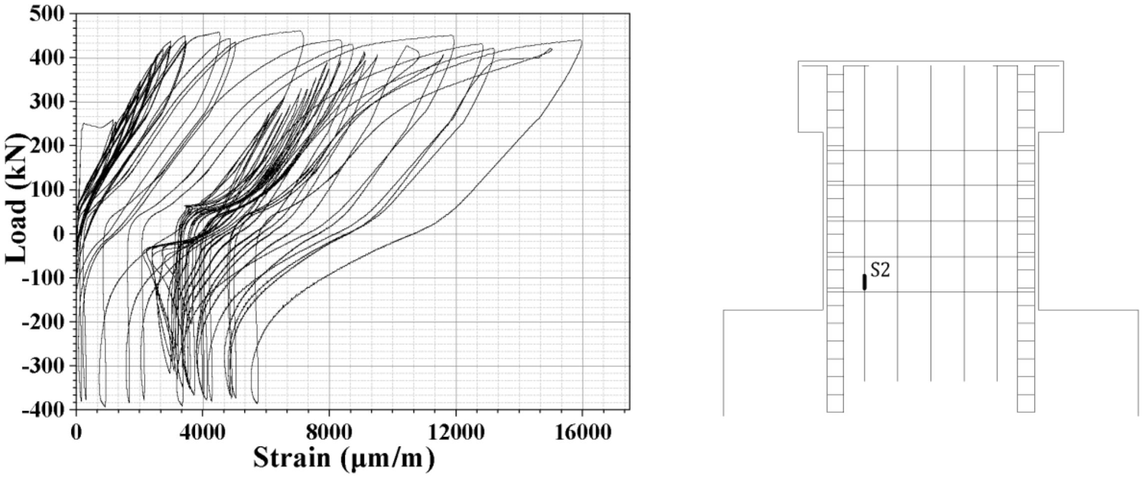

Fig. 5.33 Strain at Reinforcement Location S2 for SW_1.0-00-00

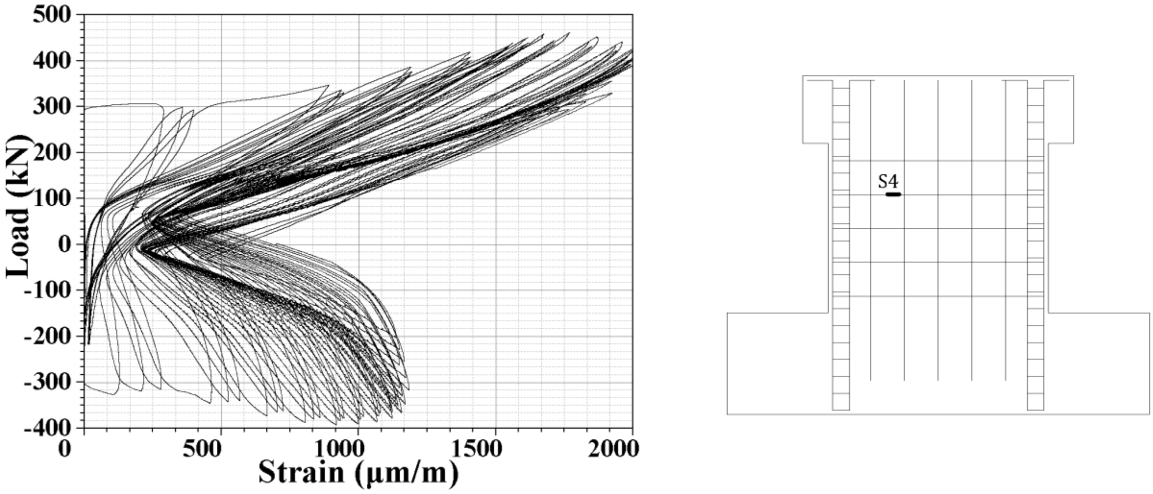

Fig. 5.34 Strain at Reinforcement Location S4 for SW-1.0-00-00

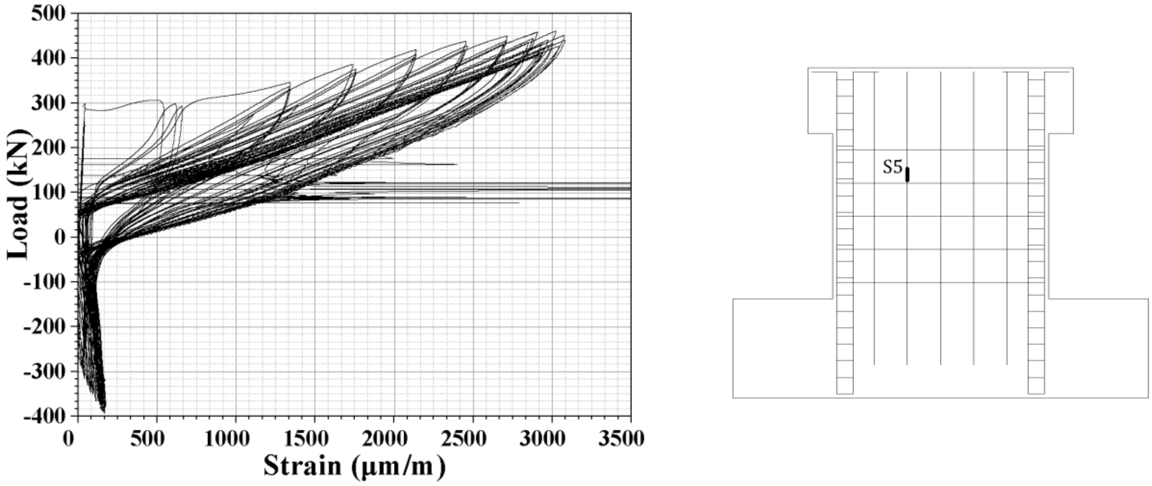

Fig. 5.35 Strain at Reinforcement Location S5 for SW-1.0-00-00

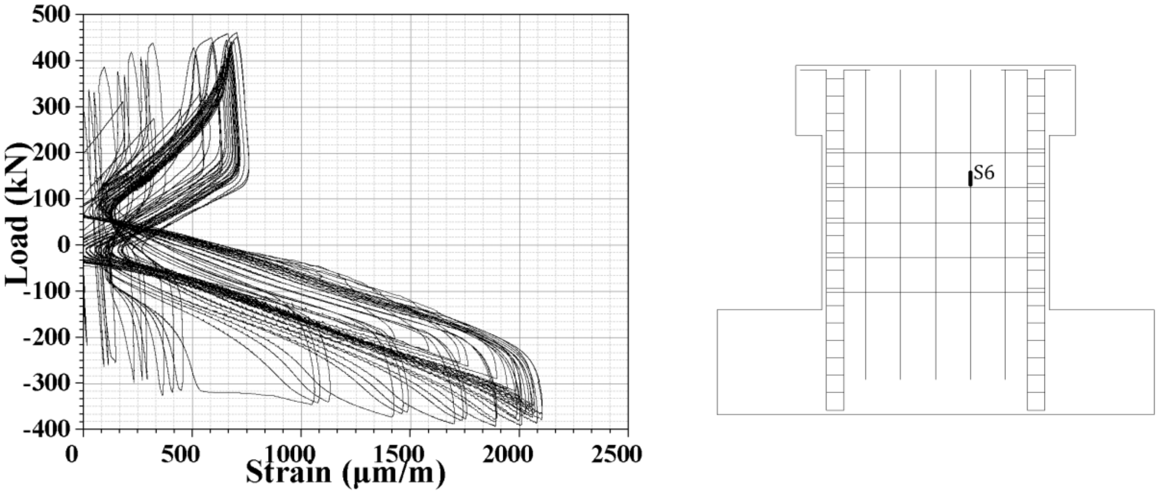

Fig. 5.36 Strain at Reinforcement Location S6 for SW-1.0-00-00

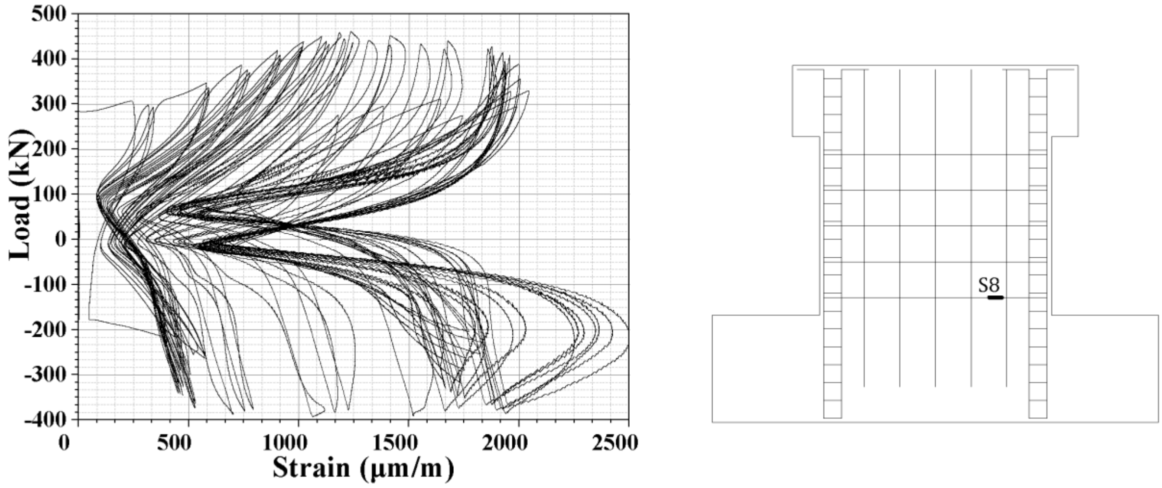

Fig. 5.37 Strain at Reinforcement Location S8 for SW-1.0-00-00

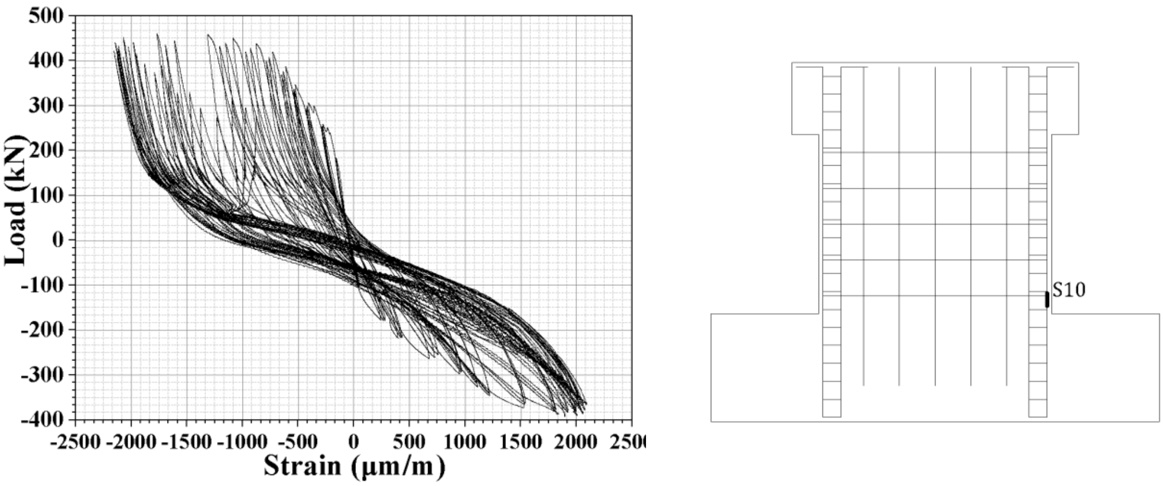

Fig. 5.38 Strain at Reinforcement Location S10 for SW-1.0-00-00

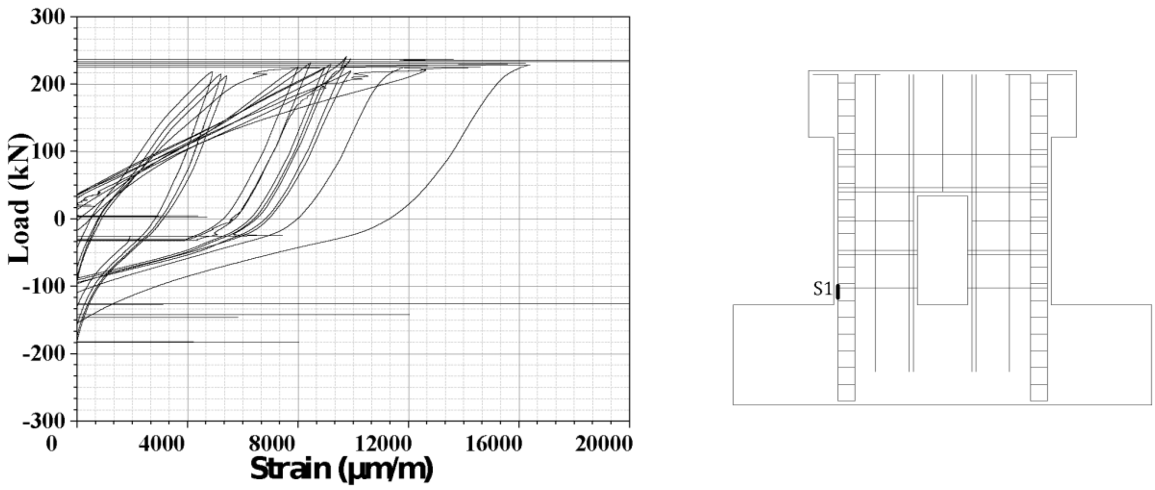

Fig. 5.39 Strain at Reinforcement Location S1 for SW-1.0-CD-00

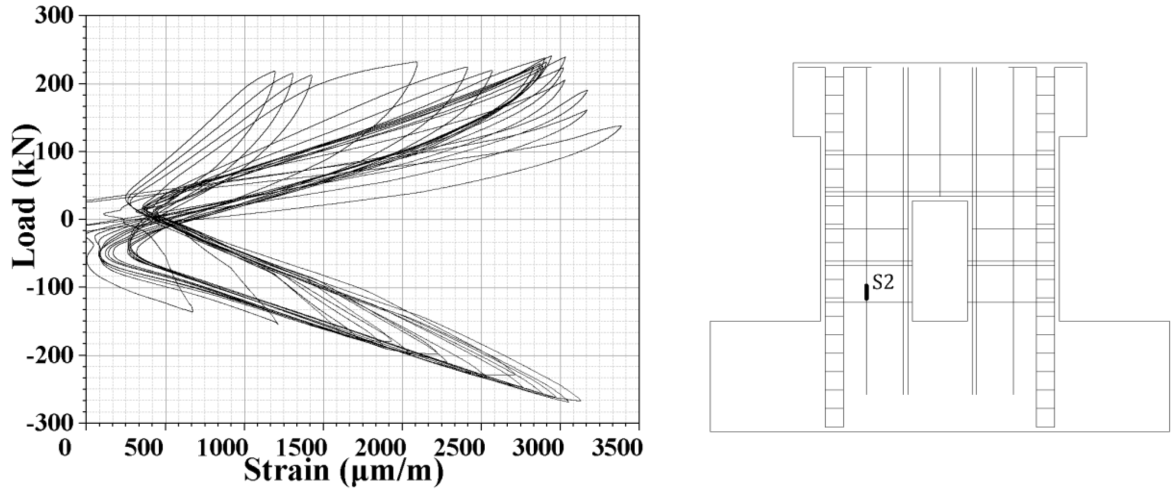

Fig. 5.40 Strain at Reinforcement Location S2 for SW-1.0-CD-00

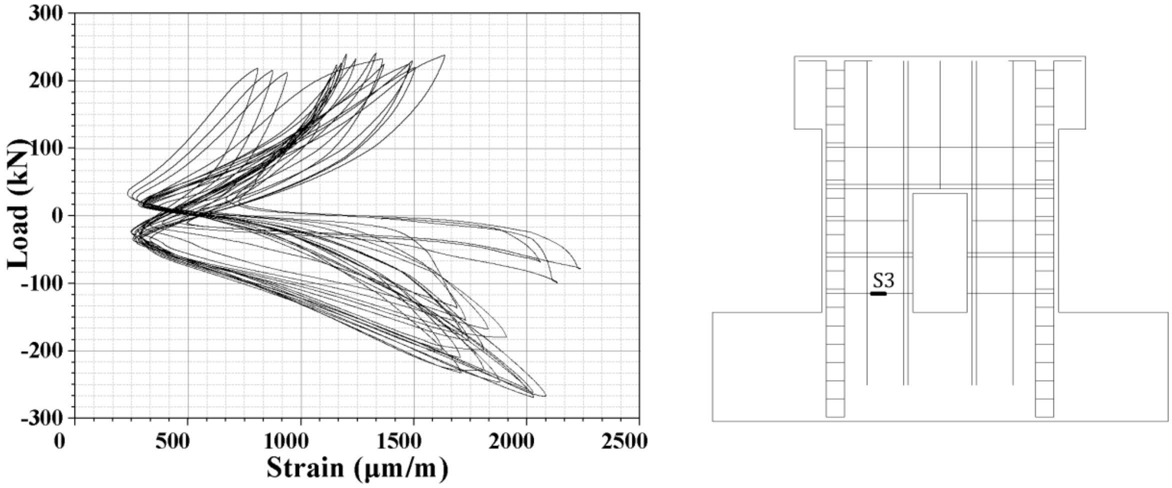

Fig. 5.41 Strain at Reinforcement Location S3 for SW-1.0-CD-00

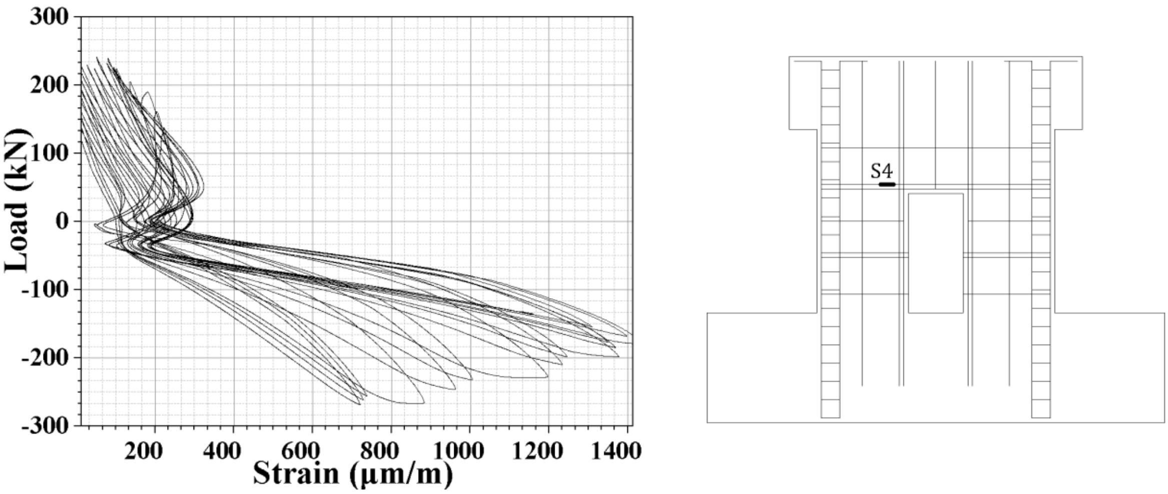

Fig. 5.42 Strain at Reinforcement Location S4 for SW-1.0-CD-00

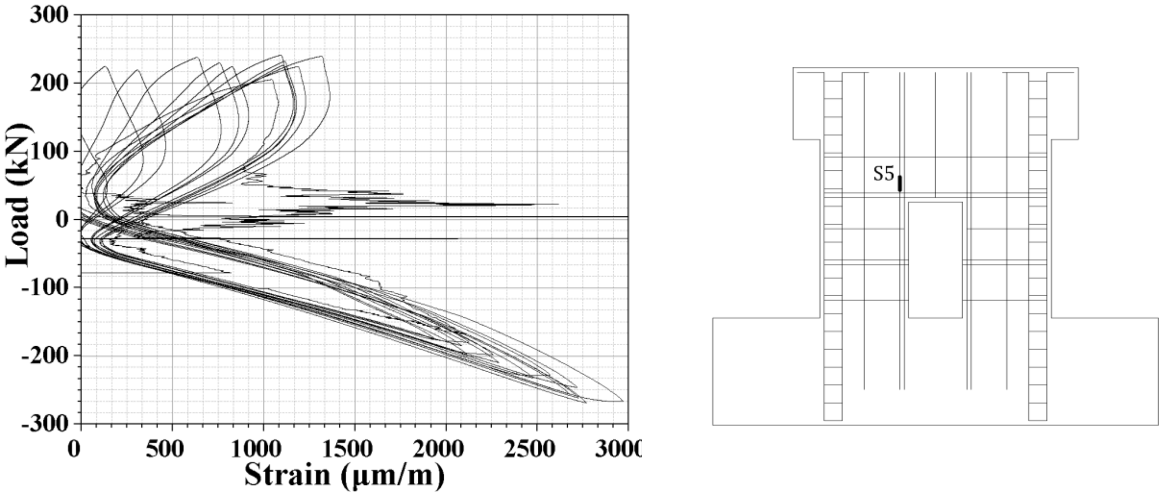

Fig. 5.43 Strain at Reinforcement Location S5 for SW-1.0-CD-00

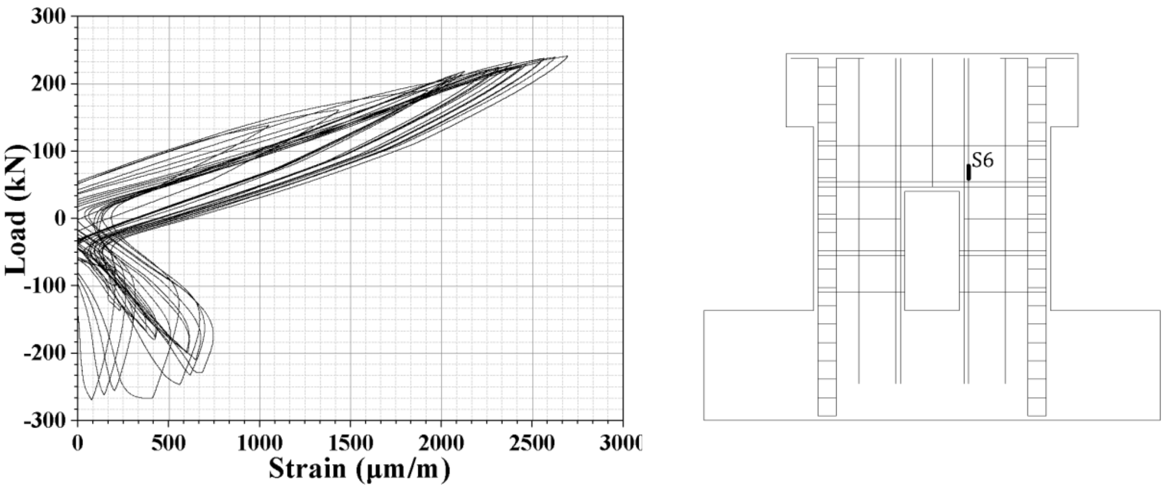

Fig. 5.44 Strain at Reinforcement Location S6 for SW-1.0-CD-00

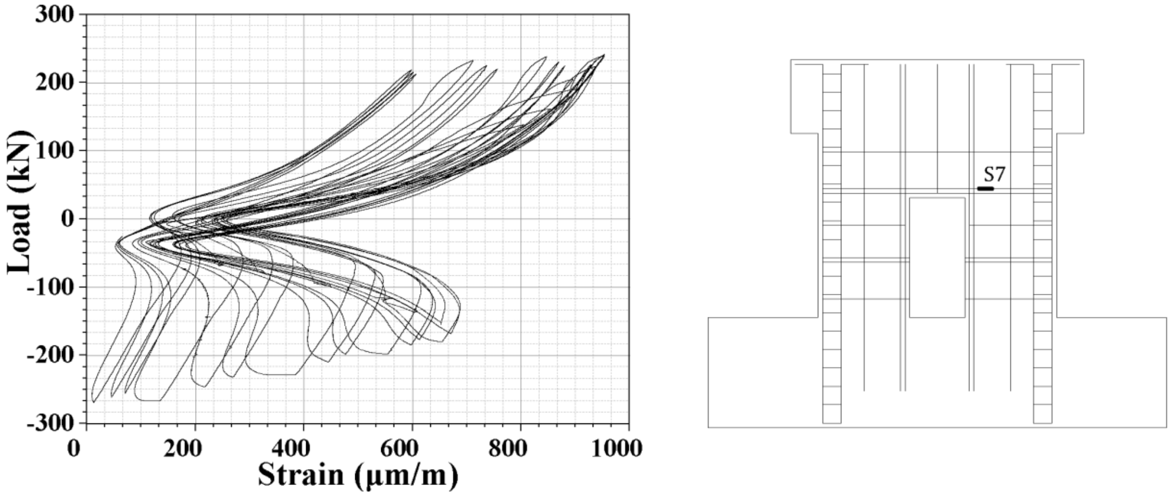

Fig. 5.45 Strain at Reinforcement Location S7 for SW-1.0-CD-00

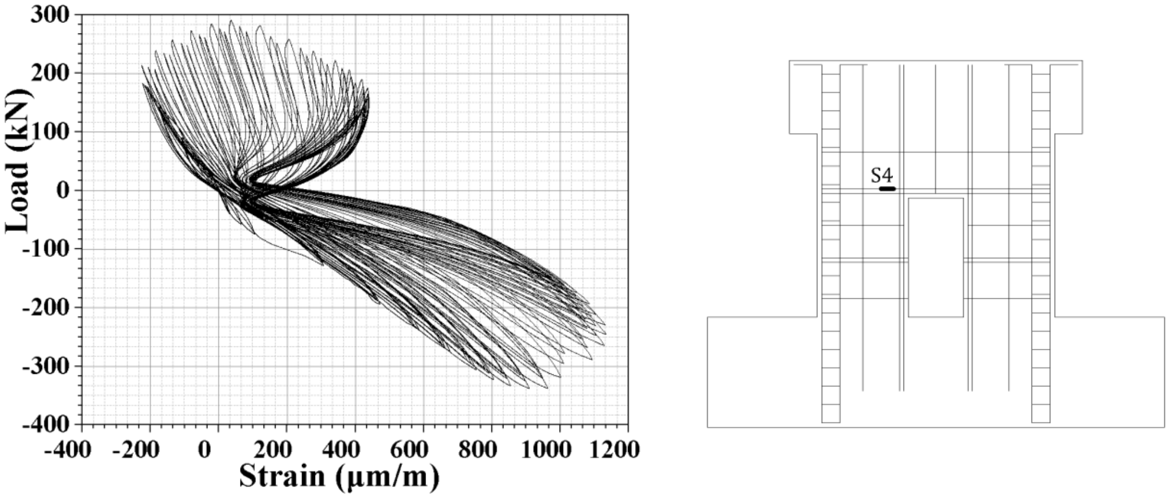

Fig. 5.46 Strain at Reinforcement Location S4 for SW-1.0-CD-FRC

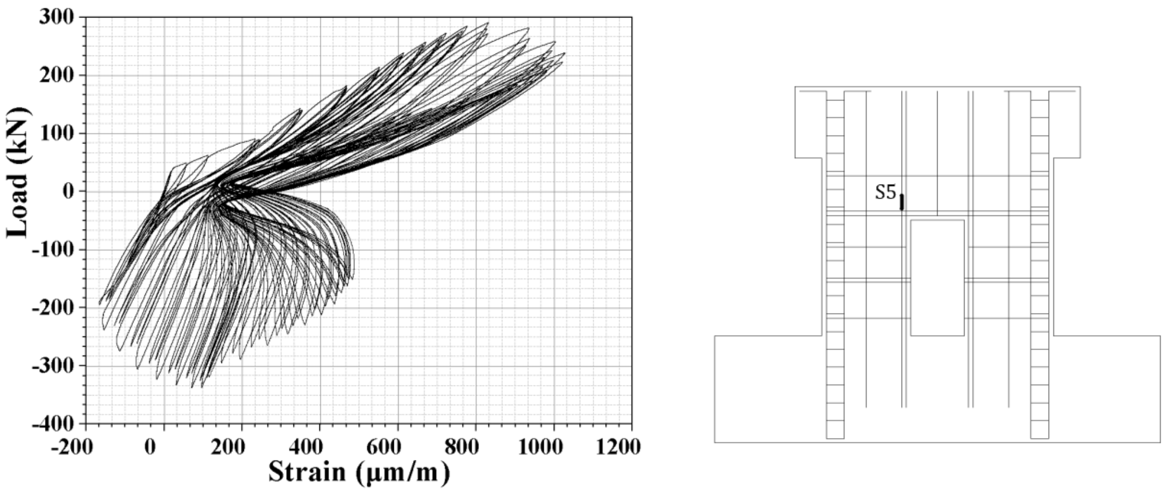

Fig. 5.47 Strain at Reinforcement Location S5 for SW-1.0-CD-FRC

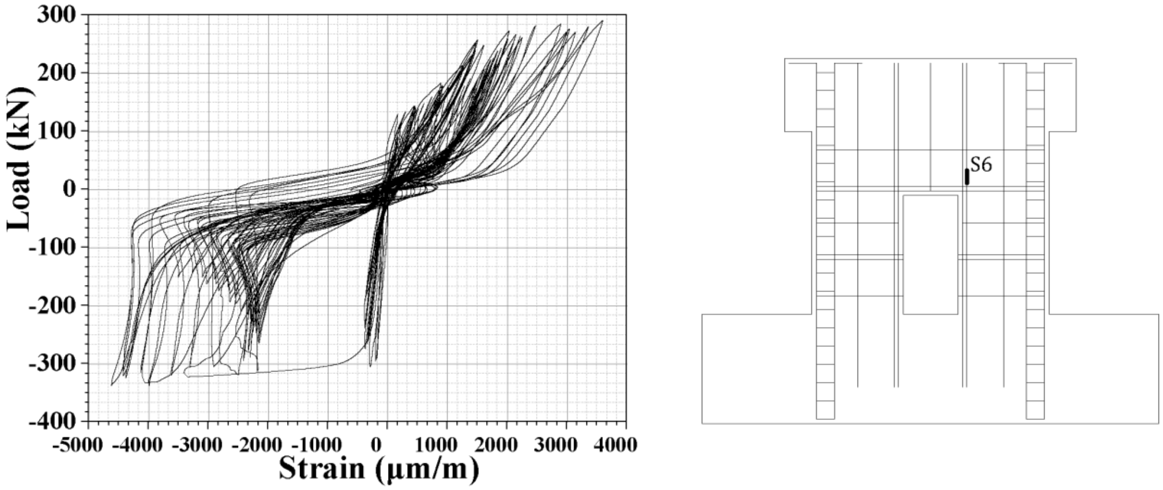

Fig. 5.48 Strain at Reinforcement Location S6 for SW-1.0-CD-FRC

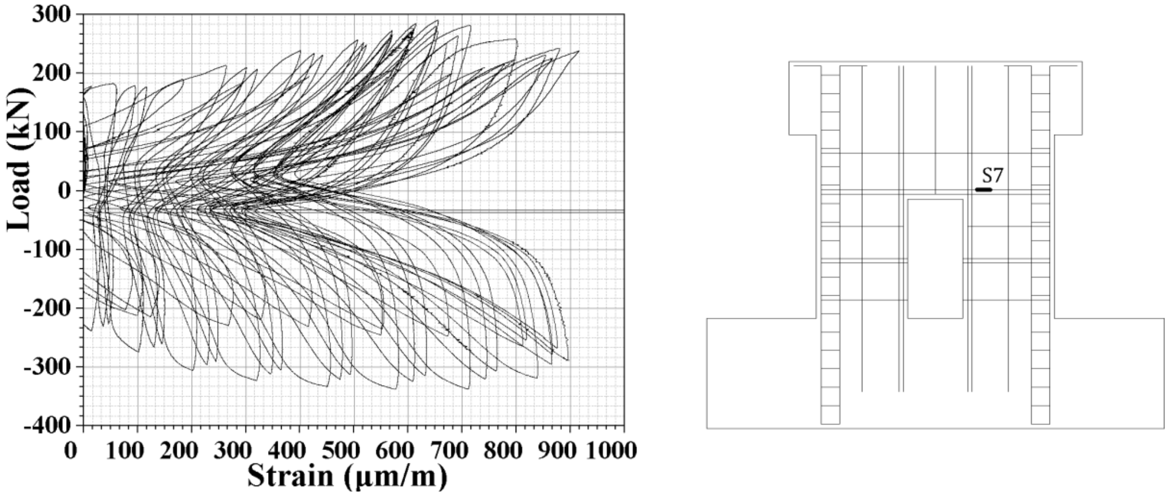

Fig. 5.49 Strain at Reinforcement Location S7 for SW-1.0-CD-FRC

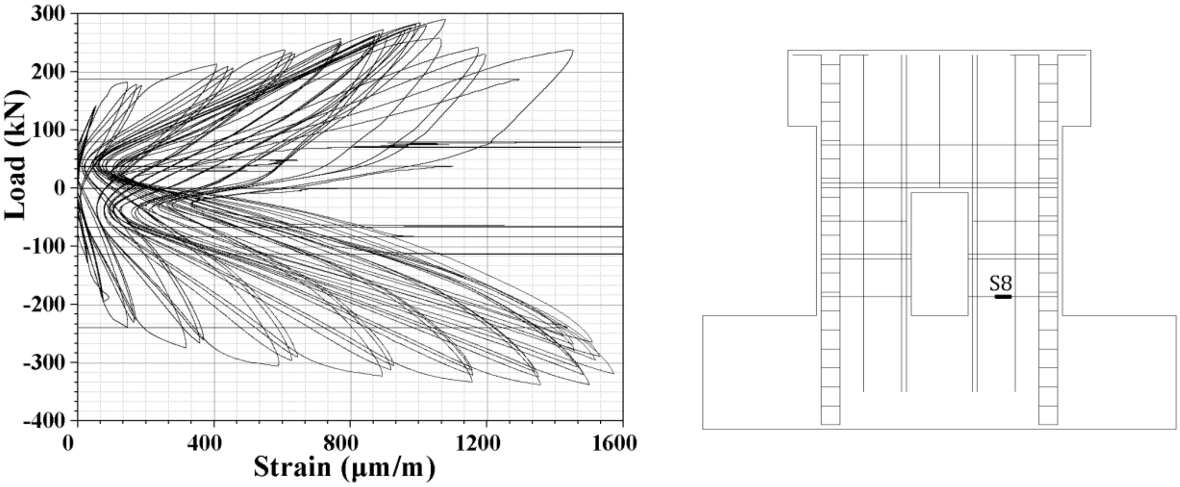

Fig. 5.50 Strain at Reinforcement Location S8 for SW-1.0-CD-FRC

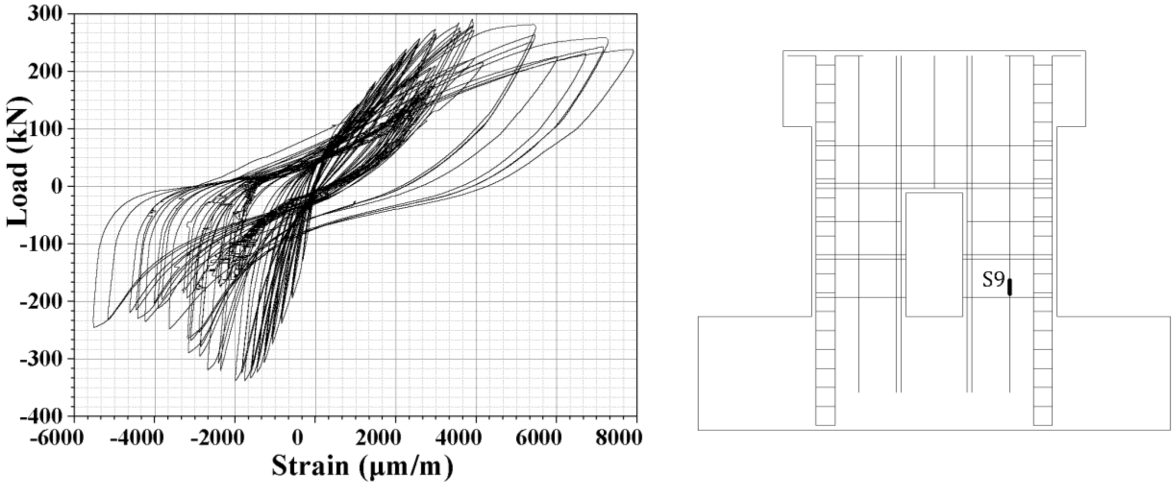

Fig. 5.51 Strain at Reinforcement Location S9 for SW-1.0-CD-FRC

CHAPTER 6

NUMERICAL STUDY ON REINFORCED CONCRETE SQUAT SHEAR WALLS WITH AND WITHOUT OPENING

6.1 INTRODUCTION

Numerous Experimental analyses have been widely carried out to study shear walls with various sizes, materials and under loading conditions. Experimental studies provide actual behaviour of structures, but it is expensive and time consuming. With development of sophisticated numerical tools for analysis like finite element analysis programmes, it is possible to model and analyse complex reinforced concrete structures. This chapter presents numerical analysis of shear walls with openings using FRC as strengthening material around openings.

6.2 FINITE ELEMENT ANALYSIS

Finite element analysis (FEA) is widely used to analyse many structural components, as it is much faster than experimental methods with very high cost effectiveness. In the present study finite element package ANSYS 15.0 is used for modelling. ANSYS 15.0 includes great number of new and advanced features that make it easier, faster and cheaper for customers to bring new products to market, with a high degree of confidence in the ultimate results they will achieve. The product suite delivers new benefits in three major areas.

a) **Greater Accuracy and Fidelity:** As Engineering requirements and design complexity increase, simulation software must produce more accurate results that reflect changing operating conditions over time.

b) **Higher Productivity:** ANSYS 14.5 includes dozens of features that minimize time and effort product development teams invest in simulation.

c) **More Computational Power:** For some Engineering simulations, ANSYS 14.5 can provide speedup ratios that are 5 to 10 times greater than previous software releases. Even complex Multiphysics simulations can be accomplished more quickly and efficiently, speeding up product development and market launch initiatives. ANSYS 15.0 builds on foundation of previous ANSYS releases, taking product development to next level by continuing evolution of smart Engineering Simulation, by compressing design cycles, optimizing product performance across multiple physics, maximizing accuracy of virtual 15 prototypes, and automating simulation process, ANSYS is making it easier and faster than ever to bring innovative new products to market, which has become imperative in today's difficult economy.

6.3 Modelling of the Wall

The finite element method (FEM) is the dominant discretization technique in structural mechanics. The basic concept in physical interpretation of FEM is subdivision of mathematical model into disjoint (non-overlapping) components of simple geometry called finite elements or elements for short. Then assemble these elements at the nodes to form an approximate system of equations for whole structure (forming element matrices). These system of equations involving at nodes are solved to find unknown quantities. Finite element modelling of specimen in ANSYS consists of three phases.

- Selection of element type.
- Assigning material properties
- Constructing and meshing the geometry

6.3.1 Geometrical Details of the Wall

Geometric dimensions of walls are 1000 mm x 1000 mm x 125 mm; and of boundary elements are 150 mm x 300 mm. Percentages of reinforcement adopted are 0.48% in vertical and horizontal directions and 1.0% in boundary elements respectively. Materials are M30 grade concrete, Fe500 grade steel reinforcement and steel fibres with aspect ratio 30 with a volumetric fraction of 1.0%. Geometry of wall is shown in Figure 6.1.

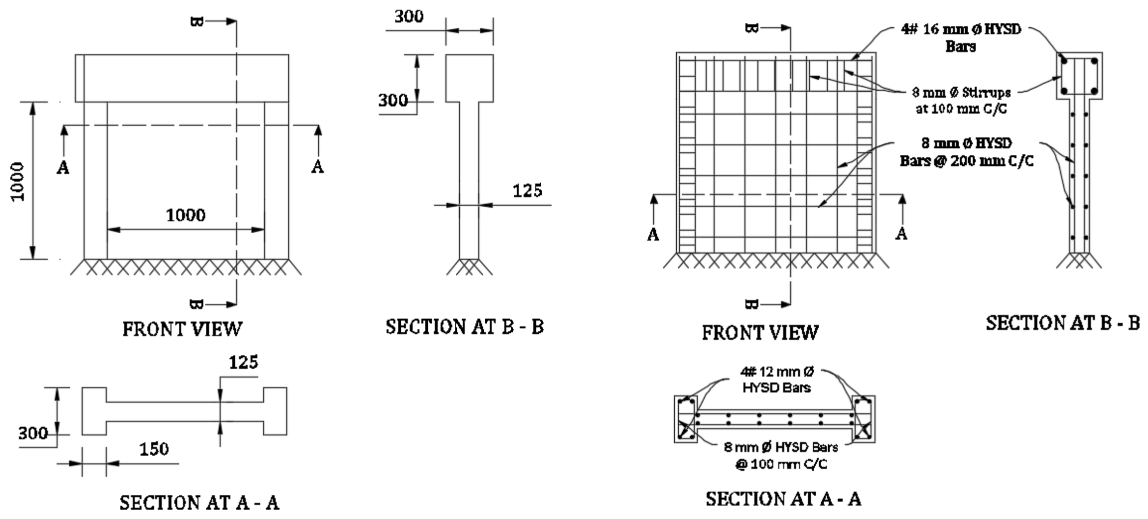

(a) Geometry of the wall (b) Reinforcement Details of the wall

Fig. 6.1 Geometrical Details of the Wall

6.3.2 Elements Used

Selection of proper element types is another important criterion in finite element analysis. Three types of elements are adopted for modelling shear walls. Eight noded SOLID65 (Concret65) element type for modelling concrete, two noded LINK 8 elements for modelling reinforcement and eight noded solid 185 elements for modelling loading steel plate. FRC is modelled as concrete with smeared fibre property with different orientation angle as possible for stimulating random distribution as shown in Figure 6.2.

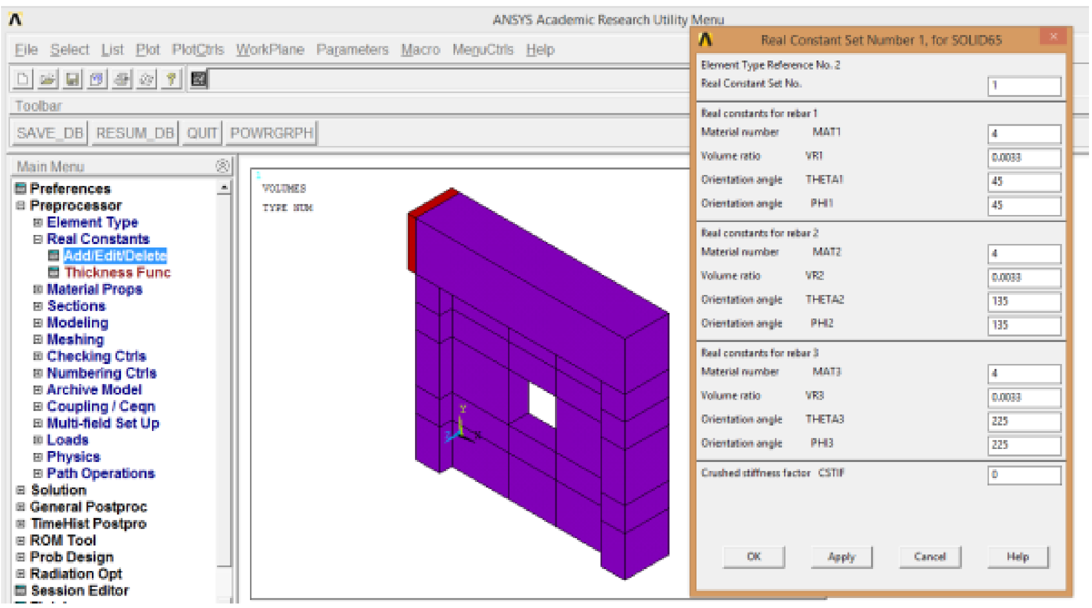

Fig. 6.2 Details of Smeared Model for Steel Fibres

d) LINK180

LINK180, a 3-D spar that is useful in a variety of engineering applications. Element can be used to model trusses, sagging cables, links, springs, and so on. Element with uniaxial tension-compression possess three degrees of freedom at each node: translations in the nodal x, y, and z directions. Tension-only (cable) and compression-only (gap) options are supported. As in a pin-jointed structure, no bending of the element is considered. Plasticity, creep, rotation, large deflection, and large strain capabilities are included. By default, LINK180 includes stress-stiffness terms in any analysis that includes large-deflection effects. Elasticity, isotropic hardening plasticity, kinematic hardening plasticity, Hill anisotropic plasticity, Chaboche nonlinear hardening plasticity, and creep are supported. To simulate tension-/compression-only options, a nonlinear iterative solution approach is necessary; therefore, large-deflection effects must be activated (NLGEOM,ON) prior to solution phase of analysis.

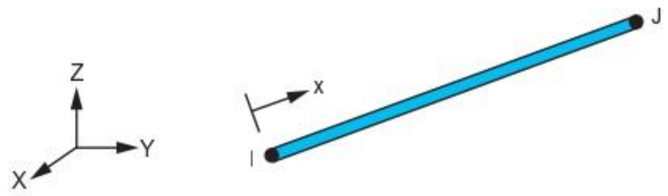

Fig. 6.3 LINK180 Element

e) SHELL281

SHELL281 is suitable for analyzing thin to moderately-thick shell structures. It is a four-node element with six degrees of freedom at each node: translations in x-, y-, and z-directions, and rotations about x-, y-, and z-axes. (If membrane option is used, element has translational degrees of freedom only). Degenerate triangular option should only be used as filler elements in mesh generation. SHELL281 is well-suited for linear, large rotation, and/or large strain nonlinear applications. Change in shell thickness is accounted for in nonlinear analyses. In element domain, both full and reduced integration schemes are supported. SHELL281 accounts for follower (load stiffness) effects of distributed pressures.

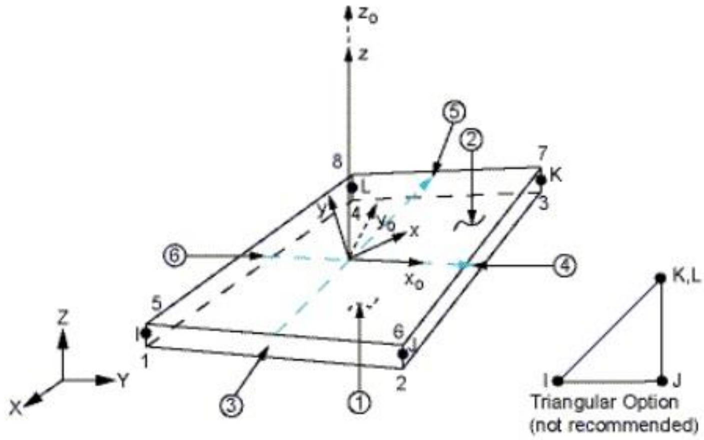

Fig. 6.4 Shell281 Element

f) SOLID65

Structural Solid is suitable for modelling general 3-D solid structures. It allows for prism and tetrahedral degenerations when used in irregular regions. Various element technologies such as B-bar, uniformly reduced integration, and enhanced strains are supported.

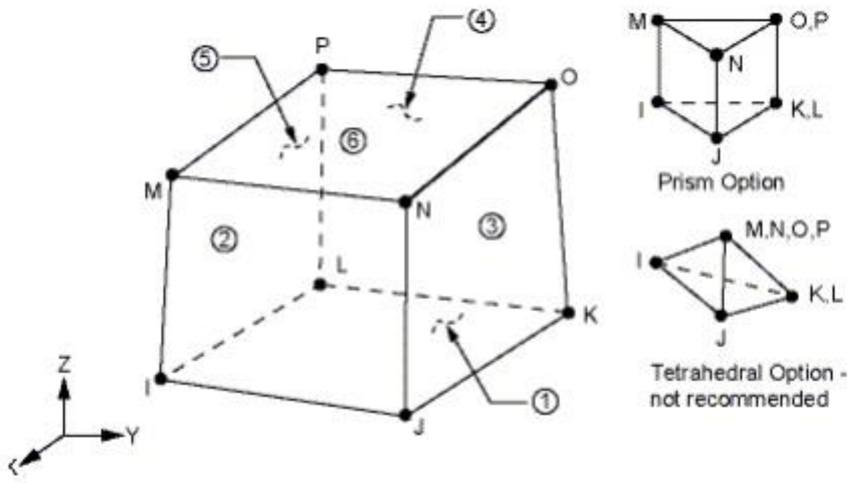

Fig. 6.5 Solid65 Element

Geometry and node locations for this element are shown in Figure 6.5. Element is defined by eight nodes and orthotropic material properties. Default element coordinate system is along global directions. You may define an element coordinate system using ESYS, which forms basis for orthotropic material. Special feature in SOLID65 is crack pattern.

6.3.3 Material Property

6.3.3.1 Concrete

Concrete is a quasi-brittle material and has different behaviour in compression and tension. Tensile strength of concrete is around 8-15% of compressive strength of concrete. Concrete is a quasi-brittle material with Strain–softening behaviour, indicating a reduction in stress beyond peak with an increase in deformation. Although ductility of concrete is several orders of magnitude lower than steel, it still exhibits considerable deformation before failure. Figure 6.6 shows a typical stress-strain curve for normal weight concrete.

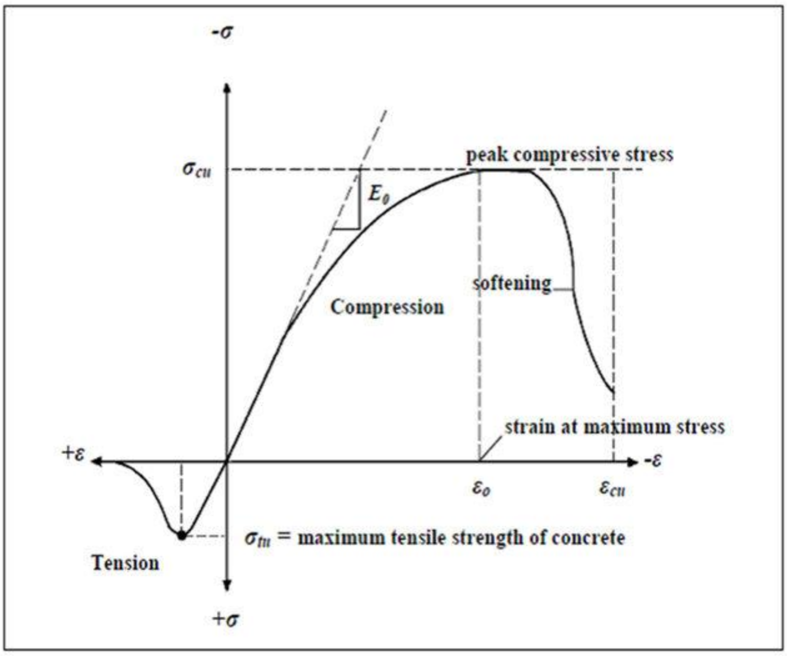

Fig. 6.6 Typical stress-strain curve for normal weight concrete

In compression, stress-strain curve for concrete is linearly elastic up to about 30 percent of maximum compressive strength. Above this point, stress increases gradually up to maximum compressive strength. After it reaches maximum compressive strength σ_{cu} , curve descends into a softening region, and eventually causing crushing failure at an ultimate strain ε_{cu} . In tension, stress-strain curve for concrete is approximately linearly elastic up to maximum tensile strength in tension. After this point, concrete cracks and strength decreases gradually to zero. In general, development of a model for achieving the true behaviour of concrete is a challenging task.

As per ANSYS concrete model, two shear transfer coefficients, one for open cracks and other for closed ones, are used to consider amount of shear transferred from one end of crack to another.

Following are input data required to create material model for concrete in ANSYS.

- Elastic Modulus, (E_c)
- Poisson's Ratio, (ν)
- Ultimate Uniaxial compressive strength, (f_{ck})
- Ultimate Uniaxial tensile strength, (f_t)
- Shear transfer coefficient for opened crack, (β_0)
- Shear transfer coefficient for closed crack, (β_c)

Elastic modulus and ultimate uniaxial tensile strength of concrete is found using IS 456:2000 as follows,

$$E_c = 5000\sqrt{f_{ck}}$$

$$f_{cr} = 0.7\sqrt{f_{ck}}$$

Where, Ec - Modulus of Elasticity of Concrete (MPa)

f_{ck} - Charecteristic compressive strength of Concrete (MPa)

f_t - Tensile strength of concrete (MPa)

Poisson's ratio for concrete is assumed as 0.15 for all models. Shear transfer coefficient, β_t, represents conditions of crack face. Value of β_t ranges from 0.0 to 1.0, with 0.0 representing a smooth crack (complete loss of shear transfer) and 1.0 representing a rough crack (no loss of shear transfer). Damien Kachlakev et.al. (2001) conducted numerous investigations on full-scale beams and they found out the shear transfer coefficient for opened crack is 0.2 and for closed crack is 0.9-1.0. Two shear transfer coefficients are used to consider re-tension of shear stiffness in cracked concrete.

In this study, stress-strain curve for concrete constructed by using Desayi et al. (1964) equations. It is assumed that curve is linear up to 0.3 fc' as shown in Figure 6.7. Therefore, elastic stress-strain relation is enough for finding out strain value.

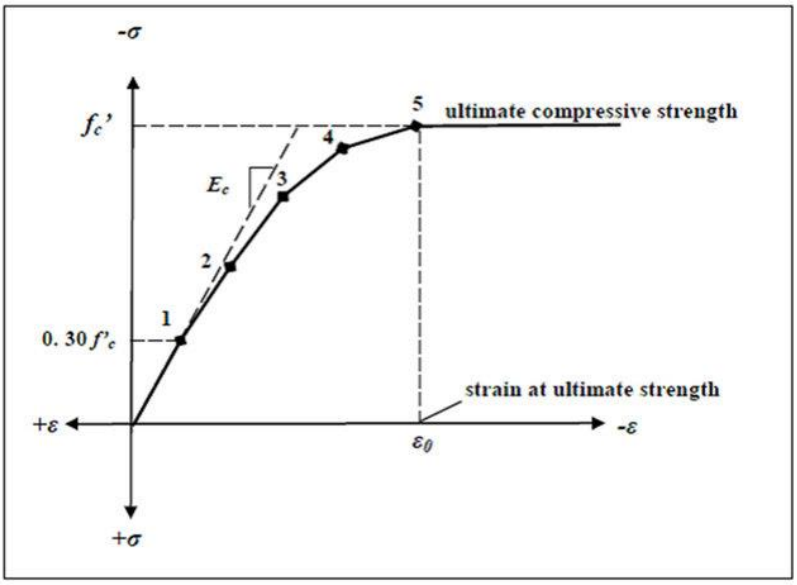

Fig. 6.7 Simplified Uniaxial Compressive Stress-Strain curve for Concrete

Stress at any strain, ε is found,

$$f = \frac{E_c \varepsilon}{1+\left(\frac{\epsilon}{\epsilon_0}\right)}$$

Strain at ultimate compressive stress, f_c' is

$$\varepsilon_0 = \frac{2f_c'}{E_c}$$

Above input values are given as material properties for concrete to define non-linearity. ANSYS has its own non-linear material model for concrete. Its reinforced concrete model consists of a material model to predict failure of brittle materials, applied to a three-dimensional solid element in which reinforcing bars may be included. Material is capable of cracking in tension and crushing in compression. It can also undergo plastic deformation and creep. Three different uniaxial materials, capable of tension and compression only, may be used as a smeared reinforcement, each one in any direction. Plastic behaviour and creep can be considered in the reinforcing bars too. For plain cement concrete model, reinforcing bars can be removed.

6.3.3.2 Steel Reinforcement

Steel in finite element models was assumed as an elastic-perfectly plastic material identical in tension and compression. Young's modulus given is 2e5 MPa and yield stress as 500 MPa for steel reinforcement used in this FEM study. Poisson's ratio of 0.3 was used for steel. Bilinear kinematic material model is adopted in this study. The tangent modulus for steel elements is assumed as zero, which means that there will be a large deflection after yield point, i.e, strain is independent of loading after yield point. Figure 6.8 shows the stress-strain relationship adopted in this study.

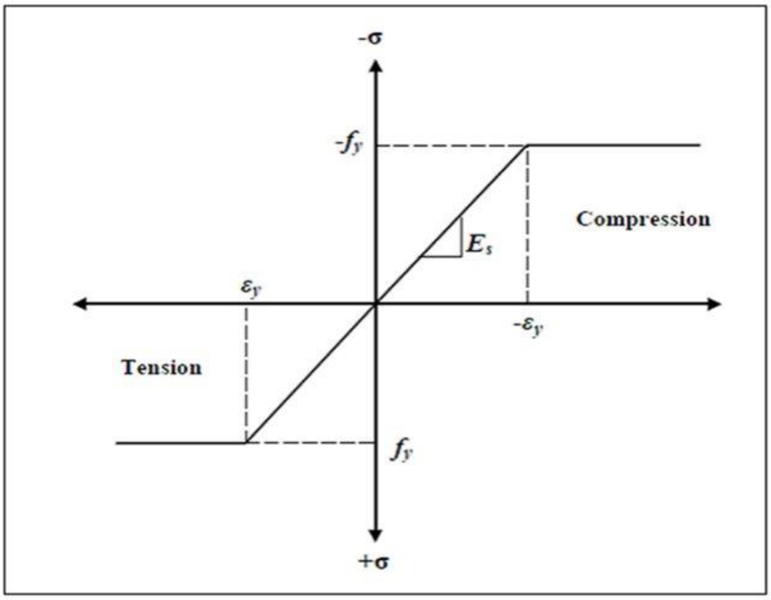

Fig. 6.8 Bilinear Stress-Strain Curve for Steel

Reinforcement and steel plate used are assumed to exhibit elasto-plastic response with identical properties in tension and compression. Portions of FRC in wall are discretised by smeared concrete model. The input material properties are enlisted in Table 6.1.

Table 6.1 Material Property for Shear Wall Modelling (N, mm)

S. No.	Element Type	Material	Material Properties		
1	Solid65	Concrete	Linear Isotropic		
			Ex		27386
			PRXY		0.15
			Multilinear Isotropic		
			Point 1	0	0
			Point 2	0.00044	10
			Point 3	0.0005	10.95445
			Point 4	0.0010	18.25742
			Point 5	0.0015	23.47382
			Point 6	0.0020	30
			Point 7	0.0035	30
			Concrete		
			Open Shear Transfer Coeff.		0.1
			Closed Shear Transfer Coeff.		0.9
			Uniaxial Cracking Stress		3.83
			Uniaxial Crushing Stress		30

2	Link180	Steel Reinforcement	Linear Isotropic	
			Ex	200000
			PRXY	0.3
			Bilinear Isotropic	
			Yield Stress	500
			Tangent Modulus	0
3	Solid185	Steel Loading Plate	Linear Isotropic	
			Ex	200000
			PRXY	0.3
			Bilinear Isotropic	
			Yield Stress	250
			Tangent Modulus	0
4	Smeared Model for Steel Fibre	Steel Reinforcement	Linear Isotropic	
			Ex	200000
			PRXY	0.3
			Bilinear Isotropic	
			Yield Stress	800
			Tangent Modulus	0

6.3.4 Mesh Convergence Study

Mesh convergence study has been performed to find an appropriate mesh size of each element in the numerical model. Here, this study is performed using plain concrete shear wall without reinforcement. Six concrete shear walls of dimensions 1000 x 1000 x 125 mm are modelled in ANSYS 15.0 with increasing number of elements 616, 4928, 16632, 39424, 77000, 133056 corresponding to mesh size 75, 37.5, 25, 18.75, 15 and 12.5 mm respectively using Solid65 element as shown in Figure 6.9.

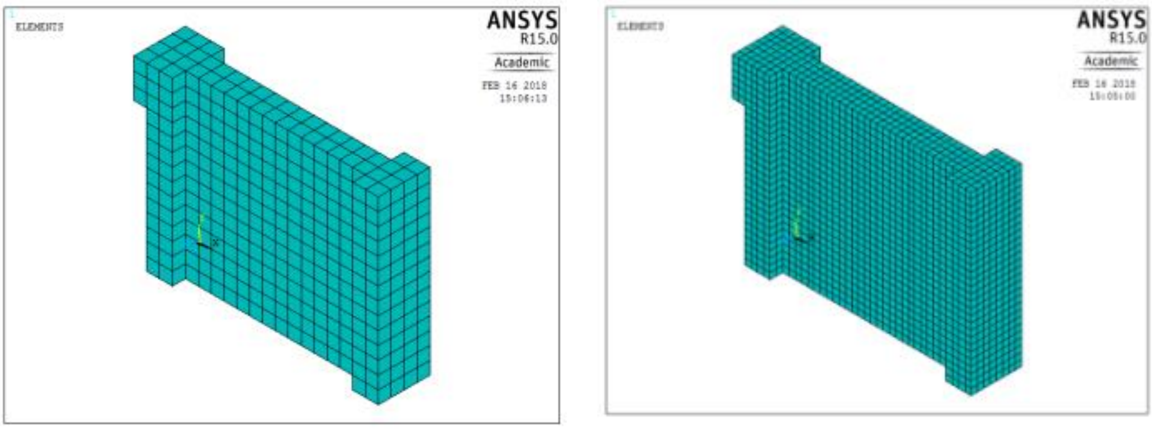

(a) 616 Elements

(b) 4928 Elements

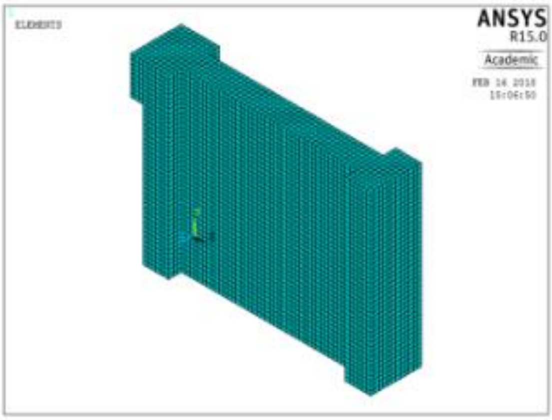

(c) 16632 Elements

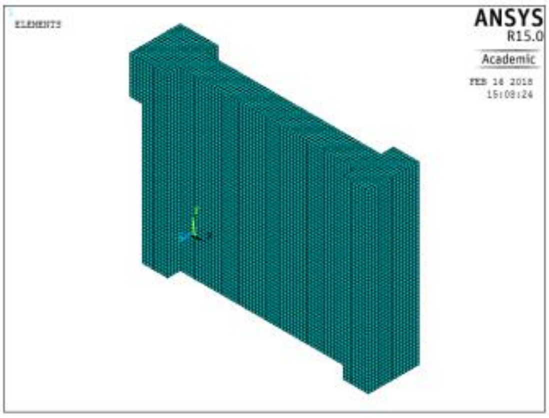

(d) 39424 Elements

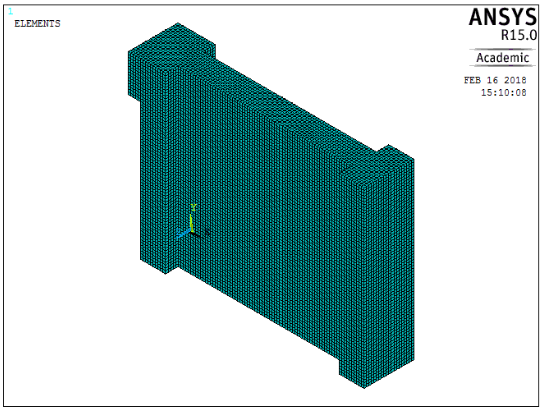

(e) 77000 Elements

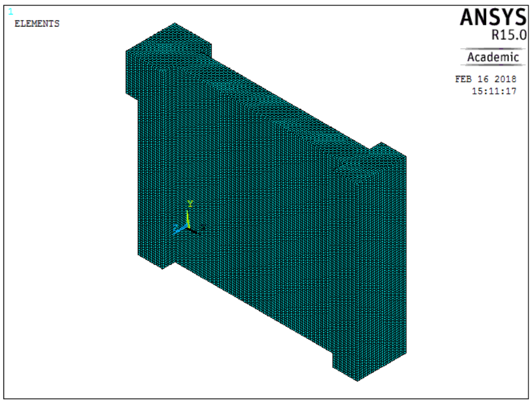

(f) 133056 Elements

Fig. 6.9 Wall Model Used for Convergence Study

Variation of number of elements to lateral deflection is shown in Figure 6.10, delineates that deflection remains nearly constant from 16632 elements to 133056 elements. So that finite element model consisting of 16632 concrete elements corresponds to mesh size 25 mm is used for this entire study.

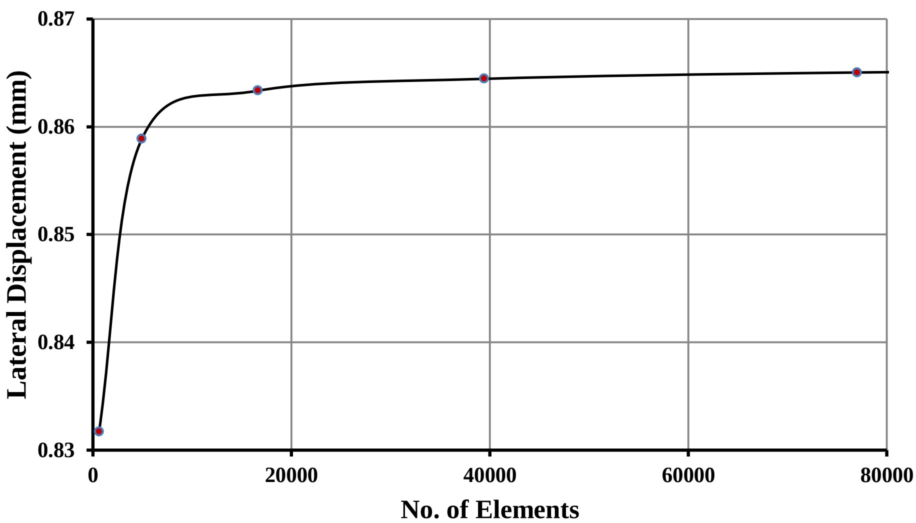

Fig. 6.10a Mesh Convergence Study (Lateral Displacemet)

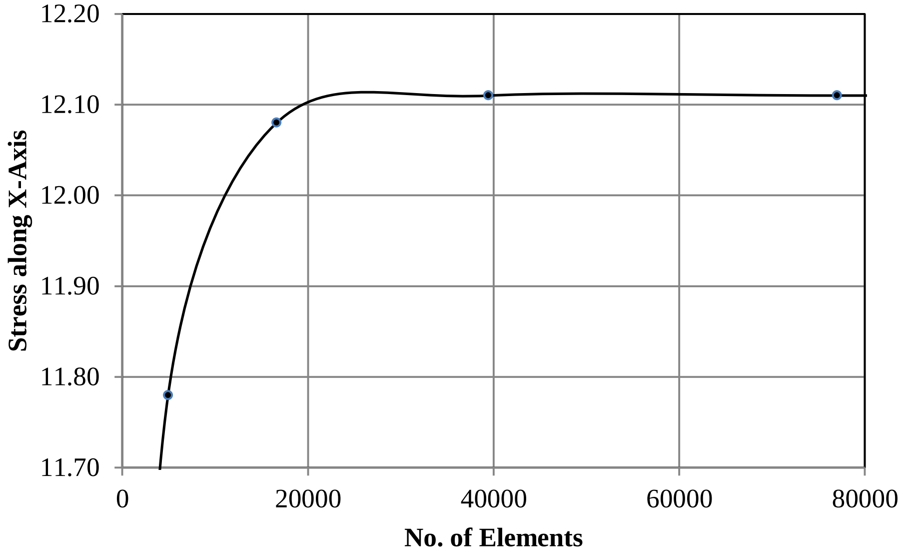

Fig. 6.10b Mesh Convergence Study (Stress along X-axis)

6.3.5 Constructing and Meshing

Full wall has been constructed using lines and volumes command for reinforcement and concrete respectively as shown in Figures 6.11, 6.12 & 6.13. Advantage of symmetry in the geometry is not considered as lateral load is applied only from one side of wall.

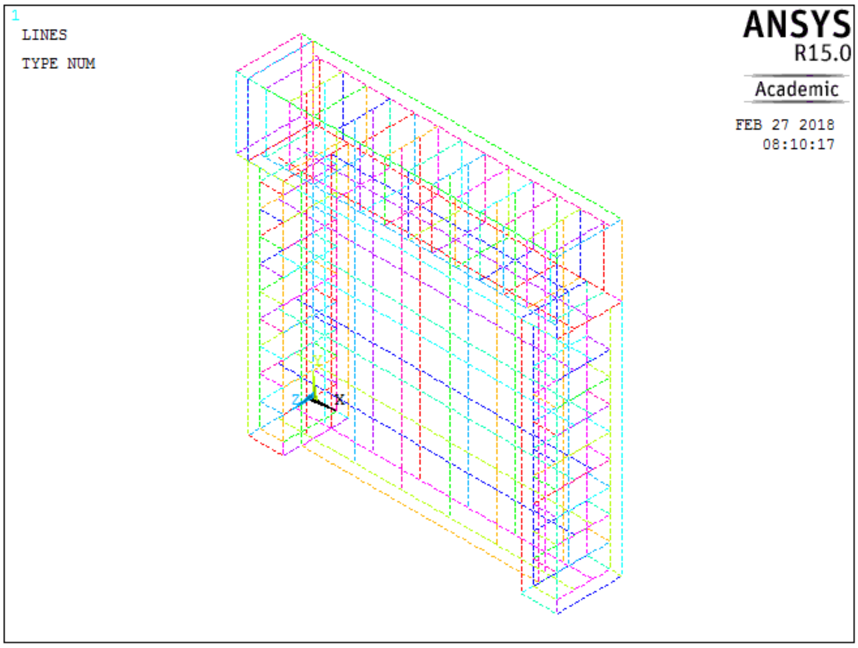

Fig. 6.11 Reinforcement Model in ANSYS

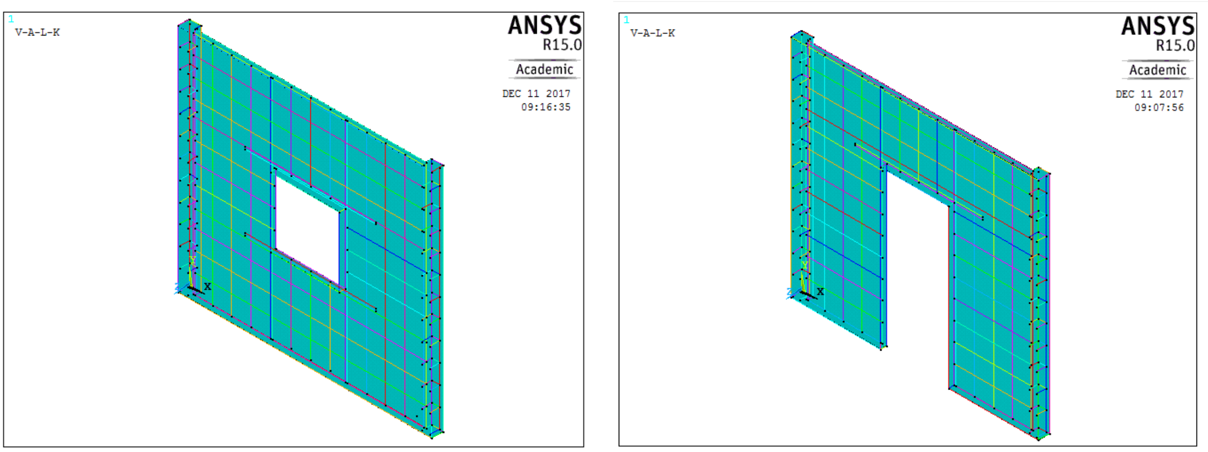

Fig. 6.12 Reinforcement Model in ANSYS for walls with Opening

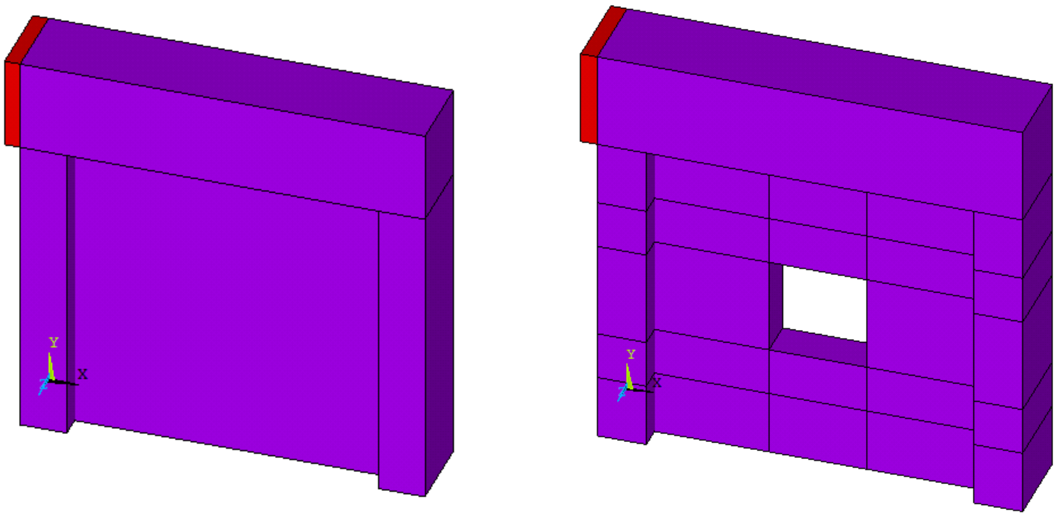

Fig. 6.13 Concrete Model in ANSYS for walls with and without Opening

Material models are assigned for respective materials. Concrete and steel models are discretised and meshed with 25 mm mesh size which is obtained from mesh convergence study as shown in Figure 6.14. Merge operation is used for bonding concrete and steel in the model. Hence composite action was assured using merge operation. This means that it has been assumed full proper bonding between concrete and steel.

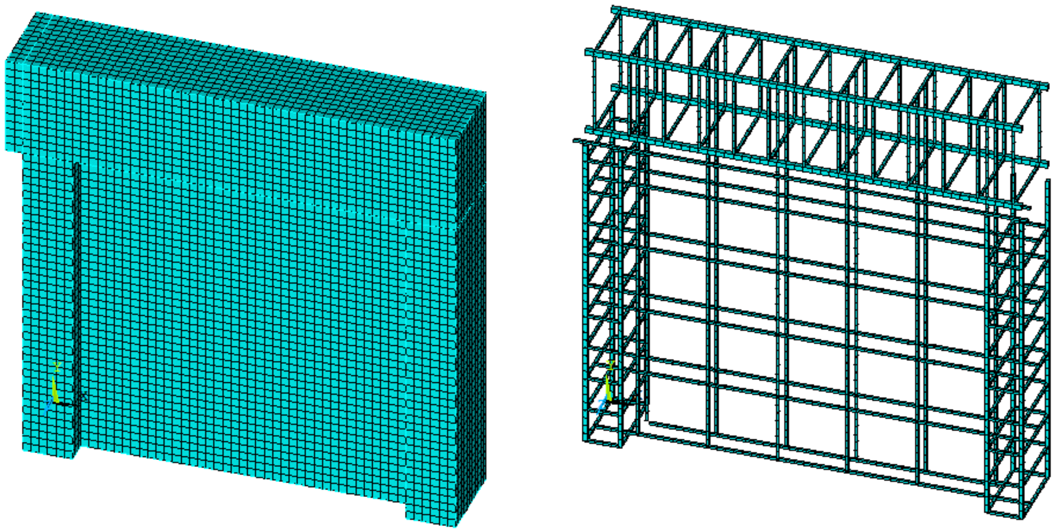

Concrete Steel Reinforcement

(a) Wall without Opening

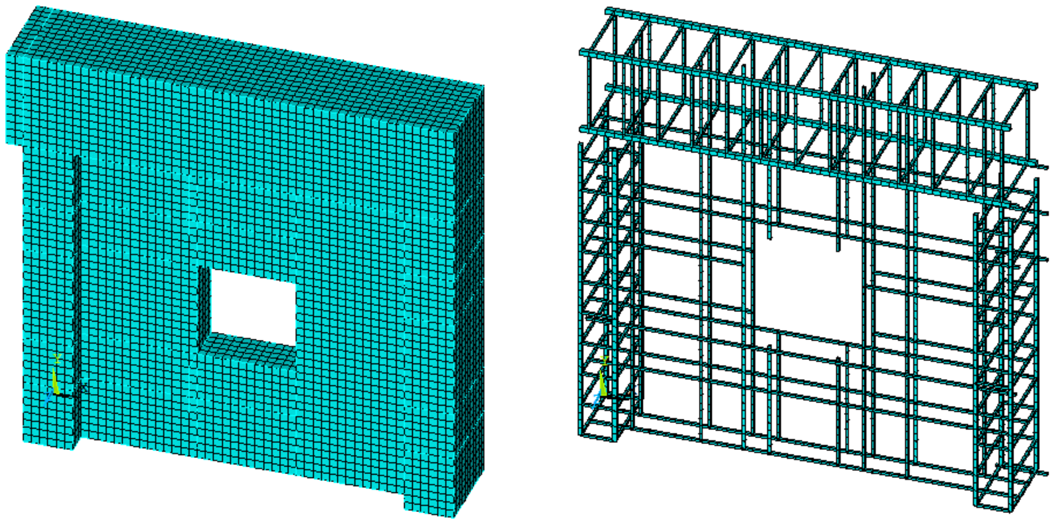

Concrete Steel Reinforcement

(b) Wall with Opening

Fig. 6.14 Meshing View of Walls with and without Opening

6.3.6 Loading and Boundary Condition

Boundary conditions are required to avoid rigid body motion of the structure. All degrees of freedom are arrested at the base of shear wall in order to provide fixed support. Axial load ratio of 10% is adopted for this study. Lateral load is applied on the loading plate. Figure 6.15 shows the loaded and constrained model view.

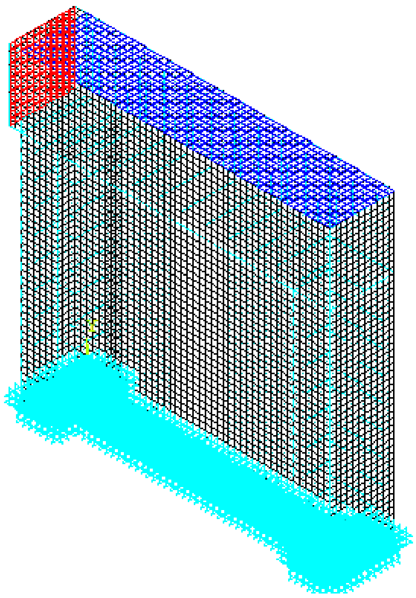

Fig. 6.15 Loading and Boundary Condition of the wall

6.3.7 Solution Controls

A nonlinear structural analysis is performed to study the nonlinear material behaviour of the wall. ANSYS15.0 employs "Newton-Raphson" method to solve nonlinear problems as shown in Figure 6.16. Load is sub-divided into series of load increments as load steps. A nonlinear structural analysis is performed to study nonlinear material behaviour of wall. ANSYS15.0 employs "Newton-Raphson" method to solve nonlinear problems.

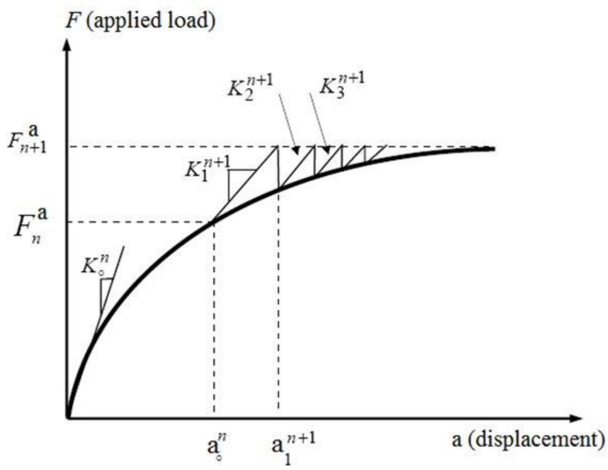

Fig. 6.16 Newton-Raphson Method

Load is sub-divided into series of load increments as load steps. Large displacement static condition is considered for analysis and tolerance limits are kept in the order of 10^{-2} and are shown in Figure 6.17 & 6.18.

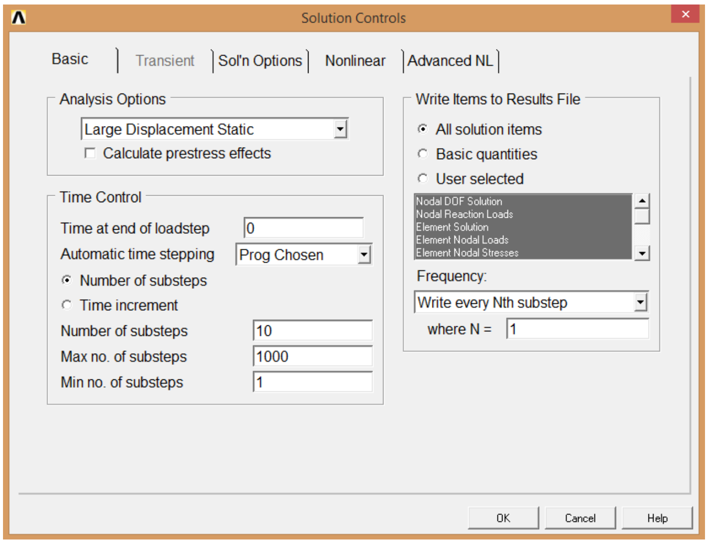

Fig. 6.17 Load Steps for the walls

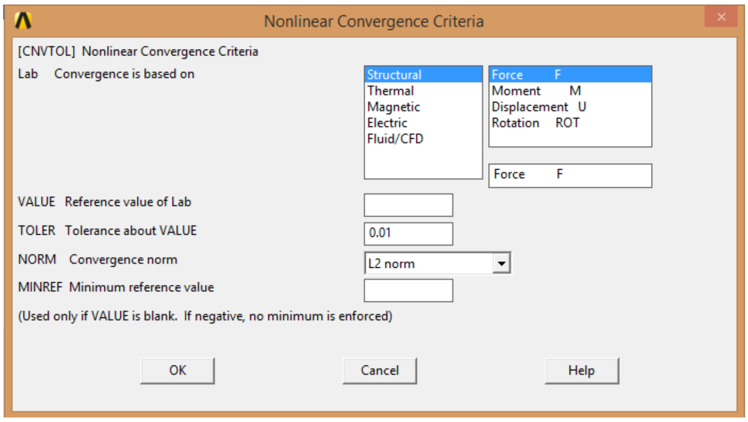

Fig. 6.18 Tolerance Limit for the walls

6.3.8 Failure Criteria for Concrete

Non-linear concrete model is based on William-Warnke failure criteria in ANSYS. As per the William-Warnke failure criteria, In every single elements of FEM model, two strength parameters are used to define the failure surface. Principal stresses in compression and tension viz., σ1 and σ2 are used in this calculation by the programme which is being calculated for every step of applied lateral force to the shear wall. The William Warnke failure criteria is assigned as the input for limiting the stresses for convergence criteria in the analysis steps. As the applied lateral force increases, the σ_1 and σ_2 also increases, FEA programme plots these principal stress values to check whether the points fall withing or on the bounding curve defined by the William Wanrke. Analysis terminates without converging, if the point falls outside this curve. At this stage. the physical structure as per the William Warnke, crushes or cracks in the zones reaching the bounding values defined by him. This yield criterion has the functional form,

$$f(I_1, J_2, J_3) = 0$$

Where, I_1 is the first invariant of the Cauchy stress tensor, and J_2, J_3 are the second and third invariants of the deviatoric part of the Cauchy stress tensor. the Willam-Warnke yield criterion can be expressed as,

$$f: = \sqrt{J_2} + \lambda(J_2, J_3)\left(\frac{I_1}{3} - B\right) = 0$$

Where,   is a function that depends on J_2, J_3 and the three material parameters and B depends only on the material parameters.

When failure surface is reached, stresses in that direction drops suddenly to zero. This essentially denotes that there is no strain softening, neither in compression nor in tension. Hence the descending portion of strain-strain curve of concrete is not used in ANSYS non-linear concrete model. The salient points marked in the plot are point 1= 25,0; point 2= 7,7; point 3 = 0,25 for M25 grade concrete. The curve plotted is by the equations proposed by William Warnke.

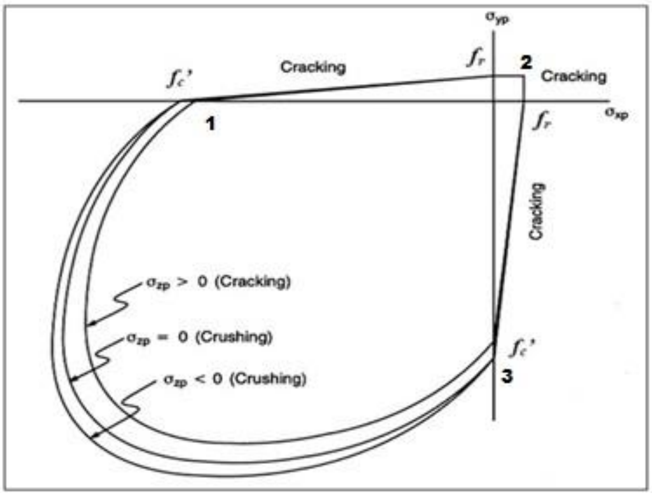

Fig. 6.19 3-D Failure Surface for Concrete

6.4 RESULTS AND DISCUSSION

6.4.1 Shear Strength of wall without opening

This numerical model is performed by varying concrete grade M25 and M30 grade concrete and also changing axial load as 250 kN and 300 kN, numerical model. Various empirical and semi-empirical equations for predicting shear strength of RC shear wall without opening are found around the globe in various codes and literature which are described in Chapter 2 are considered for evaluation of numerical results. Shear strength of RC wall from numerical analysis is compared with those equations are listed in Table 6.2.

Table 6.2 Comparison of Shear Strength of Shear wall without Opening

Eq. No.	**Code/ Literature**	**Shear Strength (kN)**	
		M25	**M30**
1	*IS : 456 (2000)*	485	**517**
2	*ACI : 318 (2014) (Ch 11 – Walls)*	383	454
3	*ACI : 318 (2019) (Ch. 18 – Sp. St. walls)*	**404**	**484**
4	*ASCE/SEI 43 (2005)*	**396**	465
5	*MCBC (2004)*	**416**	**485**
6	*EC8 (2004)*	295	335
7	*AIJ (1999)*	324	408
8	*AS : 3600 (2009)*	**421**	**496**
9	*NZ : 3101.1 (2006)*	303	367
10	*Barda et al. (1977)*	473	560
11	*Wood (1990)*	306	341
12	*Hernandez et al. (1980)*	534	635
13	*Sanchez et al. (2010)*	**396**	**470**
14	*Gulec et al. (2011)*	225	273
15	*Kassem et al. (2010)*	708	855
16	*Luna et al. (2019)*	509	**519**
17	*Present Study*	**432**	**504**

It is evident that there is an appreciable variation in prediction of shear strength of shear wall using various equations. Shear strength of wall computed using numerical analysis of this study is found to be close to prediction by *IS : 456 (2000), ACI : 318 (2019) (Ch. 18 – Special St. walls), MCBC (2004), AS : 3600 (2009), Sanchez et al. (2010)* and *Luna et al. (2019).* From this research, it has been concluded in Chapter 3 that prediction by *ACI : 318 (2019)* and *Sanchez et al. (2010)* performs better among these predictive equation. This in turn strengthens the numerical results obtained from ANSYS 15.0. Lateral displacement of the wall is shown in Figure 6.20. Cracking pattern of wall is shown in Figure 6.21. The stress distribution is shown in Figure 6.22.

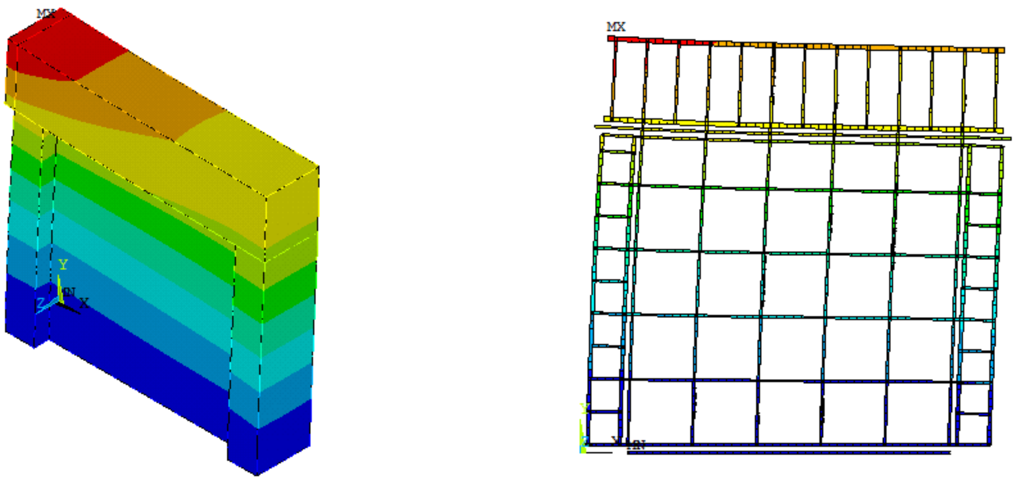

Fig. 6.20 Lateral Displacement of the wall

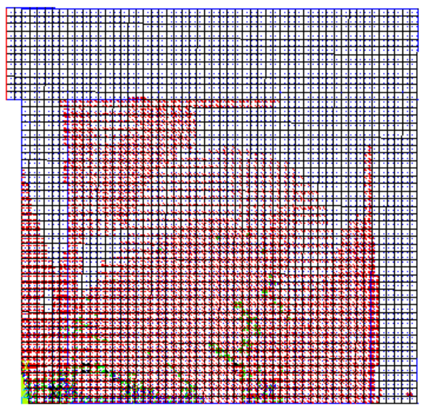

Fig. 6.21 Crack Pattern of shear wall without opening

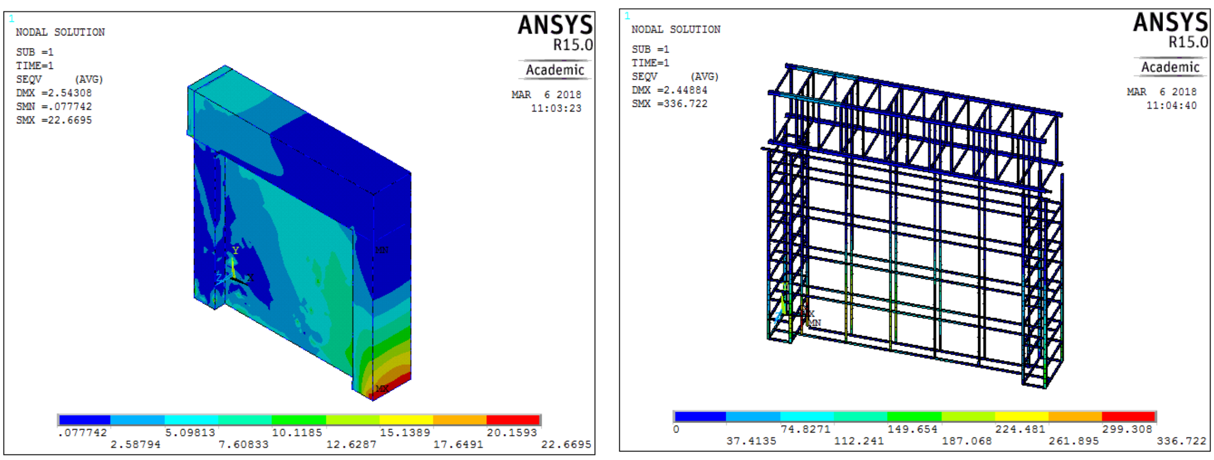

(a) Von mises Stress Distribution

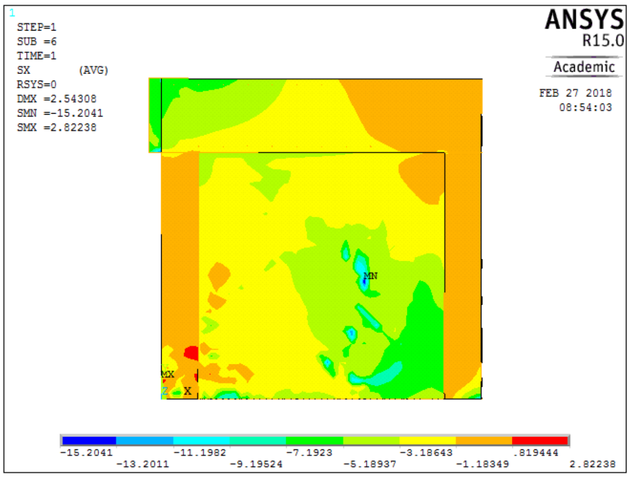

(b) Principal Stress Distribution along Length of the wall

Fig. 6.22 Stress Distribution View of the wall

6.4.2 Shear Strength of wall with opening

Region around opening is vulnerable to stress concentration and cracking. Instead of providing FRC throughout, it is provided only around opening. Figure 6.23 shows addition of FRC around opening up to a depth of 150 mm from opening edge.

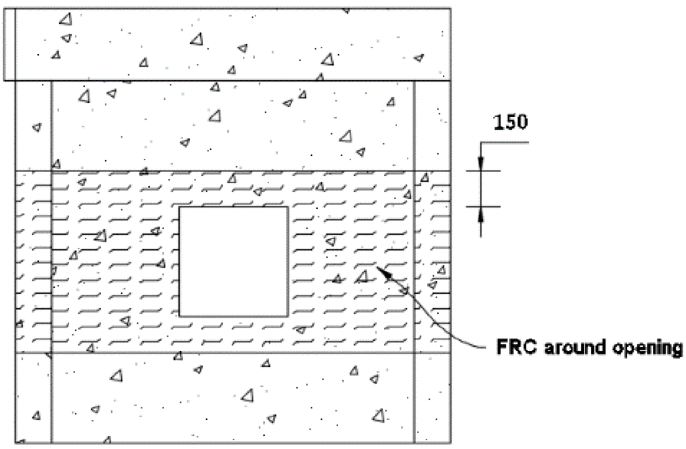

Fig. 6.23 Fibre Reinforced Concrete (FRC) around opening

For walls without opening, first crack observed at top left corner of wall and slowly developed as diagonal crack. Simultaneously, crack was observed at bottom of wall as well. For wall with opening, first crack was observed at top left corner of opening and progressed gradually towards corner of wall. Meanwhile, another crack started at bottom right corner of opening and develops towards bottom right corner of wall as shown in Figure 6.24. Figure 6.25 shows the von-mises stress distribution for walls with opening.

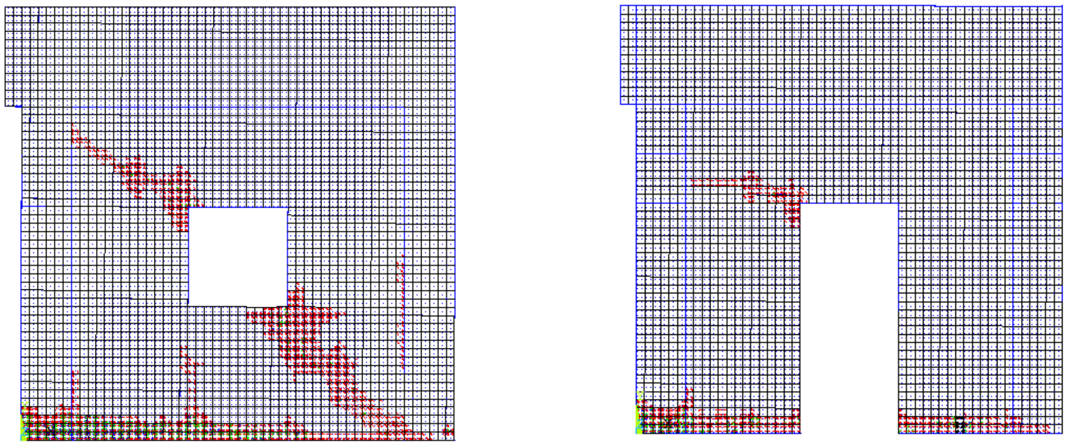

Window Opening Door Opening

Fig. 6.24 Crack Pattern of shear wall without opening (L) and with opening (R)

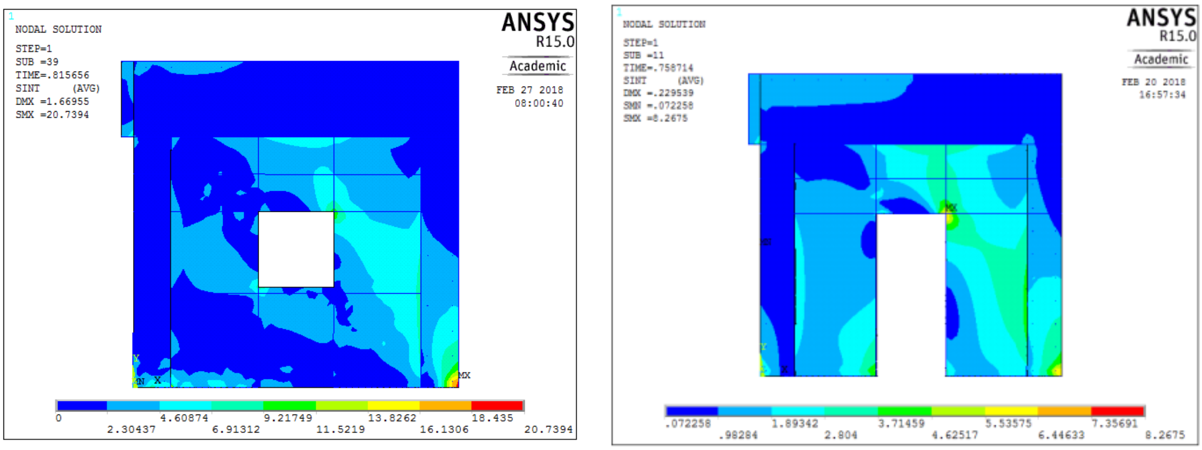

Window Opening Door Opening

Fig. 6.25 Von Mises Stress Distribution: Wall with opening

Load-deflection response of walls with and without opening is reported in Figure 6.26 and Figure 6.27 for M25 and M30 grade concrete respectively. It has been observed that with addition of FRC around opening improves not only strength but also lateral stiffness of wall up to certain extent.

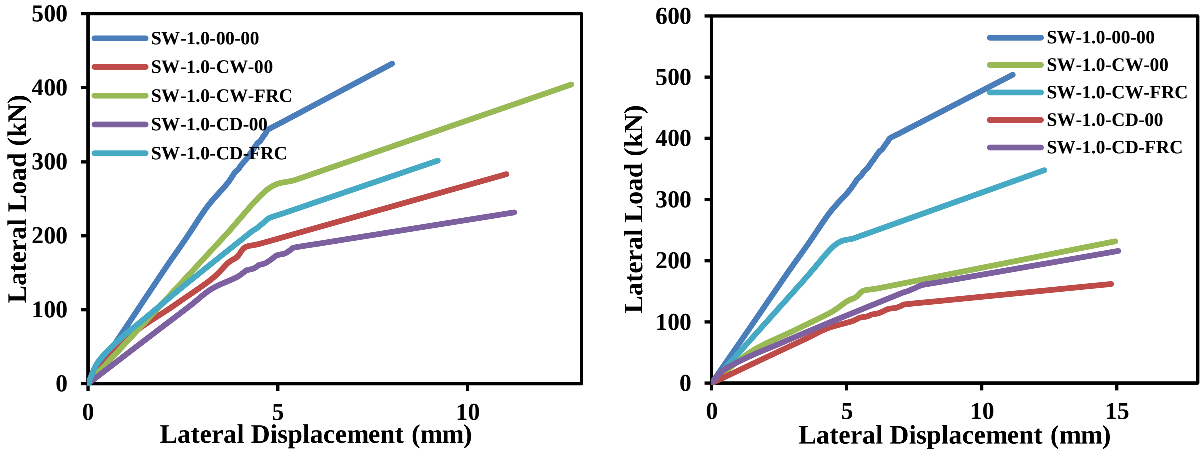

(a) M25 with Axial Load 250 kN (b) M30 with Axial Load 300 kN

Fig. 6.26 Load - Deflection Plot

The load displacement comparative graphs for numerical and experimental studies are shown in Fig. 6.27.

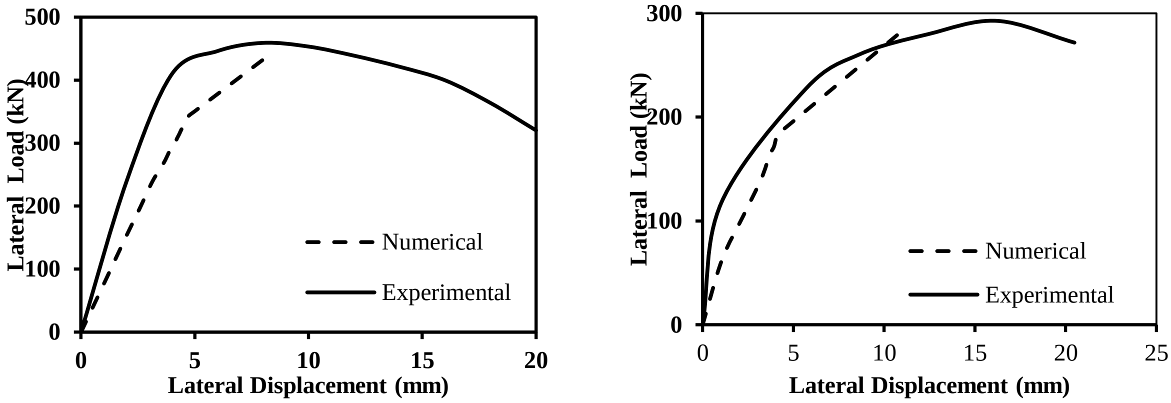

(a) SW-1.0-00-00 (b) SW-1.0-CW-00

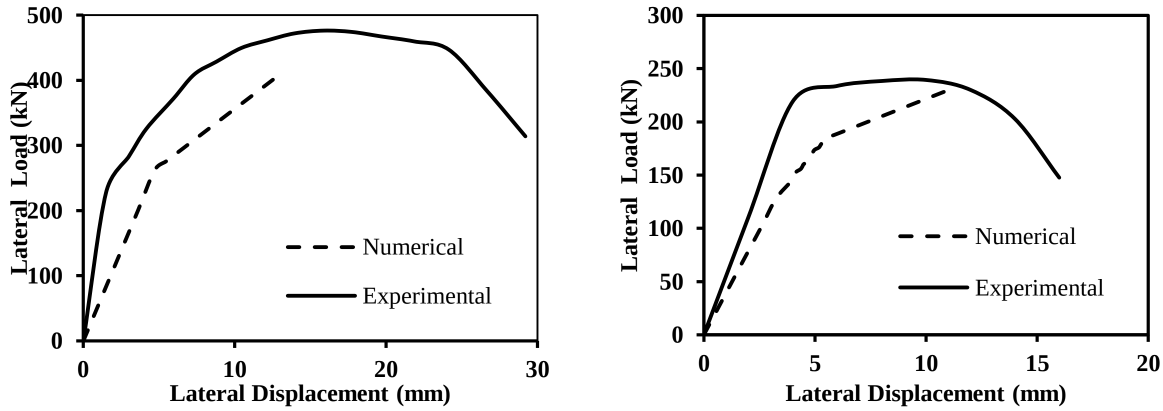

(c) SW-1.0-CW-FRC (d) SW-1.0-CD-00

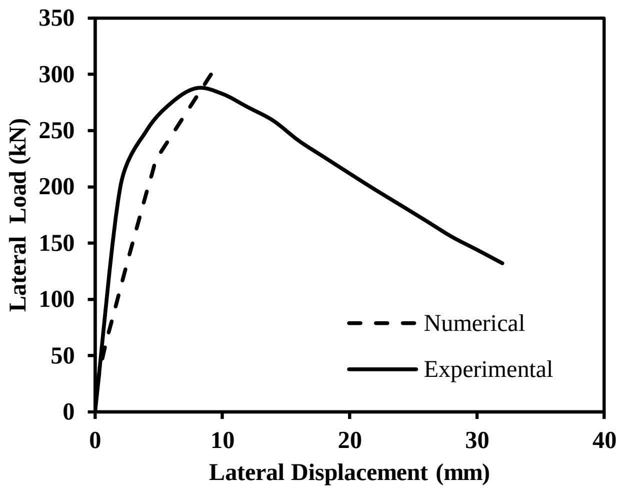

(e) SW-1.0-CD-FRC

Fig. 6.27 Comparison of Load - Deflection Plot

6.4.3 Discussion

It is observed from numerical analysis that crack originates at opposite tension corners of opening and progresses towards corresponding corner of wall. Table 6.3 shows details of shear strength and drift of shear walls.

Table 6.3 Shear strength and Drift of the squat shear walls

	V_{Peak} (kN)		$(V_{peak})_{sw\text{-}1.0}/V_{peak}$		Δ_{peak}/H (%)	
	M25	**M30**	**M25**	**M30**	**M25**	**M30**
SW-1.0-00-00	433	504		-	0.80	1.14
SW-1.0-CW-00	283	231	0.65	0.46	1.10	1.49
SW-1.0-CW-FRC	405	348	0.94	0.69	1.27	1.23
SW-1.0-CD-00	232	162	0.54	0.32	1.12	1.47
SW-1.0-CD-FRC	302	216	0.70	0.43	0.92	1.50

Presence of opening affects shear strength of wall. FRC around openings improves shear strength and ductility of shear wall. Lateral stiffness of wall has been improved with addition of FRC around opening. Use of FRC an alternate solution for strengthening of shear wall with opening is also clear from this numerical study.

6.5 CONCLUDING REMARKS

Finite element analysis (FEA) is widely used to analyse many structural components, as it is very cost effective. Important thing to be noted from this numerical analysis and experimental analysis is that axial load over wall with opening. As axial load increases, shear strength decreases drastically in case of wall with opening. This happens because axial load weakens plane of failure around opening. Behaviour described here with axial load is in contrary to wall without opening. However, more studies are needed for understanding effect of axial load on wall with opening to evaluate this stated behaviour.

CHAPTER 7

SUMMARY AND CONCLUSIONS

7.1 SUMMARY

Shear strength is the most important property of shear walls. During the past five decades, a considerable study has been made by researchers around the globe on reinforced concrete squat shear walls. Various codes of practice and researchers proposed several empirical and semi-equations for predicting the shear strength of RC walls. Sixteen such predictive equations for finding shear strength have been collected from the codes of practice and literature; *IS 456-2000, ACI 318-14, ACI 318-19, ASCE/SEI 43-05, MCBC-04, EC 08-04, AIJ-99, AS 3600-09, NZ 3101.1-06, Barda et al. (1977), Wood (1990), Hernandez et al. (1980), Sánchez et al. (2010), Gulec et al. (2009), Kaseem et al. (2010), Luna et al. (2019).* Prediction by various empirical, semi-empirical and code equations is highly deviating. The accuracy of such predictions is a great concern for the designers. Such deviation in the prediction needs to be addressed. Hence, these equations have been assessed through statistical based 333 selective experimental data points. The data base on RC squat shear walls from 333 experimental results have been selected from various sources by *Galletly (1952), Benjamin et al. (1953), Muto et al. (1953), Antebi et al. (1960), Ryo (1963), Tsuboi et al. (1967), Alexander et al. (1973), Hirosawa (1975), Barda et al. (1977), Cardenes et al. (1978), Sugano et al. (1980), Pauley et al. (1992), Aoyagi et al. (1984), Maier et al. (1985), Wiradinata et al. (1986), Tanabe et al. (1987), Fukuzawa et al. (1988), Lefas et al. (1990), Kabeasawa et al. (1992), Mo (1993), Gupta et al. (1998), Jiang et al. (1999), Salonikios et al. (1999), Pedro et al. (2002), Dabbage (2005), Farvashany et al. (2008), Kuang et al. (2008), Massone et al. (2009), Luna et al. (2015), Yoshizuaki et al. (2015)*. A detailed statistical assessment has been performed. The statistical parameters such as mean, median, coefficient of variation, coefficient of determination, predictor error, scatter plot, frequency distribution and whisker plot has been evaluated using sixteen equations and the best one has been found.

The behaviour of RC shear walls with openings is not clearly understood. Not many efforts have been made so far to understand the behaviour of RC squat shear walls with openings. The performance of shear wall seems to be significantly influenced by the shape of opening, its dimensions and location in walls. Even several national codes do not include provisions for detailing of reinforcement in shear walls with openings, but few national codes recommend additional corner reinforcement around openings. Further, strengthening of shear wall with openings also addressed.

Experimental programme includes selection and processing of materials, dimensions and preparation of specimens, reinforcement detailing, test set-up, loading protocol and testing to understand horizontal strength and behaviour of RC shear walls with and without openings. Test series includes five one-third scaled RC squat shear wall with and without openings. It is presumed that the cantilever wall subjected to constant vertical load and static cyclic lateral load exhibits similar behaviour of shear wall under earthquake loading. The shear walls consist of three components. First component is top beam through which vertical and lateral loads are transferred to the wall. The second component is the wall web which is to be tested. The third component is the bottom beam which anchors to the strong floor for fixity. The five shear walls designed for experimental study consist of; without opening (SW-1.0), with concentric window opening (SW-1.0-CW), FRC with concentric window opening (SW-1.0-CW-FRC), with concentric door opening (SW-1.0-CD) and FRC with concentric door opening (SW-1.0-CD-FRC).

7.2 CONCLUSIONS

7.2.1 Assessment of Shear Strength of Reinforced Concrete Squat Shear Walls

Equations considered in this study do not account for effect of out-of-plane and eccentric loading. Results and conclusions made from this study are discussed in brief as follows.

5. The shear strength predictions by *ACI 318-19, MCBC–04, AS3600-09, NZ 3101.1-06* and *Luna et al. (2019)* result in the mean shear strength ratios of 1.03, 1.05, 0.97, 1.00 and 1.07 respectively. Prediction seems to be in closer to mean shear strength ratio.

6. The shear strength predictions by *IS 456-2000, ACI 318-19 (Ch. 18), MCBC-04* and *Luna et al. (2019)* show comparatively better median of 1.06, 0.94, 0.97 and 1.03 respectively.

7. The shear strength equation proposed by *Sánchez et al. (2010)* shows best prediction of ultimate shear strength with a coefficient of variation (CoV) of 0.34.

8. The shear strength equations by *ASCE/SEI 43-05, Sánchez et al. (2010)* and *Gulec et al. (2009)* show better prediction with a coefficient of determination of about 0.77.

9. The shear strength equations by *ACI 318-19, AS3600-09* and *NZ 3101.1-06* show the lowest overestimate percentage of shear strength of about 3.0, 3.0, and 1.0% respectively.

10. Substantial scatter of data points can be seen from scatter plot diagram according to the sixteen shear strength equations. The equations by *ACI 318-14, Sánchez et al. (2010)* and *Gulec et al. (2009)* show comparatively least scatter with minimum deviation from mean.

11. The shear strength equation by *Hernandez et al. (1980)* and *Sánchez et al. (2010)* show better frequency distribution comparing with other equations.

12. A box and whisker plot, as shown in Fig. 4, is useful to indicate skewness of scatter data distribution. Predictions by *ACI 318-19, MCBC-04, AS 3600-09* and *Luna et al. (2019)* show relatively least skewness as P mean line crosses almost centre of interquartile range box (IQR) in distribution.

13. All the predicting equations show entirely different scatter due to their form and level of influence of parameters selected.

14. The prediction by *ACI 318-14* based on semi-empirical modified truss analogy performing relatively unsatisfactory. It is noticed that performance of this equation is relatively unsatisfactory. In *ACI 318-19*, equation in chapter 11 is replaced with equation in chapter 18. This replacement holds good, which is confirmed by this study.

15. Shear strength predictions by *ACI 318-19* and *Sánchez et al. (2010)* are closely agreeable with experimental results.

16. Improvement of the shear strength prediction needs to be attempted incorporating all parameters including influence of boundary elements.

7.2.2 Behaviour of RC Squat Shear Walls with Openings under Cyclic Loading

Five reinforced concrete shear walls, designed with and without openings, tested as per standard loading protocol under reverse cyclic loading. The performance parameters include shear strength, ductility, shear strength degradation, lateral stiffness degradation and energy dissipation in shear walls.

- The wall without opening failed by crushing of concrete in both toes of boundary elements and sheared off horizontally due to reversed cyclic displacements. For the wall with window opening, failure mode was due to shearing off weaker plane of wall (i.e) across opening. For the wall without opening and with window opening using FRC, failure mode occurred due to crushing of concrete at both left and right toes of boundary elements. Interestingly, addition of FRC around window opening alters cracking pattern of wall. In case of door opening, cracking and failure are similar in RC squat walls cast with normal concrete and with fibre reinforced concrete.

- The shear strength of RC walls with opening rapidly reduced, about 68% with window opening and 61% with door opening, of that of RC squat wall without opening. Steel fibres used in concrete in and around corners of opening improved shear strength by about 29 and 14% respectively as compared with RC squat wall cast with normal concrete with opening.

- The ductility of RC walls with opening reduced significantly, about 51% with window opening and 70% with door opening, of that of RC squat wall without opening. Steel fibres used in concrete in and around corners of opening improved shear strength by above 23 and 40% respectively as compared with RC squat wall with normal concrete with opening.

- Reduction of shear strength of RC wall with opening is rapid during subsequent consecutive cycles after load cycle in which highest peak load was observed. Addition of FRC in wall with opening minimizes loss of strength in comparison with that of wall without opening.

- Initial stiffness of walls with openings is about 60% of that of wall without opening. Stiffness degradation has been rapid in walls with normal concrete, while showing gradual reduction in wall cast with FRC.

- Addition of FRC with openings improves ductility. Energy dissipation capacity has been found to be significantly reduced by openings. However, addition of fibres in concrete improved energy dissipation in wall with opening.

- Observed shear strength of squat wall is agreeable with shear strength predicted by *ACI 318–19, ASCE/SEI 43-05, MCBC–04, AS3600–2009* and *Sanchez et al. (2010).* Though shear strength predicted by *ACI 318* equations in walls with openings is closely agreeable with test results, it does not state shape of opening. Moreover, as suggested by *ACI 318* that weak plane coincides with horizontal in opening, which is not observed from experimental investigations.

7.3 IMPORTANT CONTRIBUTIONS

- Important guidance has been proposed for design engineers for designing the shear wall effectively with safety.
- Proposed an effective strengthening methodology for shear wall with openings.
- Pointed out important weakness in *ACI 318-19* regarding recommendations for calculating shear strength of shear wall with opening with experimental observation.

7.4 SCOPE FOR THE FUTURE WORK

There is a need to continue research work as more studies are needed in shear wall area. Present study can be extended as follows.

- Improvement of shear strength prediction needs to be attempted incorporating all parameters including influence of boundary elements.
- Similar study should be carried out for displacement capacity predictions also which are available in codes and literature.
- Unlike wall without opening, there is no proper demarcation line for squat and slender wall in case of wall with opening in terms of aspect ratio. It should be explored in future.
- It is seen from literature that studies carried with higher axial load and higher concrete grade is very much limited.
- Study can be extended to multiple and eccentric opening which is much seen in practical.

REFERENCES

[1] **ACI 318** (2014) Building Code Requirements for Structural Concrete. *American concrete Institute,* Rarmington Hill, Michigan.

[2] **AIJ (Architectural Institute of Japan) (**1999**)** Structural Design Guidelines for Reinforced concrete Buildings.

[3] **Alexander, C. M., Heidebrecht, A. C., and Tso, W. K.** (1973) Cyclic Load Tests on Shear Wall Panels. *Proceedings, Fifth World Conference on Earthquake Engineering*, Rome, Italy, pp. 1116-1119.

[4] **Ali, A., and Wight, J. K.** (1991) RC Structural Walls with Staggered Door Opening. *Journal of Structural Engineering*, Vol. 117, No. 5, pp. 1514 – 1531.

[5] **American Society of Civil Engineers**, (2005) Seismic Design crieteria for Structures, systems and Components in Nuclear Facilities. (ASCE/SEI 43-05)

[6] **Antebi, J., Utku, S., and Hansen, R. J., (**1960), "Response of Shear Walls to Dynamic Loads," Department of Civil and Sanitary Engineering, Massachusetts Institute of Technology, Cambridge, pp. 177.

[7] **AS 3600 (Australian Standard) (2009)** *Concrete structure.*

[8] **Aoyagi, Y., and Yamada, K.** (1984) Strength and Deformation Characteristics of Reinforced Concrete Shell Elements Subjected to In-plane forces. *Concrete Library International, JSCE,* No.4, pp.129-160.

[9] **Barda, F., hanson, J. M., and Corley, W. G.** (1977) Shear strength of Low-Rise walls with Boundary Elements. *SP-53, American Concret Institute*, pp. 149-202.

[10] **Benjamin, J. R., and Williams, H. A.** (1953) Investigation of Shear Walls, Part 3-Experimental and Mathematical Studies of the Behaviour of Plain and Reinforced Concrete Walled Bents under Static Shear Loading. *Technical Report,* No. 1, Part 3, Department of Civil Engineering, Stanford University, pp. 63.

[11] **Bing, L., Kai, Q., and Hui, W.** (2016) Flange effects on seismic performance of reinforced concrete squat walls with irregular or regular openings, *Engineering Structures*, V-110, pp. 127-144.

[12] **Bismarck, N. L., Jonathan, P. R., and Anderw, S. W.** (2015) Seismic Behavior od Low-Aspect-Ratio Reinforced Concrete Shear Walls, *ACI Str. Journal*, T. No. 112-S48, V-5, pg. 593-604, Sep-Oct 2015.

[13] **Cardenes, A. S., Russell, H. G., and Corley, W. G.** (1978) Strength of low-rise structural walls, *Publication SP-63, American Concrete Institute*, Detroit, pp. 221-241.

[14] **Christian, G., and Pierino, L.** (2005) Static cyclic tests on lightly reinforced concrete shear walls, *Engineering Structures*, V-27, pp. 1703-1712.

[15] **Christidis, K, I., and Karagiannaki, D.,** (2020) Evaluation of flexural and shear deformations in medium rise RC shear walls, *Journal of Building Engineering*, V-42, pp 1-18.

[16] **Cosmin, P., Gabriel, S., Thomas, B., and Biorn, T. (**2015) Concrete walls weakened by opening as compression members – A Review, *Engineering Structures*, V-89, pp. 172-190.

[17] **CSA (Canadian Standards Association) A23.3** (2014) - *Design of concrete structures*.

[18] **Dabbage, H.** (2005). “Strength and ductility of high-strength concrete shear walls under reverse cyclic loading”, *Ph.D. Thesis, The University of New South Wales*, Sydney, Australia.

[19] **Daniel, P., and Frank, J.V.** (2002) Behavior of Three-Dimensional Reinforced Concrete Shear Walls. *ACI Structural Journal*, V-99, No. 1, pp. 81-89.

[20] **Daniel, P., and Vecchio, F.J.** (2002) Behaviour of Three dimensional Reinforced Concrete Shear walls. *ACI Structural journal*, V-99 , No. 1 Title no. 99-S, pg. 81 – 89, Jan-Feb 2002.

[21] **Edward, D.T., Maria, E.P., Ricardo, P., Maria, E.M., and Julio, F.** (2009) Simplified model for damage in squat RC shear walls. *Engineering Structures,* V-31, pp. 2215-2223.

[22] **Elmorsi, M., Kianoush, M. R., and Tso, W. K.** (1998) Nonlinear Analysis of Cyclically Loaded Reinforced Concrete Structures. *ACI Structural Journal,* V-95**,** No. 6**,** pp. 725-739.

[23] **Endo, T. Adachi H., and Nakanishi, M.** (1980) Force-Deformation Hysteresis Curves of Reinforced Concrete Shear Walls, *Proceedings*, Seventh World Conference on Earthquake Engineering, Istanbul, Turkey, Vol. 6, pp. 315-322.

[24] **Eurocode 08** (2004) Design of Stuctures in Seismic Regions, *Institution of Civil Engineers..*

[25] **Fahjan, Y.M., Kubin, J., and Tan, M.T.** (2010) Nonlinear Analysis Methods for Reinforced Concrete Buildings with Shear walls. *14th European Conference on Earthquake Engineering,* August 30 – September 3, in Ohrid, Republic of Macedonia.

[26] **Farvashany, F. E., Foster, S. J., and Rangan, B. V.** (2008) Strength and Deformation of High-Strength Concrete Shear walls. *ACI Structural Journal*, T. No. 105-S03, V-105, No. 1, PP. 21-29.

[27] **Fukuzawa, R., Chiba, O., Hatori, T., Yagishita, K., and Watabe, M.** (1988) Study on Load-Deflection Charecteristics of Heavily Reinforced Shear Wall. *Proceedings of Ninth World Conference on Earthquake Engineering*, V-4, pp. 517-522.

[28] **Galletly, G. D.** (1952) Behavior of Reinforced Concrete Shear Walls Under Static Load. *Department of Civil and Sanitary Engineering*, Massachusetts Institute of Technology, Cambridge, pp 123.

[29] **Greeshma, S., Jaya, K.P., and Sheeja, A.L.** (2011) Analysis of Flanged Shear wall using ANSYS concrete model. *Int. journal of civil and structural engineering,* V-2, No 2, pp. 454 – 465.

[30] Gulec, C. K., Andrew, S.W., and Bozidar, S. (2009) Peak Shear Strength of Squat Reinforced Concrete Walls with Boundary Barbells or Flanfes. *ACI Structural Journal*, V-106, No. 3, pp. 368-377.

[31] Gupta, A., and Rangan, B. V. (1998) High-strength Concrete (HSC) structural walls. *ACI Structural Journal*, V–95(2), pp. 194-205.

[32] Hernandez, O., and Zermeno, M. E. (1980) Strength and Behavior of Structural Walls with shear failure. *Seven world conference on Earthquake Engg*., V-4, pp. 121.

[33] Hirosawa, M. (1975) Past experimental results on reinforced concrete shear walls and analysis on them. *Building Research Institute*, Ministry of Construction, Japan. (In Japanese).

[34] Hong, G.P., jang, W.B., Jae, L., and Hyun, S. (2015) Cyclic Loading Tests for Shear Strength of Low-Rise Reinforced Concrete Walls with Grade 550 MPa Bars. *ACI Structural Journal* , V-112, No. 3, pp. 299-310.

[35] IS 13920 (2016) Ductile Detailing Of Reinforced Concrete Structures Subjected To Seismic Forces - Code of Practice.

[36] Jiang, H., and Lu, X. (1999) Shear wall (R01 ~ R02). Static test database of components and nodes of State Key *Laboratory of Disaster Prevention in Civil Engineering of Tongji University*, pp. 69 – 85. (In Chinese).

[37] Kabeasawa. T., Kuramoto, H., and Matsumoto, K. (1992) Tests and analyses of high strength shear walls. *Proc., 1st Meeting of the Multilateral projects on the use of High Strength Concrete*, Japan, pp. 1-26.

[38] Kaseem, W., and Elsheikh, A. (2010) Estimation of Shear Strength of Structural Shear walls. *Journal of Structural engineering ASCE,* V-136, No. 10, pp. 1215 – 1224.

[39] Kuang, J. S., and Ho, Y. B. (2008) Seismic Behaviour and Ductility of Squat Reinforced Concrete Shear Walls with Non Seismic Detailing. *ACI Structural Journal*, T. No. 105-S24, V-105, No. 2, pp. 225–231.

[40] Kwak, H. G., and Kim, D. Y. (2004) Material Nonlinear Analysis of RC Shear Walls

Subjected to Cyclic Loadings, *Elsevier Engineering Structure*, V-26**,** pp. 1423-1436.

[41] **Kwak, H. G., and Kim, D. Y.** (2004) Material Nonlinear Analysis of RC Shear Walls Subjected to Monotonic Loading. *Elsevier Engineering Structure*, V-26**,** pp. 1517-1533.

[42] **Lefas, L. D., Kotsovos, M. D., and Ambraseys, N. N.** (1990) Behaviour of reinforced concrete structural walls: Strength, deformation charecteristics and failure mechanism. *ACI Structual Journal*, V–87, pp. 23-31.

[43] **Leonardo, M. M.** (2010) Strength prediction of squat structural walls via calibration of shear-flexure interaction model, *Engineering Structurals 32*, pp. 922-932.

[44] **Massone, L. M., Kutay, O., and John W.W.** (2009) Modelling of Squat Structural Walls Controlled by Shear. *ACI Structural Journal*, V-106, No. 5, pp. 646-655.

[45] **Lin, C.Y, and Kuo C. L.** (1988) Behaviour of shear walls with opening. *In: Proc. of the ninth world conf. on earthquake eng.*, V-IV, pp. 535–540.

[46] **Luna, B. N., Jonathan, P. R., and Whittaker, A. S.** (2015) Seismic Behavior of Loe-Aspect Ratio Reinforced Concrete Shear Walls. *ACI Structural Journal*, Vol-112, No. 5, pp. 593 – 603.

[47] **Luna, B. N., and Whittaker, A. S.** (2019) Peak Strength of Shear-Critical Reinforced Concrete Walls. *ACI Structural Journal*, Title No. 116-S46, Vol-116, No. 2, pp. 257-266.

[48] **Maier, J., and Thurliamman, B.** (1985) Bruchversuche an Satahlbeton-scheiben (Fracture Test on reinforced concrete plates). *Institut fur Baustatil und konstruktion ETH*, Zurich, pp 130.

[49] **Marius, M.** (2013) Seismic behaviour of reinforced concrete shear walls with regular and staggered openings after strong earthquakes between 2009 and 2011. *Engineering Failure Analysis*, V-34, pp. 537–565.

[50] **Marius, M.** (2014) Failure analysis of RC walls with staggered openings under seismic loads. *Engineering Failure Analysis*, V-41, pp. 48-64.

[51] **Mazen, A, M.** (2013) Analysis of Shear Walls with Opening using Solid65 Element, *Jordan Journal of Civil Engineering*, V-7, No. 2, pp. 164-173.

[52] **MCBC (Mexico City Building Code)** (2004) Normas Tecnicas Complementarias para Diseno y Construcción de Estructuras de Concreto. Distrito Federal (DF): Gaceta Oficial del Distrito Federal. [in Spanish].

[53] **Merin, M., and Prabha. C.** (2013) Structural behaviour of shear wall based on nonlinear analysis. *American journal of Engineering Research RASE2013*, pp. 44 – 49.

[54] **Mo, S. T.** (1993) Dynamic tests on reinforced concrete shear walls. *National science council project* Rep. No. NSC81-0410-E006-521.

[55] **Musmer, M.A.** (2013) Analysis of Shear Wall with Openings Using Solid65 Element, *Jordan Journal of Civil engineering*, V-7, No. 2, pg. 164 – 173.

[56] **Muto, Kiyoshi, and Kokusho, S.** (1953) Experimental Study on Two-Story Reinforced Concrete Shear Walls.' *Architectural Institute of Japan (Tokyo)*, No. 47, pp. 7 – 15.

[57] **Oesterle, R. G., Aristizabal, O., and Corley, W. G.** (1984) Web crushing of reinforced concrete structural walls. *ACI Structural Journal*, V–81, pp. 231 - 241.

[58] **Okamura, H. and Maekawa, K.** (1991) Nonlinear analysis and constitutive models of reinforced concrete, Gihodo Press, Tokyo, Japan, pp. 182.

[59] **Palermo, D., and Vecchio, F. J.** (2003) Compression Field Modelling of Reinforced Concrete Subjected to Reversed Loading: Formulation. *ACI Structural Journal*, V-100, No. 5, pp. 616-625.

[60] **Paulay, T., and Loeber, P. J.** (1974) Shear Transfer by Aggregate Interlock. *ACI Structural Journal*, Detroit, Michigan, pp. 1-15.

[61] **Pauley, T., and Priestley, M.J.N.** (1992) Seismic design of reinforced concrete and masonry building. *A Wiley Interscience Publication*.

[62] **Pedro A. H., Christian A. L., and Rodrigo M. J.** (2002) Seismic Behavior of Squat Reinforced Concrete Shear Walls. *Earthquake Spectra*, V-18, No. 2, pp 287–308.

[63] **Pilakoutas, K., and Elnashai, A.** (1995) Cyclic Behaviour of Reinforced Concrete Cantilever Walls, Part I: Experimental Results. *ACI Structural Journal*, V-92**,** No. 3**,** pp. 271-281.

[64] **Pilakoutas, K., and Elnashai, A.** (1995) Cyclic Behaviour of Reinforced Concrete Cantilever Walls, Part II: Discussions and Theoretical Comparisons. *ACI Structural Journal*, V-91**,** No. 4**,** pp. 425-434.

[65] **Rong, X., Zheng, S., Zhang, Y., Zhang, X., and Dong, L.** (2019) Experimental study on the seismic behavior of RC shear walls after freeze-thaw damage, *Engineering Structures,* V-206, pp. 1-17.

[66] **Ryo, S.** (1963) Experimental Study on strength and stiffness of reinforced concrete frame with infill wall, *Annual Convention of AIJ,* pp. 61-64. (In Japanese).

[67] **Saeid, S. G., and Salaheddin, M.** (2015) Experimental investigation on stiffened steel plate shear walls with two rectangular openings, *Thin-Walled Structures*, V-86, 2015, pp. 55-66.

[68] **Salonikios, T. N., Kappos, A. J., Tegos, L., A., and Penelis, G. G.** (1999) Cyclic Load Behaviour of Low-Slenderness Reinforced Concrete Walls: Design Basis and Test Results, *ACI Structural Journal*, T. No. 96-S73, V-96, pp. 649-661.

[69] **Sanchez, A. A., and Alcocer, S. M.** (2010) Shear Strength of squat reinforced concrete walls subjected to earthquake loading – Trends and models, *Engineering Structures 32,* pp. 2466-2476.

[70] **Sato S., Ogata Y., Yoshizaki S., Kanata K., Yamaguchi T., Nakayama T., Inada Y., and Kadoriku J.** (1989) Behavior of Shear Wall Using Various Yield Strength of Rebar Part 1: An Experimental Study. *Transactions*, Tenth International Conference on Structural Mechanics in Reactor Technology, H09/293, Anaheim, CA.

[71] **Sharmin, R.C., Rahman, M.A., and Das, A.K.** (2012) Effect of Opening in Shear Wall on Seismic Response of Structures. *International Journal of Computer Applications*, V-59, No. 1, pp. 10-13.

[72] **Sittipunt, C., and Wood, S. L.** (1993) Finite Element Analysis of Reinforced Concrete Shear Walls, Report No. 584, University of Illinois, Urbana, Illinois, pp-384.

[73] **Sivakumar, N., Asha, M., Gowtham, P., and Manikandan, R.** (2014) Analytical study on Flanged Shear wall under lateral loading. *Int. journal of Structural and Civil Engg Res*, V-3, N. 1, pp. 22 – 30.

[74] **Sotomura, K., Murazumi, Y., Yoshizaki, S., and Korenaga, T.** (1985) Ultimate Shear Strength of Shear Wall in Nuclear Power Plant. *International Association for Structural Mechanics in Reactor Technology (ISMiRT)*, pp. 145 – 150.

[75] **Su, R.K.L., and Wong, S.M.** (2007) Seismic behavior of slender reinforced concrete shear walls under high axial load ratio. *Engineering Structures*, V-29, 2007, pp. 1957-1965.

[76] **Sugano, S. and Fugimura, M.** (1980) Aseismic Strengthening of Existing Reinforced Concrete Building. *Proc., of 7WCEE, Istanbul*, Turkey, pp. 449 – 456.

[77] **Tanabe, T., and Yoshikawa, H.** (1987) Constitutive equation of a cracked reinforced concrete panel. *IABSE Colloquium on Computational Mechanics of concrete structures*, pp. 17-34.

[78] **Trevor, K.** (2007) A Blind Prediction Test Of Nonlinear Analysis Procedures For Reinforced Concrete Shear Walls", Bulletin of the New Zealand Society for Earthquake Engineering, V-40, No. 3, pp 142 – 159.

[79] **Tsuboi, Y., Suenaga, Y and Shigenobu, T.** (1967) Fundamental study on Reinforced Concrete Shear Wall Structures – Experimental and Theoretical study of Strength and Rigidity of Two-Directional Structural walls subjected to combined stresses. *Transactions of the Architectural Institute of Japan*, No. 131.

[80] **Vishal, A.I., and Uttam B.K.** (2015) Effect of Openings in Shear Wall on Seismic Response of Structure. *International Journal of Engineering Research and Applications*, V-5, Issue 7, pp. 41-45.

[81] Wiradinata, S., and Saatcioglu, M. (1986) Tests of Squat Shear Wall under Lateral Load Reversals. *Proceedings*, 3rd U.S. National Conference on Earthquake Engineering, Charleston, V-2, pp. 1395-1406.

[82] Wood, S. L. (1990). Shear strength of Low-Rise Reinforced Concrete walls. *ACI Structural Journal*, V-87, pp. 99-107.

[83] Xu, J., Jinsuo N., Charles, H., and Syed, A. (2007) FE analysis of JNES/NUPEC Seismic Shear Wall Cyclic and Shaking Table test Data. *Proc. of ASME PVP*, pp. 1–11, Texas, US.

[84] Yanez, F. V., Park, R., and Paulay, T. (1992), Seismic Behaviour of walls with irregular openings. *Earthquake Engineering, Tenth World Conference*, Rotterdam, pp. 3303 – 3308.

[85] Youkai, P., Hui, W., and Yan, Z. (2015) Strength and drift capacity of squat recycled concrete shear walls under cyclic loading. *Engineering Structures*, V-100, pp. 356-368.

[86] Zhang, L. X., and Hsu, C. T. T. (1998), Behaviour and Analysis of 100 MPa Concrete Membrane Element. *ASCE Journal of Structural Engineering*, V-124**,** No. 1**,** pp. 24-34.

[87] Zhang, Y., and Wang, Z. (2000) Seismic Behaviour of Reinforced Concrete Shear Walls Subjected to High Axial Loading. *ACI Structural Journal*, T. No. 97-S75, V-97, No. 5, pp. 739-750.

[88] Zhang, H., Lu, X., and Weijian, Y. (2018) Experimental Investigation on Stress Redistribution and Load-Transfer Paths of Shear Walls with Openings, *Journal of Structural Engineering*, Vol. 144, No. 9, pp. 1 – 16.

APPENDIX

Table A-1 Geometric Details of Experimental Shear Wall Specimen

Source	Designation	Geometrical Properties						Material Properties					Axial Load, N (kN)	Shear Strength V (kN)
		h_w (mm)	l_w (mm)	h_w/l_w	b_w (mm)	l_c (mm)	b_c (mm)	f_c' (MPa)	f_y (MPa)	ρ (%)	ρ_v (%)	ρ_h (%)		
Luna et al. (2015)	SW1	2867	3050	0.94	203	0	0	25	462	0.00	0.67	0.67	0	1125
	SW2	1647	3050	0.54	203	0	0	48	434	0.00	1.00	1.00	0	2504
	SW3	1647	3050	0.54	203	0	0	54	434	0.00	0.67	0.67	0	2082
	SW4	1647	3050	0.54	203	0	0	29	462	0.00	0.33	0.33	0	1005
	SW5	1007	3050	0.33	203	0	0	30	462	0.00	1.00	1.00	0	3229
	SW6	1007	3050	0.33	203	0	0	26	462	0.00	0.67	0.67	0	2540
	SW7	1007	3050	0.33	203	0	0	26	462	0.00	0.33	0.33	0	1415
	SW8	1647	3050	0.54	203	0	0	24	462	0.00	1.50	1.50	0	2771
	SW9	1647	3050	0.54	203	0	0	30	462	0.00	1.50	0.67	0	2767
	SW10	1647	3050	0.54	203	0	0	32	462	0.00	1.50	0.33	0	2202
	SW11	1647	3050	0.54	203	0	0	34	462	1.50	0.67	0.67	0	1886
	SW12	1647	3050	0.54	203	0	0	34	462	2.00	0.33	0.33	0	1624
Massone et al. (2009)	test1	1520	1520	1.00	152	0	0	26	424	3.12	0.43	0.28	0	633
	test2	1520	1520	1.00	152	0	0	31	424	1.70	0.40	0.28	0	453
	test3	1520	1520	1.00	152	0	0	31	424	1.70	0.40	0.28	0	491
	test4	1520	1520	1.00	152	0	0	44	424	3.12	0.43	0.28	0	749
	test5	1220	1370	0.89	152	0	0	28	424	1.33	0.23	0.28	589	753
	test6	1220	1370	0.89	152	0	0	31	424	1.33	0.23	0.28	654	819
	test7	1220	1370	0.89	152	0	0	32	424	1.33	0.23	0.28	332	648
	test8	1220	1370	0.89	152	0	0	32	424	1.33	0.23	0.28	333	682
	test9	1220	1370	0.89	152	0	0	30	424	1.33	0.23	0.28	0	443
Maier et al. (1985)	S1	1200	1180	1.02	100	400	100	37	574	1.13	1.16	1.03	433	680
	S2	1200	1180	1.02	101	400	100	35	574	1.13	1.16	1.03	1653	928

Source	Designation	Geometrical Properties h_w (mm)	l_w (mm)	h_w/l_w	b_w (mm)	l_c (mm)	b_c (mm)	Material Properties f_c' (MPa)	f_y (MPa)	ρ (%)	ρ_v (%)	ρ_h (%)	Axial Load, N (kN)	Shear Strength V (kN)
	S3	1200	1180	1.02	102	400	100	37	530	1.13	2.46	1.03	424	977
	S4	1200	1180	1.02	103	100	236	33	574	1.13	1.05	1.03	262	392
	S5	1200	1180	1.02	104	400	100	37	574	1.13	1.16	1.03	416	701
	S6	1200	1180	1.02	105	400	100	36	479	1.13	1.13	0.57	416	667
	S7	1200	1180	1.02	106	400	100	34	555	1.13	1.13	1.01	1657	836
	S8	1200	1180	1.02	107	400	100	34	555	1.13	1.13	1.01	416	510
	S9	1200	1180	1.02	108	100	118	29	560	1.13	0.98	0.00	260	342
	S10	1200	1180	1.02	109	111	179	31	496	1.13	2.00	0.98	262	670
Kabeasawa et al. (1993)	NW1	3000	1700	1.76	80	200	200	94	1001	0.85	0.84	0.53	1764	1468
	NW2	3000	1700	1.76	80	200	200	56	1001	0.85	0.65	0.25	1764	714
	NW3	3000	1700	1.76	80	200	200	55	753	0.85	0.88	0.25	1372	784
	NW4	3000	1700	1.76	80	200	200	60	753	0.85	1.07	0.49	1568	900
	NW5	3000	1700	1.76	80	200	200	65	753	0.85	1.15	0.49	1372	1056
	NW6	3000	1700	1.76	80	200	200	103	753	0.85	0.84	0.53	1568	1670
	W08	2000	1700	1.18	80	200	200	138	1079	0.85	0.84	0.53	1764	1719
	W12	2000	1700	1.18	80	200	200	71	1079	0.85	1.42	0.35	2313	1254
	N1	2000	1700	1.18	80	200	200	65	792	0.85	1.34	0.21	1568	1100
	N2	2000	1700	1.18	80	200	200	72	792	0.85	1.54	0.53	1568	1378
	N3	2000	1700	1.18	80	200	200	103	792	0.85	1.54	0.53	1568	1696
	N4	2000	1700	1.18	80	200	200	77	792	0.85	1.54	0.49	2617	1158
	N5	3000	1700	1.76	80	200	200	74	792	0.85	1.69	0.72	1568	1411
	N6	2000	1700	1.18	80	200	200	72	792	0.85	1.84	0.92	1568	1498
	N7	2000	1700	1.18	80	200	200	76	792	0.85	2.17	1.34	1568	1639
	N8	2000	1700	1.18	80	200	200	63	810	0.85	1.00	0.74	1568	1049
	W35X	2000	1700	1.18	80	200	200	61	810	0.85	1.00	0.74	1764	1054
	W35H	2000	1700	1.18	80	200	200	58	810	0.85	1.00	0.74	1921	958
	W30H	2000	1700	1.18	80	200	200	62	810	0.85	1.00	0.74	1862	1020
	P35H	2000	1700	1.18	80	200	200	60	810	0.85	1.00	0.74	1470	1011

Source	Designation	Geometrical Properties h_w (mm)	l_w (mm)	h_w/l_w	b_w (mm)	l_c (mm)	b_c (mm)	Material Properties f_c' (MPa)	f_y (MPa)	ρ (%)	ρ_v (%)	ρ_h (%)	Axial Load, N (kN)	Shear Strength V (kN)
	MW35H	2000	1700	1.18	80	200	200	94	810	0.85	0.84	0.53	1666	1468
Lefas et al. (1990)	SW11	750	750	1.00	70	0	0	45	470	0.00	2.49	1.10	0	260
	SW12	750	750	1.00	70	0	0	46	470	0.00	2.49	1.10	230	340
	SW13	750	750	1.00	70	0	0	35	470	0.00	2.49	1.10	355	330
	SW14	750	750	1.00	70	0	0	36	470	0.00	2.49	1.10	0	265
	SW15	750	750	1.00	70	0	0	37	470	0.00	2.49	1.10	185	320
	SW16	750	750	1.00	70	0	0	44	470	0.00	2.49	1.10	460	355
	SW17	750	750	1.00	70	0	0	41	470	0.00	2.49	0.37	0	247
Yoshizaki et al. (2015)	165-1-56-2	860	800	1.08	60	0	0	24	433	0.00	0.22	0.23	0	102
	166-1-56-8	860	800	1.08	60	0	0	24	433	0.00	0.73	0.82	0	147
	167-1-88-4	860	800	1.08	60	0	0	24	433	0.00	0.44	0.41	0	135
	168-1-88-8	860	800	1.08	60	0	0	24	433	0.00	0.73	0.82	0	159
	169-1-88-12	860	800	1.08	60	0	0	24	433	0.00	1.17	1.17	0	175
	170-2/3-36-2	860	1200	0.72	60	0	0	25	433	0.00	0.24	0.23	0	160
	171-2/3-36-8	860	1200	0.72	60	0	0	25	433	0.00	0.78	0.82	0	235
	172-2/3-52-4	860	1200	0.72	60	0	0	25	433	0.00	0.44	0.41	0	220
	173-2/3-52-8	860	1200	0.72	60	0	0	25	433	0.00	0.78	0.82	0	260
	174-2/3-52-12	860	1200	0.72	60	0	0	25	433	0.00	1.17	1.17	0	275
	175-1/2-27-2	860	1200	0.72	60	0	0	26	433	0.00	0.22	0.23	0	199
	176-1/2-27-8	860	1200	0.72	60	0	0	26	433	0.00	0.80	0.82	0	322
	178-1/2-42-8	860	1200	0.72	60	0	0	26	433	0.00	0.80	0.82	0	382
	179-1/2-42-12	860	1200	0.72	60	0	0	26	433	0.00	1.17	1.17	0	422
Gupta et al. (1998)	S-1	1000	1000	1.00	75	375	100	79	545	1.06	1.06	0.52	0	428
	S-2	1000	1000	1.00	75	375	100	65	545	1.06	1.06	0.52	610	720
	S-3	1000	1000	1.00	75	375	100	69	545	1.06	1.06	0.52	1230	850

Source	Designation	Geometrical Properties h_w (mm)	l_w (mm)	h_w/l_w	b_w (mm)	l_c (mm)	b_c (mm)	Material Properties f_c' (MPa)	f_y (MPa)	ρ (%)	ρ_v (%)	ρ_h (%)	Axial Load, N (kN)	Shear Strength V (kN)
	S-4	1000	1000	1.00	75	375	100	75	545	1.06	1.06	0.52	0	600
	S-5	1000	1000	1.00	75	375	100	73	545	1.61	1.61	0.52	610	790
	S-6	1000	1000	1.00	75	375	100	71	545	1.61	1.61	0.52	1230	970
	S-7	1000	1000	1.00	75	375	100	71	545	1.06	1.06	1.06	610	800
	S-F	1000	1000	1.00	75	375	100	61	545	1.06	1.06	0.52	310	487
Mo et al. (1993)	HN4-1	650	860	0.76	70	170	80	32	302	4.60	0.72	0.81	14	205
	HN4-2	650	860	0.76	70	170	80	32	302	4.60	0.72	0.81	14	247
	HN4-3	650	860	0.76	70	170	80	32	302	4.60	0.72	0.81	14	202
	HN6-1	650	860	0.76	70	170	80	30	302	4.60	0.72	0.81	12	255
	HM4-1	650	860	0.76	70	170	80	38	302	4.60	0.72	0.81	14	223
	HM4-2	650	860	0.76	70	170	80	38	302	4.60	0.72	0.81	14	231
	HM4-3	650	860	0.76	70	170	80	40	302	4.60	0.72	0.81	12	250
	LN4-1	650	860	0.76	70	170	80	18	302	4.60	0.58	0.81	13	193
	LN4-2	650	860	0.76	70	170	80	18	302	4.60	0.58	0.81	13	217
	LN4-3	650	860	0.76	70	170	80	30	302	4.60	0.58	0.81	13	203
	LN6-1	650	860	0.76	70	170	80	31	443	4.60	0.58	0.81	13	246
	LN6-2	650	860	0.76	70	170	80	30	443	4.60	0.58	0.81	13	200
	LN6-3	650	860	0.76	70	170	80	30	443	4.60	0.58	0.81	13	210
	LM6-1	650	860	0.76	70	170	80	39	443	4.60	0.58	0.81	12	219
	LM6-2	650	860	0.76	70	170	80	37	443	4.60	0.58	0.81	13	205
	LM6-3	650	860	0.76	70	170	80	35	443	4.60	0.58	0.81	13	210
	LM4-3	650	860	0.76	70	170	80	66	302	4.60	0.58	0.81	12	227
Barda et al. (1977)	B1-10	955	1905	0.50	102	610	102	29	543	1.83	0.73	0.44	0	1217
	b2-1	955	1905	0.50	102	610	102	16	552	6.46	1.26	0.44	0	978
	B3-2	955	1905	0.50	102	610	102	27	545	4.17	0.97	0.44	0	1107
	B6-4	955	1905	0.50	102	610	102	21	496	4.17	0.75	0.44	0	876
	B7-5	475	1905	0.25	102	610	102	26	531	4.17	0.96	0.41	0	1139
	B8-5	1905	1905	1.00	102	610	102	24	527	4.17	0.96	0.48	0	885

Source	Designation	Geometrical Properties						Material Properties					Axial Load, N	Shear Strength
		h_w (mm)	l_w (mm)	h_w/l_w	b_w (mm)	l_c (mm)	b_c (mm)	f_c' (MPa)	f_y (MPa)	ρ (%)	ρ_v (%)	ρ_h (%)	(kN)	V (kN)
Cardenas et al. (1980)	SW7	1905	1905	1.00	76	0	0	43	449	0.00	0.02	0.00	0	519
	SW8	1905	1905	1.00	76	0	0	43	449	0.00	0.03	0.00	0	569
	Sw9	1905	1905	1.00	76	0	0	43	449	0.00	2.87	1.00	0	679
	SW11	1905	1905	1.00	76	0	0	38	449	0.00	1.64	0.75	0	609
	SW12	1905	1905	1.00	76	0	0	38	449	0.00	1.64	1.00	0	658
Dabbagh et al. (2005)	SW1	1000	1000	1.00	75	375	100	86	536	6.43	2.52	0.45	1200	992
	SW2	1000	1000	1.00	75	375	100	86	498	6.43	3.22	1.34	1200	1190
	SW3	1000	1000	1.00	75	375	100	96	498	6.43	2.82	0.75	1200	1107
	SW5	1000	1000	1.00	75	375	100	83	498	6.43	3.22	0.45	1200	1134
	SW6	1000	1000	1.00	75	375	100	83	498	6.43	2.95	0.94	1200	1141
Pedro et al. (2002)	1	2000	1000	2.00	120	0	0	19	392	0.00	0.25	0.13	0	198
	2	2000	1000	2.00	120	0	0	20	402	0.00	0.25	0.25	0	270
	4	2000	1000	2.00	120	0	0	20	402	0.00	0.25	0.38	0	324
	6	1800	1300	1.38	120	0	0	18	314	0.00	0.26	0.13	0	309
	7	1800	1300	1.38	120	0	0	18	471	0.00	0.13	0.25	0	364
	8	1800	1300	1.38	120	0	0	16	471	0.00	0.26	0.25	0	374
	9	1800	1300	1.38	100	0	0	18	366	0.00	0.26	0.26	0	258
	10	1800	1300	1.38	80	0	0	16	367	0.00	0.25	0.25	0	187
	11	1400	1400	1.00	100	0	0	16	362	0.00	0.26	0.13	0	235
	12	1400	1400	1.00	100	0	0	17	366	0.00	0.13	0.26	0	304
	13	1400	1400	1.00	100	0	0	18	370	0.00	0.26	0.26	0	289
	14	1200	1700	0.71	80	0	0	17	366	0.00	0.25	0.13	0	255
	15	1200	1700	0.71	80	0	0	19	366	0.00	0.13	0.25	0	368
	16	1200	1700	0.71	80	0	0	19	366	0.00	0.25	0.25	0	362
	21	1800	1300	1.38	100	0	0	24	0	0.00	0.00	0.00	0	258
	22	1800	1300	1.38	100	0	0	17	0	0.00	0.00	0.00	0	222
	23	1800	1300	1.38	100	0	0	24	431	0.00	0.00	0.25	0	333
	24	1800	1300	1.38	100	0	0	24	431	0.00	0.25	0.00	0	323

Source	Designation	h_w (mm)	l_w (mm)	h_w/l_w	b_w (mm)	l_c (mm)	b_c (mm)	f_c' (MPa)	f_y (MPa)	ρ (%)	ρ_v (%)	ρ_h (%)	Axial Load, N (kN)	Shear Strength V (kN)
		Geometrical Properties						**Material Properties**						
	25	1400	1400	1.00	100	0	0	24	0	0.00	0.00	0.00	0	352
	26	1400	1400	1.00	100	0	0	18	0	0.00	0.00	0.00	0	262
	27	1400	1400	1.00	100	0	0	24	431	0.00	0.00	0.25	0	491
	28	1400	1400	1.00	100	0	0	23	431	0.00	0.25	0.00	0	258
	29	1050	1500	0.70	80	0	0	23	0	0.00	0.00	0.00	0	400
	30	1050	1500	0.70	80	0	0	18	0	0.00	0.00	0.00	0	356
	31	1050	1500	0.70	80	0	0	23	431	0.00	0.00	0.25	0	391
	32	1050	1500	0.70	80	0	0	23	431	0.00	0.25	0.00	0	344
Alexander et al. (1973)	1	1372	2743	0.50	100	0	0	25	359	0.00	0.30	0.30	0	329
	2	1372	2743	0.50	100	0	0	25	359	0.10	0.30	0.30	0	556
	3	1372	2743	0.50	100	0	0	25	359	0.10	0.30	0.30	350	698
	4	1372	1829	0.75	100	0	0	25	359	0.10	0.30	0.30	175	378
	5	1372	914	1.50	100	0	0	25	359	0.10	0.30	0.30	175	214
Salonikios et al. (1999)	LSW1	1200	1200	1.00	100	240	100	22	500	1.70	0.57	0.57	0	262
	LSW2	1200	1200	1.00	100	240	100	22	500	1.30	0.28	0.28	0	191
	LSW3	1200	1200	1.00	100	240	100	24	500	1.30	0.28	0.28	201	268
	LSW4	1200	1200	1.00	100	240	100	23	500	1.30	0.28	0.28	0	232
	LSW5	1200	1200	1.00	100	240	100	25	500	1.30	0.28	0.28	0	247
Kuang et al. (2008)	U1.0	1200	1200	1.00	100	0	0	30	520	0.00	0.92	1.05	365	360
	U1.5	1800	1200	1.50	100	0	0	35	520	0.00	0.92	1.05	419	277
	C1.0	1200	1200	1.00	100	0	0	35	520	0.00	1.05	1.05	422	455
	C1.5	1800	1200	1.50	100	0	0	34	520	0.00	1.05	1.05	410	304
	U1.0-BC	1200	1200	1.00	100	0	0	31	520	1.11	0.92	1.05	376	415
	U1.5-BC	1800	1200	1.50	100	0	0	34	520	1.11	0.92	1.05	406	280
	U1.0-BC2	1200	1200	1.00	100	0	0	34	520	1.11	0.92	1.05	409	368
	U1.0-CT	1200	1200	1.00	100	0	0	38	520	0.00	0.92	1.05	452	378
Farvashany et al. (2008)	HSCW1	1100	700	1.57	75	375	90	104	500	1.00	1.26	0.47	540	735
	HSCW2	1100	700	1.57	75	375	90	93	500	1.00	1.26	0.47	954	845

Source	Designation	Geometrical Properties						Material Properties					Axial Load, N	Shear Strength
		h_w (mm)	l_w (mm)	h_w/l_w	b_w (mm)	l_c (mm)	b_c (mm)	f_c' (MPa)	f_y (MPa)	ρ (%)	ρ_v (%)	ρ_h (%)	(kN)	V (kN)
	HSCW3	1100	700	1.57	75	375	90	86	500	1.00	0.75	0.47	953	625
	HSCW4	1100	700	1.57	75	375	90	91	500	1.00	0.75	0.47	2364	866
	HSCW5	1100	700	1.57	75	375	90	84	500	1.00	1.26	0.75	955	801
	HSCW6	1100	700	1.57	75	375	90	90	500	1.00	1.26	0.75	550	745
	HSCW7	1100	700	1.57	75	375	90	102	500	1.00	0.75	0.75	952	800
Fukuzawa et al. (1988)	1	1058	2300	0.46	80	300	300	34	410	1.04	1.20	1.20	363	1658
	2	1058	2300	0.46	80	300	300	40	410	1.04	0.80	0.80	365	1475
	3	1058	2300	0.46	80	300	300	34	410	1.44	1.60	1.60	365	1677
	4	1058	2300	0.46	80	300	300	35	410	1.76	2.00	2.00	363	1823
	5	1058	2300	0.46	80	300	300	32	410	1.04	1.20	1.20	726	1515
	6	644	2300	0.28	80	300	300	33	410	1.04	1.20	1.20	364	1617
	7	1449	2300	0.63	80	300	300	33	410	1.04	1.20	1.20	363	1343
	8	1058	2300	0.46	80	300	300	29	410	1.04	0.60	0.60	364	1246
	9	1058	2300	0.46	80	300	300	30	410	1.04	0.80	0.80	365	1307
	10	1058	2300	0.46	80	300	300	29	410	1.04	1.20	1.20	5	1146
	11	1058	2300	0.46	80	300	300	35	410	1.04	0.00	0.00	363	1192
	12	1058	2300	0.46	80	300	300	35	410	1.04	0.30	0.30	363	1283
	13	1058	2300	0.46	80	300	300	34	410	1.76	2.40	2.40	365	2003
	14	1058	2300	0.46	80	300	300	32	410	1.76	2.80	2.80	362	1732
	15	1058	2300	0.46	80	300	300	32	410	1.04	0.00	0.00	0	744
	16	1058	2300	0.46	80	300	300	32	410	1.04	0.00	0.00	723	1421
	17	1058	2300	0.46	80	300	300	35	410	1.04	0.60	0.60	0	1151
	18	1058	2300	0.46	80	300	300	34	410	1.04	0.60	0.60	726	1698
	19	644	2300	0.28	80	300	300	34	410	1.04	0.60	0.60	365	1871
	20	1449	2300	0.63	80	300	300	34	410	1.04	0.60	0.60	364	1275
	21	644	2300	0.28	80	300	300	34	410	1.76	2.00	2.00	363	2081
	22	1449	2300	0.63	80	300	300	34	410	1.76	2.00	2.00	366	1656
Hirosawa (1975)	Hirosawa_7-1	1700	1700	1.00	160	160	170	17	407	5.68	0.50	0.26	544	825

Source	Designation	Geometrical Properties h_w (mm)	l_w (mm)	h_w/l_w	b_w (mm)	l_c (mm)	b_c (mm)	Material Properties f_c' (MPa)	f_y (MPa)	ρ (%)	ρ_v (%)	ρ_h (%)	Axial Load, N (kN)	Shear Strength V (kN)
	Hirosawa_7-2	1700	1700	1.00	160	160	170	21	407	5.68	0.50	0.26	544	740
	Hirosawa_7-3	1700	1700	1.00	160	160	170	21	407	5.68	0.50	0.57	544	830
	Hirosawa_7-4	1700	1700	1.00	160	160	170	14	407	5.68	0.50	0.57	544	825
	Hirosawa_7-5	1700	1700	1.00	160	160	170	15	407	5.68	0.50	1.08	544	820
	Hirosawa_7-6	1700	1700	1.00	160	160	170	18	407	5.68	0.50	1.08	544	930
	Hirosawa_8-1	1700	1700	1.00	160	160	170	21	407	2.51	0.50	0.61	544	700
	Hirosawa_8-2	1700	1700	1.00	160	160	170	14	407	2.51	0.50	0.61	544	630
	Hirosawa_8-3	1700	1700	1.00	160	160	170	15	407	2.51	0.50	1.08	544	720
	Hirosawa_8-4	1700	1700	1.00	160	160	170	18	407	2.51	0.50	1.08	544	775
	Hirosawa_9-1	1700	850	2.00	160	160	85	21	407	9.91	0.40	0.57	272	328
	Hirosawa_9-2	1700	850	2.00	160	160	85	18	407	9.91	0.40	0.57	272	340
	Hirosawa_9-3	1700	850	2.00	160	160	85	18	407	8.44	0.40	1.08	272	330
	Hirosawa_9-4	1700	850	2.00	160	160	85	21	407	8.44	0.40	1.08	272	375
	Hirosawa10-1	1700	1700	1.00	160	160	170	23	483	2.10	0.71	1.28	544	725
	Hirosawa10-2	1700	1700	1.00	160	160	170	23	483	2.10	0.71	1.28	544	735
	Hirosawa10-3	1700	1700	1.00	160	160	170	21	436	2.10	0.71	1.11	544	650
	Hirosawa10-4	1700	1700	1.00	160	160	170	21	436	2.10	0.71	1.11	544	670
	Hirosawa11-1	1700	1700	1.00	100	100	170	24	413	0.84	1.91	0.81	437	465
	Hirosawa11-2	1700	1700	1.00	100	100	170	24	413	0.84	1.91	0.81	437	440
	Hirosawa11-3	1700	1700	1.00	100	350	100	22	435	1.86	1.06	0.81	437	600
	Hirosawa11-4	1700	1700	1.00	100	350	100	22	435	1.86	1.06	0.81	437	615
Sugano et al. (1980)	Sugano_2-1	1800	3960	0.45	120	360	360	21	571	1.77	0.66	0.66	0	2400
	Sugano_2-2	1800	3960	0.45	120	360	360	21	571	1.77	0.66	0.66	0	3000
	Sugano_2-3	1800	3960	0.45	120	360	360	21	571	1.77	0.66	0.66	0	3200
	Sugano_2-4	1800	3960	0.45	120	360	360	20	571	1.77	0.32	0.33	0	1850
	Sugano_2-5	1800	3960	0.45	120	360	360	21	571	1.77	0.33	0.33	0	1950
	Sugano_2-6	1800	3960	0.45	120	360	360	21	284	1.77	0.69	0.66	0	2180
	Sugano_2-7	1800	3960	0.45	120	360	360	20	284	1.77	0.69	0.66	0	2020
	Sugano_2-8	1800	3960	0.45	120	360	360	21	397	1.77	0.77	0.74	0	2350

Source	Designation	Geometrical Properties						Material Properties					Axial Load, N	Shear Strength
		h_w (mm)	l_w (mm)	h_w/l_w	b_w (mm)	l_c (mm)	b_c (mm)	f_c' (MPa)	f_y (MPa)	ρ (%)	ρ_v (%)	ρ_h (%)	(kN)	V (kN)
Aoyagi et al. (1984)	Aoyagi_1-1	1520	2720	0.56	80	320	320	20	353	1.74	0.71	0.76	0	950
	Aoyagi_1-2	1520	2720	0.56	80	320	320	26	353	1.74	0.71	0.76	0	1050
	Aoyagi_1-3	1520	2720	0.56	160	320	320	29	339	1.74	0.58	0.62	0	1585
	Aoyagi_1-4	1520	2720	0.56	80	320	320	24	353	6.48	0.71	0.76	0	1525
	Aoyagi_1-5	1520	2720	0.56	160	320	320	29	339	6.48	0.58	0.62	0	2355
Jiang et al. (1999)	SSW-2	933	1667	0.56	67	67	95	18	325	3.10	1.00	1.00	200	522
	SSW-3	933	1667	0.56	67	67	95	18	325	3.10	1.00	1.00	400	587
	DSW-1A	933	827	1.13	67	67	95	19	325	3.10	1.00	1.00	0	316
	DSW-1B	933	827	1.13	67	67	95	19	325	3.10	1.00	1.00	200	400
	DSW-1C	933	827	1.13	67	67	95	19	325	3.10	1.00	1.00	400	488
	DSW-2A	933	827	1.13	67	67	95	17	325	3.10	1.00	1.00	0	307
	DSW-2B	933	827	1.13	67	67	95	17	325	3.10	1.00	1.00	200	381
	DSW-2C	933	827	1.13	67	67	95	17	325	3.10	1.00	1.00	400	469
	DSW-3A	933	827	1.13	67	67	95	16	325	3.10	1.00	1.00	0	308
	DSW-3B	933	827	1.13	67	67	95	16	325	3.10	1.00	1.00	200	394
	DSW-3C	933	827	1.13	67	67	95	16	325	3.10	1.00	1.00	400	473
Ryo (1963)	29	1449	2300	0.63	78	250	250	23	335	2.55	0.18	0.18	0	966
	30	1449	2300	0.63	75	250	250	33	335	2.55	0.19	0.19	0	932
	31	1457	1550	0.94	80	250	250	17	485	2.55	0.17	0.18	0	608
Muto et al. (1953)	46	215	430	0.50	23	145	30	20	323	0.71	0.70	0.73	0	29
	47	215	430	0.50	24	145	30	19	323	0.71	0.67	0.70	0	28
	50	366	430	0.85	27	145	30	14	402	1.52	0.40	0.38	1	24
	51	366	430	0.85	24	145	30	14	323	1.52	0.45	0.43	1	24
	52	366	430	0.85	22	145	30	16	323	1.52	0.50	0.48	1	20
	53	366	430	0.85	16	145	30	14	323	1.52	0.69	0.66	0	20
	54	366	430	0.85	22	145	30	18	323	1.52	0.73	0.72	0	25
	55	366	430	0.85	22	145	30	17	323	1.52	0.73	0.72	1	26
Tanabe et al.	101	479	570	0.84	20	60	60	34	284	4.70	1.83	1.83	0	63

Source	Designation	Geometrical Properties						Material Properties					Axial Load, N	Shear Strength
		h_w (mm)	l_w (mm)	h_w/l_w	b_w (mm)	l_c (mm)	b_c (mm)	f_c' (MPa)	f_y (MPa)	ρ (%)	ρ_v (%)	ρ_h (%)	(kN)	V (kN)
(1987)	102	479	570	0.84	20	60	60	30	284	4.70	1.83	1.83	0	75
	103	479	570	0.84	20	60	60	35	284	4.70	1.83	1.83	0	63
	104	479	570	0.84	30	60	60	36	284	4.70	1.22	1.22	0	94
	105	479	570	0.84	30	60	60	34	284	4.70	1.22	1.22	0	90
	106	479	570	0.84	30	60	60	34	284	4.70	1.22	1.22	0	86
	107	479	570	0.84	40	60	60	33	284	4.70	0.92	0.92	0	98
	108	479	570	0.84	40	60	60	35	284	4.70	0.92	0.92	0	97
	109	479	570	0.84	40	60	60	36	284	4.70	0.92	0.92	0	102
	110	479	570	0.84	10	60	60	46	294	4.70	1.83	1.83	0	43
	111	479	570	0.84	10	60	60	43	294	4.70	1.83	1.83	0	44
	112	479	570	0.84	20	60	60	43	294	4.70	1.83	1.83	0	69
	113	479	570	0.84	20	60	60	49	294	4.70	1.83	1.83	0	71
	114	479	570	0.84	30	60	60	40	294	4.70	1.22	1.22	0	71
	115	479	570	0.84	30	60	60	46	294	4.70	1.22	1.22	0	77
	116	479	570	0.84	40	60	60	45	294	4.70	0.92	0.92	0	78
	117	479	570	0.84	40	60	60	43	294	4.70	0.92	0.92	0	77
Tsuboi et al. (1967)	131	897	507	1.77	67	107	120	31	296	8.26	1.97	1.89	0	162
	134	502	507	0.99	67	107	120	30	296	3.96	1.97	1.89	0	195
	135	502	507	0.99	67	107	120	29	296	8.26	1.97	1.89	0	185
Sugano et al. (1980)	70	1449	2300	0.63	74	250	250	24	549	2.54	0.18	0.18	0	834
	71	1449	2300	0.63	83	250	250	25	461	2.54	0.07	0.07	0	804
	140	911	3960	0.23	120	360	360	21	572	1.77	0.66	0.66	1514	2354
	141	911	3960	0.23	120	360	360	21	572	1.77	0.66	0.66	2737	2942
	142	911	3960	0.23	120	360	360	21	572	1.77	0.66	0.66	1956	3138
	143	911	3960	0.23	120	360	360	20	572	1.77	0.32	0.33	1198	1814
	144	911	3960	0.23	120	360	360	21	572	1.77	0.33	0.33	1254	1912
	145	911	3960	0.23	120	360	360	20	284	1.77	0.69	0.66	1384	2138

Source	Designation	Geometrical Properties h_w (mm)	l_w (mm)	h_w/l_w	b_w (mm)	l_c (mm)	b_c (mm)	Material Properties f_c' (MPa)	f_y (MPa)	ρ (%)	ρ_v (%)	ρ_h (%)	Axial Load, N (kN)	Shear Strength V (kN)
	146	911	3960	0.23	120	360	360	20	284	1.77	0.69	0.66	1299	1981
	147	911	3960	0.23	120	360	360	21	397	1.77	0.77	0.74	1473	2305
Aoyagi et al. (1984)	150	1523	2720	0.56	160	320	320	29	339	1.74	0.58	0.62	0	1555
	152	1523	2720	0.56	160	320	320	29	339	6.48	0.58	0.62	0	2310
Paulay et al. (1992)	W1	1710	3000	0.57	100	100	200	27	300	0.81	0.81	1.61	28	810
	W3	1710	3000	0.57	100	500	100	26	300	1.36	0.39	1.61	31	786
Wiradinata et al. (1986)	W1	1140	2000	0.57	100	0	0	25	434	0.00	0.80	0.25	15	574
	W2	660	2000	0.33	100	0	0	25	434	0.00	0.80	0.25	10	681
Antebi et al. (1960)	6	1154	1803	0.64	51	191	127	22	271	2.09	0.25	0.25	0	360
	10	1154	1803	0.64	51	191	127	23	271	4.72	0.25	0.25	0	454
	13	1154	1803	0.64	51	191	127	18	393	2.09	0.50	0.50	0	414
	25	1154	1803	0.64	51	191	127	41	331	2.09	0.50	0.50	0	409
	32	1154	1803	0.64	51	191	127	27	345	2.09	0.50	0.50	0	445
	35	1154	1803	0.64	51	191	127	26	345	2.09	0.50	0.50	0	405
	37	1154	1803	0.64	51	191	127	28	345	2.09	0.50	0.50	0	360
	41	1154	1803	0.64	51	191	127	23	323	4.72	0.50	0.50	0	472
	45	1154	1803	0.64	76	191	127	20	313	2.09	0.25	0.25	0	409
	49	1154	1803	0.64	76	191	127	14	319	2.09	0.25	0.25	0	400
	50	1154	1803	0.64	76	191	127	16	306	2.09	0.50	0.50	0	409
	51	1154	1803	0.64	76	191	127	17	343	2.09	0.50	0.50	0	503
	54	1154	1803	0.64	76	191	127	14	346	2.09	0.50	0.50	0	427
	55	1131	3327	0.34	51	191	127	23	361	2.09	0.50	0.50	0	494
	58	1131	3327	0.34	51	191	127	20	348	2.09	0.50	0.50	0	489
	60	1131	3327	0.34	51	191	127	20	350	2.09	0.50	0.50	0	601
Benjamin et al. (1953)	4BII - 1	671	610	1.10	51	127	102	20	341	2.21	0.50	0.50	0	89
	4BII - 2	631	914	0.69	51	127	102	21	341	2.21	0.50	0.50	0	155

Source	Designation	Geometrical Properties						Material Properties					Axial Load, N (kN)	Shear Strength V (kN)
		h_w (mm)	l_w (mm)	h_w/l_w	b_w (mm)	l_c (mm)	b_c (mm)	f_c' (MPa)	f_y (MPa)	ρ (%)	ρ_v (%)	ρ_h (%)		
	4BII - 3	610	1219	0.50	51	127	102	19	341	2.21	0.50	0.50	0	202
	4BII - 4	587	1778	0.33	51	127	102	26	341	2.21	0.50	0.50	0	294
	3BI - 1	985	1727	0.57	51	95	127	21	341	4.19	0.50	0.50	0	187
	1BII - 1	985	1727	0.57	51	191	127	20	341	2.09	0.25	0.25	0	205
	1BII - 2a	985	1727	0.57	51	191	127	22	341	2.09	0.50	0.50	0	463
	1BII - 2b	985	1727	0.57	51	191	127	24	341	2.09	0.50	0.50	0	374
	3BI - 3	985	1727	0.57	51	305	127	23	341	1.31	0.50	0.50	0	294
	3AII - 1	631	914	0.69	44	127	102	25	341	3.31	0.50	0.50	0	205
	3AII - 2	631	914	0.69	44	127	102	19	341	3.31	0.25	0.25	0	138
	1BII - 1a	492	864	0.57	25	95	64	21	341	2.01	0.50	0.50	0	90
	1BII - 3	1477	2591	0.57	76	286	191	21	341	2.00	0.50	0.50	0	685
	NV - 1	826	1651	0.50	51	127	127	27	341	1.76	0.50	0.50	0	301
	NV - 11	1143	1143	1.00	51	127	127	25	341	4.96	0.50	0.50	0	222
	NV - 18	645	1956	0.33	51	127	127	21	341	1.76	0.50	0.50	0	374
	VR - 3	985	1727	0.57	51	191	127	21	341	2.09	0.50	0.50	0	302
	R - 1	985	1727	0.57	51	191	127	21	359	2.09	0.25	0.25	0	316
	A1 - A	587	1778	0.33	44	127	102	22	341	2.21	1.00	1.00	0	311
	A1 - B	587	1778	0.33	44	127	102	23	341	2.21	1.00	1.00	0	367
	A2 - B	587	1778	0.33	44	127	102	20	341	2.21	1.50	1.50	0	329
	M - 1	913	1575	0.58	51	191	121	22	359	2.25	0.25	0.25	0	214
	M - 4	913	1575	0.58	51	191	121	21	359	2.25	0.25	0.25	0	178
	MR - 2	526	1645	0.32	44	127	127	20	359	3.20	0.25	0.25	0	245
	MR - 4	526	1645	0.32	44	127	127	14	359	3.20	0.25	0.25	0	245
	VRR - 1	915	1727	0.53	51	178	127	22	293	2.29	0.50	0.50	0	329
	MS - 1	800	1600	0.50	51	127	127	22	293	4.96	0.25	0.25	0	274
	MS - 5	584	2337	0.25	51	127	127	25	293	4.96	0.27	0.27	0	380
	SD - 1A	695	1219	0.57	51	102	102	16	293	2.75	0.50	0.50	0	178
	SD - 1B	695	1219	0.57	51	102	102	16	293	2.75	0.50	0.50	0	178

Source	Designation	Geometrical Properties						Material Properties					Axial Load, N (kN)	Shear Strength V (kN)
		h_w (mm)	l_w (mm)	h_w/l_w	b_w (mm)	l_c (mm)	b_c (mm)	f_c' (MPa)	f_y (MPa)	ρ (%)	ρ_v (%)	ρ_h (%)		
	SD - 1C	695	1219	0.57	51	102	102	16	293	2.75	0.50	0.50	0	160
Galletly (1952)	A - 8	658	914	0.72	44	102	102	36	345	4.91	0.79	0.79	0	274
	A - 4	658	914	0.72	44	102	102	30	345	4.91	1.57	1.57	0	318
	B - 8	658	914	0.72	44	102	102	34	345	2.76	0.79	0.79	0	227
	B - 4	658	914	0.72	44	102	102	34	345	2.76	1.57	1.57	0	285
	C - 8	658	914	0.72	44	102	102	32	345	5.51	0.79	0.79	0	191
	C - 4	658	914	0.72	44	102	102	30	345	5.51	1.57	1.57	0	245

Note: 80% of cube strength (f_c') is taken as concrete cylinder strength, if required.

LIST OF PUBLICATIONS ON THE BASIS OF THIS RESEARCH WORK

1. Paper(s) Published in Refereed Journal(s)

a) **Sivaguru, V., and Appa Rao, G.,** (2020), "Structural Behaviour of RC Squat Shear Walls with Openings", *ACI Structural Journal*, USA (Accepted and Under publication).

b) **Appa Rao, G., and Sivaguru, V.,** (2020), "Prediction of Shear Strength of Reinforced Concrete Squat Shear Walls-Comparable Studies", *Journal of Structural Engineering*, SERC, India, Vol. 47, N. 4, pp. 319—343.

2. Paper(s) Published in Conference Proceeding(s) as Full Paper

a) **Sivaguru, V., and Appa Rao, G.** (2016), "Shear Strength of RC Squat Shear Walls – A Review", *Proceedings of Structural Engineering Convention (SEC-2016),* Dec 21-23, pp. 130 – 135.

b) **Sivaguru, V., and Appa Rao, G.** (2018), "Numerical study on effect of steel fibres on the shear strength of reinforced concrete squat shear walls with opening", *Proc. of the 12th fib International PhD Symposium in Civil Engineering, Prague, Czech Republic,* 2018, August 29-31, pp. 781-789.

c) **Sivaguru, V., and Appa Rao, G.** (2019), "Behaviour of reinforced concrete squat shear walls with utility openings", *Proc. of 10th International Conference on Fracture Mechanics of Concrete and Concrete Structures (FraMCoS – X), Bayonne, France,* , June 24 – 26.

DOCTORAL COMMITTEE

CHAIR PERSON:	Dr. Manu Santhanam, Professor and Head, Department of Civil Engineering.
GUIDE:	Dr. G. Appa Rao, Professor, Department of Civil Engineering.
MEMBERS	Dr. Amlan K Sengupta, Professor, Department of Civil Engineering.
	Dr. Benny Raphael, Professor, Department of Civil Engineering.
	Dr. C. Sujatha, Professor, Department of Mechanical Engineering.